DISSERTATION

MODEL BASED ANALYSES OF THE CESIUM DYNAMICS IN POND 4, SAVANNAH RIVER SITE

Submitted by

Vivien Miller

Department of Environmental and Radiological Health Sciences

In partial fulfillment of the requirements

For the Degree of Doctor of Philosophy

Colorado State University

Fort Collins, Colorado

Fall 2018

Doctoral Committee:

Advisor: Thomas E. Johnson

Alexander Brandl
Ralf Sudowe
Jennifer Hoeting

ABSTRACT

MODEL BASED ANALYSES OF THE CESIUM DYNAMICS IN POND 4, SAVANNAH RIVER SITE

A number of experiments have added radionuclides, or their stable analogs, into small ponds and described the transport and fate of the added material as measured by their changing concentrations in the pond's biota during the following days, weeks and months. Several of these studies have been concerned with the fate of cesium (Cs) isotopes (Pendleton and Hanson 1958; Kolehmainen *et al*., 1967; Hakonson and Whicker, 1975; Vanderploeg *et al.*, 1975a, 1975b), but few of these experiments have investigated or speculated on the relative importance of the pathways and processes by which the released Cs isotopes have passed through the various components of the system or evaluated the likelihood of the Cs exiting the system. This lack of investigation may be due, in part, to the measurements of mostly Cs concentrations in biotic components with limited data on the relative masses of these components. Masses are required to estimate the inventories of Cs retained in the biota and the Cs fluxes (*i.e.*, the masses of Cs being transferred between biotic components per unit of time) and therefore, the intermediate and ultimate fates of the released Cs in an aquatic system. The modelling techniques of this dissertation are unique in that they assess the inventory of Cs in the pond, or descriptors of the dynamic Cs behavior dependent on knowing this inventory. Overall, the models seek to provide site specific insight on the ^{133}Cs dynamics in Pond 4 and to create a reverse-engineering type of model where different conditions (i.e. scenarios) could be applied and assessed.

All of the models are based on the well documented results of an experimental addition of ^{133}Cs into the 11.4 ha Pond 4 on the Savannah River Site, South Carolina. The experimental data set used includes measures of ^{133}Cs in multiple biotic species and the water over a 500 day period. While ^{133}Cs is stable, it is an analog to the radioisotopes of Cs. The radioisotopes of Cs are important to model because they are some of the major contaminants resulting from nuclear related operations, either as allowable small amounts or unintended larger amounts from accidents that could be detrimental for humans or the environment. The model framework is a basic food web system and includes the 8 primary biotic components in Pond 4, which includes the largemouth bass as the apex predator and a large population of submerged macrophytes and periphyton. One of the reverse engineering scenarios applied is the extension of the model to ^{134}Cs, the radioisotope of Cs with the shortest half life.

Overall, three modeling approaches were assessed: 1) a tabular model, 2) an ordinary differential equation (ODE) compartment model, and 3) Markov chain models. Methods two and three utilize the same parameterization for transfer of ^{133}Cs between the different components. The first model, the tabular model, was developed to estimate the daily inventories of ^{133}Cs in the biotic and water components and to estimate the daily fluxes amongst the components. The tabular model was also useful in identifying the water-periphyton-lake chub-largemouth bass food chain as the highest flux of Cs in the system. The second model, the ODE kinetic model, is an empirical compartment model that predicts daily ^{133}Cs inventories for Pond 4 based on a set of ordinary differential equations. A set of transfer coefficients was optimized such that the Cs inventories matched those of the tabular model both in magnitude and temporally within a factor of two fit for 300+ days in all components.

Subsequently, these transfer coefficients were used as transition probabilities for the application of Markov chain methods to develop and assess three Markov chain based approaches: 1) the Markov simulation; 2) the Markov matrix model; and 3) the time inhomogeneous Markov (TIM) model. The Markov chain methods were explored as an alternative method to the more traditional ODE kinetic compartment model. The Markov chain models of this work assess quantitative and stochastic aspects relating to the distribution, cycling, and fate of Cs atoms transitioning among the various model components. Additionally, the TIM model assesses possible effects of seasonal water temperature variation on the biota, particularly the largemouth bass.

Since the dynamic process of Cs movement is characterized by discrete movements of the individual atoms of the released radionuclide between all the compartments of the ecosystem, the matrix of Markov transition probabilities approach was utilized to create a Markov simulation of this movement. The output is stochastic in that no two replications of individual atoms result in the same distributions of atoms among the components or the same fluxes of atoms along pathways through the system. The mean of 30 realizations of the simulation for one million atoms was comparable with the results of the ODE kinetic model; specifically, the biota daily ^{133}Cs inventories were within five percent of each other with the exception of plankton and *Chaoborus* larvae due to their low probability of uptake. Results of the simulation support small inherent variability overall in the Pond 4 system, and that the largest component relative variability occurs 1) during time periods when components have smaller inventories of ^{133}Cs and 2) for those components with smaller retention probabilities of retaining the ^{133}Cs atoms per unit time. In this system, the largest variability was observed in the primary consumers that had a smaller retention probability.

The Markov simulation model was also used to conduct an assessment of the pathway behavior of the atoms in each component, specifically the cycling of the atoms occurring through the different components and the residence time from entry to exit of the atoms in the individual components. The use of this technique enables quantification of the number of times an atom would return to the same component over a user specified period, which was two years for this work. The results showed that the largest cycling behavior occurred in the macrophytes (twice that of the periphyton), and minimal cycling occurred for the largemouth bass. The quantification of the cycling behavior increases our understanding of the dynamics of ^{133}Cs occurring in the pond. In addition to an assessment of the cycling behavior, exponential distributions were fit to the atom residence time results for each biotic component. These exponential distributions can be used to assess the probabilities that an atom stays in a certain component for user selected time spans.

Depending on the desired level of detail in the assessment of a reverse engineering scenario, the Markov simulation may be too time intensive at approximately 30 minutes computing time for one million atoms. However, the Markov transition probability matrix was found to be useful in developing the deterministic Matrix model as an alternative to the more traditional ODE kinetic model. The Markov matrix model produced an output comparable to the ODE kinetic model (overall average deviation in biota of less than 10 percent between the two models) with minor temporal improvements in its fit to the tabular model. The model computation is a basic linear algebra equation simply implemented by software such as R or Matlab. The model has the advantage of not needing to specify the differential equations of the system and was 10 times faster solving comparable problems using R. Additionally, the matrix

model transition probability matrix was easily extended to subsequent analysis of the probability of exiting the system through use of absorbing Markov chain calculations.

The Pond 4 Markov model can be considered as an absorbing Markov chain since it includes at least one component that is a "sink"; once the Cs transitions to this state it does not leave (in the unmodified Pond 4 model this is the adjacent run-off Pond 5, though the sediments are nearly a sink). The absorbing Markov Chain procedures provide a mathematically simple method to calculate values descriptive of the absorbing nature of the system and also indicative of the cycling occurring in each component prior to exiting the system. More specifically, the absorbing Markov chain methods were useful to augment the previously created reverse engineering model of Pond 4 Cs dynamics by providing information on the 1) mean time prior to Cs exiting the system; 2) number of state changes prior to the Cs exiting the system; and 3) probabilities of the different routes of exiting the system. This information cannot be obtained in traditional compartment models, but is useful in describing system dynamics and assessing the behavior of reverse engineering scenarios.

Lastly, potential effects of water temperature on biota elimination and uptake were incorporated in the development of a time-inhomogeneous Markov model. This type of Markov chain is characterized by time varying transition probabilities. Elimination probabilities were varied over time in the biota by use of the Q_{10} rule (with $Q_{10} = 2$, such that for every decrease in 10 degrees in an aquatic system, the biotic organisms metabolic activity decreased by a factor of two) and three different approaches were investigated as methods to decrease the elimination by fish during colder periods. Of these approaches, the most appropriate for the Pond 4 Markov model was to decrease the elimination rates by a constant rate over the modeled period. The

TIM model was optimized for the largemouth bass for subsequent computation of daily estimates of bass concentration ratios and internal dose.

For the TIM model, no temperature based variability behavior is apparent over the first 300 days of the largemouth bass output and a small sinusoidal behavior of less than 10% deviation from the general increase in Cs inventory is observed between days 300 and 500. The behavior over the first 300 days matches the available data from the experiment for comparable sized largemouth bass. Limited data from the experiment exists for largemouth bass of comparable sizes between days 300 to 400, and it is not possible to assess whether there was a temperature driven behavior in the data over this period of time. It is possible that there is a temperature driven trend in comparable sized bass data between days 400 to 500, where a slight decrease followed by an increase occurs. If it exists, this trend matches the general behavior of the TIM model during this period.

The TIM model predicted sinusoidal behavior of peaks and valleys between day 300 and 500 is different than the behavior of seasonal trends in fish from studies where the transitions of Cs between fish and water are in equilibrium (Peles *et al.* 2000; Kolehmainen, 1979) suggesting different seasonal behavior of Cs in largemouth bass after an acute addition. This conclusion should be investigated further with subsequent refinements to the TIM model. Overall, the TIM model is a reasonable baseline that could be improved by further refining and investigation of all the Pond 4 biotas' uptake and elimination behavior under varying temperatures.

ACKNOWLEDGEMENTS

I would like to acknowledge Dr. John Pinder for sharing his extensive knowledge on radioecology and the Pond 4 study, and for his encouragement to investigate Markov chains as a methodology to model the Pond 4 experimental data. The original Pond 4 study was planned, proposed and performed by Dr. Thomas G. Hinton, and would not have been possible without the assistance of Dr. Pinder along with the following individuals: A.E. De Biase, D. Coughlin, J. Gariboldi, K. Guy, A. Hays, B. Jackson, M. Johannsen, M. Jones, J. Joyner, R. Lide, L. Marsh, J. Novak, B. E. Taylor, F. W. Whicker, and Y. Yi. The original experiment was funded by DOE Contract No. DE-FC09-96SR18546 and some of the sample analyses were supported through a U.S. Department of Energy Reactor Sharing Program with Oregon State University. I am also appreciative of the U.S. Air Force for funding my PhD course requirements; please note that the views expressed in this dissertation are mine and do not reflect official policy or position of the U.S. Air Force, Department of Defense, or the U.S. Government. Additionally, I would like to acknowledge Tyler Eike for his IT support at Colorado State University (CSU). Also, I would like to thank my advisor, Dr. Thomas Johnson, for all his support and belief in me, and thank the members of my committee for their input and willingness to be on my committee. Finally, I must express my deepest appreciation to my family and friends for all their support; particularly, the never failing encouragement of my husband Matt and of my wonderful children Brady and Derek, who encouraged me simply by watching their boundless energy.

DEDICATION

In Memory

of John E. Pinder III,

whom was the spark that ignited this work

Dedicated to my children

Braden Abraham Miller

and Derek Simeon Miller

"Think left and think right, think low and think high.
Oh, the thinks you can think up if you only try!" -Dr. Seuss

TABLE OF CONTENTS

CHAPTER ONE. INTRODUCTION AND BACKGROUND

1.1 Overall Objectives

The overall objective of this work was to assess methods of developing a site specific model of the dynamics of cesium movement in Pond 4, using data from a ^{133}Cs addition experiment, for use in assessing reverse engineering scenarios. Pond 4 is a mesotrophic ecosystem, located at the Savannah River Site, South Carolina.

To achieve this objective, the following models were created, and are described in each of the given chapters:

Chapter (3): Tabular model of daily ^{133}Cs inventories and daily fluxes of ^{133}Cs

Chapter (4): ODE kinetic model, an inventory based Ordinary Differential Equation (ODE) compartment model

Chapter (5): Markov Matrix model, a Markov chain based model that results in a daily inventory output of ^{133}Cs

Chapter (5): Markov Simulation model, a stochastic simulation based on creating multiple Markov chains for ^{133}Cs movement

Chapter (7): Time inhomogeneous Markov model, a Markov chain model, similar to 3) above with the exception that transition probabilities of Cs movement vary over time

The ODE kinetic model was extended to a Markov chain based model as this enabled unique analysis of the Cs dynamics in the pond that would not be possible with an ordinary compartment model alone. Chapter 6 of this dissertation addresses the use of absorbing Markov chain techniques to evaluate parameters such as mean time until exiting the Pond 4 system, and

applies them to two reverse engineering scenarios: 1) extension of the model to ^{134}Cs, a radioisotope of ^{133}Cs, and 2) analysis of different remobilization probabilities of ^{134}Cs and ^{133}Cs from the pond's sediments to the water.

Figure 1.1. below illustrates the general process of using the ^{133}Cs addition experiment data in achieving these objectives.

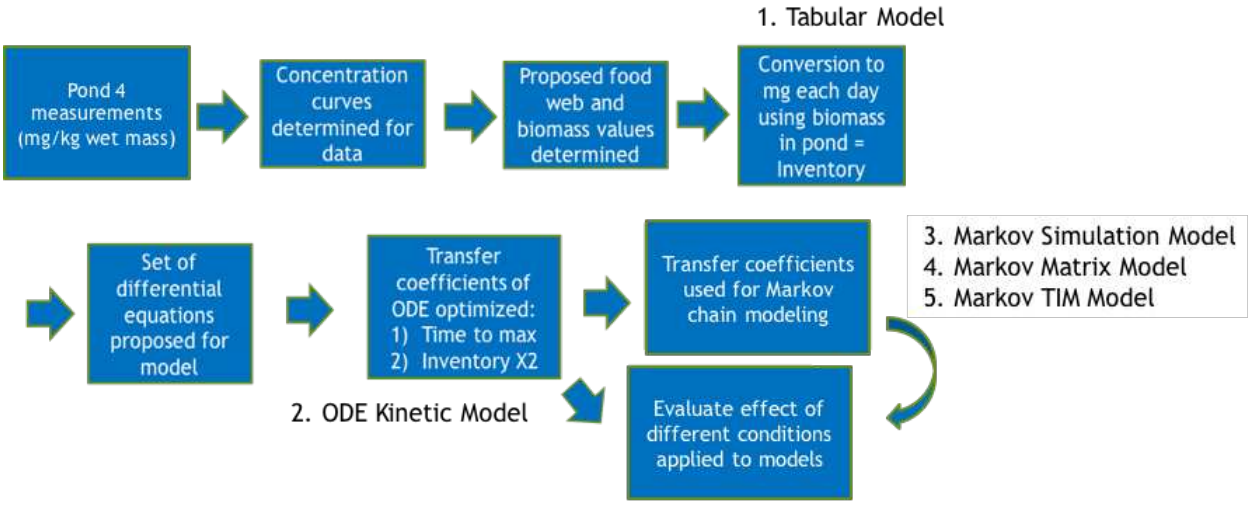

Figure 1.1: Diagram of general process

1.2. Pond 4 History and Background

Pond 4 is a 11.4 hectare impoundment located at the Savannah River Ecology Laboratory (SREL), which is near the town of Aiken and in the lower Coast Plain region of South Carolina, USA. It was constructed in 1961 as part of a network of cooling ponds that were used for P-reactor of the previously operating nuclear power and reprocessing plant; a map of the pond network is illustrated in Figure 1.2 below.

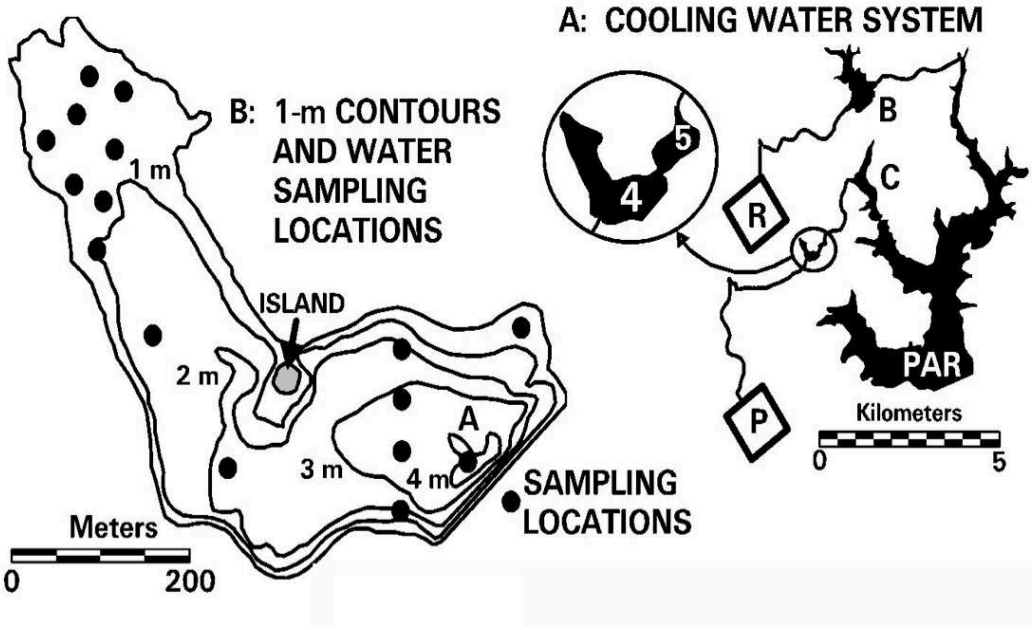

Figure 1.2. Diagram of formerly used cooling pond system at the Savannah River Site (A) and map of Pond 4 indicating depth contours and the water sampling locations of Cs addition experiment (B), (Pinder, 2005).

At the full-pool elevation of 73-m above sea level, Pond 4 has a volume of 157,000 m^3, a mean depth of 1.6 m, and a maximum depth of approximately 4.4 m (Pinder *et al*., 2010). The volumes within the 0 – 1 m, 1 - 2 m, 2 – 3 m, and > 3 m deep sections of the pond (Figure 1.2 B) are 67,900, 55,700, 26,100, and 7,300 m^3, respectively (Pinder *et al*., 2010). Water temperatures, conductivities, pH, and concentrations of dissolved oxygen (O_2) and dissolved potassium (K) in Pond 4 (as reported in Pinder *et al*., 2010) are similar to those in regional ponds and neighboring reservoirs (Tilley, 1975; Evans *et al*., 1983; Chimney *et al*., 1985a, 1985b; Alberts *et al*., 1987; Newman and Schalles, 1990). Water temperatures range from approximately 5ºC in late January to maximums of >30ºC in August (Figure 3 in Pinder *et al*., 2010). Differences between surface and deep water temperatures are usually less than 2ºC to 7ºC, but these differences are sufficient to cause intermittent periods of chemostratification during summer months. Stratification is a

behavior in lakes that occurs when the warmer layer, termed the epilimnion, is formed as a separate layer above an anoxic portion of the lake. The epilimnion is where the majority of biotic activity takes place. A lake or pond must have adequate depth and appropriate environment (i.e., temperature) for stratification to occur (Barnes, 2009). Stratification in Pond 4 was indicated by 1) declines in oxygen concentrations in deeper waters from > 10 mg L^{-1} in mid-winter to < 2 mg L^{-1} in mid-summer, and 2) increases in Mn concentrations in deeper waters from > 10 µg L^{-1} in mid-winter to > 100 µg L^{-1} in mid-summer (Figure 6 in Pinder *et al*., 2010). The concentrations of potassium in pond water ranged from minimums of approximately 50 µg L^{-1} in the summer to maximums of > 400 µg L^{-1} in winter (Figure 7 in Pinder *et al*., 2010) with the winter maximums possibly being related to the release of K from decomposing macrophytes.

After the pumping of thermally elevated water into the pond stopped, the pond developed an extensive aquatic community that includes representatives of three trophic levels: 1) primary producers which obtain their energy by photosynthesis and absorb Cs from the water column; 2) first order consumers that obtain their energy and Cs by consuming primary producers; and 3) secondary consumers that primarily obtain their energy and cesium by consumption of the first order consumers. The primary producers include an extensive community of macrophytes which occurs in the shallows along the shore and a pelagic community of phytoplankton and zooplankton in the deeper open waters of the pond.

This macrophyte community was divided into zones of emergent, floating-leaf, and submerged species. Important emergent species, such as cattails (*Typha latifolia* L.; botanical nomenclature follows Radford *et al*., 1968), occur around the margin of the pond at water depths < 1 m. A floating-leaf zone of mostly waterlilies (*Nymphaea odorata* Aiton) extends from water depths < 1 m to $\leq$ 2 m. The open water area beyond the emergent and floating-leaf vegetation

contains 1) a zone of submerged macrophyte species dominated by water-milfoil (*Myriophyllum spicatum* L.) and floating bladderwort (*Utricularia inflata* Walter) that extends to water depths ≤ 3 m and 2) a zone beyond water depths of 3 m where macrophytes do not occur. The underwater surfaces of the macrophytes are colonized by periphyton, which is a complex mixture of various alga species, cyanobacteria, and plant detritus. Periphyton is consumed by invertebrate species such as snails and vertebrate species such as fish (fishbase.org).

A pelagic, planktonic community in the open deeper water is composed of various microscopic phytoplankton species which are consumed by a variety of microscopic animal species (zooplankton) that are fed upon by fish. During the addition experiment, the sampling procedure for the planktonic community combined both phytoplankton and zooplankton into a common sample which is termed "plankton" in this analysis.

1.3. Overview of the ^{133}Cs Addition Experiment

On 1 August 1999, the experimental addition commenced, and four kilograms of stable cesium, ^{133}Cs, was uniformly added to the top one meter of the pond. The ^{133}Cs was added as 691 separate 43 mL injections of a 1.0M solution of ^{133}CsCl over the open water sections (light blue sections in Figure 1.3 below) of the pond using a small motor boat. This open water area was either above the submerged macrophytes or in areas where they do not grow. ^{133}Cs was not added in areas where emergent or floating-leaf macrophytes prevented the free passage of the boat. The ^{133}Cs injections occurred at 10-m intervals in both north-south and east-west directions from a small outboard motorboat (see Pinder *et al*., 2009 for details of the Cs addition). Each injection took approximately two seconds, and all of the injections were applied within a six hour timeframe. Each injection occurred approximately one meter behind the outboard motor's propeller to ensure dispersion within the pond's water.

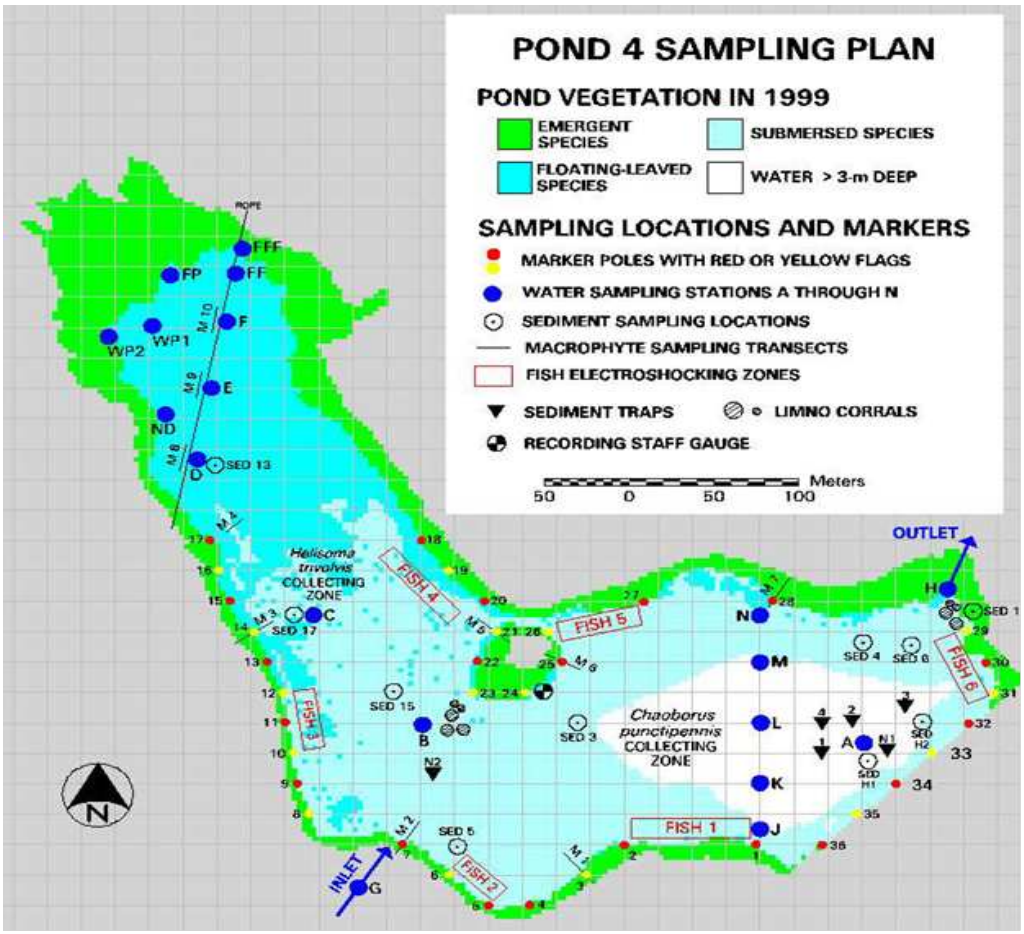

Figure 1.3: Sampling Sites for Biotic Components and Water (Pinder, 2006)

The following is a list of sampled media that was accomplished during the experiment, with sampling locations indicated in Figure 1.3:

1) Water (dissolved and particulate fractions of ^{133}Cs)
2) Sediment
3) Submerged macrophytes (*i.e.,* vegetation)
4) Biota
    a. Primary Producers: periphyton and plankton

b. Primary Consumers: aquatic snails (*Helisoma trivolis)*, the larvae of the fly *Chaoborus punctipennis*, the fish lake chubsucker (*Erimyzon sucetta*)

c. Secondary Consumers: the fish bluegill (*Lepomis macrochirus*) and largemouth bass (*Micropterus salmoides*)

Note that in this dissertation lake chubsucker will be referred to as lake chub, but it should not be confused with *Couesius plumbeus,* a minnow whose common name is lake chub.

Multiple species of submerged macrophytes were sampled during the addition experiment, but sampling results from *Myriophyllum spicatum* were used for the models of this work since it was a predominant species in the center of the pond. Table 1.1 provides an

Table 1.1. Summary of Cs addition experiment sampling

Component	Type of Sample	Approximate Number of Samples	Day Range Sampled
Water – filtered	Individual	44	0,1,2,3,4,5,7,10,12,15,19,22,26, then ~weekly-biweekly – 500+
Sediment	Core and Traps	14	0 - 120
Submerged Macrophytes	Bulk	10	0 - 88
Periphyton	Bulk	20	0 - 59
Snails	Bulk	32	0 - 65
Plankton	Bulk (40 individual hauls per day)	19	0 - 67
Chaoborus	Bulk	28	0 - 65
Lake chubs	Individual	87	0 - 226
Bluegill	Individual	26	0 -87, 348, 354, 495

Largemouth Bass, Small and Larger	Individual	130	0 – 226, 256,348-500

overview on the sampling conducted during the experiment with the methods explained further in the following sections and detailed in several papers published on results of the experiment (Pinder *et al.*, 2004, 2006 & 2009). In addition to day zero, the biota were sampled within two to four weeks prior to the start of the experiment. During the course of the experiment, the biota were sampled on average every two to four days at the beginning of the experiment and every one to two weeks after about the first two weeks (during the day ranges specified in Table 1.1).

1.3. Summary of the sampling and analysis for ^{133}Cs after addition

1.3.1. Basic limnological measurements

The basic limnological measurements began 11 January, 1999 (approximately 6 months before the start of the experiment) and continued to > 500 days following the Cs addition on August 1, 1999. The depth profiles of water temperatures, dissolved oxygen concentrations and conductivities were measured at 0.5-m depth intervals at the deepest point in the pond, termed station A (Figure 2B), using a submersible Hydrolab (Qunta Model SDI-12). From January, 1999 until the 1 August ^{133}Cs additions, these limnology measurements were made at approximately 14-day intervals. Following the ^{133}Cs addition, these measurements occurred on days 5, 13, 19, and 27, with weekly measures through day 110 and biweekly measures through day 522 (4 January, 2001). Changes in pond depths and water volumes were continuously measured using a recording gauge (Stevens Type F).

1.3.2. Sampling to measure Cs concentrations and inventories in Pond 4 water

Changes in the concentrations of dissolved ^{133}Cs in the surface waters of Pond 4 were estimated by measuring concentrations at various locations (Figure 1B) and times using disposable, self-contained syringe and filter assemblages. The filter size was 0.45 μm. These measurements were taken at approximately 7-day intervals through day 109 following the addition and at 14-day intervals until day 522 (Pinder *et al*., 2005). In addition to ^{133}Cs, concentrations of K, Fe, and Mn were also measured in these water samples, after adding HNO_3 to prevent adhesion to container surfaces, using inductively-coupled plasma mass spectrometry (ICP-MS) at SREL. The temporal pattern in depth distributions of both ^{133}Cs and ^{137}Cs in the dissolved and particulate fractions were measured at 0.5-m or 1-m intervals to the maximum depth of 4 m at the centrally located sampling station A in Figure 2B before the ^{133}Cs addition and at 1, 2, 3, 4, 5, 7, 9, 12, 15, 19, 22, 26, and 32 days following the addition (as described in Pinder *et al.*, 2005). The ^{133}Cs content in the particulate fractions in water did not have a temporal trend and the amount of Cs suspended in the water particulates was not differentiated from the sediment in the models discussed in this dissertation.

1.3.3. Sediment related measurements

Five limnocorrals that enclosed 0.9-m diameter, cylindrical columns of pond water were installed before the ^{133}Cs addition and consisted of a tube of flexible, 0.45-mm thick PVC plastic suspended from a floating ring and anchored onto the sediments with weights (see Hinton *et al*., 2006 and Pinder *et al*., 2010 for details). The waters contained in these limnocorrals (which ranged from 1.3 to 1.5 m deep) were in contact with the sediments and the atmosphere, but isolated from the surrounding pond waters. Sufficient ^{133}Cs was added to each of these limnocorrals to produce an initial ^{133}Cs concentration of 450 μg L^{-1} on 1 August, 1999, and the

disposable syringe and filter assemblies were used to measure dissolved ^{133}Cs, K, Fe, and Mn at varying intervals from 1 to 486 days following the addition (see Pinder *et al.*, 2010 for details). The limnocorrals were primarily used to measure ^{133}Cs exchanges between the water and the sediments, especially the remobilization of ^{133}Cs from the sediments to the water column during periods of anoxia when NH_4^+ ions are formed in the sediments and displace Cs atoms from adsorption sites on the sediment particles as reported in Pinder *et al*., 2010.

Sediment samples were taken during the experiment, but the available results do not indicate a statistical increase over natural ^{133}Cs background levels measured prior to the experiment (Pinder, 2004). Additionally, though sediment core samples were accomplished, depth profiles are not part of the available data set. Due to these two factors it is not possible to directly estimate the daily inventories of ^{133}Cs in the sediments due to the addition.

1.3.4. Sampling to measure Cs concentrations and inventories in Pond 4 biotic components

During the experiment, the ^{133}Cs concentrations in the pond's primary biotic components were measured by either inductively-coupled plasma mass spectrometry (PerkinElmer SCIEX Elan DRC Plus; ICP-MS) conducted at SREL or neutron activation analysis (NAA) conducted at the Oregon State University Radiation Center. The ^{133}Cs concentrations in oven-dried samples of plankton, periphyton, *Chaoborus* larvae, and the soft tissues of the snails were analyzed by NAA procedures which involved measuring Cs contents of activated samples on a high purity germanium detector after irradiation in a TRIGA reactor (Pinder *et al*., 2014). The ^{133}Cs concentrations in oven-dried samples of submerged vegetation and fish muscle tissues were measured using ICP-MS (see Pinder *et al*., 2006 for details). Oven drying temperatures and durations varied among samples to ensure drying without causing damage to the sampled

material. Further details on the sampling for biota and biomass measurements are available in Appendix A of this dissertation.

CHAPTER TWO. LITERATURE REVIEW

2.1. Modelling principles as applied to aquatic radioecology

One way of differentiating models is into two broad categories of either deterministic or stochastic models. Deterministic models result in one value for each output variable of the model and utilize only one input value for each model parameter. Such models "determine" the outcome utilizing mathematical equations. Stochastic models are probabilistic, and the variables utilized have a random component. A simple example is formulating a normal distribution that describes an input value and computing multiple model outputs each selecting a different random value from this distribution. The outcome of a stochastic model does not take on one set value, but a range or distribution of values (Dixon *et al.*, 2012). This general approach is applied in evaluating the ODE kinetic model (Chapter 4) of this dissertation. Simulation is a different method of obtaining a stochastic model output, and a form of simulation is used applied in this work to determine the inherent variability due to ^{133}Cs taking different pathways in the pond without making any changes to the input parameters of the Pond 4 model.

Another descriptor of models is whether they can be considered as process-based models or empirical models. Process-based models are mechanistic and are composed of mathematical equations that characterize known processes (Acevedo, 2004). In ecology, process based models can be further characterized as either "fundamental process specific" or "environmental process specific." Fundamental process specific models are based on primary laws of science (i.e., physics or chemistry laws) and are typically characterized by multiple sub-models. Environmental process specific models utilize environmental characteristics, such as water pH or biota potassium levels, to model the radionuclide behavior (Monte, *et al.,* 2003). Some

environmental process specific models can be considered a hybrid between process-based and empirical models in that they empirically determine some of their model parameters and use process-based sub models for other parameters. Empirical models, as described in Simulation of Ecological and Environmental Models, "build a quantitative relationship between variables based on data without explicit consideration of the process yielding that relationship" (Acevedo, 2004). The Pond 4 models of this manuscript are empirical models with some environmental process-based parameters.

There is substantial debate on whether it is better to utilize a fundamental process specific model or a more general empirical model (Monte *et al*., 2003). Fundamental process specific models can be considerably harder to develop and can still not be an accurate descriptor of the system. The uncertainty can be increased by a large number parameters of the sub-models utilized in such models. A common argument is that simple, and at least partially empirical, models are often a better representation of environmental behavior (Smith, 2000). Monte, *et al.* suggest developing "macroscopic models with aggregated environmental components to evaluate systems for quantitative, observable, and experimentally based relationships" (Monte *et al.*, 2003). The Pond 4 models in this work are developed to identify such experimentally based relationships in Pond 4; for example, a decreased sediment remobilization results in what relative change in the largemouth bass inventory level and what change in mean amount of time prior to the ^{133}Cs exiting to Pond 5. Some arguments against empirical models are that they do not provide accurate understanding of the fundamental processes occurring and that combining too many physical processes into one parameter can also increase model uncertainty and cause unacceptable error (Mueller, 1997 and Monte *et al*, 2003). It is worth mentioning that it is not

the goal of the Pond 4 models to assess fundamental processes. Sources of model uncertainty are discussed in subsequent chapters.

Models of the behavior of radionuclides in aquatic environments are typically developed to 1) be predictive; or 2) be descriptive (i.e., provide insight about the system being modeled); or 3) a combination of both. These approaches are all challenging since radionuclide movement is very specific to the aquatic system being modeled (NCRP 154, 2007) due to multiple factors (such as water pH levels, sediment composition, and the structure of the ecosystem itself). Many aquatic environmental models in radioecology are developed to be predictive in nature, with input parameters that can be adjusted to match site specifications if known. Predictive radioecology models can either estimate the current levels of radionuclides or doses in non-sampled biota based on measured levels (for example, in water or sediments) or can be predictive of what levels in the future will be given a known initial condition. Models are all simplified to some degree and the degree of simplification depends on the desired output. The area of interest for this review are time-based models; i.e., those models that are dynamic in nature and either predict or assess the behavior of radionuclides in aquatic systems over time and do not solely make calculations or parameter determinations at equilibrium conditions.

Compartment models or "box models" are a primary tool in radiological health sciences for deterministic evaluation of radioactive material's behavior over time. Such models can be process-based, empirical, or a combination of these approaches. In radioecology, compartment models have a long history of being used to model transfer of radioactive material through the environment for a combination of predictive and descriptive goals (Higley and Bytwerk, 2007). The mathematical basis of compartment models is fairly straightforward. One or more compartments are defined for a given system, and the flow(s) in and out of the compartments are

defined (Higley and Bytwerk, 2007). The system is then transcribed into a set of ordinary differential equations. The benefit of using compartment models is that the kinetic behavior of Cs can be evaluated and equilibrium does not need to exist in the system.

Equilibrium in a compartment system occurs at the point when the flows in and out of the model components over time are constant. Equilibrium in one component can also be considered to occur when its concentration is in constant relative relationship with the water. The timeline for equilibrium to occur after addition of a radionuclide can vary widely depending on species. For example, in a spike study adding ^{137}Cs to a montane lake ecosystem, the amphipods and zooplankton reached equilibrium with the water within about three weeks. At 260 days after the addition, the levels in the trout compared to water were not yet in equilibrium (Hakaonson, et al. 1975).

Though the accumulation of radionuclides in aquatic biota is dynamic, the use of compartment models often incorporates the use of concentration ratios (Higley, 2007). Concentration ratios have several names in the literature, to include bioaccumulation factors, bioconcentration factors, and concentration factors. NCRP 154 recommends the use of the term concentration ratio. This ratio is defined as the concentration of radionuclide in the specified organism compared to a reference concentration (NCRP 154, 2007), where typically the reference concentration is that of the body of water where the aquatic organism resides. It is important to note that the water concentration is that of filtered water versus total cesium in unfiltered water samples (in the latter the sample includes suspended solids) and the concentration ratio should be specified for wet versus dry mass of the biota.

A large amount of study has been developed to measuring these concentrations ratios for multiple biota and radionuclides, and an international compilation of concentration ratios at

equilibrium conditions from different sites exists (IAEA, ICRP 108). Some radioecological models are only concerned with that time period when the system is presumed to be at a state of equilibrium and widely use these concentration ratios for their model calculations. Other models have dynamic components, but utilize concentration ratios to extrapolate what that concentrations will be in certain biotic components, such as fish. The concentration ratios used in many models are based on the aggregate of multiple studies and individually can range over two orders of magnitude (NCRP 154, 2007).

In radioecology, compartment models have been developed for the dynamic behavior of concentrations of radionuclides. There is minimal, if any, literature on the modeling of flow of inventories (mass) of radionuclides through the populations in ecosystems, and specifically, lake ecosystems. Concentrations are evaluated as this is what is typically measured from field environmental samples, limits (such as human consumption) are based on concentrations, and dose due to the radionuclide can be estimated based on concentrations. Additionally, the ubiquitous use of concentration ratios in radioecology also encourages this approach. The use of concentrations in compartment modeling of aquatic systems assumes the following:

1) Constant input factor to water over time
2) Constant mass of the compartments over time

The effect that any violations to these assumptions have on concentration models is accepted as uncertainty and unavoidable error in such models (IAEA, 2000). Since the Pond 4 models estimate inventories and not concentrations, assumption number two above is not necessitated; however, the biomass was assumed to be constant in development of the tablular model (described further in Chapter 3). The first assumption does apply to the Pond 4 models;

however, in the experiment, the ^{133}Cs addition was a one time input, and there is no additional input over time.

2.2 Examples of lake modeling

Compartment model theory is utilized to develop the ODE kinetic model of this paper, though the aspect being modeled differs (mass versus concentration), The following general review of some concentration based radiological contaminant models provides a basis for understanding the similarities and unique aspects of the Pond 4 models. A substantive resource on models of Cs in lakes is the International Atomic Energy Agency's Validation of Environmental Model Predictions (VAMP) Aquatic Working Group's report *Modeling of the Transfer of Radiocaesium from Deposition to Lake Ecosystems* (VAMP, 2000). This working group's objective was to evaluate different lake models and specifically assess how the models could be applied to different types of lakes. The modeling approaches from four different European agencies are described in the VAMP report, and the data from seven lakes (primarily the Baltic region that experienced notably more fallout from the Chernobyl Nuclear Power Plant accident than neighboring areas) was used in the evaluation of the models. The group ultimately proposed an aggregate generic model, termed the VAMP model.

All of the models were similar in that they evaluated concentrations and utilized to at least some extent a first order ordinary differential equation approach. The models include: 1) the MARTE model (Model for Assessing the migration of Radionuclide Transport) developed by Luigi Monte; 2) LAKECO by Rudie Heling; 3) Studsvik model by Ulla Bergstrom and Sture Nordlinder; 4) An empirical, mixed, and generic model developed by Uppsala University (UU) by Lars Håkanson; 4) DETRA (Doses via Environmental Transfer of RAdionuclides), originally

developed by Ilkka Savolainen and Riitta Korhonen from VTT Technical Research Center of Finland and used by Vesa Suolanen, also at VTT. A combination of different aspects of these models produced a new model simply termed VAMP. The VAMP project resulted in six new modeling tools, two of which could be used in modeling work regarding Pond 4, these are: 1) a seasonal variability moderator; and 2) an estimator for relationships between prey and predator fish biomass (VAMP, 2000).

Another useful description of lake models is given in the article by Monte, et al. (2003). This publication includes the models discussed in the VAMP document, and additionally includes the model AQUASCOPE developed by J. Smith (2002). The following table provides a synopsis of the different aspects of various Cs models from the VAMP report and other publications. All of the models are, at least, partial compartment models. Generic indicates that the model is developed not be site specific. Whether or not concentration ratios (CR) were utilized in the model is indicated.

Table 2.1. Summary of Selected Cs Lake Models

Model Name	**Reference/ modeler**	**Components modeled**	**Framework**	**CR used?**	**Sub-models applied**
MARTE	L. Monte	water, suspended matter, sediment (three layers), fish[1]	generic; non biotic components emphasized	Y	suspended matter absorption; drainage into lake; fish
LAKECO	Rudie Heling	surface water, suspended matter, sediments, pore water; fish	process specific-utilizes physical parameters; generic	Y	molecular diffusion; sediment mixing; sedimentation; burial
Studsvik	Ulla Bergstrom; Sture Nordlinder	water, drainage area, sediment (three layers), 3-5 generic biotic compartments	primarily generic-developed for Nordic lakes; semi-empirical rate constant based	Y	sediment; uptake to biota seasonal

UU (empirical, mixed, and generic models)	Lars Håkanson;	empirical- 3 fish; plankton; algae; sediment; mixed- water, small and pike fish	empirical- developed for Swedish lakes	N- empirical N- generic Y-mixed	retention rate based; potassium moderated bio-concentration factor
DETRA- Doses via Environmental Transfer of Radionuclides	Savolainen, et al. (VTT energy)	water, sediment (two layers), four generic fish species	generic; accuracy factor of 10	N	lake dilution, infiltration, and erosion
VAMP LAKE	IAEA VAMP team	water, plankton	generic	N	seasonal; water retention; outflow; sediment
AQUASCOPE	Smith et al.	water[2], sediment	compartment model[2]	Y	open vs closed lake models; water potassium level dependent fish uptake (size corrected for predatory fish)
Eutrophic lake model	Vanderploeg et al.	water, interstial water, sediment, POM, macrophytes, plankton, an invertebrate, three fish species	Lake type specific; compartment model	N	temperature

Notes:
[1] In MARTE, fish concentrations are approximate and the model focuses on the abiotic compartments;
[2] A three component exponential equation is used to drive the water compartment, comparable as is done in Pond 4 models of this manuscript

Vanderploeg, *et al.* developed a dynamic compartment model of ^{137}Cs that was unique in that it included a model for specific activity in addition to concentration in an eutrophic lake. A separate model was developed for an oligotrophic lake. The concentration data utilized to calibrate their model's transfer coefficients was from a ^{137}Cs spike study by Kolehmainen, *et al*. The biota studied are given in Table 2.1, where POM is particulate organic matter, which overlies the sediment as a thin layer. They utilized a driving function to match the water

component to the data. Additionally, each of the fish were modeled as two coupled compartments. A temperature coefficient was applied to convert all the measurements to be equivalent to what would be expected at 15°C. The temperature coefficient utilized was based on the Q_{10} law, which states that there is an approximately two-fold change for every 10 degree change of water temperature (Leveque, 2003). In this eutrophic lake model evaluation, the authors state that an inventory based model was not attempted due to not having measurements or information necessary to determine reasonable levels of biomass for the biotic components. Instead, they conducted a comparison between the specific activity approach and the concentration approach (Vanderploeg, *et al*., 1975).

Models have also been developed for ocean and terrestrial ecosystems using a concentration based approach similar to that previously described for aquatic systems. Alva (2016) describes a multi-compartment model for movement of ^{137}Cs through an ocean food chain with the killer whale as the apex predator. Two examples of terrestrial concentration based compartment modelling of radionuclide movement are the movement of radionuclides through a forest system (Schell, 318) and the movement through the Arctic ecosystem, lichen-reindeer-man pathway (Golikov, 2004).

While less common, inventory based contaminant movement models have been developed and utilized. A notable model is CalTOX, A Multimedia Total Exposure Model, which evaluates exposure due to multiple pathways for a range of contaminants. These contaminants include radionuclides, though its primary usage, based on available literature, is for organic and inorganic chemicals. This modeling program was originally developed in 1993. It is still utilized in the US and applied internationally, as seen by a recent review of the model use in Sweden (Alberg, 2015). Though CalTOX displays its end results in concentration, its

underlying mathematical basis depends on the movement of inventory amounts through general compartments of soil, air, water, etc. (McKone, 1993).

2.3 Markov Chain Models

Markov chains are time based, with one application of use being modeling and studying processes. Given the knowledge of probabilities of movement or change, Markov chains can be used to characterize dynamic systems. The theory of Markov chains is described to much greater detail in Chapters 5 and 6 of this dissertation. Use of Markov chains to physically model processes is common across multiple and widely varying disciplines, with some examples being behavioral science, industrial sciences, and ecology. Markov chains are also used in the numerical calculation technique Markov Chain Monte Carlo, but that is not the application of Markov chains in this work, and such applications were not considered for the examples reviewed for this section. However, to the author's knowledge there are no examples of using Markov chains to model the physical behavior of radionuclide dynamics in an aquatic ecosystem. As a result, general examples of Markov chains in the literature, with a focus on ecology, are briefly discussed in this section.

The use of Markov chains can produce either a stochastic or deterministic result, dependent on whether a simulation approach or the mathematical calculations approach is used. While not commonly utilized in the field of radioecology, Markov chains have been more commonly applied in the broad field of ecology. One use is that of vegetation coverage over time, specifically forest. For example, four ecological roles can be used to characterize tree species behavior. These roles involve whether or not the trees need to have a gap in the tree canopy to grow well (shade tolerance) and whether or not the trees themselves are large enough to create a gap in the canopy. The likeliness that a tree will move between these different states

is characterized by what is termed a Markov chain transition probability matrix. Use of random numbers can drive a stochastic simulation that illustrates how the system becomes a steady state within 10 year of simulation time (Acevedo, 2004).

Another stochastic example in ecology is use of a Markov chain model simulation of disease transmission in plants of the aphid-transmitted barley yellow dwarf virus (McElhany *et al.,* 1995). A third example is the temporal evaluation of species trophic relationships through use of a simulation-based Markov chain model called SIENA (Simulation Investigation for Empirical Network Analysis) (Johnson *et al.*, 2009). SIENA was initially developed by Snijders for the evaluation of social networks of relationships between actors such as companies (Snijders, 2001). The transition probabilities utilized in Johnson's application of SIENA were the seasonal probabilities of changes to predator-prey relationships occurring in the Chesapeake Bay food web. The simulation was effective in enabling statistical evaluation of seasonal patterns of biotic component relationships, for example, changes in numbers of components and links between the winter and summer (Johnson *et al.*, 2009).

There are multiple examples of use of the Markov chain methods, with one example being the use of Markov process models for migration of marine shrimp spatially and temporally (Matis *et al*, 1992 and Grant *et al*, 1991). Additionally, when a Markov chain can be classified as an absorbing Markov chain, further calculations can be computed to assess the dynamics of leaving the defined system. This concept is described extensively in Chapter 6, but is applicable to any system that includes a sink as a component. A couple examples of absorbing Markov chain models are of 1) the transitional dynamics of Mycobacterium Tuberculosis (Alhassan and Nokoe, 2016) and 2) the protein-ligand binding process for the analysis of small protein

molecule interactions (Pacholczyk *et al.*, 2013). Further examples of Markov chains are described in Chapters 5 and 6 of this dissertation.

CHAPTER THREE. INVENTORY AND FLUX ESTIMATION AMONG THE POND'S MAJOR BIOTIC COMPONENTS*

3.1 Introduction and Objectives

The ^{133}Cs addition experiment differed from previous studies in that procedures were employed to estimate the masses of some of the important biotic components of the pond. In this chapter, a model is developed utilizing these biomass measurements and simple extrapolations of the masses of other components in order to produce a model of the accumulation of ^{133}Cs in the biota and the fluxes (*i.e*., the masses of ^{133}Cs being transferred among the biotic components) per unit time. This model, termed the "tabular model," is in the form of a table of inventories (*i.e.*, mg of ^{133}Cs per pond) and presumed fluxes (*i.e*., the masses of ^{133}Cs being transferred among the biotic components) for each of the 500 days following the addition of ^{133}Cs. It was developed to increase our understanding of how the added Cs was redistributed and recycled among the biotic components. The subsequent purpose is to use the tabular model in the development of a rate-based, kinetic model of the ^{133}Cs added into Pond 4 that may be used to investigate reverse engineering scenarios such as: 1) the various temperature regimes that could have occurred in Pond 4; 2) the effects of increases or decreases in biota biomass (that may reflect gradients of oligotrophic to eutrophic lake conditions); and 3) the effectiveness of potential remedial efforts to reduce Cs accumulation by the biota.

---

*Jeong, H., Miller, V.J., Johnson, T.E., Hinton, T., Pinder J.E. III, 2018a. Model-based analyses of the cesium dynamics in the small mesotrophic reservoir, Pond 4. I. Estimating the inventories of and the fluxes among the pond's major biotic components. Journal of Environmental

Radioactivity. In Press. Note: Miller, V.J. is a primary author and the corresponding author of this manuscript.

The objectives of this chapter are:

A. Development of an ecosystem model for Pond 4 with daily ^{133}Cs inventory amounts in each of the food chain components

B. Calculation and assessment of fluxes for identification of the primary pathway of ^{133}Cs flow in the pond

C. Comparison of ^{133}Cs transport and fate over time among the pond's primary producers, primary consumers, and second order consumers.

3.2. Theory and Methods

3.2.1. Food web model structure for the transfers of Cs

Following the addition of ^{133}Cs to Pond 4, its concentrations were measured over an extended time period in seven abundant and important members of the pond's flora and fauna. These included: 1) three primary producers, which accumulated their Cs by absorption from the water column; 2) three first-order consumers, which feed upon and primarily assimilate Cs from the primary producers; and 3) two second-order consumers, which feed upon and primarily assimilate Cs from the first-order consumers.

The primary producers included: 1) the submerged macrophytes species *Myriophyllum spicatum*; 2) periphyton; and 3) plankton. The first-order consumers included: 1) *Chaoborus* larvae (*i.e*., the larvae of the insect *Chaoborus punctipennis*) an insect larvae, which feeds on plankton (Winner and Greber, 1980; Moore, 2006); 2) the snail (*Heliosoma trivolis*), which feeds on periphyton (Eversole, 1978; Boeger, 1975) and 3) the lake chub (*Erimyzon sucetta)* which is a fish that feeds primarily on periphyton (Becker, 1983; *fishbase.org)*.

The second-order consumers included two fish species: 1) bluegill (*Lepomis macrochirus*) and 2) largemouth bass (*Micropterus salmoides*). As individuals of these two fish species grow, their diets can progress from algae and plankton through a mixture of zooplankton, insects, and small fish, to predominantly larger fish (Hodgson and Kitchell, 1987; Taylor *et al*., 1991; Liao *et al*., 2002; Nobriga and Feyrer, 2007). Despite these variations, the bluegill is primarily an intermediate predator on zooplankton, crustaceans, insects, and snails (Flemer and Woolcott, 1966; Kitchell and Windell, 1970; Taylor *et al*., 1991; Lobinske, *et al*., 2002; *fishbase.org*) and the larger individuals of largemouth bass are apex predators feeding primarily on fish (Clady, 1981; Hodgson and Kitchell, 1987; Liao *et al*., 2002; Nobriga and Feyrer, 2007; *fishbase.org*). Because the *Chaoborus* larvae feed upon both the phytoplankton and the zooplankton, they may be considered as both first-order and second-order consumers, but for the purpose of this analysis they are considered first-order consumers. Additionally, since the plankton were a bulk sample and not analyzed separately for species, phytoplankton and zooplankton are considered as one component in all Pond 4 modeling.

The basic components and connections of the food web model, with the component designator listed next to the biotic species name, are illustrated in Figure 3.1. Transfers of Cs between biotic components due to the feeding of one component on another are illustrated with shaded arrows, and the variable $F_{c,j->n}$ indicates the daily flux due to consumption of biota *j* by biota *n*. Transfers of Cs from the water column to the primary producers (*i.e.,* absorption) are illustrated by open arrows, and the variables U_2 and U_3 indicate the daily uptake fluxes due to absorption by periphyton and plankton, respectively. Transfers of Cs from the water column to the primary consumers and secondary consumers are not included in the Pond 4 food web model due to literature documenting that this pathway of uptake is negligible (Hewett and Jeffries, 1976

and 1978; Morgan *et al*., 1993; Topcuoglu, 2001; Malek *et al*., 2004). For simplicity, arrows for the elimination of Cs by animals to the water or the leaching of Cs from plants to the water have been omitted.

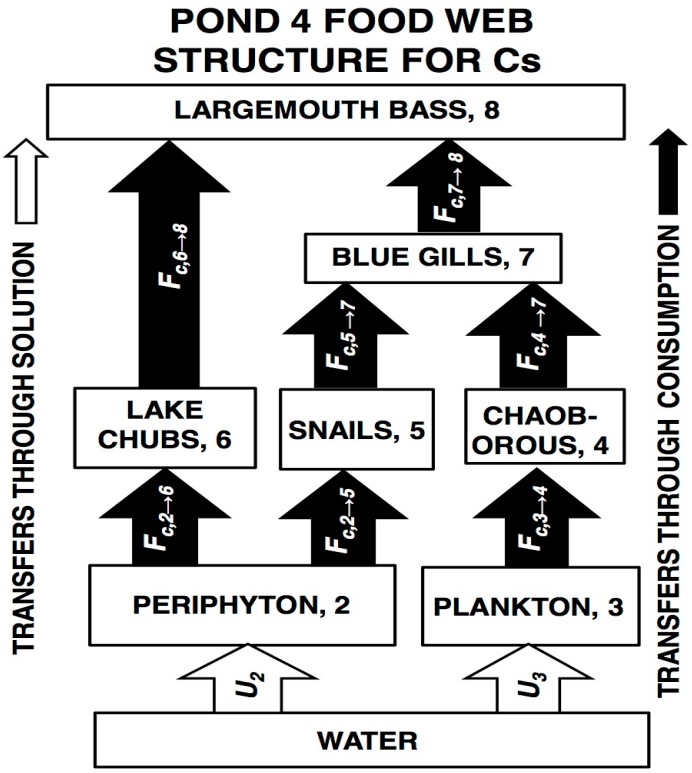

Figure 3.1. Food web model used in tabular model

Although the food web model in Figure 3.1 is a relatively simple and incomplete representation of the Pond 4 food web, it does include three separate, though overlapping food chains, leading to the bass. These include: 1) periphyton (PE) to lake chub (LC) to bass (B) (hereafter, PELCB); 2) periphyton to snails (S) to bluegill (BG) to bass (hereafter, PESBGB); and 3) plankton (PL) to *Chaoborus* larvae (CL) to bluegill to bass (hereafter, PLCLBGB). These specific biota were selected because of 1) their apparent abundance in the pond, 2) their ease of

sampling during the experiment, and 3) their common and representative occurrence in pond communities in this region. The selected species do not present a complete summary of the biomass in each trophic level.

The submerged macrophytes are not fed upon by any of the sampled primary consumers and are therefore not included in the structure of the food web model in Figure 3.1. They are included in this analysis because of 1) their initial large-scale absorption of Cs from the water column; 2) their subsequent, prolonged release of this Cs back into water; and 3) their important role as structure to support the functional role of periphyton. Due to these reasons, they should be included in the subsequent dynamic models which will be derived from the inventories and fluxes of the tabular model explained in this chapter.

3.2.2. Measurement or estimation of the wet masses of the biotic components in Pond 4

In order to estimate the inventories of ^{133}Cs retained in the components of the biota, the masses of the biotic components in Pond 4 were either 1) measured directly by sampling procedures in the pond or 2) estimated indirectly from the mass of other measured components in the pond that supported their presence. The masses of submerged macrophytes, periphyton, and plankton were estimated from samples of mass per unit area or mass per unit volume and are given in Table 3.1:

Table 3.1. The estimated wet masses of the biotic components of Pond 4.

Component	Component Number	Wet Biomass, M_n (kg per pond)	Procedure
Submerged macrophytes	1	35,000	Sampling
Periphyton	2	6,000	Sampling
Plankton	3	9	Sampling
Chaoborus larvae	4	1	Estimation

Snails	5	50[1]	Estimation
Lake chubs	6	550	Estimation[2]
Bluegills	7	125	Estimation[2]
Largemouth bass	8	360	Estimation[2]

[1] Does not include shells

[2] Estimation adjusted for the relative abundance of the species as observed in sampling by electroshocking

In the absence of measured values of biomass at intervals following the Cs release, the biomass values in Table 3.1 were assumed to be constant the 500 days over which sampling of concentrations were measured following the release. Whereas constant masses may be appropriate for the first 90 days, the masses of the biomass are likely to vary over the following 410 days. Some biota may show periods or patterns of increasing masses, and these may not be consistent or synchronous among the biota. In the absence of data on possibly changing quantities of biomasses, the simplifying assumption of constant biomass was employed. Additionally, the fish species biomasses are anticipated to vary less than the other biota due to the longer lifespans of fish. This is advantageous since the fish accumulate ^{133}Cs over the longest periods of time (Pinder, 2011). The largest fluctuations in biomass may be expected to occur for the macrophytes as the summer passes into autumn. However, monthly studies of myriophyllum biomass for August through September and October for Ponds in Tennessee (Stanley *et al*., 1976) and Wisconsin (Adams and McCracken, 1974) suggest variations among these months in myriophyllum biomass from 1.3 to 1.75.

Resources were not available during the period of data collection on Pond 4 to estimate the masses for all the biotic components by sampling. Instead, the masses of these other components were estimated by applying a typical biomass pyramid structure detailed by Odum,

1971, for the unfertilized Weber Lake which is comparable in nature to Pond 4. Within this structure the ratio of the masses of first order consumers to primary producers is 0.1. The ratio for the masses of second order consumers to first order consumers is 0.5. The ratio of masses of third order consumers to second order consumers is 0.5. Thus, for a third order consumer such as the largemouth bass, the ratio of the bass to that for the primary producer is 0.025 (*i.e.*, $(1)\cdot(0.1)\cdot(0.5)\cdot(0.5) = 0.025$). A specific example from the model is that the sum of the biomasses for snails and lake chubs equals 600 kg (= 550 + 50), which is 10% of that of the 6000 kg biomass for periphyton.

The fish biomass estimations were adjusted for the relative abundance of the species as observed in sampling by electroshocking (Hinton, *unpubl. data*). This adjustment resulted in an exception to the pyramid structure as seen in the sum of the biomasses for the snails and the *Chaoborus* of 51 kg (= 50 +1), which is less than the 125 kg of the secondary consumer bluegills. This is due to the faster turnover rates for snails and *Chaoborus* than bluegill. As applied in the tabular model, these biomass values represent the average biomass over the period of the experiment. However, in reality, the composition of the mass of the biota and its ^{133}Cs content is in a constant state of flux with individual organisms being lost to consumption by prey or mortality. These rates of loss and replacement may involve: 1) days for single cell organisms in the phytoplankton; 2) days to weeks for zooplankton; 3) weeks or months for *Chaoborus* larvae with those lost individuals potentially replaced by densities on sediment surface of greater than 4000 individuals per m^2 in the sediments (B.E. Taylor, *pers comm*); and 4) months for snails, but years for the long lived fish species, especially the largemouth bass.

Based on 1) this pyramid structure, 2) the complexity of some forms (*e.g.*, bluegills, which feed on alternative organisms at varying trophic levels), and 3) the relative abundances of

the difference fish species as indicated by the results of electroshocking (Hinton, unpublished data), the biomass pyramid estimation procedure resulted in wet biomass values of 1 kg for *Chaoborus* larvae, 50 kg of edible tissues (*i.e*., non-shell) for snails, 125 kg for bluegills, 550 kg for lake chubs and 360 kg for largemouth bass. The total computed wet biomass of the sampled biotic components in Pond 4 was 42,095 kg. Of this amount 97.4 % was estimated by sampling and the remaining 2.6% was estimated by extrapolation.

In larger lakes and ponds with more extensive open-water (*i*.e., pelagic) areas, plankton may be more abundant than periphyton. As a result, the biomass pyramid for these aquatic systems may be inverted with the larger biomass of the upper consumers being supported by a smaller biotic mass which have 1) greater productivity and 2) increased turnover rates in the smaller organisms of the lower trophic levels (Odum, 1971). However, the current biomass pyramid was deemed more appropriate because of the small size of Pond 4, its mesotrophic nature, and the preponderance of the grazing food chains based on the periphyton. Possibly the extrapolation with greatest uncertainty was for *Chaoborus* larvae. The mass of *Chaoborus* larvae was based on sampling the water column, and could have been 100 times greater if estimated from sediment samples (B. E. Taylor, *pers. comm*.). This error would apply only to the mass of *Chaoborus* larvae and not their Cs concentrations, as the Cs concentrations were determined by measurements of *Chaoborus* larvae sampled from Pond 4.

3.2.3. Procedures for calculating and describing the temporal pattern of ^{133}Cs concentrations and inventories in water

The temporal patterns of the concentrations of the ^{133}Cs in the biotic components and the water were previously published in Pinder *et al.* 2009 and Pinder *et al.* 2011, and are included in this chapter as these concentrations are an integral component in the development of this tabular

model. The patterns and rates of decline in ^{133}Cs concentrations in the water column following the experimental addition were approximated using a multi-component exponential equation (Whicker and Shultz, 1982) of the form:

$$W(t) = \sum_i a_i \cdot e^{(-b_i \cdot t)} \tag{3-1}$$

where $W(t)$ = the dissolved ^{133}Cs concentration in the water (μg L^{-1}) at day t where a_i = the initial concentration of the *ith* component (μg L^{-1}), and b_i = the rate constant (d^{-1}) for exponential decline in the *ith* component. The patterns of decline in the concentrations of ^{133}Cs in the pond's water were adequately approximated using three separate components of decline ($i = 3$). The a_i and b_i terms and their asymptotic SE were estimated using the PROC NLIN procedure of SAS (SAS Institute Inc., 1989) for the data of ^{133}Cs concentrations in the top one meter of water (Pinder, *et al*. 2006) and are given the Table 3.2:

Table 3.2. Estimated initial ^{133}Cs concentrations in the Pond 4 water (a_i values from Equation 3-1) and estimated rates of decline (b_i values from Equation 3-1), and their standard errors

Phase of Decline	Estimated Initial Concentrations (a_i) (μg L^{-1})	Rates of Decline (b_i) (d^{-1})
1	36.24 ± 1.166	0.783 ± 0.0593
2	13.27 ± 0.974	0.0624 ± 0.00980
3	4.68 ± 0.699	0.00310 ± 0.00118

The upper one meter of the water column is relevant for entry of Cs into the biota through absorption by the photosynthetic activity of the primary producers (i.e., macrophytes, periphyton, and plankton) in this photic zone of the pond.

The daily inventories of ^{133}Cs in the water were calculated using a similar manner to the concentrations. Equation 3-1 was applied to the values of ^{133}Cs inventories using three

components, and the a_i (units of g) and b_i (d^{-1}) terms and their asymptotic SE were again estimated using the PROC NLIN procedure of SAS (SAS Institute Inc., 1989) and are given in Table 3.3. The ^{133}Cs inventory values were calculated based on concentration measurements from the full water column depth where the water was at least three meters deep and the corresponding volume of the pond as determined by a bathymetric study (Pinder *et al* 2006). The ^{133}Cs concentrations in the surface and 3-m deep waters rapidly became similar and were not notably different 10 to 14 days after the addition (Pinder *et al.,* 2010; Figs. 7 and 9).

Table 3.3. Estimated initial ^{133}Cs inventories in the Pond 4 water (a_i values from Equation 3-1) and estimated rates of decline (b_i values from Equation 3-1), and their standard errors

Phase of Decline	Estimated Initial Inventory (a_i) (g)	Rates of Decline (b_i) (d^{-1})
1	1133 ± 543	0.259 ± 0.116
2	1711 ± 508	0.0587 ± 0.0182
3	905 ± 90	0.00403 ± 0.000541

Although the three components of decline from Equation 3-1 could adequately model the changing concentrations and inventories, they could not be clearly associated with different physical components of the water (*e.g*., dissolved or particulate fractions), different portions of the water column (*i.e*., depth intervals), or different areas of the pond (*e.g*., pelagic or littoral). Because of a lack of clear association with these features of the pond, they are assumed to reflect the complex interactions of 1) water mixing, 2) sorption and desorption from both bottom and suspended sediments, and 3) the pond's diverse mix of biota.

3.2.4. Procedures for calculating and describing the temporal pattern of ^{133}Cs concentrations in biota

A simple uptake and loss equation (Whicker and Shultz, 1982) summarizes the transient behavior of ^{133}Cs concentrations in a biotic component, *n,* as follows:

$$\frac{dB_n(t)}{dt} = u_n\, W(t) - k_n\, B_n(t) \qquad (3-2)$$

where $B_n(t)$ is the concentration of ^{133}Cs (mg kg^{-1}) in the biotic component *n* (*n* as indicated in Table 3.1 and Figure 3.1), $W(t)$ is the dissolved ^{133}Cs concentration in water (mg L^{-1}), u_n is an uptake constant with units L kg^{-1} d^{-1} , and k_n is a first-order loss rate constant with units d^{-1}. The term $u_n\, W(t)$ is used to relate the temporal pattern of ^{133}Cs in the water to that in the biota and should not be interpreted as inferring ^{133}Cs uptake directly from the water for the higher trophic levels. u_n merely relates the transfer of Cs from the water through the intermediate trophic levels.

Estimates of u_n and k_n were obtained by fitting the following equation (Whicker and Shultz, 1982) to the time series of ^{133}Cs concentration measurements of biota *n* using PRO NLIN of SAS (SAS Institute, 1989):

$$B_n(t) = u_n \sum_{i=1}^{3} \frac{a_i}{(k_n - b_i)}\,(e^{-b_i t} - e^{-k_n t}) \qquad (3-3)$$

where the a_i and b_i values are those determined from Equation 3-1 and presented in Table 3.1 with a_i converted from µg L^{-1} to mg L^{-1}. These values are based on ^{133}Cs measurements in the upper one meter of the water column which is the relevant photic zone of the pond for entry of Cs into the biota through absorption by primarily photosynthetic activity of the primary producers (i.e., macrophytes, periphyton, and plankton). Additionally, the majority of the pond's biomass was in the upper 1-m of the water column. The estimates of the u_n and k_n values and

their standard errors have been compiled from previous publications on Pond 4 and are given in Table 3.4. Equation 3-3 was used to determine the daily concentrations, $B_n(t)$, of each biotic component *n*.

Table 3.4 Coefficients u_n and k_n from the non-linear regression equation, Equation 3-3, for the ^{133}Cs concentrations as milligrams per kg wet mass for the components of the food web model.

Biotic component	Number of samples	$u_n \pm$ SE (L kg^{-1} d^{-1})	$k_n \pm$ SE (d^{-1})	Source
Periphyton	26	215 ± 75.6	0.249 ± 0.091	Pinder *et al.* 2011
Plankton	23	55.6 ± 130	0.457 ± 0.12	Pinder *et al.* 2011
Snails	24	730 ± 26.4	0.153 ± 0.0063	Pinder *et al.* 2011
Chaoborus Larvae	24	97.8 ± 5.4	0.0891 ± 0.0059	Pinder *et al.* 2011
Lakechubs	87	45.8 ± 7.8	0.0104 ± 0.0032	Pinder *et al.* 2009
Bluegills	26	24.3 ± 3.4	0.0054 ± 0.0032	Pinder *et al.* 2009
Largemouth Bass (large, >300mm)	43	26.9 ± 4.3	0.0019 ± 0.0008	Pinder *et al.* 2009

The fitted regression equations for daily ^{133}Cs concentrations of the biotic components are given in Figure 3.2. The u_n values from Pinder *et al.* 2011 have been converted to wet-mass values using conversion factors of 10 for submerged macrophytes, periphyton, and plankton and 5 for the *Chaoborus* larvae. The largemouth bass parameters are based on the data for large fish of length greater than 30 mm total length.

The general approach described by these equations has been used previously to predict Cs movement through lake food webs (Monte *et al*., 2003), in the models AQUASCOPE (Smith *et al*., 2005) and ECOPRAQ (Comans *et al*., 2001). Thomann (1981) used a similar approach for modeling ^{239}Pu and ^{137}Cs in aquatic food chains. Smith *et al*. (2002) used Equation 3-1 to examine the temporal dynamics of ^{137}Cs in Chernobyl contaminated lakes.

The parameters u_n and k_n in these equations will be referred to as uptake and loss rather than absorption and elimination because their estimated values may measure more than just physiological processes. For primary producers (e.g., periphyton) which absorb Cs directly from the water column, u_n is an estimate of absorption rate, and the transfer between the water and the producer component may be expressed as $u_n\ W(t)$. As discussed above, u_n is not a measure of absorption from the water column for the animal components. Rather, its proper interpretation is as a measure of the transfer through the pathways from the primary producers to the consumers. During these transfers, u_n increases with the magnitudes of the transfers and declines with the number of transfers between absorption of the ^{133}Cs from the water by a primary producer and its ingestion by the consumer.

The factors affecting u_n for consumers become increasingly complex with increases in the number of trophic levels and increases in the number of alternative pathways from the water to the consumer. For this reason, u_n may decline as trophic position increases despite an increase in assimilation efficiencies of ^{133}Cs absorption from ingested material at higher trophic levels. This interpretation of u_n for the fish species assumes that ^{133}Cs is primarily absorbed from ingested materials, which is consistent with studies that conclude relatively little Cs is directly absorbed from water by fish (Hewett and Jeffries, 1976 and 1978; Morgan *et al*., 1993; Topcuoglu, 2001; Malek *et al*., 2004).

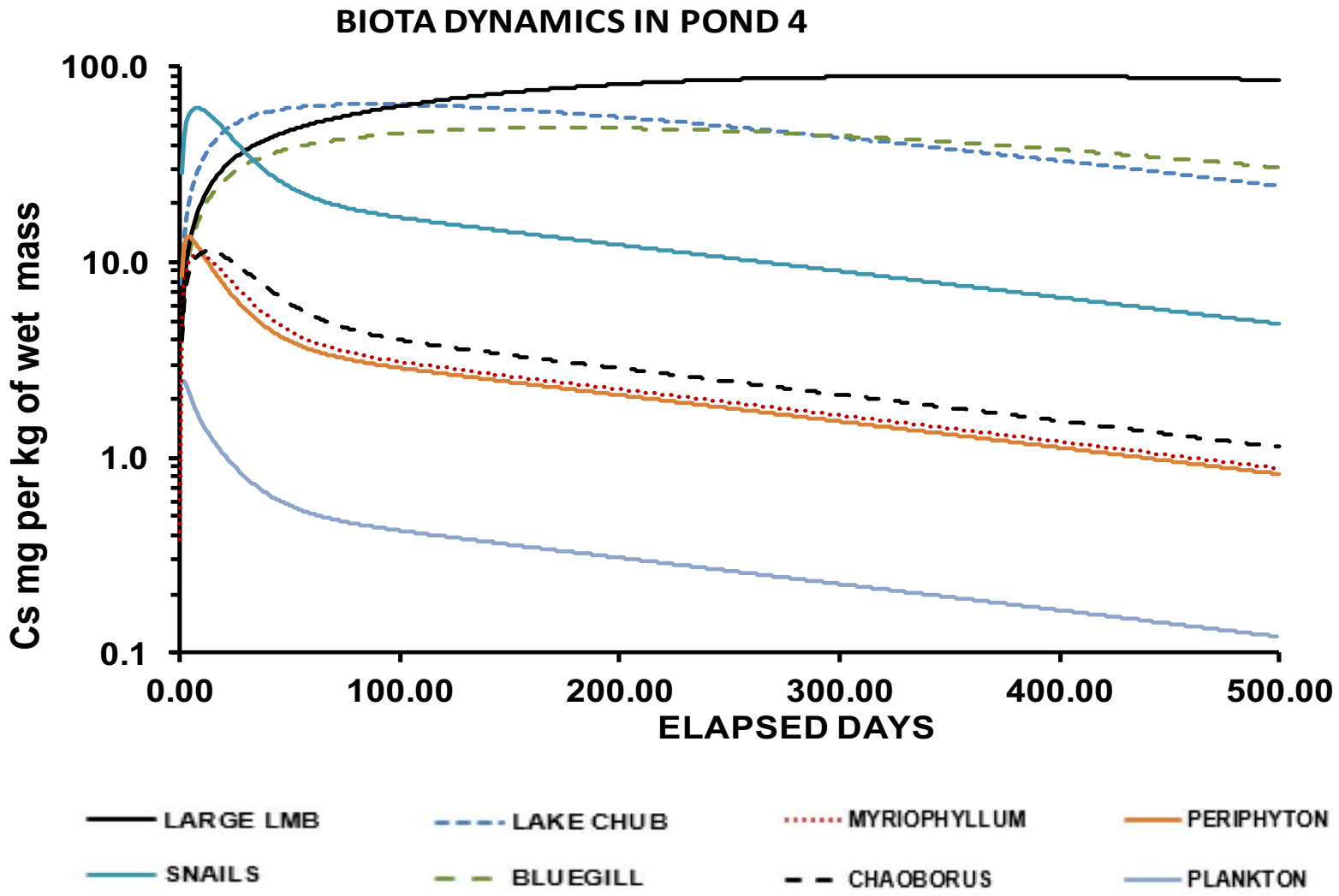

Figure 3.2. Daily Concentration Estimates for Model Food Web Components

3.2.5. Procedures for calculating and describing the temporal pattern of ^{133}Cs inventories in biota

The daily inventories, $I_n(t)$, of ^{133}Cs in each biotic component *n* were computed using Equation 3-4, where $B_n(t)$, is the daily concentration for each day from Equation 3-3, and M_n is the biomass of the biotic component *n* as described in the subsequent section 6.3.1. and listed in Table 3.1.

$$I_n(t) = B_n(t)\, M_n \qquad (3-4)$$

The $I_n(t)$ values are estimates of wet mass inventories in units of milligrams in Pond 4.

3.2.6. Procedures for estimating the flux of ^{133}Cs among the biotic components

The tabular model utilized the ^{133}Cs inventory of each component on each day through the first 500 days following the initial ^{133}Cs addition and estimated the mass of ^{133}Cs being transferred from one compartment to another each day (i.e., the flux) using a top-down approach beginning with the largemouth bass. These ^{133}Cs fluxes are due to consumption of biotic component *j* by biotic component *n,* $F_{c,j\rightarrow n,}$, and due to uptake from water to periphyton, U_2, and plankton, U_3, and are indicated in Figure 3.1. The flux due to elimination to water, $F_{e,n}$ is not pictured in Figure 3.1., though these fluxes are computed in the tabular model. Each flux due to consumption, $F_{c,j\rightarrow n,}$ was calculated on a daily time step, starting with day 1. Table 3.4 explains the variables used in the flux estimation.

The first day loss of ^{133}Cs from the largemouth bass compartment was estimated as the product of the largemouth bass' initial ^{133}Cs inventory and the daily loss rate due to elimination, $F_{e,8}$. Since the bass is the apex predator in this model, there is no loss in the bass compartment due to consumption. Hence, the required input to the largemouth bass to have the correct inventory on day 2 is equal to the elimination loss plus the increase in the largemouth bass

inventory between days one and two. This required input was replaced from the inventories of the lake chubs and bluegills that the largemouth bass feed upon. This same procedure was then completed for the remaining biota, where the daily amount required was determined by the change in inventory from the previous day plus the losses due to consumption and elimination.

Where the ^{133}Cs input requirement from one component was replaced using ^{133}Cs drawn from more than one component (*i.e.*, bass feeding on lake chubs and bluegills, and bluegills feeding on snails and *Chaoborus* larvae), the amount of ^{133}Cs that was drawn from each of these components was in proportion, p_j, to their relative biomass in the pond in a manner similar to that recently employed in Haque *et al.* (2017). The assumption that the largemouth bass and bluegills were feeding on their prey in proportion to the relative abundances of the prey was necessitated by 1) a lack of diet data for Pond 4 and 2) insufficient literature data that was appropriate for Pond 4. This assumption was only needed for the bluegill and largemouth bass as they are the only biota in the Pond 4 model ecosystem that consume more than one species.

This process of replacing ^{133}Cs loss from a consumer biota by ^{133}Cs from the consumed biota was continued until the fluxes were drawn from the water by the primary producers, and then repeated for subsequent days up to 500 days. Estimates of the rates of ^{133}Cs loss, K_n, were based on literature sources for the fish components. Specifically, the loss values used were 0.008 d^{-1} for largemouth bass (Peters and Newman, 1999), 0.009 d^{-1} for bluegill (Rowan and Rasmussen, 1995), and 0.0086 d^{-1} for lake chub (Tostowarky, 2000). The rates of ^{133}Cs loss due to elimination by the remaining biota and leaching from vegetation were estimated from the Equation 3-3 model presented in this chapter and previous Pond 4 literature (Pinder *et. al*., 2005, 2006 and 2011), and are given in Table 3.4.

This procedure of determining the flux of Cs, $F_{c,j\rightarrow n,}$ from the consumed biota *j* to consumer biota *n,* is expressed mathematically by utilizing the concept that the change in inventory, $\Delta I_{n,}$ in biota *n* between day *t* and the previous day, *t-1,* is equal to the total daily uptake (required input) to the biotic component, $U_n(t)$, minus the total daily loss, $L_n(t)$.

$$\Delta I_n = I_n(t) - I_n(t\text{-}1) = U_n(t) - L_n(t) \tag{3-5}$$

This loss is comprised of the loss due to consumption by biota(s) *m,* $F_{c,n\rightarrow m}$ and the loss due to elimination, $F_{e,n}$:

$$L_n(t) = F_{e,n}(t) + F_{c,n\rightarrow m}(t) \tag{3-6}$$

where the loss due to elimination or leaching, $F_{e,n}(t)$, is determined as follows:

$$F_{e,n}(t) = I_n(t\text{-}1)\, K_n \tag{3-7}$$

and K_n equals the loss rate from consumer inventory due to elimination or leaching (fraction per day) and is either from literature sources or Table 3.4. Equation 3-5 applies a discrete form, with $\Delta t=1$, of the differential equation of uptake and loss, Equation 3-2, except for inventory instead of concentration. The uptake and loss values at day *t* are the estimated flux that occurred between the previous day, *t-1*, and current day, *t.* Table 3.5. below provides a description of the variables and constants used in the flux calculation.

Table 3.5. Description of symbols used in calculation of fluxes.

Parameter	Explanation	Value
n	Biota index (subscript)	See Table 3.1 for biotic component numbers
j	Index for biota(s) that is consumed by biota *n*	
m	Index for biota(s) that consume biota *n*	

$F_{c,j\rightarrow n}(t)$	Daily ^{133}Cs flux due to consumption of biota *j* by biota *n*	Positive
ΔI_n	Change in ^{133}Cs inventory between day *t* and *t-1*	Positive or negative
$U_n(t)$	Total daily uptake (needed input) to biotic component *n* between day *t* and *t-1*	Positive
$L_n(t)$	Total daily loss to biotic component *n* between day *t* and *t-1*	Positive
$F_{e,n}(t)$	Daily loss (flux) due to elimination to water from component *n* between day *t* and *t-1*	Positive
K_n	Loss coefficient for biotic component *n*	Constant, 0 to 1
$F_{c,n\rightarrow m}(t)$	Daily loss (flux) due to consumption of biota *n* by biota *m* over between day *t* and *t-1*	Positive
M_j	Biomass of consumed biota *j*	Positive constant, given in Table 3.1
p_j	Relative biomass factor of biota(s) *j* consumed by biota *n*	Constant, 0 to 1

The daily uptake, $U_n(t)$, can be calculated by rearranging Equation 3-5 and Equation 3-6 as:

$$U_n(t) = \Delta I_n + F_{e,n}(t) + F_{c,n\rightarrow m}(t) \quad (3\text{-}8)$$

ΔI_n values are calculated for the discrete daily time step from the daily ^{133}Cs inventory values given by the continuous Equation 3-4 for $I_n(t)$. ΔI_n values are positive or negative depending on the day t at which they are calculated. Additionally, the only biota to have loss due to consumption by more than one consumer is the periphyton, $n = 2$, which are consumed by snails and lake chub and hence for periphyton $F_{c,2\text{-}\rightarrow m}(t) = F_{c,2\rightarrow 5}(t) + F_{c,2\rightarrow 6}(t)$.

The fluxes due to consumption of biota(s) j by biota n is equal to this calculated uptake with a relative biomass factor, p_j, in the pond, of the biotic component j being consumed by biotic component n:

$$F_{c,j\rightarrow n}(t) = U_n(t)\ p_j \tag{3-9}$$

where p_j, is equal to the biomass, M_j, of the directly consumed species j divided by the total biomass of the species consumed by biota n, M_t.

$$p_j = \frac{M_j}{\sum_j M_{j,i}} \tag{3-10}$$

The biomass values, M_n of each biotic component are given in Table 3.1. The relative biomass term, p_j, is a weighting function that applies the assumption that the biotic component n consumes component j in proportion to the biomass in the pond of what it consumes. The relative biomass term, p_j, is equal to one when the biotic component n consumes only one species j; under this condition $F_{c,j\rightarrow n}(t) = U_n(t)$.

To determine the fluxes due to consumption the fore described top down approach was applied, and the uptake for the largemouth bass component between day 0 (addition) and day 1 was determined first using the above process. The flux due to consumption, $F_{c,n\rightarrow m}(t)$, is zero for the largemouth bass. The largemouth bass uptake, $U_{n=8}(t)$, was calculated by using Equation 3-8 and setting $F_{c,n\rightarrow m}(t)$ to zero:

$$U_8(t) = \Delta I_8 + F_{e,8}(t)$$

The calculated value for largemouth bass uptake, $U_8(t)$, was used to determine the fluxes due to consumption by the lower trophic level species, j. As can be seen in Figure 3.1, the flux due to consumption of the lake chub and of the bluegills by largemouth bass equals the uptake into the largemouth bass component:

$$F_{c,7\rightarrow 8}(t) + F_{c,6\rightarrow 8}(t) = U_8(t)$$

Applying this for the lake chub and bluegill to largemouth bass fluxes gives:

$$F_{c,7\rightarrow 8}(t) = U_8(t)\ p_7 = U_8(t)\ \frac{M_7}{M_7+M_6}$$

$$F_{c,6\rightarrow 8}(t) = U_8(t)\ p_6 = U_8(t)\ \frac{M_6}{M_7+M_6}$$

The calculated $F_{c,j\rightarrow n}$ values are utilized in the subsequent calculations of Equation 3-6 for $U_n(t)$ of the lower trophic level as the appropriate $F_{c,n\rightarrow m}$ terms until $U_n(t)$ values are determined for the periphyton and plankton. $U_1(t)$, $U_2(t)$, and $U_3(t)$ are each the ^{133}Cs flux due to absorption from the water to the submerged vegetation, periphyton, and plankton ,respectively. The submerged macrophytes uptake is calculated using Equation 3-6; however, since it is not consumed in this model, the term $F_{c,n\text{-}\rightarrow m}(t)$ is equal to zero.

The calculations used to determine each of the fluxes, $F_{c,j\rightarrow n,}$ are given in entirety in Appendix B of this dissertation. An example of applying the above equations in solving for the flux of ^{133}Cs from snails (j = 5) to bluegills (n = 7) on day twenty, $F_{c,5\rightarrow 7}(t=20)$, is given below:

$$\Delta I_7 = I_7(t=20) - I_7(t=19) = 3275 \text{ mg} - 3191 \text{ mg} = 84 \text{ mg} \quad (\text{for } \Delta t = 1)$$

$$U_7(t=20) = \Delta I_7 + F_{e,7}(t=20) + F_{c,7\rightarrow 8}(t=20)$$

$$F_{e,7}(t=20) = I_7(t=19)\ K_7 = 3191 \text{ mg } (0.0092 \text{ d}^{-1}) = 29 \text{ mg d}^{-1}$$

Note 1: K_7= 0.0092 d^{-1} is derived from Rowan and Rasmussen, 1995

$$F_{c,7\rightarrow 8}(t=20) = 72 \text{ mg d}^{-1}$$

Note 2: $F_{c,7\rightarrow 8}(t=20)$, the loss in the bluegills due to consumption by largemouth bass (m = 8) at day 20, is calculated prior to the calculation in this example (see Appendix B for further detail); it is this aspect that necessitates a top down approach (i.e., largemouth bass fluxes are calculated first, followed by the fish that consume the bass, followed by those biota that consume the fish, etc.).

$$U_7(t=20) = 84+29+72 = 184 \text{ mg d}^{-1}$$

$$p_{j=5} = \frac{M_j}{\sum_i M_{j,i}} = \frac{M_5}{M_4+M_5} = 50 \text{ g} / (50 \text{ g}+1 \text{ g}) = 0.98$$

Note 3: The wet biomass values, M_j, are for those biota directly consumed by the bluegills (*i.e.,* snails, $j=5$, and *Chaoborus* larvae, $j=5$), and are given in Table 3.1.

$$F_{c,5\rightarrow 7}(t=20) = U_7(t=20)\ p_5 = 181 \text{ mg d}^{-1}$$

A limitation of this tabular model is that it is inherently stable and eventually produces a steady state between 1) all losses of ^{133}Cs from the biota to the water column, $\sum F_{e,n(t)}$, and 2) the replacement of these losses by the uptake of ^{133}Cs from the water by the primary producers. This steady state occurs due to the top-down computation process where ^{133}Cs loss from the upper trophic levels to the water column is replaced by the uptake by primary producers. This inherent steady state property should have little effect on the estimation of fluxes in this analysis because: 1) this steady state is not reached until day 327; 2) the relative proportions of the ^{133}Cs inventory in the individual biota are still varying through time within the overall steady state; and 3) it does not result in a steady state between the relative proportions of ^{133}Cs in the biota and the water, as the inventory in the water continues to decline due to losses to the sediments and to Pond 5.

3.3. Results

3.3.1. The temporal patterns of the ^{133}Cs concentrations and inventories of the water following the addition on 1 August 1999.

The patterns of the declines in ^{133}Cs concentrations in surface waters of one meter depth (Figure 3.3A) and inventories (Figure 3.3B) below were adequately approximated using versions of Equation 3-1 with the parameter estimates given in Tables 3.2 and 3.3; however, the rates of the initial declines (*i.e.*, the b_i) differed between the concentrations and the inventories (Figure 3.3, Tables 3.2 and 3.3). The water concentration data were for the surface one meter of the pond, and the water inventory values were assessed for the full water volume of the pond. The temporal patterns of ^{133}Cs inventories in the water volume of the pond declined at a slower rate than the concentrations in the surface waters. The mean concentrations in the surface water declined by 60% in the first 3 days, and this rapid initial decline probably reflects vertical mixing. The subsequent decreases in water concentrations represented a combination of 1) adsorption to the sediments, 2) absorption by the biota, and 3) continuing mixing of surface and deeper waters.

3.3.3. The patterns of increasing and decreasing concentrations in the biotic components

The patterns of increasing and decreasing concentrations in the components of the biota, as illustrated in Figure 3.2, matched the patterns observed in other similar studies with maximum concentrations occurring later for organisms at higher trophic levels. Maximum ^{133}Cs concentrations for plankton, periphyton, and submerged macrophytes were 2.5 mg kg^{-1}, 13.5 mg kg^{-1} and 11 mg kg^{-1}, respectively, and these maxima occurred three, four, and eight days after the spike, respectively.

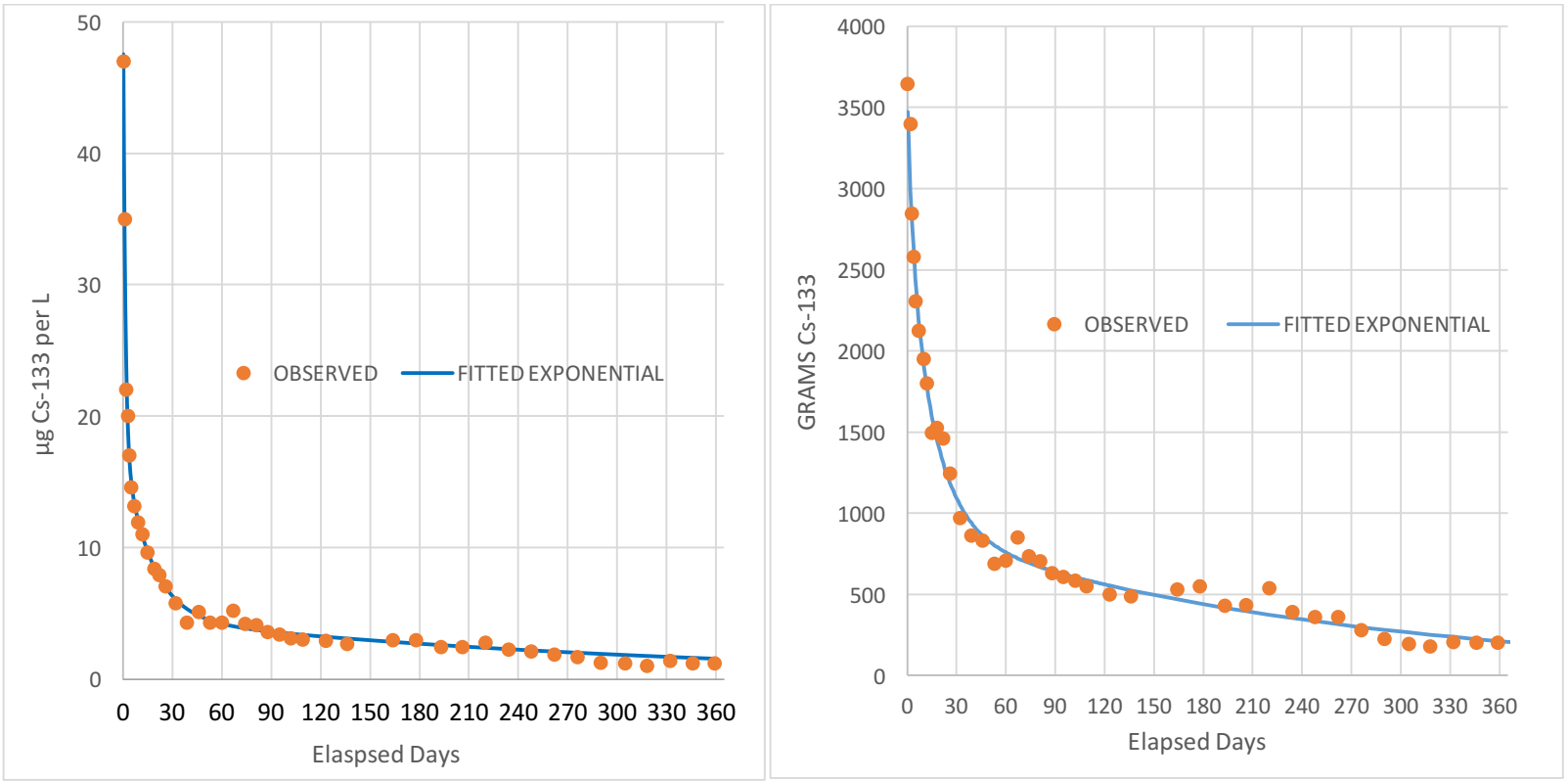

Figure 3.3. Comparison of water ^{133}Cs concentration curve and ^{133}Cs inventory curve; concentration curve observed data is for top one meter of Pond 4's open water areas and inventory curve values are representative of the full depth of the open water area

The maximum ^{133}Cs concentrations and the day of the maximum concentrations for the first-order consumers snails, *Chaoborus* larvae, and lake chubs, which feed on the primary producers, were 61 mg kg^{-1} on day 8, 11 mg kg^{-1} on day 13, and 64 mg kg^{-1} on day 86, respectively. The projected maximum ^{133}Cs concentrations and the days of these maxima for the higher trophic levels of the second-order consumers of bluegills and largemouth bass which feed on other animal forms were, respectively, 49 mg kg^{-1} on day 177 and 90 mg kg^{-1} on day 358.

Although the sequences of these days of maximum concentrations follow the expected pattern due to the trophic position of the biota, these estimated days must be considered approximate due to the distributions of elapsed days between sampling intervals. This may be especially true for the primary producers and the first-order consumers of *Chaoborus* larvae and snails, whose concentrations were changing rapidly during these first 15 days.

3.3.2. The patterns of increasing and decreasing inventories in the biotic components.

Because the measured or extrapolated biomass values for the each of the biotic components were held constant, the days of maximum inventories occurred on the same days as the maximum concentrations. The maximum levels and corresponding days they occur are given in Table 3.6.

Table 3.6 Maximum inventory levels in biota and days of occurrence

Biotic Component	**Max Inventory (g)**	**Day of Max Inventory**
Submerged Macrophytes	384	8
Periphyton	73	6
Plankton	0.016	3

Snails	3.1	10
Chaoborus	0.011	13
Bluegill	2	105
Lake chub	16	61
Largemouth Bass	6.4	358

The maximum ^{133}Cs inventory summed across the biotic components was 484 g and occurred on day 8. This maximum represented 12.1 % of the added ^{133}Cs. Approximately 98 % of this maximum inventory occurred in the primary producers, especially the submerged macrophytes. Following this maximum ^{133}Cs inventory in the biota, the total inventory demonstrated a continuous decline with the rate of this decline also declining. After day 50, the total ^{133}Cs in the biota declined at an approximate rate of 0.003 d^{-1}. This rate of decline for the sum of the inventories in the biota is similar to that for the inventories of ^{133}Cs in the water, which was approximately 0.004 d^{-1} (Table 3.3).

Each component's inventories (mg) are given Figures 3.4A, 3.4B, and 3.4C for the primary producers, primary consumers, and secondary consumers, respectively. The inventories of ^{133}Cs in the individual biota components when the maximum total biota inventory occurred increased in the sequence of 11 mg for the *Chaoborus* larvae, 16 mg for the plankton, 2 g for the bluegill, 3.1 g for the snails, 6.4 g for the largemouth bass, 16 g for the lake chubs, 73 g for the periphyton, and 384 g for the submerged macrophytes. Although these amounts may contain ^{133}Cs that was present in the pond before the release, the rapid increases in ^{133}Cs concentrations following the addition suggests that the majority of these amounts are due to the release of the added ^{133}Cs.

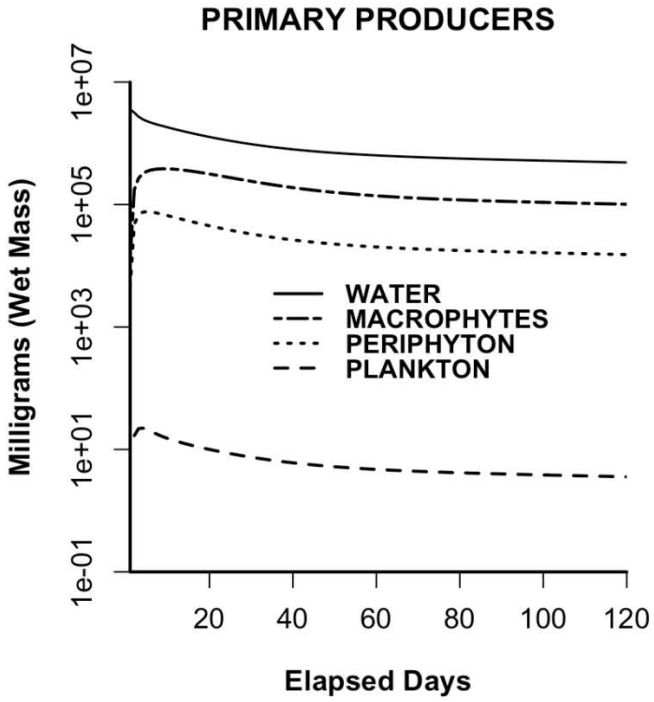

Figure 3.4A Primary Producer ^{133}Cs tabular Model Daily Inventories

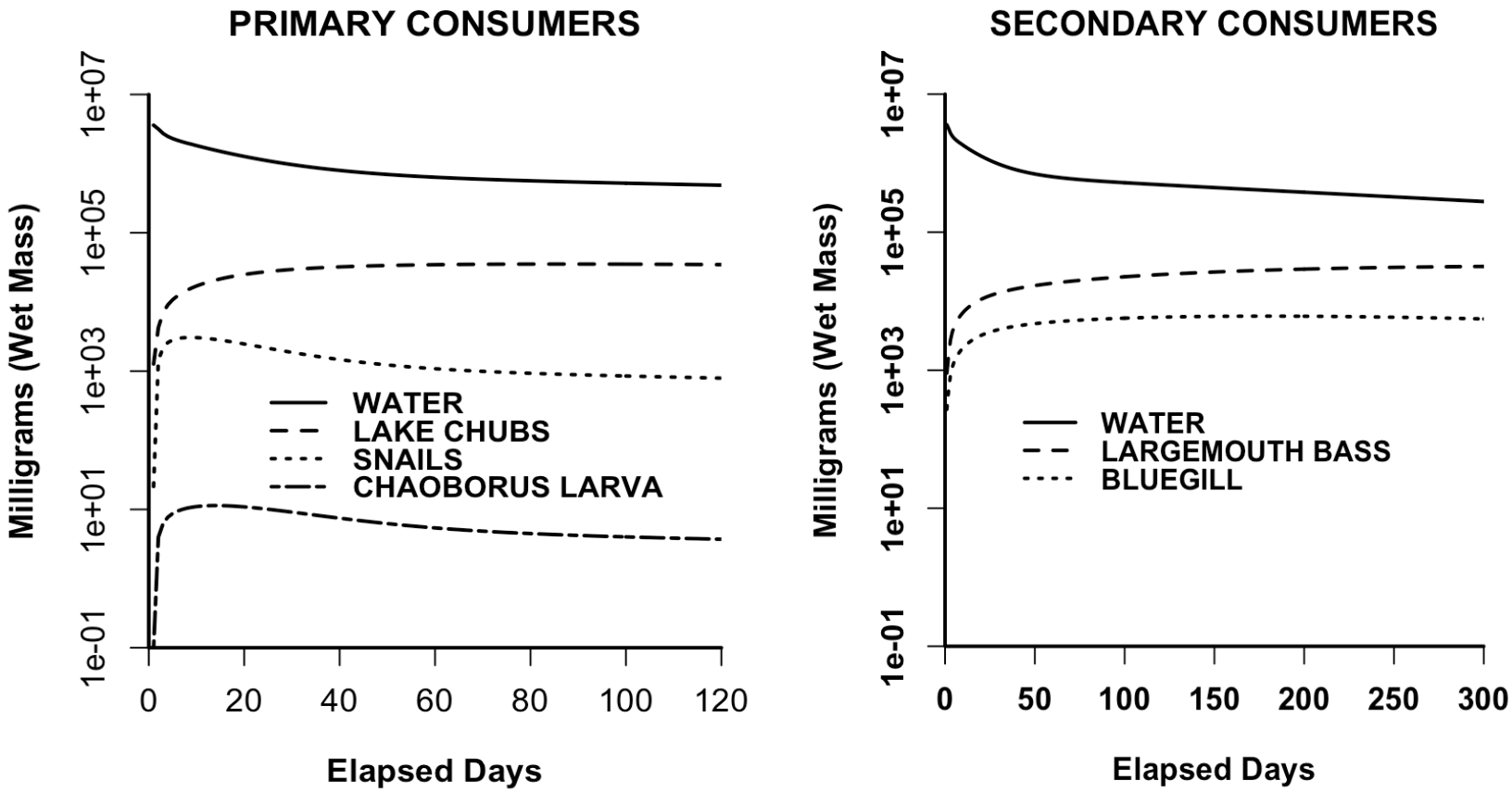

Figure 3.4B and 3.4C. Primary and secondary consumer ^{133}Cs tabular model inventories (B on left and C on right)

Although projections past 100 days may be less certain than those in the first 90 days when sampling was most intensive, the projected total ^{133}Cs inventories in the biota for 100, 200, 300, 400, and 500 days were 190, 157, 128, 104, and 84 g, respectively. If only those biota participating in the pond's food web are considered (*i.e.,* all biota except for the submerged macrophytes), the maximum inventory of these biota was 102 g which occurred on day 5. The total ^{133}Cs inventories in these biota for 50, 100, 200, 300, 400 and 500 days were 80, 82, 79, 71, 62, and 53 g, respectively. The projected fraction of ^{133}Cs in the food-web components out of the total ^{133}Cs in the biota continually increased to 0.63 on day 500.

The maximum inventory for the primary producers of 457 g ^{133}Cs occurred on day seven and was largely due to the rapid assimilation of ^{133}Cs by the submerged macrophytes. The maximum ^{133}Cs inventory in the submerged macrophytes was 384 g ^{133}Cs on day eight. The maximum ^{133}Cs inventory in the plankton of 22 mg ^{133}Cs occurred on day three. The maximum for periphyton of 81 g of ^{133}Cs occurred on day four.

The ^{133}Cs inventories in the three primary producer components demonstrated similar temporal patterns with a rapid increase to a maximum value and slow rates of decline. The submerged vegetation's maximum daily amount of ^{133}Cs uptake was 165 g on day one. The maximum daily ^{133}Cs loss from the submerged vegetation was 5.6 g on day eight. The maximum ^{133}Cs inventory in the periphyton was approximately 81 g on day four with maximum Cs assimilation of 53 g d^{-1} occurring on day one, and maximum ^{133}Cs released back to the water of 2.3 g d^{-1} on day four.

The patterns of ^{133}Cs accumulation and decline differed among the first-order consumers and reflected their life forms and trophic positions. Maximum inventories for *Chaoborus* larvae, snails, and lake chubs occurred on days 13, 8, and 86 with inventories of 0.01, 3, and 35 g ^{133}Cs,

respectively. The similar rates of declines in *Chaoborus* larvae and snail inventories may indicate a greater consumption of snails by bluegills when compared to the consumption of *Chaoborus* larvae by bluegills.

In contrast to the primary producers and first-order consumers which reached maximum concentrations and inventories within the first 90 days, neither the bluegills nor the bass reached maxima within the first 90 days. The graph for these species is extended past 90 days to illustrate their continuing increases in concentrations and inventories. The projected maximum ^{133}Cs inventories for the bluegill and the bass occurred on days 177 and 358, respectively. Their respective projected maximum inventories on these dates were 61 g and 32 g. For the bass, this continuing increase in inventories past 200 days is supported by continuing measures of ^{133}Cs concentrations in bass (Pinder *et. al.,* 2009).

3.3.3. The estimated fluxes of ^{133}Cs through the biotic components expressed as the mass of ^{133}Cs passing through each component per day.

For the total biota, the rate of ^{133}Cs uptake from the water and entry into the biota via the primary producers was at a maximum on day one of 253 g d^{-1} with 74 % of this being due to the macrophytes. This uptake rate declined rapidly to 27 mg d^{-1} by day 50. Following day 50 the rate of ^{133}Cs uptake per day declined 0.35% per day on average. The rate of loss from all the combined forms of the biota to the water reached a maximum of 75.8 g d^{-1} on day six and declined to 29 g d^{-1} by day 50, with the submerged vegetation contributing the most to this loss.

If only those forms involved in the food web (*i.e.*, periphyton and plankton through largemouth bass) are considered, the sum of the daily fluxes of ^{133}Cs among these forms reached a maximum on day two of 6.7 g with the major transfers occurring from 1) the periphyton to the snails (1.3 g) and 2) the periphyton to the lake chubs (3.7 g). The sum of the fluxes among the

components of the food-web biota declined rapidly to 1.2 g on day 50 and declined more slowly to 0.97 g on day 200.

3.3.4. The ^{133}Cs fluxes through the separate food chains from periphyton and plankton to bass

The fluxes of ^{133}Cs through the separate food chains are illustrated in Figs. 3.5A, 3.5B, and 3.5C. Note the differences in the scales among the separate figures. The differences in the flux from the bluegills to the bass between Figure 3.5B (*i.e.*, > 50 mg ^{133}Cs per day) and the flux from the bluegills to the bass in Figure 3.5C (*i.e.*, < 5 mg per day) reflect the greater flux from periphyton to snails to bluegills than that for the flux of ^{133}Cs from plankton to *Chaoborus* larvae to bluegills. The fluxes through the lower trophic organisms in a food chain are greater than those in the upper trophic organisms which reflects the losses from the lower organisms to the water column through leaching or elimination.

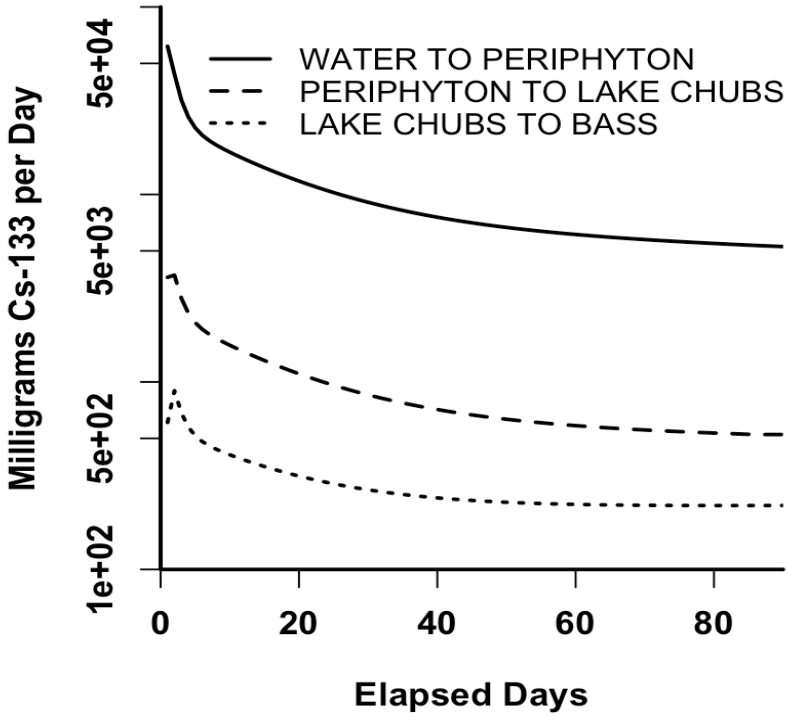

Figure 3.5A. Estimated daily fluxes of ^{133}Cs in Pond 4.

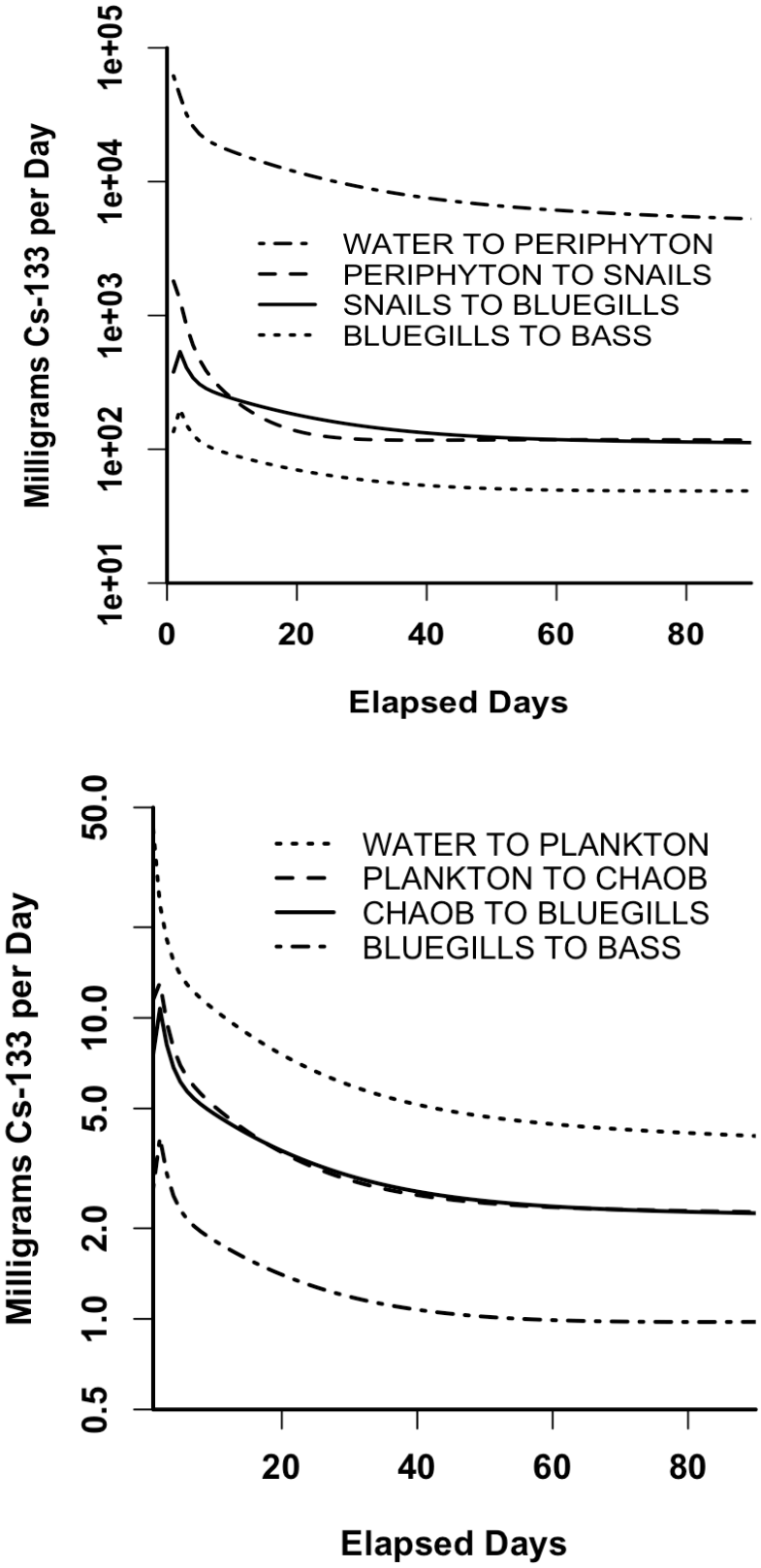

Figure 3.5B (top) and Figure 3.5C (bottom). Estimated daily fluxes of ^{133}Cs in Pond 4.

It is important to note in Figs. 3.5A, 3.5B, and 3.5C that the fluxes for all of the biotic components are greater for the lower trophic levels (*e.g.*, the ^{133}Cs fluxes for the periphyton to snails to bluegills to bass in Figure 3B decline in the order periphyton to snails to bluegills to bass). Any deviation from this pattern would question the appropriateness of the procedures employed in estimating these fluxes and the food web structure in Figure 3.1.

3.3.5. Comparing the ^{133}Cs fluxes through the food chains from periphyton and plankton to bass

The separate fluxes for the PELCB, PESBGB and PLCLBGB food chains to bass are compared in Figure 3.6 for first 90 days.

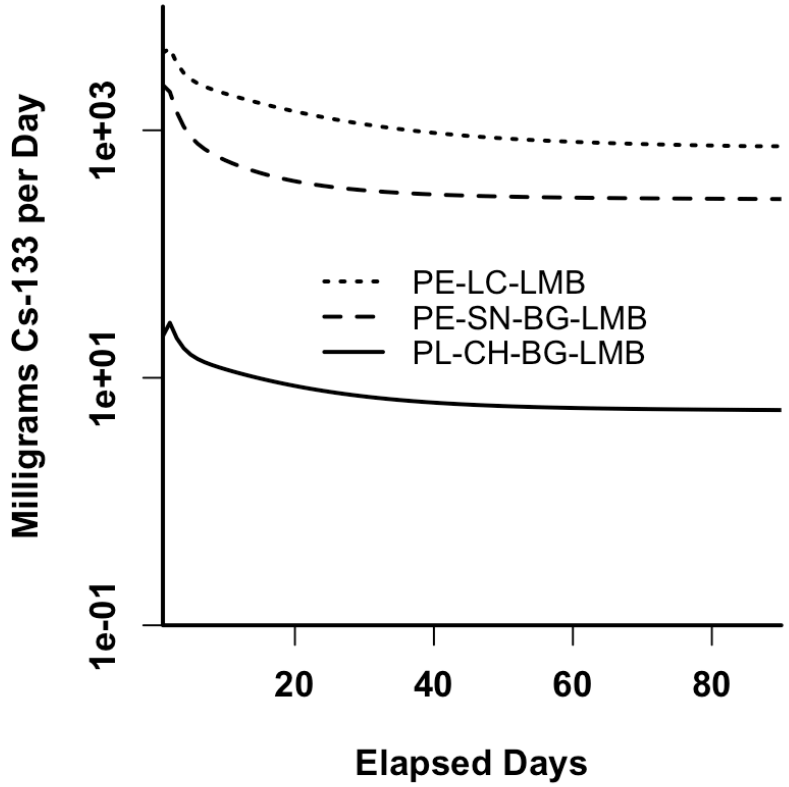

Figure 3.6. Comparison of daily fluxes of ^{133}Cs occurring in each food chain (primary producer to apex predator, the largemouth bass) estimated by the tabular model

The largest flux to bass occurs via the PELCB food chain. Due to the rapid ^{133}Cs assimilation by periphyton, this short chain results in a total flux of 2,059 mg d^{-1} on day 10 with 423 mg d^{-1} due to the flux from lake chub to largemouth bass. The relative contributions of ^{133}Cs from the three

food chains, were 76.9 % for PELCB, 22.7% for PESBGB and 0.5% for PLCLBGB, and these remain relatively constant across the declining flux during the first 90 days.

3.4. Discussion

3.4.1. Temporal behavior predicted by the tabular model

Although the temporal patterns from the tabular model inventories may be approximate and representative of the maxima levels versus the actual day of maxima that occurred during the experiment, they do demonstrate one important aspect of accuracy. This important aspect is that the successive days of maxima in the tabular model consistently increase with tropic position. For example, the days of maxima inventories for the food chain involving the periphyton, the snails, the bluegills, and bass increase in the sequence of 6, 10, 105, and 358 days. Similar patterns of increasing days to maxima occur for the other food chains in the model. Had errors in the timing of maxima occurred where earlier days of maxima occurred for consumers rather than the food sources they were consuming, this would have raised serious questions about the model's structure.

3.4.1. Fluxes predicted by the tabular model

The observation that the greatest flux from the primary producers to the apex predator largemouth bass originates from periphyton could be anticipated given the greater biomass of periphyton than that of plankton in Pond 4. However, this expectation is based on an assumption of relatively comparable levels of ^{133}Cs concentrations. If the measured concentrations of plankton were higher than those of periphyton, than the amount of Cs flux through the plankton based food chain (as estimated by the tabular model) would have been higher. In actuality, the measured concentration levels of plankton were about five times less than that of periphyton, as

can be seen in Figure 3.2. This observation highlights the need of both measures of biomass and ^{133}Cs concentrations to predict the highest flux food chain pathway.

Another expected outcome validated by the tabular model was that the flux from the periphyton through the lake chubs to bass should be greater than that for the flux from the periphyton through the snails to the bluegills to the bass because of 1) the greater mass for lake chubs than for snails and 2) the fewer number of intermediate transfers within the PELCB food chain. Although these expectations are based on the relative masses of the biotic components and the relative number of transfers before reaching the bass, they may only suggest the different relative importance of the pathways.

If the estimated abundance of *Chaoborus* larvae is an underestimation of their total mass in the pond with a corresponding underestimate of the importance of the fluxes through the PLCLBGB food chain, it would require a 45-fold increase in *Chaoborus* larvae ^{133}Cs concentrations and/or their mass to approximate the same importance as the PESBGB food chain or a 200-fold increase in the ^{133}Cs concentrations and/or the masses to approximate the same relative importance as the PELCB food chain. A more reasonable potential 10-fold error would have a small effect on the relative importance of the littoral and pelagic food webs.

3.4.2. Developing a more complete model of the movement of ^{133}Cs through the biotic components of Pond 4

As discussed in Pinder *et al*. (2011) sections 3 and 7.2, the limitations in sampling and analytical resources allowed only a small fraction of the pond's diverse biota to be studied. The current model structure (Figure 2) is largely a flow-through system where ^{133}Cs in the water is absorbed by periphyton and plankton which are subsequently consumed, with these consumers being subsequently consumed by larger consumers. For all these forms, ^{133}Cs is returned to the

water primarily by leaching and elimination which are not illustrated in Figure 3.1. Once returned to the water, the Cs may be adsorbed by the sediments before it can be absorbed by periphyton or plankton and returned to the food web. ^{133}Cs accumulation in the sediments is supported by the observation of aged ^{137}Cs being mobilized from the sediments into the water column due to displacement by the added ^{133}Cs (Pinder *et al.,* 2005).

A more complete model would include more components, or more interactions among these components, or both. Potential additional components relevant to Pond 4 could include: 1) the benthic forms, such as crayfish; 2) small minnow-like fish, such as mosquito fish (*Gambusia affinus*) which feed upon plankton and insect larvae (*fishbase.org*); and 3) catfish (*e.g.*, *Ameiurus nebulosus*) which feeds on benthic insects and crustaceans (*fishbase.org*). The addition of catfish and crayfish, which are also potential scavengers of deceased animal forms, may include addition of a pathway by which ^{133}Cs would be recycled through the biota without having to pass through the water with a potential subsequent loss to the sediments. Some additional interactions that could be added to the model are: 1) the relatively limited feeding of bluegills on periphyton or macrophytes (Kitchell and Windell, 1970); 2) the feeding of bluegills on mosquito fish that were feeding on zooplankton (*fishbase.org*); 3) the feeding of snails on small quantities of macrophytes (Lombardo, 2002); and 4) smaller bass also feeding on mosquito fish. Although adding these components may have increased the model's realism and accuracy, the data on the ^{133}Cs concentrations and masses of these components and their appropriate prey items were not collected during the Pond 4 study due to limited resources.

Additionally, a level of uncertainty in the model results exists for the biota, with the exception of the fish, because the modeled periods of time extend past 1) the 75-day period of the most rapid declines in water concentrations, 2) the 90 day periods of most frequent sampling

for all biota. They also extend into and through the autumn and winter periods during which levels of biological activity decline with the declining water temperatures. Water temperatures ranged from approximately 30 ºC on day 1 to 5 ºC on day 180 with a return to > 30 ºC on day 360 (Figure 3 in Pinder *et al*., 2010). For the relatively short-lived forms of plankton and *Chaoborus* larvae, these periods may also extend into populations composed largely of individuals that were not exposed to the initially large concentrations immediately following the release.

The present model structure does not permit an assessment of the effects of changes in temperatures and population structures on the assimilation and release of ^{133}Cs. However, a principal objective of this study is to develop a subsequent rate-based kinetic model for the movement of ^{133}Cs through this system. In such a model, the effects of temperatures may be investigated by using temperature dependent rates for u and k in simulations of the responses of the biota to the release to determine if temperature driven changes in these parameters modify the ability of the model to accurately simulate the observed temporal patterns for concentrations and inventories.

3.5. Conclusions and Further Considerations

The greater importance of the littoral community (*i.e,.* submerged macrophytes and periphyton) in controlling the transport and fate of the added ^{133}Cs is not surprising given their greater masses and larger spatial extents, but this analysis allows a quantification of their relative importance. Although the submerged macrophytes do not appear to contribute ^{133}Cs directly to the pond's food web, their presence has two major impacts on the movement of ^{133}Cs through the food web. First, they provide a structural support and surface area for the periphyton, which at least in Pond 4, are the major vector by which ^{133}Cs is moved from the water to the food web

biota. Second, the rapid absorption and subsequent slower release of ^{133}Cs prolongs the availability of ^{133}Cs to the other biota. If the surface area of the sediments occupied by the submerged macrophytes was directly exposed to the water column, there may have been a much more rapid adsorption and partial sequestration of the ^{133}Cs into the sediments with a corresponding reduced availability of ^{133}Cs to the biota. This factor may be of importance in designing and managing ponds to sequester Cs from aquatic releases.

The lesser importance of the planktonic community (*i.e.,* plankton and *Chaoborus* larvae) is not unexpected but the documentation of a 50-fold reduction in absorption and transfer of the ^{133}Cs to the apex predator compared to the periphyton quantifies their relative importance. This degree of difference between the two communities suggests that for them to be of similar importance would require a much larger water body with steep shorelines to 1) provide space for the planktonic community and 2) limit the space available for the littoral community.

Subsequent analyses in the Pond 4 study will utilize these inventories and fluxes in the biotic components with the inventories and fluxes among the abiotic components of water and sediments to develop, test, and employ a rate-based ordinary differential equation kinetic model for the pond's abiotic and biotic components. This rate-based kinetic model is developed for reverse engineering scenarios such as 1) testing the effects of varying temperature regimes, 2) the effects of increases or decreases in biota biomass (that may reflect gradients of oligotrophic to eutrophic lake conditions) or 3) potential remedial actions to reduce the accumulation of radioactive Cs isotopes in pathways leading to human food sources.

CHAPTER FOUR. INVENTORY BASED KINETIC MODEL OF CESIUM MOVEMENT IN POND 4*

4.1. Introduction and objectives

The objectives of the deterministic kinetic model are as follows:

1) Develop a deterministic model of the Pond 4 proposed ecosystem's inventories
2) Evaluate how close this deterministic model can match the inventory curves described in the previous chapter of this dissertation
3) Perform selected model tests to evaluate behavior

The purpose of the ODE kinetic model is to employ the tabular model's time series results of ^{133}Cs inventories and fluxes, as detailed in Chapter 3 of this dissertation, to develop a rate-based dynamic kinetic model of the Pond 4 system. This model could be used to 1) assess how the added ^{133}Cs was redistributed and recycled among the biotic components before being largely sequestered in the pond's sediments or 2) evaluate how changes in the Cs transfers among the biotic components may affect the ultimate fate of the added ^{133}Cs for this pond's environment, along with other user determined scenarios (such scenarios are referred to as "reverse engineering" in this dissertation).

---

*Jeong, H., Miller, V.J., Johnson, T.E., Hinton, T., Pinder J.E. III, 2018b. Model-based analyses of the cesium dynamics in the small mesotrophic reservoir, Pond 4. I. II. Development of a Rate-Based Kinetic Model. Journal of Environmental Radioactivity. In Press. Note: Miller, V.J. is a primary author and the corresponding author of this manuscript.

4.2. Methods

4.2.1. ODE Kinetic Model framework

The model food web used is the same as that of the tabular model, and includes the seven key components of the biota and the water. Additionally, macrophytes, sediment, and Pond 5 are added as components, bringing the total number of biotic and physical components to 11. Recall, Pond 5 is an adjacent pond to Pond 4 (see Figure 1.1). The water component of the model is composed of three sub-components, as will be subsequently explained. Figure 4.1. illustrates the structure of the model. The blue arrows indicate transfer back to the Pond 4 water or from Pond 4 water to Pond 5 water. The black arrows indicate transfer amongst the biotic components, and the green arrows indicate transfer from the water.

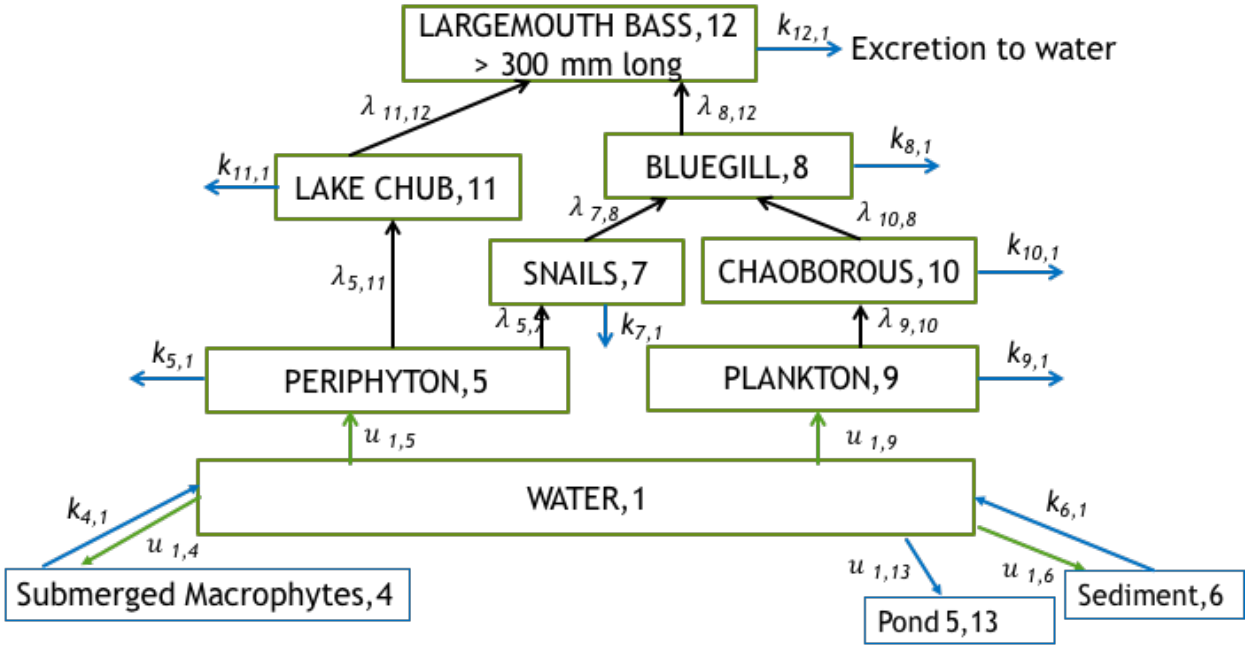

Figure 4.1. ODE Kinetic Model Structure

4.2.2. Developing a rate-based kinetic model of the Pond 4

The Pond 4 ODE kinetic model is dynamic and utilizes a compartment model framework of the aforementioned food web structure with corresponding differential equations. Unlike some aquatic contaminant models, such as those discussed in the literature review (Chapter 2) of this dissertation, this model is characterized by mass flow rather than by concentration of the contaminants, and it includes representation of multiple trophic levels within the pond ecosystem. The flow of Cs through the system is based on determining a set of transfer coefficients that provide the best fit between the data based tabular model inventories of each component and the numerical solutions to the set of differential equations.

The accuracy of this ODE kinetic model is evaluated as its ability to reproduce the temporal pattern of inventories depicted in Figures. 3.3B and 3.4A-C of Chapter 3 within a factor of two. If a sufficiently accurate model can be developed, it could also be used as a tool to test the effects of various treatments and experimental manipulations that could not be applied to the pond. Treatments and experimental manipulations could include, though not be limited to, the effect of different temperature regimes and the effectiveness of different remedial actions to reduce ^{133}Cs accumulation in pond fish used as human food. Different temperature regimes may be simulated by either 1) uniform model-wide increases or decreases in the transfer coefficients in response to increases or decreases in pond water temperatures; or 2) applying changes in transfer coefficients that reflect the measured temperature gradients and seasonal cycles following the addition (Pinder *et al.*, 2010). Similarly, the effects of potential remediation actions may also be examined by modifying those transfer coefficients that the proposed remediation activities are intended to affect, such as: 1) increased rates of sequestration in the sediments due to the application of clays into the water column (Hinton *et al.,* 2006); 2)

reductions in the rate of ^{133}Cs absorption by the biota in response to the release of K into the water column (Smith *et al.*, 2003), or 3) the relative effects of adding K on the uptake rates of ^{133}Cs versus the remobilization of ^{133}Cs from the sediments to the water column due to K displacing ^{133}Cs from adsorption sites in the sediments (Smith *et al.*, 2003).

The current model structure is largely a pass through system where ^{133}Cs in the water is absorbed by periphyton and plankton, which are subsequently consumed by first order consumers, and with these consumers being subsequently consumed by the larger second order consumers. For all these forms, ^{133}Cs is returned to the water primarily by leaching and elimination. Once returned to the water, the ^{133}Cs may be absorbed by and largely sequestered in the sediments, or again be absorbed by periphyton and plankton and returned to the food web. Although not a complete representation of the Pond 4 ecosystem, the model does contain sufficient diversity and connectivity to include both pelagic and littoral food chains.

4.2.3. The differential equations used in the ODE kinetic model

The ODE kinetic differential equations have the following form, where y_i is the inventory amount (mg) of ^{133}Cs in the component, *i* (numbering as listed in Table 3.1):

$$\frac{dy_i}{dt} = \text{uptake} - \text{loss} \qquad (4\text{-}1)$$

Uptake of ^{133}Cs is given by the appropriate uptake transfer coefficient(s) multiplied by the components which contribute to the increase in y_i, and the loss of ^{133}Cs is obtained by each of the corresponding loss transfer coefficients multiplied by y_i. The differential equations used in the kinetic model are as follows, where for clarity in these equations the transfer coefficients are separately designated as *k, u*, and λ (and illustrated above in Figure 4.1):

k – loss from compartment to water

u – uptake from water (to macrophytes (4), periphyton (5), and plankton (9); also transfer from water to sediment (6) and Pond 5 (13))

λ – transfer between biota compartments

Water, W_i (for i=1,2,3; three subcomponents as subsequently explained)

$$\frac{\partial W_i(t)}{\partial t} = k_{6i} * y_6(t) + k_{5i} * y_5(t) + k_{4i} * y_4(t) + k_{7i} * y_7(t) + k_{8i} * y_8(t) + k_{9i} * y_9(t) + k_{10i} * y_{10}(t) + k_{11i} y_{11} * (t) + k_{12i} * y_{12}(t) - (u_{i6} + u_{i5} + u_{i4}) * W_i(t) \quad (4\text{-}2)$$

Submerged Macrophytes, y_4

$$\frac{\partial y_4(t)}{\partial t} = u_{i4} * W_i(t) - k_{4i} * y_4(t) \quad (4\text{-}3)$$

Periphyton, y_5

$$\frac{\partial y_5(t)}{\partial t} = u_{51} * W_i(t) - (k_{5i} + \lambda_{511} + \lambda_{57}) y_5(t) \quad (4\text{-}4)$$

Sediment, y_6

$$\frac{\partial y_6(t)}{\partial t} = u_{i6} * W_i(t) - k_{6i} * y_6(t) \quad (4\text{-}5)$$

Snails, y_7

$$\frac{\partial y_7(t)}{\partial t} = \lambda_{57} * y_5(t) - (k_{7i} + \lambda_{78}) y_7(t) \quad (4\text{-}6)$$

Bluegill, y_8

$$\frac{\partial y_8(t)}{\partial t} = \lambda_{78} * y_7(t) - (k_{8i} + \lambda_{8\,12}) y_8(t) \quad (4\text{-}7)$$

Plankton, y_9

$$\frac{\partial y_9(t)}{\partial t} = u_{i\,9} * W_i(t) - (k_{9i} + \lambda_{9\,10}) y_9(t) \quad (4\text{-}8)$$

Chaoborus Larvae, y_{10}

$$\frac{\partial y_{10}(t)}{\partial t} = \lambda_{9\,10} * y_9(t) - (k_{10\,i} + \lambda_{10\,8}) y_{10}(t) \quad (4\text{-}9)$$

Lake Chubs, y_{11}

$$\frac{\partial y_{11}(t)}{\partial t} = \lambda_{5\,11} * y_5(t) - (k_{11i} + \lambda_{11\,12}) y_{11}(t) \quad (4\text{-}10)$$

Largemouth Bass, y_{12}

$$\frac{\partial y_{12}(t)}{\partial t} = \lambda_{11\,12} * y_{11}(t) + \lambda_{8\,12} * y_{48}(t) - k_{12i} * y_{12}(t) \quad (4\text{-}11)$$

Pond 5 Sink, y_{13}

$$\frac{\partial y_{13}(t)}{\partial t} = u_{i\,13} * W_i(t) \quad (4\text{-}12)$$

R 3.3.0 (2016-05-03) by The R Foundation for Statistical Computing was the primary computing platform used to numerically solve the differential equations with the proposed set of transfer coefficients using the package deSolve (Soetaert *et al.*, 2010) utilizing a Runge-Kutta 4 method. The subsequent paragraphs provide more detail about the parameterization of the model.

The water component has three subcomponents. These sub-components describe the dynamics of ^{133}Cs in the water column, but the data are insufficient to clearly associate the three sub-components with more precise structural aspects within the water column (*e.g.*, suspended sediments) or different sections of the water column (*i.e.*, various water depths, such as for

example the surface 0 – 1 m depths). However, the dynamics may be related to observed sudden increases of ^{133}Cs concentrations on predominantly FeMn particulates of ≥ 3 μm diameter followed by rapidly declining ^{133}Cs concentrations in these particulates in the following several days (Hinton, *unpubl*. data).

Because of the nearly negligible mass of the pond's total biota when compared to that of the water column (Table 3.1), the initially high rates of ^{133}Cs decline from each of the water subcomponents are presumed to represent transfers of ^{133}Cs from the water to the sediments. Because of the presence of naturally-occurring ^{133}Cs in the sediments underlying the 6.3-ha area where the ^{133}Cs was added, attempts to measure the accumulation of the added ^{133}Cs into these sediments were unsuccessful due to the relatively small amount of ^{133}Cs added relative to the naturally occurring abundance of ^{133}Cs contents in the sediments (Hinton, *unpubl.* data). Instead, the adsorption of ^{133}Cs to the sediments was inferred from the increased ^{137}Cs concentrations in the water column following the addition, which is presumed to result from the displacement of this previously existing ^{137}Cs contamination from the sediments due to the addition of the ^{133}Cs (Pinder et al., 2005).

All model parameters are constrained by the a_i and b_i components of Equation 3-1. The ratio of the a_i components is applied to the initial level of Cs added, giving the following initial conditions for water: W(0)1 = 1.2E6 mg; W(0)2 = 1.8E6 mg; and W(0)3 = 1.0E6 mg. The following paragraphs provide further details on the transfer coefficient development.

4.2.4. Estimating the transfer coefficients for the exchange of ^{133}Cs between the water and the sediment.

The accumulation of ^{133}Cs in the sediments, which could not be measured but only estimated as the unaccounted ^{133}Cs in the other components, was treated as a reversible process

with the rates of remobilization from the sediments to water being approximately 100× less than the rate of accumulation (Comans *et al*., 2003; Evans *et al.,* 1983). The ^{133}Cs released from the sediments to the water was, as was the case for the ^{133}Cs released from the biota, redistributed in the same proportions to the three sub-components of the water as in the original release. An initial estimate of 0.0015 d^{-1} for the transfer coefficient for the release of ^{133}Cs from the sediments to the water was estimated based on ^{133}Cs remobilization rates from limnocorral data (Hinton *et al.,* 2002; and Figure 12 in Pinder *et al.*, 2010). The magnitude of this remobilization value is comparable to that driven by formation of NH_4^+ due to anoxia in the sediments of the neighboring reservoir Pond B (Evans *et al.*, 1983) and reported by an additional study by Comans *et al*. (2003). The value was adjusted to 0.0017 d^{-1} to align with the observed ^{133}Cs inventories in the water column.

4.2.5. Estimating the transfer coefficients for the exchange of ^{133}Cs among the biotic components

Both transfers of ^{133}Cs, through the exchanges of biomass or through absorption from the water column, are computed in the model using transfer coefficients which express the fraction of the ^{133}Cs in the component being transferred to another component per unit time (*i.e*., days). All transfer coefficients, hereafter $\lambda_{i,j}$ for transfers of the ^{133}Cs inventories from the $\underline{i}^{th}$ to the j^{th} components, were of the form $0 < \lambda_{i,j} < 1$, and a three-phase process was employed to estimate these transfer coefficients.

In the first phase, the tabular model was developed containing the ^{133}Cs inventory of each component on each day through the first 550 days following the release. These ^{133}Cs inventories were computed as the product of 1) the daily ^{133}Cs concentrations estimates calculated using Equation 3-3; and 2) the estimated or extrapolated mass of that component in the pond, as described in detail in the previous chapter.

In the second phase, initial estimates of the transfer coefficients were computed as the ratio between 1) the mass of ^{133}Cs being transferred from the component; and 2) the mass of the ^{133}Cs in that component for each day from the tabular model. Although the spreadsheet computations were extended to 500 days, the initial estimates of transfer coefficients used in the kinetic model were primarily drawn within the range of the estimates over the first of 25 days. Additionally, initial estimates of appropriate transfer coefficients for the loss of ^{133}Cs from the various biota to the water by elimination by the animals or leaching from the plants were obtained from literature sources (*e.g.*, Rowan and Rasmussen, 1994; Peters and Newman, 1999; Tostowarky, 2000). To maintain consistency in the ^{133}Cs dynamics, the ^{133}Cs flux from the biota to the water was presumed to follow the same dynamics as the initially added ^{133}Cs and was distributed among the three water subcomponents in the same proportions as the initial release (*i.e.,* ratio of a_i components in Equation 2). No transfer coefficients were included in the model to account for mortality among the biotic components and the subsequent release of Cs due to decomposition as this mortality was assumed to be negligible relative to that for consumption. Fluctuations in biomass may be expected to occur for the macrophytes as the summer passes into autumn. However, monthly studies of myriophyllum biomass for August through September and October for ponds in Tennessee (Stanley et al., 1976) and Wisconsin (Adams and McCracken, 1974) suggest variations among these months in myriophyllum biomass from 1.3 to 1.75, which is within the acceptable uncertainty proposed for this model.

In the third phase, the initial estimates of transfer coefficients from either phase 2 computations or the literature were adjusted so that model results through the 500 days approximated the inventory data for Pond 4 from the tabular model. The model was built piece-wise, starting with a three component model of the water, the sediment, and the macrophytes

components since these were the components with the highest proportions of the added ^{133}Cs. In adjusting the preliminary transfer coefficients, the literature-based estimates of elimination rates were more likely to be subjected to larger adjustments than the preliminary transfer coefficients from the spreadsheet-based tabular model. The transfer coefficients were varied iteratively compartment by compartment over an approximately 10 percent range for most compartments, starting with the primary producers and then moving to higher trophic levels. The iterations were stopped when it was determined that a sufficient combination of the two aforementioned priority goals was met across all of the compartments. The transfer coefficients selected in this phase represent a consensus amongst all the members of the ODE kinetic development team for the most accurate and appropriate values, with the goal of achieving model results that were within a factor of two of the inventories when compared to the tabular model.

4.2.5. The full set of transfer coefficients.

To fully characterize the model requires estimating 62 coefficients. Forty-nine of these coefficients, termed transfer coefficients, control the exchange of ^{133}Cs among components and a further 13 coefficients, termed retention coefficients, parameterize the retention of ^{133}Cs within the components. Six of the transfer coefficients are required for the exchanges of ^{133}Cs between the sediments and the water subcomponents and are given in Table 4.1.

Table 4.1. Transfer coefficients (d^{-1}) for 1) the absorption of ^{133}Cs by sediments from the three water subcomponents, 2) remobilization of ^{133}Cs from sediments to the three water subcomponents (No. 1, No.2 and No. 3), and 3) the outflow of ^{133}Cs from the three water subcomponents in Pond 4 to Pond 5.

Pathway	Transfer Coefficients (d^{-1})		
	Absorption of ^{133}Cs from the water by the sediments		
	No. 1	No. 2	No. 3
Water to Sediment	0.454	0.0994	0.00643

	Remobilization of ^{133}Cs from the sediments to the water		
	No. 1	No. 2	No. 3
Sediment to Water	3.78×10^{-4}	9.13×10^{-4}	4.45×10^{-4}

	^{133}Cs transfer from water compartments in Pond 4 to Pond 5		
	No. 1	No. 2	No. 3
Pond 4 to Pond 5	8.59×10^{-4}	8.59×10^{-4}	8.59×10^{-4}

Three coefficients are required for the transfer of ^{133}Cs from the Pond 4 water to downstream Pond 5, but these three transfer coefficients all have the same value reflecting the primarily physical nature of the ^{133}Cs transport via water flowing from Pond 4 into Pond 5. This transfer represents a net loss of ^{133}Cs in Pond 4's water column. These flows are the result of precipitation onto Pond 4 and not due to pumping of water from the canal through Pond 4. There was no pumping of water from the canal into Pond 4 during the course of the study.

Nine coefficients are required for the transfer of ^{133}Cs from the water subcomponents to the primary producers and are given in Table 4.2:

Table 4.2. Transfer coefficients (d^{-1}) for absorption of ^{133}Cs from water by the primary producers of macrophytes, periphyton and plankton from water components 1.1, 1.2 and 1.3.

Transfer from the water subcomponents	Transfers to the Primary Producers		
	Macrophytes Component # 4	Periphyton Component # 5	Plankton Component # 9
1.1	0.221	0.0557	2.29×10^{-5}
1.2	0.04583	0.0122	5.01×10^{-6}

1.3	0.00313	7.89×10^{-4}	3.24×10^{-7}

Twenty-four coefficients are required for the transfer of ^{133}Cs from the biota to the water subcomponents through either elimination or leaching in Table 4.3; however, not all of these are independent. The transfer coefficients from the biotic component to the water are partitioned into three separate coefficients with one for each of the water subcomponents being based on the relative sizes of the subcomponents of Equation 2 (a_i values, Table 3.2). Only seven estimated transfer coefficients are required for the transfer of ^{133}Cs among the biotic components, as given in Table 4.4. The 13 retention coefficients are computed as 1 minus the sum of the transfer coefficients from that component to other components, and are given in Table 4.5. While these retention coefficients are not specifically required to solve the system of differential equations that drive the Pond 4 model, they are provided because they are a concise measure of a component's rate of turnover.

Table 4.3. Transfer coefficients (d^{-1}) from the biotic components to the water subcomponents 1.1, 1.2 and 1.3 (components illustrated in Figure 7).

Biota	Component #	Water Subcomponents		
		1.1	1.2	1.3
Macrophytes	4	0.0161	0.0390	0.0190
Periphyton	5	0.0166	0.0402	0.0196
Plankton	9	0.0293	0.0444	0.0235
Chaoborus larvae	10	0.0142	0.0342	0.0167

Snails	7	0.0337	0.0814	0.0397
Lake chubs	11	9.06×10^{-5}	2.19×10^{-4}	1.07×10^{-4}
Bluegills	8	3.78×10^{-4}	9.13×10^{-4}	4.49×10^{-4}
Largemouth bass	12	8.93×10^{-4}	2.16×10^{-3}	1.05×10^{-3}

Table 4.4. Transfer coefficients (d^{-1}) between components of the biota

From Component	Component #	To Component	Component #	Transfer Coefficient (d^{-1})
Periphyton	5	Snails	7	0.0100
Periphyton	5	Lake chubs	11	0.0185
Plankton	9	Chaoborus larvae	10	0.0884
Chaoborus larvae	10	Bluegills	8	0.0211
Snails	7	Bluegills	8	0.0407
Bluegills	8	Bass	12	1.85×10^{-3}
Lake chubs	11	Bass	12	6.47×10^{-3}

Table 4.5. The coefficients for the retention of ^{133}Cs in the Pond 4 water subcomponents, the biotic components, the sediments, and Pond 5

Component No.	Component	Retention Coefficient (d^{-1})
1.1	Water 1	0.269

1.2	Water 2	0.839
1.3	Water 3	0.989
4	Macrophytes	0.926
5	Periphyton	0.895
6	Sediments	0.998
7	Snails	0.804
8	Bluegills	0.997
9	Plankton	0.814
10	Chaoborus larvae	0.914
11	Lake chubs	0.993
12	Largemouth bass	0.996
13	Pond 5	1

4.2.6. The use of a posteriori estimation of transfer coefficients

These procedures are based on a simplified model structure with empirical transfer coefficients among the components being estimated *a posteriori* from the data; a fully-independent determination of each appropriate transfer coefficient during the Pond 4's field work that could be used to form a more completely independent representation of the pond's ecosystem was not a feasible option for the study. Due to the complexity and the efforts that would be involved in independent determinations of the numerous transfer coefficients, it may continue to remain as a non-feasible option for some time to come. It may be most appropriate to consider this model as an intermediary between a whole-lake model based on *a priori* parameter estimates and results from experimental microcosms or mesocosms. The approach here is also similar to the concept of "reverse engineering" where an existing system or device is disassembled to determine the role performed by each part in the system's functioning.

Due to the number of components and the number of transfer coefficients among these components, the transfer coefficients derived from this *a posterior* procedure may 1) not be unique (*i.e.*, as other sets of transfer coefficients may be derived from the data) and 2) may not be the most accurate (as other sets of transfer coefficients may provide a more accurate representation for some, most, or all of the transfers of ^{133}Cs among the components). However, the estimated transfer coefficients in this analysis may be useful in understanding and assessing the dynamics of ^{133}Cs in Pond 4.

Despite these limitations, the transfer coefficients serve the objective of producing a reasonable model of Pond 4 whose parameters may be modified to simulate experimental procedures that would be difficult, impractical, or impossible to implement in Pond 4 itself. Moreover, experimental procedures applied to Pond 4 itself may result in prolonged effects that could compromise the validity of the results for subsequent experimental manipulations to the pond.

4.3. Results

4.3.1. Evaluation of the transfer coefficients

All transfer coefficients given in the previous tables were scrutinized, compared to the literature sources used in the tabular model, and found to be reasonable. The sum of the biota excretion rates and loss rates due to consumption were compared to the *k* values predicted by the concentration curve fit, and were comparable. Transfer coefficients from the water to the sediments and Pond 5 were assessed for their reasonability given what was expected to occur in the pond, though extensive data for the sediments and Pond 5 are not available, as previously discussed. First, the sediment release rates are less than the adsorption rates, thus the sediments are a sink and accumulate ^{133}Cs over time as would be expected. Second, the transfers to Pond 5

are at least a factor of 100× less than the transfers of ^{133}Cs from Pond 4 waters to its sediments. Transfers of ^{133}Cs from Pond 5 to Pond 4 were not included in the model as these flows are far less likely to occur (Jeong et. al., *2018a*). The retention rates also are reasonable, with the fish having the highest retention as would be anticipated per the experimental results.

4.3.2. The predicted ^{133}Cs inventory in the biotic components

The predicted sum of the ^{133}Cs inventories in the biotic components from the ODE kinetic model is shown in Figure 4.2, where a maximum inventory of approximately 6×10^5 mg occurred on day 9. The macrophytes, whose predicted inventory on this day from the kinetic model was 5.6×10^5 mg accounted for 84 % of ^{133}Cs in the biotic inventory. The periphyton accounted for 13% of the ^{133}Cs in biotic inventory, and the combined inventory of the three fish species accounted for 2.3 % of the ^{133}Cs inventory in the biota. The total inventory in the biotic components declined rapidly to 1.4×10^5 mg of ^{133}Cs on day 90 with the macrophytes still containing the largest fraction (*i.e.*, 45 %) of the inventory. The maximum inventory in the fish species occurred on day 156 and represented 67 % of the total ^{133}Cs inventory in the biota on that day.

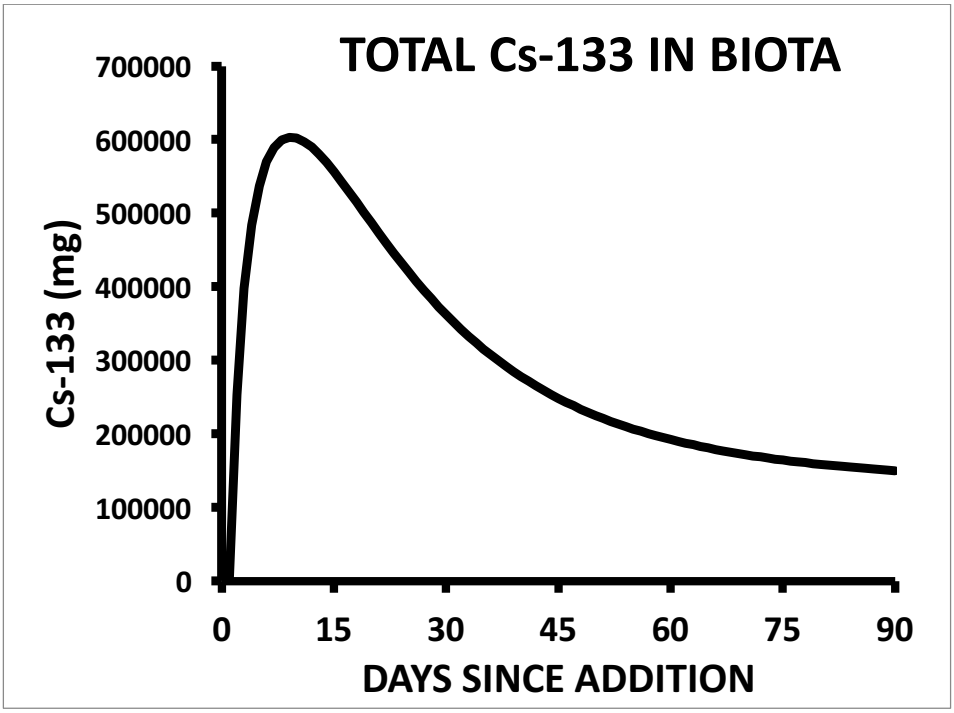

Figure 4.2. Total daily ^{133}Cs inventory in the biota as predicted by the ODE kinetic model

Graphs of the behavior of the ODE kinetic model in relation to the tabular model are given in Figure 4.3. The overall success of obtaining a fit of the ODE kinetic model to the tabular model within a factor of two can be observed in these figures. Recall that sediment and Pond 5 are not included in the tabular model due to a lack of usable concentration data and volume estimates, so comparisons of the predicted inventory results in these compartments to data based values are not possible.

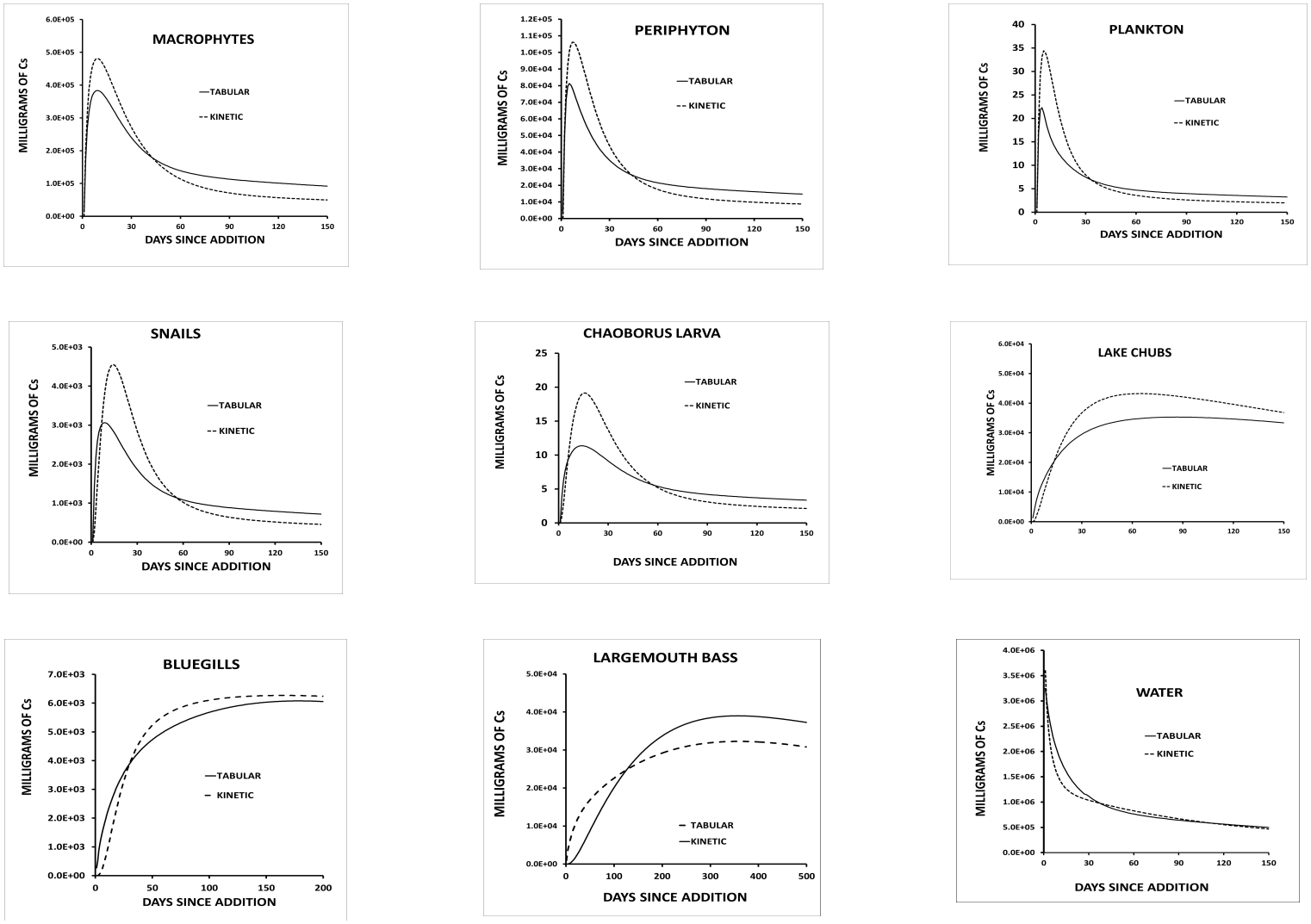

Figure 4.3. Results of ODE kinetic model for ^{133}Cs inventories in the biotic components compared to the tabular model

4.3.4. Assessments of the accuracy of the kinetic model for estimating the ^{133}Cs inventories

The initial tests of the model accuracy involved an analysis of the ratio of the inventories computed by the kinetic model to those inventories computed using the spreadsheet-based tabular model which is a smoothed representation of the observed dynamics of the ^{133}Cs added to Pond 4. Ratios of the ODE kinetic model output to the tabular model output were computed on a daily basis from days one through 500. Although most of the measurements of ^{133}Cs concentrations in the pond's biota were obtained during the first 90 days following the addition, the model was extended through as much as 500 days to determine 1) whether or not the model reached a steady state, and if so, what were the relative ^{133}Cs inventories among components at this steady state; 2) whether the model continued the patterns of declining concentrations and inventories in all components; or 3) whether the model displayed any major anomalies in behavior or accuracy when compared to the tabular model.

The median values of the ratios of the ^{133}Cs inventory in each of the biotic components for the kinetic model to that for the tabular model at each day of the first 90 days are illustrated in Figure 4.4. The median ratio for the period of day four through day 90 suggests an accuracy of approximately two (*i.e.*, ratios from ≥ 0.5 to ≤ 2). The median of these ratios over this time period is 0.872. From day seven through day 37, the ratios are greater than or equal to one, with a maximum ratio of 1.23 on days 19 through 23. The initial ratios of < 0.5, which occur before day five, could be attributed to the kinetic model being initially set to zero mg whereas the initial inventories in the tabular model ranged from 0.1 mg for Chaoborus larvae to 4500 mg for periphyton. From day seven to 39 the ratios are greater than one. The ratio on day 90 is 0.52.

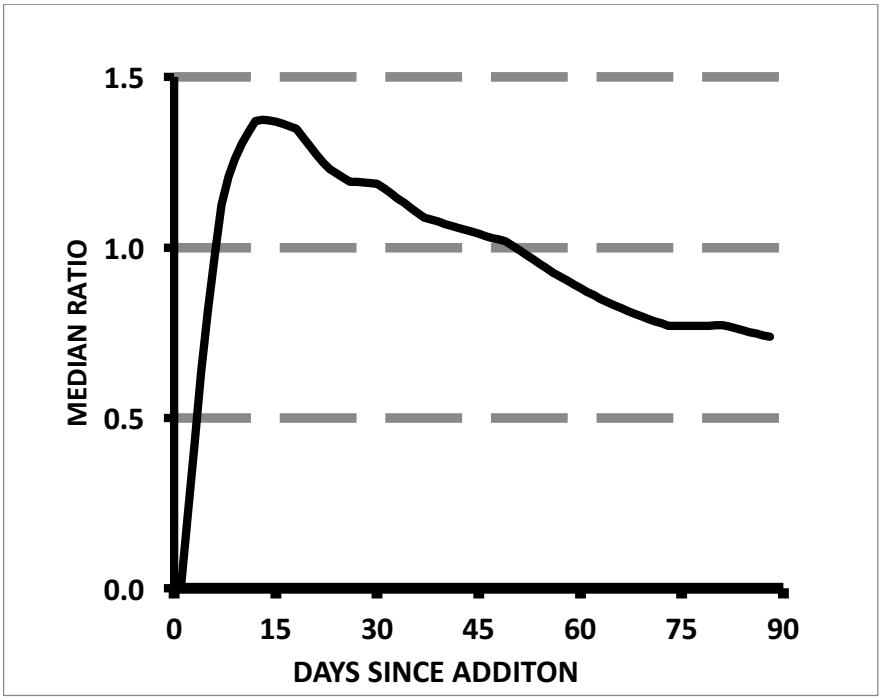

Figure 4.4. Median Ratio of Kinetic to Tabular Model

The accuracy of the ^{133}Cs inventories of the individual components of the model was also assessed. The median and the first and third quartiles of the ratios of the water and biological component inventories in the kinetic model to those of the tabular model over the first 90 and 150 days were computed and are summarized in Table 4.6:

Table 4.6. The first quartile, median and third quartile ratios of the inventories in water and biotic components from the kinetic model to those from the tabular model over the initial 90 and 150 days. Note that the three water subcomponents are combined into one for this analysis.

		Ratios				
Component	Days	First Quartile	Median	Third Quartile	Maximum	Mean
Water	90	0.980	1.241	1.285	1.303	1.140

	150	1.073	1.165	1.258	1.303	1.140
Submerged	90	0.745	0.959	1.169	1.254	0.954
Vegetation	150	0.569	0.693	1.038	1.254	0.800
Periphyton	90	0.749	0.961	1.284	1.506	1.019
	150	0.613	0.707	1.056	1.506	0.856
Snails	90	0.819	1.049	1.434	1.677	1.117
	150	0.658	0.767	1.165	1.677	0.934
Bluegills	90	1.434	1.049	0.907	1.110	0.931
	150	1.040	1.063	1.094	1.110	0.981
Plankton	90	0.724	0.850	1.192	1.861	1.007
	150	0.627	0.695	0.919	1.861	0.855
Chaoborus	90	0.846	1.078	1.449	1.697	1.141
Larvae	150	0.666	0.790	1.201	1.697	0.951
Lake Chubs	90	1.193	1.228	1.255	1.266	1.144
	150	1.128	1.181	1.238	1.266	1.144
Largemouth	90	0.222	0.484	0.690	0.841	0.453
Bass	150	0.613	0.707	1.056	1.071	0.662

These median ratios for both 90 and 150 day time spans, as given in Table 4.6, are within a factor of two (*i.e.*, ≥ 0.5 to ≤ 2) except for the largemouth bass where the inventories predicted by the kinetic model are initially much smaller than those in the tabular model. The discrepancies between the models may reflect the absence of food sources for the bass in the

kinetic model which were present in the pond. The median ratio for all eight biotic components through day 90 is 0.854. It is important to note that over-prediction of the inventories by the model can be considered conservative because it overestimates potential doses from radioactive isotopes of Cs. The maximum ratios predicted by the model are greater than those observed in the pond for all components except for the snails, where the differences are trivial.

4.3.6. Assessments of the accuracy of the kinetic model for the times to maximum inventories for the individual components

For the purpose of the kinetic model, it is important that 1) the predicted inventories are in agreement with those in the tabular model; and 2) that the temporal pattern of these inventories, expressed here as the time to maximum inventories, are also in agreement. The temporal patterns of each component compared to the observed patterns from the tabular model can be seen in Figure 4.3. Additionally, the days to maximum inventories between the kinetic and tabular models are compared in Table 4.7.

Table 4.7. The days to maximum inventories for the biotic components in the kinetic and tabular models and their ratios (kinetic/tabular).

Component	Number	Days to Maximum Inventories		Ratio
		Kinetic	Tabular	
Macrophytes	4	8	8	1
Periphyton	5	6	4	1.4
Snails	7	13	8	0.62
Bluegills	8	163	177	0.92
Plankton	9	4	3	1.25
Chaoborus larvae	10	15	13	0.87

Lake chubs	11	64	85	0.75[1]
Largemouth bass	12	356	356	1

[1]These smaller ratios may reflect the longer times to maxima as much as the difference in days

With the exception of the fish species, the differences in days are ≤ 2 days. For all of the components, the ratios of the days to maxima for the kinetic model to those for the tabular model are within a factor of two. The difference between the days of maxima for the largemouth bass is only 13 days. There are, however, greater absolute differences in days of maxima for the lake chub and the bluegill, 25 and 72 days, respectively. While the maxima for all the biota in the tabular model are subject to uncertainty from lack of sampling on multiple days around when peak values occurred, this effect may be magnified for the fish compartments given that they reach maximum levels over a longer time span.

4.3.8. Tests of the kinetics' model in response to altered inputs and transfer coefficients

Although the structure of a model may produce reasonably accurate results, or at least informative results, the use of the model to extrapolate to altered conditions requires further testing and evaluation. If the model fails to produce reasonable sets of behavior under simple test conditions, its predictions or analyses of behavior for more complex scenarios may be unreliable, and predictions from the model and extrapolations from its internal model behavior to the actual system may also be unreliable. Several tests of the behavior of the kinetic model were performed, and these tests and their results are described and evaluated in the following sections.

4.3.8.1. Responses to simulated additions of ^{133}Cs that were 0.25, 0.5, 1.5, and 2 times that in the kinetic model.

The model demonstrates linear responses in both the biotic and the physical components with the inventories through the first 150 days following the addition of 0.25, 0.5, 1.5, and 2 times that of the original 3.6 kg of ^{133}Cs. As can be seen in Tables 4.8 and 4.9, each component's inventories for either 90 or 150 days demonstrate that the increasing progression of inventories occurred in the same 1:2:4:6:8 progression of ratios as the simulated amounts of ^{133}Cs released into the pond model.

Table 4.8. The results for the water, sediment, and total biota from varied input amounts of 0.25, 0.5, 1.5, and 2 times the initial amount, compared to the original 3.6 kg addition amount on day 150 (multiplication factor of 1).

Input Amount (multiplication factor)	Water (g)	Sediment (g)	Total Biota (g)
0.25	114	727	58
0.5	229	1,454	117
1	466	2,895	239
1.5	686	4,362	352
2	914	5,816	470

Table 4.9. The results of the kinetic model with 0.25, 0.5, 1.5, and 2 times the initial amount, compared to the original 3.6 kg addition amount on day 150 (multiplication factor of 1) for the periphyton, snail, bluegill, and largemouth bass components of the model on day 90.

Input Amount (multiplication factor)	Periphyton (g)	Snails (g)	Bluegill (g)	Largemouth Bass (g)
0.25	2.89	0.156	1.52	4.65
0.5	5.78	0.312	3.04	9.29

1	11.7	0.634	6.03	18.3
1.5	17.3	0.935	9.13	27.9
2	23.1	1.25	12.2	37.2

4.3.8.2. Responses to rates of ^{133}Cs remobilization from the sediments that were 0.5, 2, 4 and 10 times that in the model.

For the transfer coefficients of ^{133}Cs remobilization from the sediments that were 0.5, 2, 4, and 10 times that in the model, the model's responses of the biotic components are not linear, but rather show a reasonably expected pattern of greater increases for primary producers, which absorb the ^{133}Cs released from the water, and smaller relative levels of increase with higher trophic levels due to the losses of ^{133}Cs back to water from the intermediate trophic levels. The ratios of the periphyton, bluegills, and largemouth bass inventories in the altered remobilization models to those in the basic model are given in Table 4.10. The increased remobilization rates from the sediments also result in 1) increased ^{133}Cs inventories in the Pond 4 water; 2) increased transfers of ^{133}Cs to Pond 5; and 3) reduced ^{133}Cs inventories in the sediments. The ratios illustrating these behaviors on select days are also given in Table 4.10:

Table 4.10. The results of simulations of varied resuspension for the water, periphyton, snail, bluegill, and largemouth bass components of the model.

Remobilization rate multiplication factor	Water Day 150	Sediment Day 150	Pond 5 Day 150	Periphyton Day 90	Bluegill Day 90	Bass Day 90
0.5	0.827	1.04	0.917	0.819	0.978	0.999
2	1.26	0.943	1.06	1.29	1.07	1.05
4	1.75	0.836	1.22	1.85	1.18	1.12

10	2.79	0.610	1.60	3.09	1.45	1.28

4.3.8.3. Responses to transfer coefficients from water to periphyton and water to plankton that are 0.5, 0.25, 0.01 times those in the model.

These declining rates simulate the possible results of increasing K concentrations in the pond water. The responses of the inventories in the primary producers to these rates are linear with inventories at day 90 that are approximately all 0.4, 0.2, and 0.08 the unmodified amounts, respectively, for rates that are 0.5, 0.25, and 0.01 of the original rates. Because the periphyton and plankton are the only pathways of ^{133}Cs transfer from the water to the biota in the model, overall, the same reductions occur in the inventories for the first and second order consumers. The reductions in the fish are slightly different, but follow the same trend. For example, the corresponding lake chub values at day 90 are 0.52, 0.27, and 0.11. Reductions of inventories to 0.54, 0.29 and 0.18 of the original values occur for largemouth bass on day 90 and remain similar to these values for subsequent time steps.

The reduced uptake of ^{133}Cs by plankton and periphyton results in increased inventories in the water that is rapidly sequestered by the sediment. The proportional increases in the Pond 4 sediments peak within the first 10 days for each scenario at values of 1.24, 1.31, and 1.36 and on day 150 are 1.03, 1.04, and 1.05. This increased sequestration by the sediments results in a decrease in the ^{133}Cs in Pond 4 water on day 150. The proportional decreases in inventories in Pond 4 water at day 150 for the reduced rates of uptake are 0.988, 0.975, and 0.964.

4.3.8.4. Responses due to loss of ^{133}Cs from the water column due to greater rates of water flow through the system into Pond 5 with ^{133}Cs washout rates of 0.01, 0.05 and 0.1 d^{-1}.

Rather than a linear or simple response to these loss rates, the responses of the inventories of ^{133}Cs in the biota are related more to trophic levels and elimination rates, and the importance of trophic levels and elimination rates increases with increasing loss rates. After 150 days at a loss rate of ^{133}Cs to Pond 5 of 0.01 d^{-1}, the inventories in the water, the primary producers, and snails and Chaoborus larvae are < 60% of those where there was no loss of ^{133}Cs from the pond whereas the inventories in the fish species are > 80% of those where no loss occurred. After 150 days at a loss rate of 0.1 d^{-1}, the inventories in the water, the primary producers, and snails and Chaoborus larvae are < 0.25 of those where no loss occurred whereas the inventories in the fish species are > 0.6 of those where no loss occurred. These results are: 1) consistent with those biotic components with lower turnover rates retaining a greater fraction of the pond's ^{133}Cs inventory; and 2) cannot be considered as an anomalous or erroneous property of the model. After 150 days at a loss rate of 0.01 d^{-1}, the sediments retain 0.86 of their inventory. At a loss rate of 0.1 d^{-1}, the sediments retain 0.47 of their inventory. These reductions in inventories with increasing through flows of water are consistent with the observations of Smith et al. (1999) for European lakes following the Chernobyl releases. The reductions in sediment inventories also reduce the flux of ^{133}Cs from the sediments to the water due to remobilization which further reduces the uptake of ^{133}Cs by periphyton and plankton and further contributes to the reduced inventories in the biota.

4.3.8.5. Responses of the predicted ^{133}Cs content of model compartments in response to independently, random resampling of transfer coefficients.

Two resampling exercises were conducted to evaluate the effect of possible uncertainties in parameter values on the model outputs. The resampling involved all 49 transfer components in the model. Each exercise used independent random sampling from uniform distributions of either $\pm$ 10% or $\pm$ 20 % for each of the transfer coefficients. Both involved 5,000 replicates for each of the $\pm$ 10 % and $\pm$ 20 % ranges. The medians of the ratios of these randomized results to those in the deterministic model for water-3, periphyton, lake chub, and largemouth bass compartments on days 90, 150, and 300 are summarized in Table 4.11. The results for these compartments are presented because the greatest flux of ^{133}Cs from the water to the bass flows through this food chain in the model.

Table 4.11. The results of random resampling of transfer coefficients where all transfer coefficients were resampled from either $\pm$ 10 % or $\pm$ 20 % uniform distributions centered on the model's transfer coefficients.

Compartment	Days Since Spike	Median Ratios of Inventories	
		10% Resampling	20% Resampling
Water 3	90	0.9722	0.9743
	150	0.9782	0.9804
	300	0.9924	0.9950
Periphyton	90	0.9858	0.9920
	150	0.9905	0.9967
	300	0.9996	1.0061
Lake Chubs	90	1.0040	1.0048
	150	0.9995	1.0018

	300	0.9999	1.0021
Largemouth Bass	90	1.0119	1.0057
	150	1.0060	1.0010
	300	1.0006	0.9950

The ranges of the median ratios among the compartments for the ± 10% and ± 20% resampling are all close to one. The first and third quartile of these ratios are within approximately 8% of the median values for the ± 10% resampling and within approximately 15% of the median values for the ± 20% resampling. The minimum and maximum ratios across all the compartments in all of the 5,000 randomizations are all within a factor of two for the ± 10% resampling, with a minimum of 0.7 and maximum of 1.7. The ratios from the ± 20% resampling had a minimum of 0.5 and a maximum of 2.3. These resampling results suggest that there is no obvious evidence of hidden instabilities in the model's structure or estimated transfer coefficients.

These ratios, and their lack of evidence of any instabilities, may be anticipated for a simple model such as that for Pond 4 where 1) the flows are mostly one-directional (*i.e.*, from the water through the biota to the water); 2) there are no direct, two-dimensional feedbacks between biota; and 3) where the computation of flows do not involve non-linear relationships between the properties of the components. Similar resampling results occur for the sediments.

4.4. Discussion

4.4.1. A general assessment of the accuracy of the kinetic model.

In some cases, a model may be sufficiently accurate so that its quantitative predictions may be directly applied to, and incorporated into, the parent system being modeled. Alternatively, the model's accuracy, although not sufficient to produce quantitative predictions, may be sufficiently accurate to produce qualitative predictions of the relative responses of the parent system. However, in most cases a model's predicted responses to altered initial values and transfer coefficients may be best evaluated by comparing the altered responses to the model's baseline behavior. Such comparisons can project the possible directions and the possible relative magnitudes of the responses at different places within the model, and characterize the relative timings of periods of increase, time of maxima and period of decline. That is, the model's responses to perturbations should be evaluated as relative (*e.g.*, % change) rather than absolute amounts of change. Depending on the level of accuracy desired, the kinetic model for Pond 4 may not be sufficiently accurate for its predictions to be used for quantitative purposes but may be sufficiently accurate to predict relative responses in inventories and the sequences of maximum inventories among the biotic components.

When evaluating and discussing the accuracy of the kinetic model in simulating the observed ^{133}Cs dynamics in Pond 4, a margin of error must be expected and accepted due to the simplification of the food web from the numerous species in the pond to the eight biotic components in the model (*i.e.*, macrophytes, plankton, periphyton, macrophytes, Chaoborus larvae, snails, bluegills, lake chubs, and largemouth bass). Overall, uncertainties may be due to 1) inaccurately measured values for the ^{133}Cs inventories in biotic components; 2) reasonably

accurate inventories but inaccurate representations of temporal dynamics; or 3) incorrect characterization of the model framework.

Although the number and diversity of the measured biotic components sampled and measured in Pond 4 is limited, the quantity of components (along with the water) is adequate to form a simplified model of the food web dynamics for ^{133}Cs of Pond 4, as illustrated in Figure 4.1. A more complete model would include additional components, more linkages among components, or more complex relationships (*i.e.*, nonlinear) between components. Additional components could include crayfish, clams, small minnow-like fish such as mosquito fish (*Gambusia affinus*) which feed upon plankton and insect larvae (*fishbase.org*), and catfish (*Ameiurus nebulosus*) which feed on benthic insects and crustaceans (*fishbase.org*). Additional interactions could include 1) the relatively limited feeding of bluegills on periphyton or macrophytes (Kitchell and Windell, 1970); 2) the feeding of bluegills on mosquito fish that were feeding on zooplankton (*fishbase.org*); 3) the feeding of snails on small quantities of macrophytes (Lombardo, 2002); and 4) smaller bass also feeding on mosquito fish. Although adding these components may have increased the model's realism, the data on the ^{133}Cs concentrations and masses of these components and their appropriate prey items were not collected during the Pond 4 study due to limited resources.

4.4.2. Summary of tests.

These tests performed on the model, although simplistic, produced results that aligned with those that might be expected for similar, physical manipulations of Pond 4. Moreover, they did provide relative estimates of the differing effects of flow from Pond 4 to Pond 5 on lower and upper trophic levels. These estimates could differ from those made without this representation, or at least a similar quantitative approach, of the pond's physical and biological components and

their biomass proportions. Additionally, the tests of changing remobilization rates from the sediments suggested an interesting result that the corresponding output is not linear. This test could be made more robust to evaluate the reverse engineering scenario of remediation activities.

4.4.3. Potential application of the model to evaluate proposed remediation activities.

Several procedures have been suggested or implemented to remediate ^{137}Cs contamination in lakes and ponds. These have included: 1) the addition of K to the water column; 2) the addition of lime to the water column; and 3) the addition of illite clays to the water.

The release of K-containing salts into the water column is designed to reduce the uptake of ^{134}Cs and ^{137}Cs by the primary producers. The observation that the bioavailability of ^{133}Cs is reduced by greater concentrations of K in the water column has been documented by comparing the concentration ratios of ^{133}Cs in biota to that in the water across a variety of natural and man-made water bodies (Smith *et al*., 2002). However, the addition of K to the water column has the potential to also increase the ^{133}Cs concentration in the water column due to an increased remobilization of ^{133}Cs from the sediments which occurs due to K displacing ^{133}Cs on sediment bonding sites. Smith et al. (2003) observed an approximate 3-fold increase in the ^{137}Cs concentrations in Lake Svyatoe following a 10-fold increase in the lake's K concentration and commented that the ^{137}Cs increase was "an unavoidable consequence of a competitor ion."

Another approach, the release of illite clay, is designed to decrease the ^{134}Cs or ^{137}Cs bioavailability by promoting greater sequestration in the sediments. Illite clay is a complex 3-layered clay minerals. Hinton et al. (2006) applied 27 kg of illite to limnocorrals containing 2.5 m^3 of water and observed a 90% reduction in the ^{137}Cs concentration in the water and a 75 % reduction in the ^{137}Cs uptake by the floating-leaved macrophyte duckweed (*Lemna gibba*).

However, these reductions required covering the sediments with a 25-mm thick layer of illite. A third example of remediation efforts is Hakanson and Andersson's (1992) report on the application of lime in various forms in numerous Swedish lakes with variable results on the accumulation of ^{137}Cs in fish.

4.4.4. Modifying the Pond 4 model to test remediation procedures

Although it may be possible to augment and modify the Pond 4 model in attempts to simulate these previous remediation tests, these modifications have the potential to be extensive. There would also be the problem of finding appropriate estimates of the transfer coefficients for the particular remediation procedure (*e.g.*, such as the release rate of ^{133}Cs from the sediments in response to K additions to the water column). An alternative approach to evaluating remedial procedures that requires less parameter estimation and utilizes the existing structure and behavior of the Pond 4 model may be to evaluate the relative level of remediation achieved compared to initial levels following the application of procedures with varying effectiveness at varying times since the addition of ^{133}Cs into the water. An example of this would be to compare the relative biotic response between two sets of simulations where: 1) the remobilization of ^{133}Cs from the sediments is decreased by a given set of factors on day 10, and 2) the remobilization is decreased by the same factors on day 20.

Rather than attempting to model the details of specific experimental procedures, a simpler and perhaps more general procedure is to assume various levels of reduction in ^{133}Cs uptake rates by primary producers, or various levels of reduction in the ^{133}Cs concentration in the water, that could be inserted into the model at various times following the ^{133}Cs addition. Monitoring these reductions for some reasonable time would suggest the degree of remediation needed to produce a given effect as a function of the time since the addition. It may be expected

that the degree of remediation required would need to be increased as time passes post-^{133}Cs-addition, due to the rapid initial incorporation of ^{133}Cs into the biotic components.

Although changes in the concentrations of ^{133}Cs in the water or uptake rates of ^{133}Cs by primary producers from any remediation procedure would likely affect the ^{133}Cs dynamics in a number of the biotic components, the interpretation of these remediation effects maybe mostly concerned with their effects on the largemouth bass as this species is the apex predator in the pond and is the most likely to be the biotic component that would be involved in the human diet. However, as the data from the Pond 4 experiment and the model suggest, much of the maximum accumulation in the bass occurred well after the initial release and was due to the delay required for ^{133}Cs-bearing prey items to become contaminated and enter the bass food web. Moreover, some of these biota could not be included in the model due to the lack of data on their rates of accumulating ^{133}Cs or their biomass in the pond. Because of this, the relationship between delay in application and effectiveness may vary among different biota that might be targeted for the remediation. This suggests that instead of the bass, the lake chub, bluegill, or other biota consumed by the bass (whose delay is less pronounced than the bass) may be better forecasters of the remediation efficacy.

4.5. Conclusion

The kinetic model demonstrated that it is possible to build and parameterize a compartment model that behaves similarly to the responses indicated by the data of the Pond 4 ^{133}Cs addition experiment. Overall, the ratios of kinetic to tabular model days to peak inventory amounts indicated agreement within a factor of 2 or less. The median of the ratios of kinetic to tabular inventory amounts of the first 90 days also indicate that the kinetic model is comparable to that of the tabular within a factor of 2 or less. As may be expected, the model response across

all the biota is not as good over a longer span of time; however, the model response of the fish components provides a better fit to the tabular data in latter time periods. In general, it is felt that the model provides a realistic enough simulation of the Pond 4 dynamics to be useful in modeling simulations of different pond conditions. The tests done so far illustrate that the model behaves as would be expected under relatively simple simulated conditions.

Subsequent use of this model, or other models of a similar framework, could include a more in depth set of simulations evaluating different scenarios by altering the transfer coefficients. Additionally, the effect of time varying transfer coefficients could be evaluated in a theoretical and relative sense by how much the result varies from the original kinetic model, or the effect could be evaluated in how time varying transfer coefficient model results compare to the data from the experiment. The effectiveness of the latter approach may be difficult to characterize, particularly for the fish components that have a large degree of variability in the data.

The modeling on the basis of inventories also allows for a different approach to stochastically assessing this system. The current kinetic approach is a mathematical model utilizing continuous ordinary differential equations that results in a deterministic value. In reality, the processes in the pond involve discrete movements of the individual atoms of the released radionuclide. These movements are random and generally occur with low probabilities, as the transfer coefficient estimates given in this paper illustrate. The result is stochastic in that no two simulations of individual atoms would result in 1) the same distributions of atoms among the components or 2) the same fluxes of atoms along pathways through the system. Such an approach would provide an estimate of the intrinsic variability for a multi-path system such as Pond 4.

CHAPTER FIVE. USE OF DISCRETE TIME MARKOV CHAINS AS AN ALTERNATIVE METHOD TO ORDINARY DIFFERENTIAL EQUATIONS IN MODELING DYNAMIC CS-133 BEHAVIOR IN POND 4*

5.1. Introduction and objectives

Multiple methods have been developed in an attempt to model, and often simplify, the short term and long term behavior of radionuclides through aquatic lake and pond food webs (Higley and Bytwerk, 2007; Monte *et al*. 2003). A common method is the ordinary differential equation (ODE) compartment model, which has been used in ecosystems modelling for several decades (Whicker 1982, Higley and Bytwerk, 2007). Often, compartment models are applied as a deterministic method, though scientific literature support for stochastic ecosystem models has also existed for several decades (Matis, 1979). A reason for the enduring popularity of deterministic models may be due to the simplicity of their application, and may also be a result of computing power being limited in the past compared to what is currently available for simulation studies. The current chapter compares Markov chain based stochastic simulation and deterministic methods for kinetic modeling of radionuclides in an aquatic ecosystem to the previously developed ODE kinetic model.

The experimental addition of radionuclides or stable analogs in a field lacustrine

---

*Miller, V.J, and Johnson, T.E., 2018. Use of Discrete Time Markov Chains as an Alternative Method to Ordinary Differential Equations in Modeling Dynamic Cs-133 Behavior in Pond 4. Pending submission to Journal of Health Physics

environment provides a unique opportunity to study the movement of the added element through an aquatic system. In the United States, these field experiments were more prevalent in the past century, with the regulatory hurdles for approval increasing in the latter part of the century. The Pond 4 addition study is one of the most recent and extensive of such studies. Details regarding Pond 4 and the addition experiment are provided in chapter one of this dissertation.

The ODE kinetic model developed in chapter four of this dissertation resulted in a set of coefficients that express the fraction of ^{133}Cs mass transferred or retained each day in each compartment. Instead of a fractional description, these coefficients can be interpreted as the probability of ^{133}Cs movement or retention over a day. This probabilistic viewpoint promotes the use of Markov chain theory in place of the former differential equation based approach for dynamic modeling. The use of Markov chain theory allows for both a deterministic approach and a stochastic simulation approach to evaluate the ^{133}Cs movement.

5.1.1. Overview of Markov chain modeling

Markov chain models have a large range of uses across multiple disciplines. A traditional and straight forward example of a Markov chain that is cited in many introductory texts is the "drunkards walk" wherein the drunk individual may randomly step left (L) or right (R), at certain probabilities. A Markov chain simulated from these probabilities for 8 time steps could be "L, L, L, R, R, L, R, L." More scientifically, Markov chains have been utilized to model the migration of shrimp between different areas of a lake (Grant *et al.,* 1991), the dynamics of pharmaceuticals in waste (Snip *et al.,* 2014), and the foodborne illness risk for humans in food supply chains (Teasley *et al.*, 2016).

While there has been limited utilization of Markov chains in radioecology and radiation protection when compared to many other disciplines, there are some published applications. An

example from the field of radiation protection is the use of Markov chain theory for calculations regarding the buildup and decay of radon progeny (Gaul and Underhill, 2001). Within radioecology, Cuculeanu *et al.*(2002) used a Markov chain model to investigate the space and time structure of a concentration field of tritium routinely released from a nuclear power plant. A second radioecology example is the use of a Markov process to evaluate Cs fixation to marine sediments (Boreetzen and Salbu, 2002). Both of these examples were deterministic applications of Markov chain models, versus a stochastic simulation.

An example in ecology of a Markov chain based stochastic simulation model is the assessment of forest coverage over time. In this simulation, four ecological roles can be used to characterize tree species behavior: 1) shade-intolerant trees that need and create a gap in the forest coverage, and grow to a large size; 2) shade-tolerant trees that create a gap and grow to a large size, but do not need a gap to grow; 3) shade-intolerant trees that need a gap but do not create a gap, and do not grow to a large size; and 4) shade tolerant trees that do not create a gap and do not need a gap, and grow to a smaller size. The likeliness that a tree will transition between these different states is characterized by a Markov transition probability matrix. Use of random numbers can drive a simulation that illustrates how the system becomes a steady state within 10 year of simulation time (Acevedo, 2004). Another example in ecology is use of a Markov chain model simulation of disease transmission in plants of the aphid-transmitted barley yellow dwarf virus (McElhany *et al.,* 1995).

Markov simulation can also be considered a type of Monte Carlo simulation due to use of random numbers, but the term Markov simulation will be used in this dissertation to avoid any confusion with Markov Chain Monte Carlo, a commonly used numerical approximation tool (Kalos, 2008). The Pond 4 Markov simulation model is a natural stochastic simulation versus a

numerical method for analytical calculation. This approach is also fundamentally different than numerical methods such as Runge Kutta 4 that are used in solving the ordinary differential equation models of complex compartment models, and was used in the ODE kinetic model of Pond 4 (Jeong, *et al., in press* 2018b*)*. However, the Markov simulation is a stochastic method that provides a solution of ^{133}Cs inventory comparable to the ODE kinetic model. As Kalos and Whitlock state in *Monte Carlo Methods*, the differentiation between precise Monte Carlo classifications is "often impossible to maintain…the same techniques directly yield both powerful and expressive simulation, and powerful and efficient numerical methods for a wide class of problems" (Kalos, 2008).

5.1.2. Objectives

In this Chapter, Markov chain methodology is proposed as a useful tool for modeling the dynamic movement of ^{133}Cs, and a potential alternative to the traditional compartment model approach. The results of the Markov chain models are compared to the ODE kinetic model developed in the previous chapter. The Markov chain methodology is used in this chapter for the following objectives:

1) A deterministic solution to the division of ^{133}Cs across the different biotic components over time very similar to that obtained by numerical approximation solutions of ordinary differential equation based compartment models
2) A method to quantify the fraction in each biotic inventory component at steady state conditions, or near steady state conditions
3) Evaluation of the inherent variability of the pond's proposed ecosystem by stochastically simulating the movement of ^{133}Cs atoms through the system

4) A method to evaluate the cycling of ^{133}Cs atoms through the system and the mean residence time distributions of ^{133}Cs in a component

This chapter does not provide lengthy proofs and mathematical descriptions of Markov chain theory, though much is available in the listed references for the interested reader and and some definitions related to Markov techniques are provided in Appendix D. As stated by Richard Durrett, a professor in mathematics over the past 30 years at Cornell and Duke Universities, it is possible to use Markov chains without an in depth knowledge of their theory just as it is possible to drive a car without in depth knowledge of combustion engines (Durrett, 2012).

5.2. Theory and Methods

5.2.1. Markov Chain Methods and Deterministic Application to Pond 4

A process can be modeled by Markov methods when the transition between states in a system can be described by a probability of occurrence and when the Markov property is upheld. The Markov property is valid when the current outcome of the process is only dependent on where the process was in the previous time step (Ross, 2007). The Pond 4 ODE kinetic model can be characterized as a Markov model wherein each compartment is considered a state (e.g., largemouth bass is one such state). Figure 5.1. illustrates the Pond 4 systems as a Markov state transition diagram:

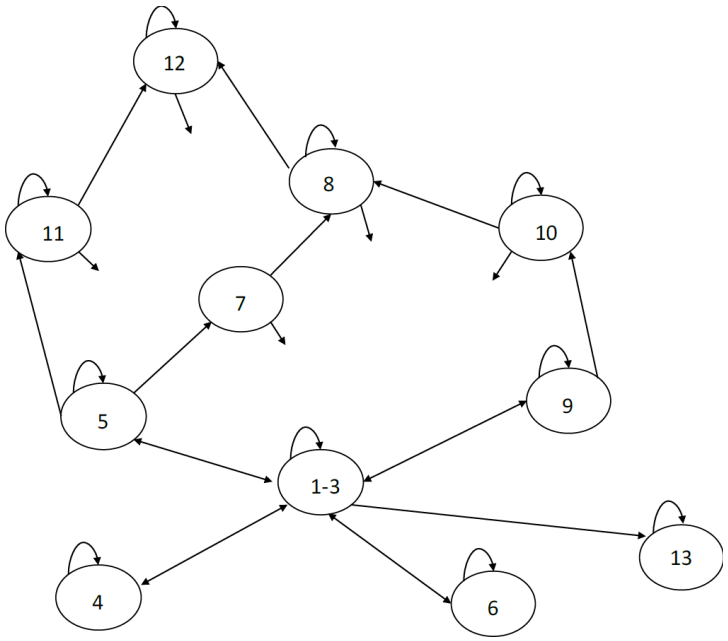

Figure 5.1. Markov state transition diagram of Pond 4 model framework

Markov processes are often illustrated through this type of diagram (Ible, 2013) that is also sometimes referred to as a tree diagram (Kemeny, 1976) or simply a Markov chain diagram (Acevedo, 2013). In the diagram, each circle is a state (a biotic or physical component of the model), and the arrows indicate those transition probabilities that are greater than zero. The index for numbering is the same as used in the previous chapter. The arrows from states 7, 8, 10, 11, and 12 are transitions to the water (states 1-3) but are not drawn completely for figure clarity. Water states 1, 2, and 3 are not directly connected to each other.

The probability of ^{133}Cs in each state at a given day is expressed as the vector $\mathbf{S}(t)$ where each entry represents a state (1 through 13 for the Pond 4 Markov model). Markov chain methods use linear algebra, and all bolded variables in this dissertation are either vectors or matrices. $\mathbf{S}(t)$ is only dependent on what it was the previous time step, $\mathbf{S}(t-\Delta t)$, and not the time steps before that; hence, the system can be expressed by the Markov property and Markov chain methodology can be applied. The term "memory-less" is often used to describe such a behavior

(Acevedo, 2013). The R software package Matrix was used for the calculations needed for the Markov model (Bates and Maechler, 2016).

Markov chain methodology postulates that the probability distribution across the states, $\mathbf{S}(t)$, at time t can be calculated by the following equation, where $\mathbf{S}_0$ is an initial distribution vector at t_0:

$$\mathbf{S}(t) = \mathbf{S}_0 \boldsymbol{P}^t \tag{5-1}$$

$\boldsymbol{P}$ is called the transitional probability matrix, where each element $p_{i,j,}$ expresses the probability of movement from state i to j, and is given in the matrix form as follows:

$$\boldsymbol{P} = \begin{pmatrix} p_{1,1} & p_{1,2} & p_{1,3} & \cdots & p_{1,m} \\ p_{2,1} & p_{2,2} & p_{2,3} & \cdots & p_{2,m} \\ p_{3,1} & p_{3,2} & p_{3,3} & \cdots & p_{3,m} \\ \cdots & \cdots & \cdots & & \cdots \\ p_{m,1} & p_{m,2} & p_{m,3} & \cdots & p_{m,m} \end{pmatrix} \tag{5-2}$$

$\boldsymbol{P}$ is a $m \times m$ matrix, where m is the number of states the process can occupy. For the Pond 4 ^{133}Cs model, m is equal to 13, resulting in transitional probability matrix dimensions of 13×13. As an example of the individual probabilities, given the same Pond 4 compartment numbering specified previously in Chapters 3 and 4 (Table 3.1), $p_{5,7}$ is the probability that the ^{133}Cs will transition from periphyton (5) to snail (7) for a day time step. Where there is no direct linkage between compartments i and j, the probability $p_{i,j}$ is simply zero. The sum of the probabilities of movements and retention in each component must equal one. Since the values of $p_{i,j}$ in each of the rows i of $\boldsymbol{P}$ account for all of the probabilities that exist for movement or retention for state I, the sum of the row entries equals one, and can be expressed as:

$$\sum_{j=1}^{m} p_{i,j} = 1 \tag{5-3}$$

When $j = i$, the probability matrix elements $p_{i,i}$ express the probability of retention in the same state over a time step (e.g., p_{55} is the probability over a day that the atom will stay in the periphyton given it is in the periphyton). ***P*** is constant over time for the most general application of a Markov chain, and this is referred to as a time-homogeneous, or simply a homogeneous, Markov model. Time variant methodologies are also utilized and these are called non-homogeneous Markov models (Kalos, 2008 and Acevedo, 2013). For this first application of a Markov model to the Cs movement in Pond 4, a homogeneous Markov model was used. It will be referred to as the "Markov matrix model" or just simply the "matrix model" in this dissertation. For all Pond 4 models, to include the Markov matrix model, the probabilities of ^{133}Cs movement and retention are discretized as to the probability over a day, $\Delta t = 1$. A day was considered appropriate, as this is the time frame that 1) effects are considered (for example, time until maximum ^{133}Cs inventory in a biotic component) and 2) sampling supports (multiple sampling events in one day were not possible with available resources, even directly after the addition). This time step is constant throughout the entire period assessed, and given this, the Pond 4 Markov model can also be classified as a discrete time Markov model.

In the Pond 4 Markov matrix model and simulation model, the transition probabilities of the matrix ***P*** are the same as the transfer coefficients estimated for the ODE kinetic model. This is possible because a transfer coefficient expresses the fraction of ^{133}Cs that moves from one compartment to another each day, and this also can be thought of as the probability of movement between states for each day.

For the Pond 4 Markov matrix model, the initial condition vector $\mathbf{S}_0$ is equal to (0.218, 0.526, 0.256, 0, 0, 0, 0, 0, 0, 0, 0, 0, 0) if expressed as probabilities of ^{133}Cs being in each state at time $t = 0$. This means that the initial distribution of the four kg addition ^{133}Cs is 21.8% in water

1, 52.6% in water 2, and 25.6% in water 3. As was done in the kinetic ODE model, these fractions were based on the ratio of the a_i values from the three component fit to the water (Equation 3-1). Using this $\mathbf{S}_0$ and Equation 5-1, the probability distribution of the inventory of ^{133}Cs, $\mathbf{S}(t)$, was obtained for each day. Multiplying this outcome by the initial input in mg for each day results in a solution to the inventories in each state. The water subcomponents were summed into one total water component, as was done for the ODE kinetic model. The behavior of the ^{133}Cs addition modeled by the Markov model is anticipated to be very similar, if not identical, to numerically solving the system of ordinary differential equations (ODE) as was done in the previous chapter for the Pond 4 ODE kinetic model. If so, when solving compartment model systems, it is worth considering the usefulness of using the Markov chain method (Equation 5-1) as an alternative to the use of numerical solutions to differential equations.

5.2.2. Stationary Distribution

The stationary distribution is another property of Markov chains that could be a useful application for model frameworks similar to the Pond 4 model. For Markov processes, a stationary distribution, $\mathbf{S}^*$, occurs at steady state (or equilibrium) conditions, as $t \to \infty$. This distribution is expressed as a vector of probabilities for each state, and it is what occurs after multiplying the probability matrix by itself many times (i.e., many time steps). This stationary distribution is a constant distribution that the process converges to at equilibrium, and it is the same independent of where the process starts. This behavior can be described by Equation 5-7 below (Acevedo, 2013) where s_j^* are the elements of the stationary distribution, $\mathbf{S}^*$:

$$s_j^* = \lim_{t\to\infty} P_{i,j}^{*\,t} \qquad (5-4)$$

Considering that as time grows large there is no change in the probability distribution over time, such that at equilibrium $\mathbf{S}(t-1) = \mathbf{S}(t) = \mathbf{S}^*$, then Equation 5-1 can be expressed as the following for steady state conditions, where **I** is an identity matrix of the same dimensions as **P** :

$$\mathbf{S}^* = \mathbf{P}\,\mathbf{S}^* \quad or \quad (\mathbf{P} - \mathbf{I})\mathbf{S}^* = 0 \qquad (5-5)$$

Equation 5-3 and Equation 5-5 along with linear algebra principles can be used to write a series of linear equations to solve for the stationary distribution (Acevedo, 2013). An alternative description of this methodology is to find the solution for the eigenvector of the probability transition matrix with eigenvalue equal to one. A software package such as the R package "markovchain" (Spedicato, 2017) implements these methods to solve for the stationary distribution, and was used for our calculations.

The use of the stationary distribution in Markov modeling to quantify the proportion inventory levels are when they reach a state of equilibrium is useful when none of the state's retention probabilities are one (*i.e.,* a sink). However, the application of the stationary distribution calculation is not applicable when there is a sink, such as Pond 5, as over a long time the state will tend towards the sink (this type of Markov chain is called an absorbing Markov chain, and does have other useful calculations that are described further in the subsequent chapter of this dissertation). Equations are not needed to conclude that eventually $\mathbf{S}^*$ would be (0, 0, 0, 0, 0, 0, 0, 0, 0, 0, 0, 0, 1). The Pond 4 probability transition matrix could also be assessed to quantify when the system comes near enough to a state of equilibrium by evaluating the change between $\boldsymbol{P}^t$ and $\boldsymbol{P}^{t+1}$ over a series of different time steps. Evaluating the stationary distribution in such a manner was beyond the scope of this work.

However, to illustrate the usefulness of the stationary distribution calculation in evaluating equilibrium conditions of Markov processes, the Pond 4 probabilities were slightly modified. Specifically, the Pond 4 model was evaluated with a situation where Pond 5 does not have a retention probability of one, and instead five percent of the daily ^{133}Cs flow into Pond 5 returns to Pond 4 (and hence $p_{11,1} = 8.6\times10^{-4}$). Though this situation may not apply to Pond 4, it is practical that it could exist, and it is an example of when the use of stationary distribution calculations could easily provide useful information on equilibrium predictions. With the change of flow back to each of the Pond 4 water components, minor adjustments are needed to the retention probabilities $p_{1,1}, p_{2,2}, p_{3,3}$ and $p_{11,11}$ to maintain the requirement of Equation 5-3 that the probabilities in each row of $\boldsymbol{P}$ sum to one.

5.2.3. Pond 4 Markov Simulation Model

While the Markov matrix model, Equation 5-1, gives a deterministic solution, the transition probability matrix can also be used for a Markov simulation model of Cs atoms to:

1) obtain a stochastic solution to the total inventories and evaluate inherent variability due to the various pathways in the system and

2) evaluate the individual pathways of the atoms to assess residence time in the biotic components and cycling through the system.

These two aspects cannot be evaluated by traditional ODE compartment models.

The use of an inventory based kinetic model of inventories allows for the Markov chain model to be applied to the movement of a Cs atom as the unit of mass. An atom was selected as this is the fundamental unit of matter that could make independent and separate movements in the pond. Assuming linearity, the probabilities of the transfer of atoms parallels the transfer of mass and can be characterized by the probability transition matrix, $\boldsymbol{P}$. When discrete Cs atom

movement is modeled, $\mathbf{S}(t)$ indicates the state the Cs atom is in on that day instead of the distribution of Cs across the states as described in the previous section. At each time step, the probability that a Cs atom is in a certain state will be one and the probability that it will be in any of the other states will be zero. For example, $\mathbf{S}(t)$ would be (0, 0, 0, 1, 0, 0, 0, 0, 0, 0, 0, 0, 0) if the atom was in the macrophytes state. To simplify this further, the Markov chain output for a simulation indicates the state that an atom is in on that time step by its component number or an alpha designator. An example output of a simulated 15 day Markov chain for Pond 4 using the model's transition probabilities, and the alpha designators of W for water, M for submerged macrophytes, and S for sediments, is W W W M M M M M W W S S S S S. The Cs atom in this simulation spent 3 days in the water, followed by 5 days in the macrophytes, 2 more days in the water, and the remaining 5 days in the sediments.

The procedure to create a simulated Markov chain is straightforward. Since each atom's movement is random, the atom's potential movement each day is based on a random number generated between 0 and 1. This number is compared to the transitional probabilities from $\boldsymbol{P}$ for the state that the atom is in to determine the atom's next location. As a general example, if there was a probability of staying in the current state of 0.7 and a probability of moving to a different state equal to 0.3, the simulation could be written so any random number between 0 and 0.7 would result in the atom staying while a random number between 0.7 and 1 would result in the atom moving.

In the simulation, each Cs atom starts in one of the three water components and the initial starting positions of the total number of atoms was set to match the proportions given from the a_i components of Equation 3-1, as has been done in the previous models of Pond 4. Specifically, out of 1×10^6 atoms, 1.475×10^5 started in water 1.1, 6.575×10^5 atoms started in water 1.2, and

1.95×10^5 atoms started in water 1.3. The Markov simulation procedure, following the logic previously described, was initially directly written and implemented using the programming language R. Ultimately it was conducted through use of the R package "markovchain" (Spedicato, 2017). Since "markovchain" utilizes a C++ underlying basis and implements parallel computing, it was notably faster then implementation in R alone. Two versions of the simulation were created; one that remembers and assesses the individual pathways of the atoms and one that does not.

The evaluation of inherent variability of the ^{133}Cs inventories does not need to remember the individual Markov chain simulations. Instead, for each day, the atom positions are tallied to provide a total number of atoms that were in each state for each day of the simulation. Since each atom has a different pathway, the resulting summed output is stochastic. A simulation of 1 million atoms can be completed in approximately 20 minutes when memory and assessment of the individual pathways is not needed. Multiple Markov simulations of 1 million atoms were used in this work to evaluate the variation amongst the different outputs, and a virtual multi-core cluster operated by the Colorado State University School of Veterinary and Biomedical Sciences was used to accomplish this objective.

Two separate sets of simulations from 30 realizations were compared to validate that 30 was a large enough number of replications for the inherent variability assessment. Two aspects were assessed to evaluate the inherent variability in each component over time: 1) the range of the 30 realizations divided by the mean at each day, and 2) the coefficient of variation (standard deviation/mean). Initial conditions or transition probabilities were not varied in the current efforts. As a result, the variation in the realizations is due solely to the different pathways taken

by the atoms and describes the inherent variability of the system. The output of the simulation was compared to that given by the ODE kinetic model.

The second objective of the simulation was the analysis of the individual atom pathways. In the analysis for this paper, 1 million atom pathways are evaluated for 1) the mean duration an atom spends from entry to exit within a given compartment and standard deviation of this value; 2) the probability distributions of these visit durations; and 3) the number of these atoms that make more than one visit to the same compartment over a 500 day period. This latter parameter will give insight into the cycling the system experiences. The biotic components were all assessed, and while select results will be subsequently given, all of the biotic component results are available in the appendices to this manuscript. The assessment of durations an atom spends in the biotic components was evaluated from a two year simulation versus a 500 day simulation to give adequate time to obtain a large enough number of visits in the less visited components such as plankton.

5.3. Results

5.3.1. Deterministic model comparison

The results of Equation 5-1 for the Pond 4 Markov matrix model to the ^{133}Cs inventory levels in the pond are very comparable to the ODE kinetic model in all components, and this similarity is illustrated for two example biotic components in Figure 5.2. Evaluating the ratio of these curves for all the biotic components indicates that most ratios are within 10% of unity with the exception of the *Chaoborus* larvae and the water, which are both within 15%.

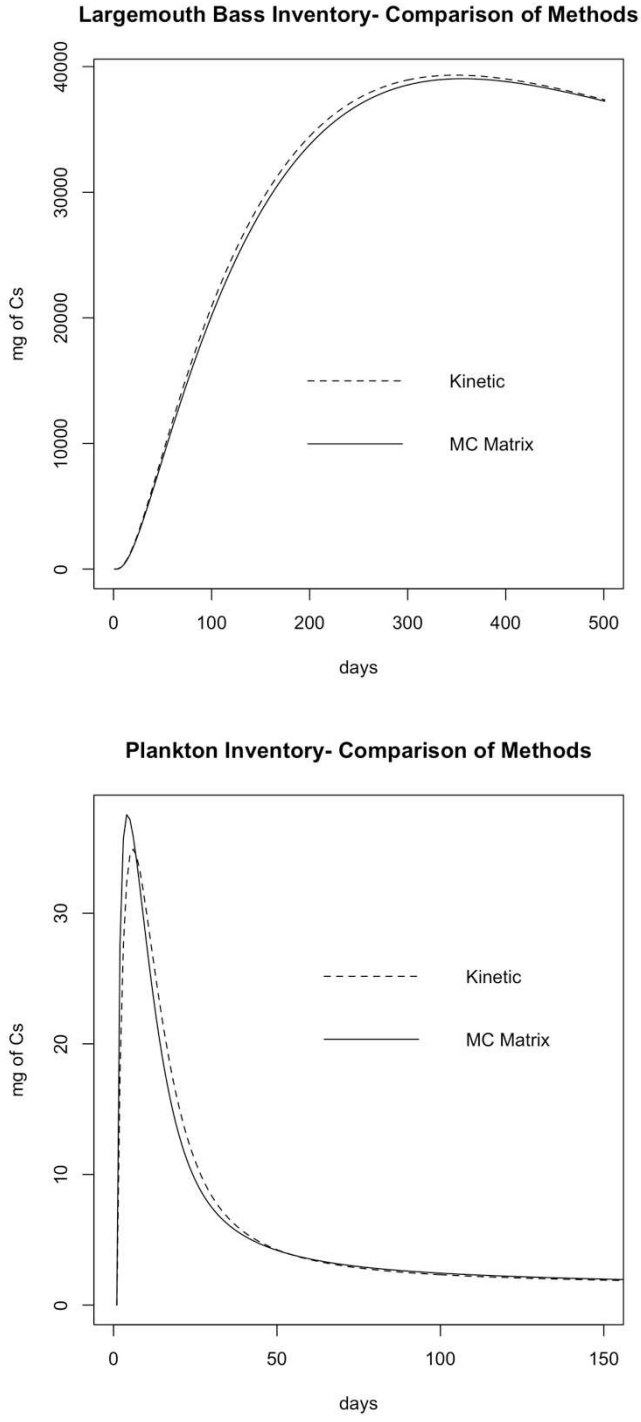

Figure 5.2. Comparison of Markov matrix model and ODE kinetic model

There are 5500 ratios of the Markov deterministic solution to the ODE solution for each compartment over a 500 day period (recall that the water components are summed for each day

into one value for the water). Of these ratios, 94% (5193/5500) are within 0.9 to 1.1 and 83% (4539/5500) are within 0.95 to 1.05. When only the ratios of the 8 biotic components are evaluated, 98.7% (3947/4000) are between 0.9 and 1.1. The largest deviations occur for the plankton, Pond 5, and water components, though these ratios are still primarily within 15 percent of unity.

Appendix E includes results of a sensitivity analysis of the behavior of the model components as a result of ±20% variation to each of the individual transition probabilities. Transitions to and from the water were varied together, for example for the assessment of sensitivity due to the water to sediments transition probabilities $p_{1,6,}$ $p_{2,6,}$ and $p_{3,6}$ were all varied ±20%. Overall, the component directly affected by the adjustment and the subsequently linked component were most sensitive to changes. One exception to this was the changes to the water to sediments transition probabilities; this resulted in 17 to 22% deviations from the unadjusted model biota output, with the smallest of these being in the largemouth bass.

Acknowledging the observation that all deviations from a ratio of one between the Markov matrix model and ODE kinetic model are small, some general trends are noted: 1) the primary producers and primary consumers initially have higher values in the Markov matrix model than in the ODE kinetic model, then they have lower values before approaching a ratio of one at 400 days; 2) overall the fish and the sediment have lower values in the Markov matrix model than in the ODE kinetic model, which are slightly closer to the data based inventory values (from the tabular model), and approach a ratio near one by approximately 300 days; and 3) the water and Pond 5 have higher ^{133}Cs inventory values in the matrix model compared to the ODE model, and the ODE kinetic model is closer to the data based tabular model between approximately days 40 to 150.

In the development of the ODE kinetic model, the method of fitting model output to the temporal behavior of the data based inventory values (i.e., tabular model) included the objective of fitting the days until maximum inventory within a factor of two. Table 5.1 compares these times to maximum inventories for the Markov matrix model, ODE kinetic model (Chapter 4), and original tabular model (Chapter 3).

Table 5.1. A comparison of the days to maximum ^{133}Cs inventories for the biotic components for the tabular data based model, ODE kinetic model, and Markov models.

State	Tabular	ODE kinetic	Ratio of ODE kinetic: tabular	Markov matrix model	Ratio of Markov matrix: tabular	Markov simulation model	Ratio of Markov simulation: tabular
Macrophytes	8	9	1.13	8	1.00	8	1.00
Periphyton	4	7	1.75	6	1.50	6	1.50
Snails	8	14	1.75	13	1.63	13	1.63
Bluegill	177	143	0.81	163	0.92	167	0.94
Plankton	3	5	1.67	3	1.00	4	1.33
Chaoborus Larvae	13	15	1.15	14	1.08	18	1.39
Lake Chub	86	60	0.70	62	0.72	62	0.72
Largemouth Bass	358	348	0.97	355	0.99	>300[1]	N/A

[1]The Markov simulation model was only run to 300 days

Differences in the time to maximum inventories are not large, though they are observed for the Markov matrix model and ODE kinetic model despite use of the same set of transfer coefficients. As can be seen in Table 5.1, the Markov matrix model is in closer agreement to the tabular model than the ODE kinetic model. The ODE kinetic model was also evaluated at a 0.25 day

time step instead of the standard one day time step, and this did not cause a change in the model's predicted days to maximum inventories.

The computing time is approximately 10 times faster for the Markov matrix model than the ODE kinetic model. This advantage is negligible when only computing one solution as this takes less than a second for each. However, when computing multiple solutions, the Markov matrix model's faster computing time is notable. For example, previously the ODE kinetic model was tested by computing 5,000 solutions of the model with the transfer coefficients varied ± 10% and a subsequent set with the transfer coefficients varied ± 20% (Jeong *et al.*, *in press* 2018b). Accomplishing this takes 42 minutes with the ODE kinetic model, and only about 4 minutes for the Markov matrix model. These times are using the previously discussed R packages on a 64-bit operating system with a 4.0 GHz AMD FX(tm)-8350 computer processor and 32 GB of RAM.

5.3.2 Stationary Distribution

Due to the adjacent Pond 5 being modeled as a sink (*i.e.,* retention probability is one), the final distribution of ^{133}Cs expressed as a vector is (0, 0, 0, 0, 0, 0, 0, 0, 0, 0, 0, 0, 1). This means that eventually, after a long time, 100% of the ^{133}Cs will move from Pond 4 and remain in Pond 5 (compartment 13). Such a conclusion is simple, and does not use a stationary distribution calculation. However, in the situation where there is movement of water from Pond 5 back to Pond 4 that stationary distribution is insightful. Utilizing the scenario explained in the methods section (5% of the daily flow into Pond 5 goes back to Pond 4 each day) results in the following stationary distribution, which is expressed as probabilities of the total added ^{133}Cs being in each state: (5.34×10^{-4}, 0.00575, 0.0408, 0.00707, 0.00126, 0.620, 6.467682×10^{-5}, 9.30×10^{-4}, 2.92×10^{-4}, 3.00×10^{-7}, 0.00338, 0.00576, 0.3141427). For such a scenario and from this stationary

distribution, it can be predicted that at equilibrium approximately 30% of the added ^{133}Cs is expected to remain in Pond 5 and 70% of the ^{133}Cs is anticipated to be in Pond 4, with 1.8% being in the biota of Pond 4.

5.3.3. Results of the Markov Simulation

The Markov simulation model was developed with two specific objectives in mind. One intent was to create a stochastic version of the model inventory output based on the random movement of the atoms that would produce a different output each time the model is run without needing to vary the model parameters. This would assess the variability in the system due to the different pathways when multiple replications of the model are computed. An example of the Markov simulation model output can be seen in Figure 5.3 blue for bluegill.

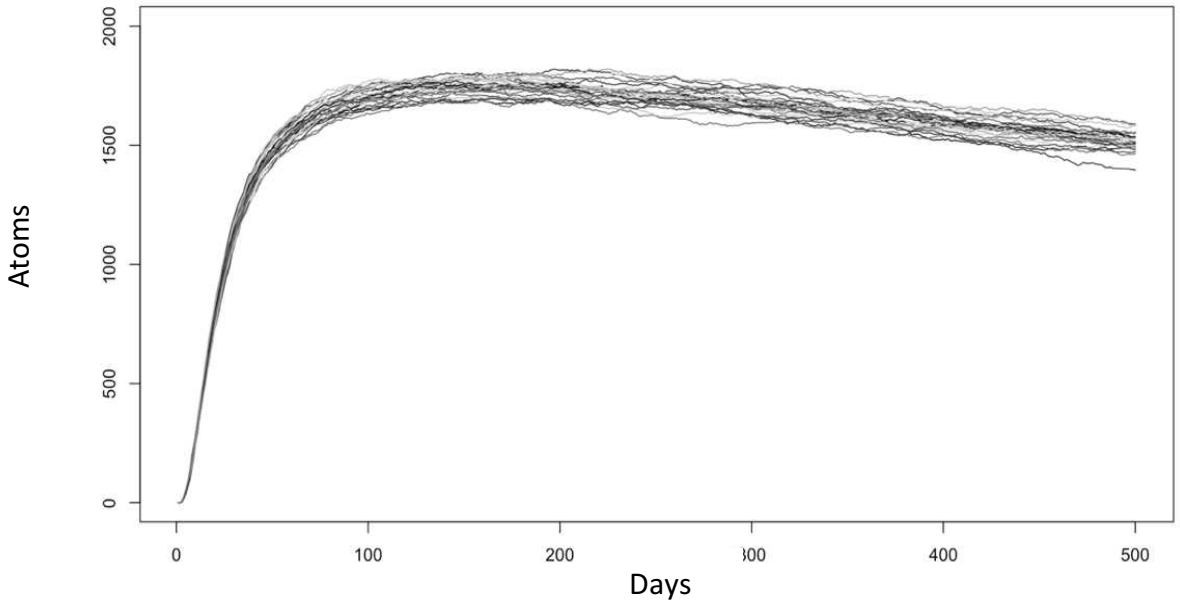

Figure 5.3. Markov simulation model output of one million atoms for bluegills

The second goal of the simulation model was to assess the aggregate behavior of the individual atoms' Markov chains to assess atom residence time in the biotic components and the number of times the atoms cycled through these components. The Markov simulation model mean output is comparable to the ODE kinetic model for all biotic components, as can be seen in

Figure 5.4 for the example biotic components of plankton and largemouth bass; graphs of the other biota are available in Appendix F. Both models' output is daily ^{133}Cs inventory of atoms for a starting amount of 1×10^6 atoms. An assessment of the ratio of the curves indicates that most ratios are within 15% of unity.

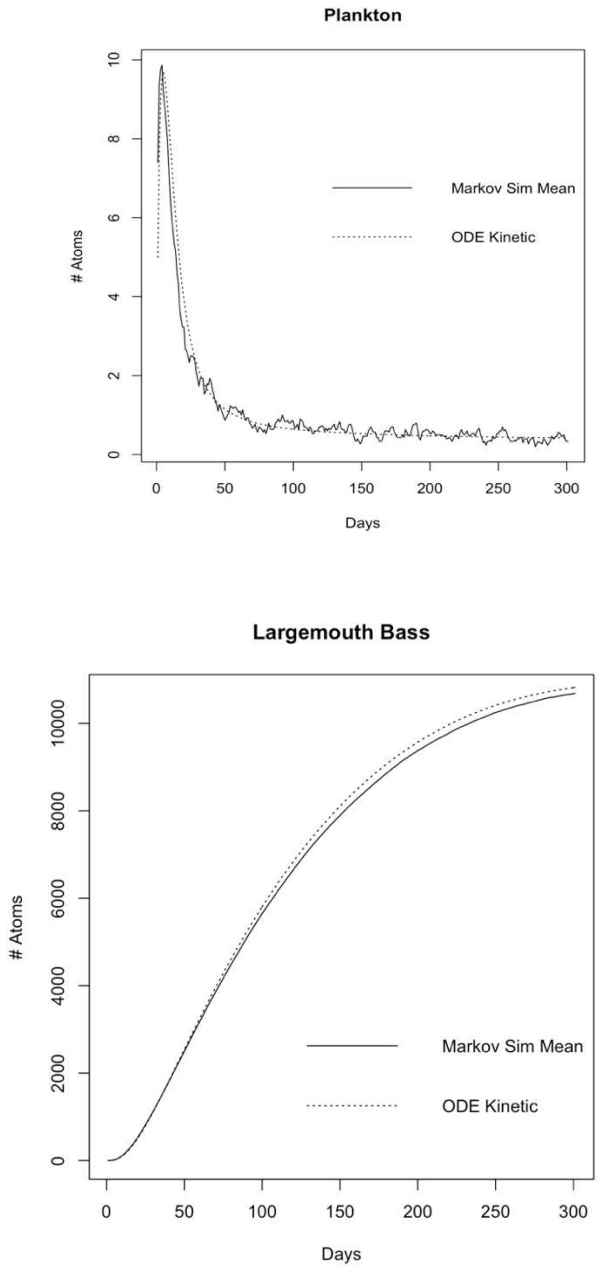

Figure 5.4. Comparison of Markov simulation model and ODE kinetic model

Table 5.1 includes results for the Markov simulation model days to peak ^{133} Cs inventory levels when compared to the tabular model. While not to the degree of the Markov matrix model, the Markov simulation model also overall performed closer to the data based tabular ^{133}Cs inventories than the ODE kinetic model.

5.3.3.1. Results of Inherent Variability Assessment

The Markov simulation was a useful and effective technique to evaluate the intrinsic variability of the Pond 4 system. Noticeable, but overall not large, intrinsic variability of the Pond 4 inventories was observed. Again, Figure 5.3 illustrates this variability for 30 realizations for the bluegill component (and 1×10^6 atoms). Thirty simulation realizations are sufficient for a repeatable evaluation of the Pond 4 system. Specifically, the mean and the coefficient of variation of the number of atoms in each compartment for each day are within 5% of each other for two separate sets of 30 realizations of $A = 1\times10^6$ atoms.

Another consideration was the appropriate value for A, the number of atoms. The simulation was run for $A = 5\times10^5$, 1×10^6, and 1×10^9 atoms (30 realizations of each). A total of 5×10^5 atoms per realization is insufficient due to the very low probability of uptake for some of the compartments, particularly the plankton. $A = 1\times10^6$ atoms is large enough to provide a plankton response where the average is comparable to that of the ODE kinetic model, however the day to day ratios of the Markov simulation to that of the ODE kinetic model varied between approximately 1.5 and 2.5 for one million atoms for the plankton and *Chaoborus* larvae components. Simulations of 1×10^9 atoms resulted in a deviation of approximately +/- 10%, and was comparable to that of the other primary producers. The 30 realizations for $A = 1\times10^6$ and $A = 1\times10^9$ atoms were compared to each other for mean daily inventories in each state and the corresponding coefficient of variation on each day. The comparison of all the daily mean

inventories for $A = 1\times10^6$ and $A = 1\times10^9$ atoms is given in Figure 5.5, and shows a near 1:1 relationship. The one to one behavior seen indicates that 1×10^6 atoms is an adequate value to assess the simulation model output.

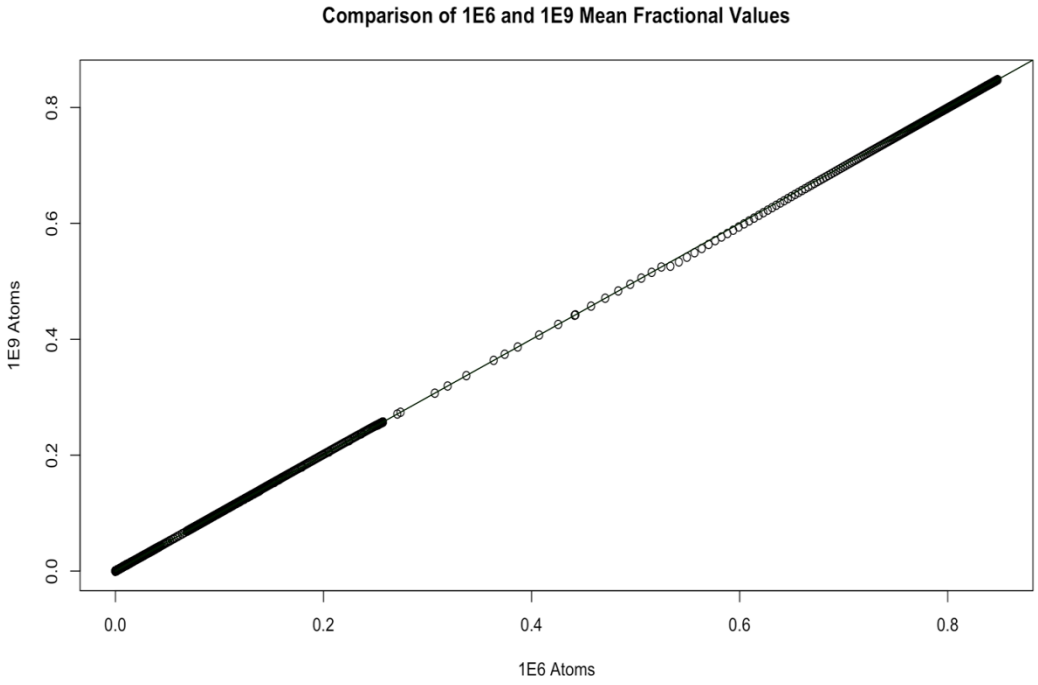

Figure 5.5 QQ plot comparing the mean fractional ^{133}Cs inventory values from all components for 30 simulations with 1×10^6 and 1×10^9 atoms.

To evaluate the maximum spread of the results across the 30 realizations, the range of the number of atoms in the compartment was divided by the mean of the 30 realizations for each day. Figures 5.6A-D and 5.7A-B are graphs of these results for both 1×10^6 atoms and 1×10^9 atoms. The decrease in the variability seen between 1×10^6 and 1×10^9 atoms is almost a factor of 40, and the relative behavior when comparing the different components within a food chain is very similar between 1×10^6 and 1×10^9 atoms. The results suggest that the most relative variability is in the plankton, *Chaoborus* larvae, and snail components. However, it is important to note that these inventories all drop to low levels after about the first 20 days post-addition.

The relative behavior of the different compartments is the same when comparing 1×10^6 atoms to 1×10^9 atoms, though the range/mean values drop by about a factor of 25 for 1×10^9 atoms. This observation is not unexpected, since the variation is anticipated to decrease as the total number of atoms increases. At 1×10^9 atoms, the daily ^{133}Cs inventory ranges are less than 20% of the mean for the biotic components, with the exception of the plankton and *Chaoborus* larvae, where the ranges of the daily inventories can be up to 10-15 times the mean daily inventories (over the first 300 days). At 1×10^9 atoms, the daily ranges are less than 1.5% of the means for the biotic components, with the exception of plankton and *Chaoborus* larvae, where the daily range approaches a value over three days that is approximately 20% of the mean.

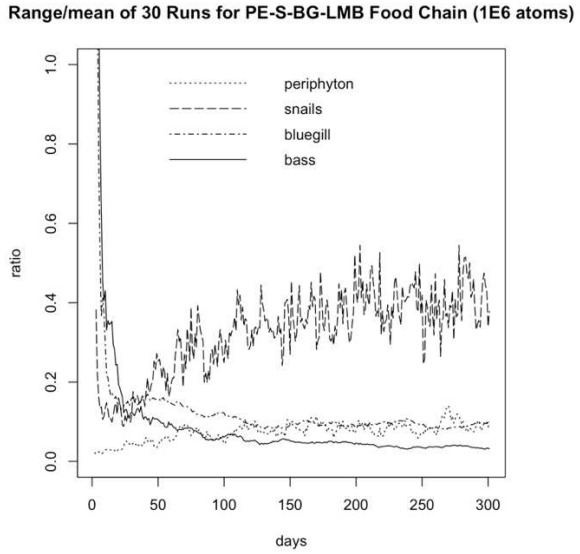

A

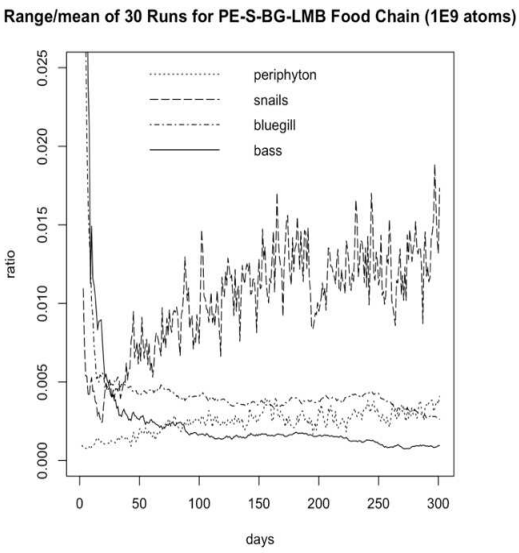

B

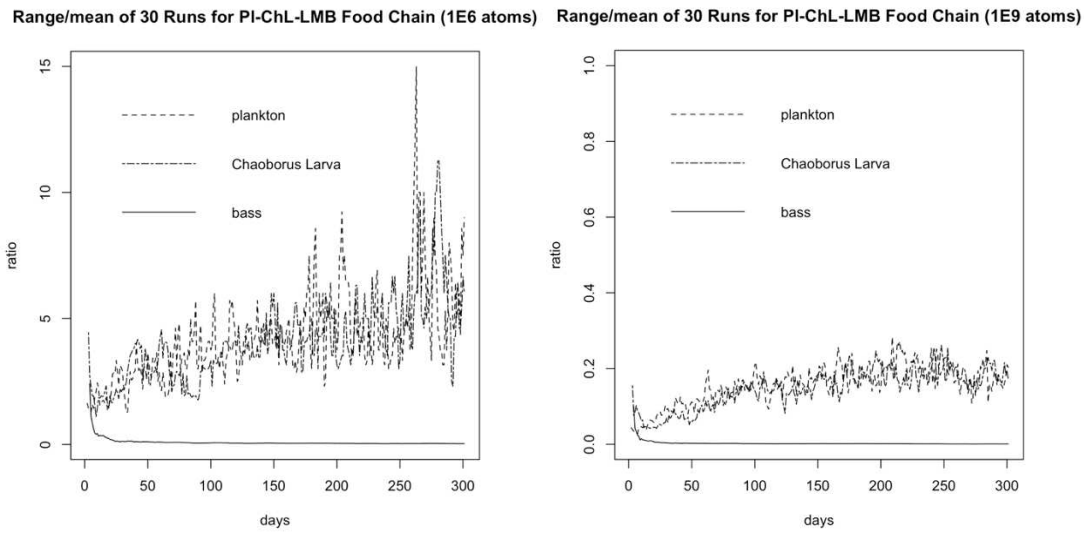

C D

Figure 5.6A-D. Illustration of the inherent variability in the simulation model for the PE-S-BG-LMB and Pl-ChL-LMB food chains for 1×10^6 and 1×10^9 atoms by assessing the range/mean for each day over a 300 day period for 30 realizations of the model output.

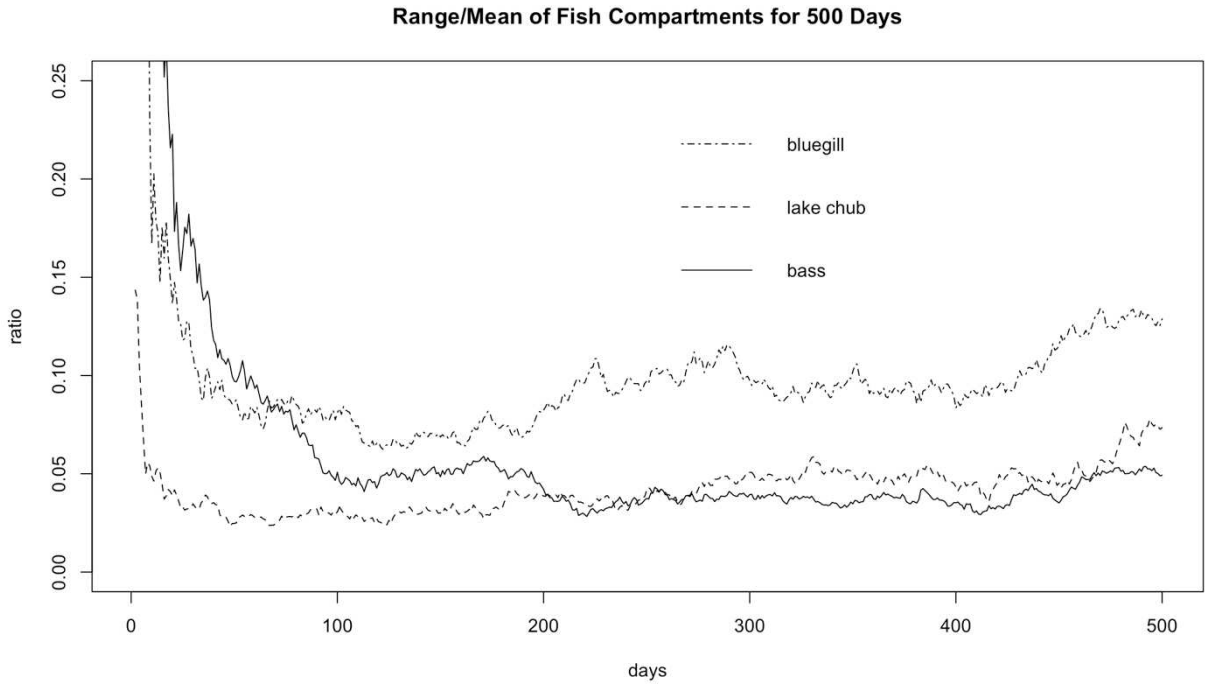

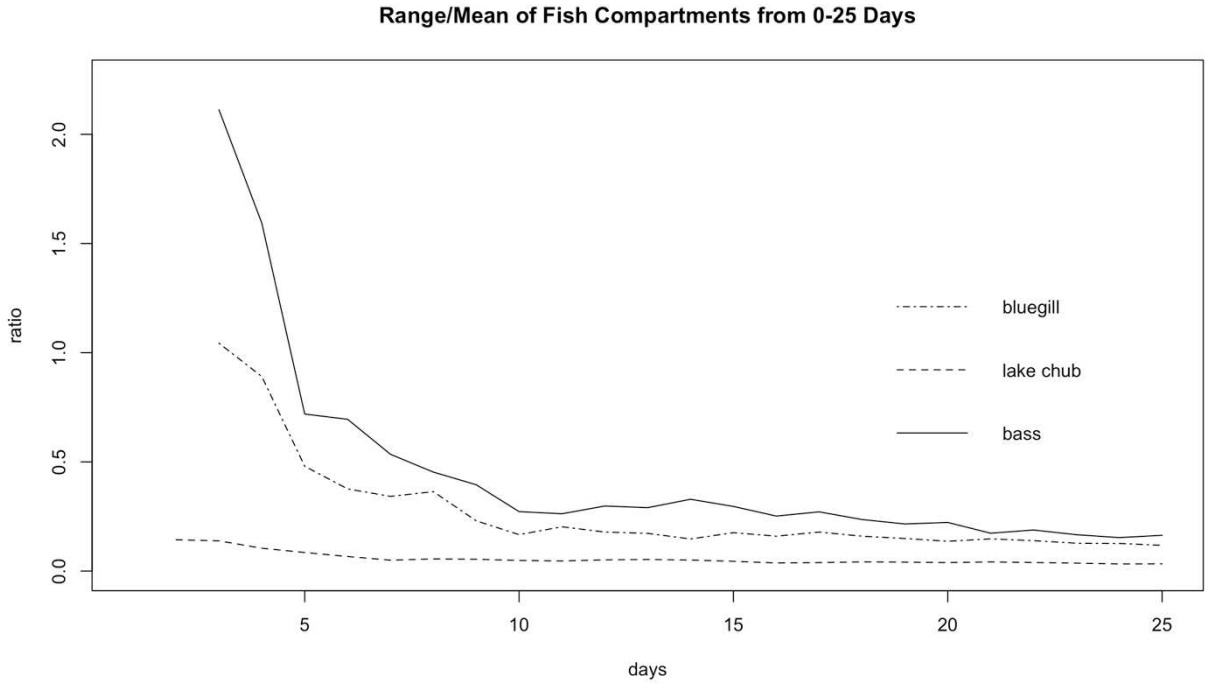

Figure 5.7A and 5.7B. Illustration of the inherent variability in the simulation model for the fish components for 1×10^6 atoms and 30 realizations over A) 500 days and B) the first 25 days.

Figure 5.7 provides the same graph of range/mean for the fish components. Figure 5.7B is the response over the first 15 days. The bass has substantially larger relative variability initially, as would be expected due to its position at the top of the food chain and small initial inventory of atoms in the bass. However, this trend does not continue; instead the variability decreases rapidly, and after about day 60, the bass has the smallest relative variability. In Figure 5.7A, the bluegills have the largest variability amongst the fish over three hundred days. This is expected, since bluegills are directly feeding on snails, which is the component with the largest relative variability. The observation that this variability is not seen in the largemouth bass may be supported by the conclusion from the tabular model that the largest flux of ^{133}Cs flows through the periphyton-lake chub-large mouth bass food chain.

5.3.3.2. Results of Stochastic Pathway Assessment

The Markov simulation provides unique insight on the cycling occurring in the system, Specifically, Table 5.2. includes the mean parameters of 1) the number of atoms that visit (enter and exit) the specified component over the time period; 2) the percentage of these atoms that revisit the compartment one time; 3) the percentage that visit two times over the time period; and 4) the percentage of atoms that revisit the compartment more than twice. Ten realizations of the simulation were assessed, and the values were all very close; specifically, the coefficient of variation (standard deviation/mean) was less than 0.1 for all parameters, with the exception of the percent of atoms that revisit the macrophytes one time.

Table 5.2. Descriptors of cycling occurring from evaluating the pathways of 1 million atoms for the given components over a two year period.

Component	Number of visits	Percent of atoms that visit once	Percent of atoms that visit twice	Percent of atoms >2 visits
Bass	24,721	98.7%	1.3%	0%

Lake chub	34,619	98.5%	1.5%	0%
Periphyton	189,363	89%	10%	1%
Macrophytes	888,483	57%	26%	17%
Plankton	87	100%	0%	0%

The macrophytes state had the largest cycling behavior with 26% of the atoms visiting twice and 17% visiting three or more times. A small number of atoms, approximately 0.2% of the total, transitioned through the macrophytes state seven times over the two year period.

The results of the pathway analysis for mean duration of the Cs atom, and the standard deviation, for the primary producers, lake chub, and the largemouth bass are provided in Table 5.3. The residence time is the duration the atom spends in a component (time from an atom's entry into the component to the time it leaves). The atom residence time distributions can be approximated by an exponential distribution, and the rate parameters and their standard errors are also provided in Table 5.3. These descriptors of the exponential distributions were determined using the "MASS" package in R (Venables, 2002) to perform the maximum likelihood fit. For an exponential distribution, the rate is also equal to one divided by the mean (Ible, 2013).

Table 5.3. Mean duration and standard deviation of visits (entry to exit) in select components from evaluating the pathways of 1 million atoms over a two year period.

Biotic Component	Mean residence time of Cs atom (days)	Standard Deviation (days)	Rate Parameter for Exponential Distribution and Standard Error
Bass	114	91	8.806×10^{-3} (5.559×10^{-5})
Lake Chub	104	94	9.535×10^{-3} (5.090×10^{-5})
Periphyton	9.5	8.9	0.1064 (2.224×10^{-4})

Macrophytes	13.3	12.8	7.560×10^{-2} (8.040×10^{-5})
Plankton	5.1	4.5	0.2059 (0.02158)

Figure 5.8A and 5.8B are graphs of the distribution of mean residence times for lake chub and periphyton from the Markov simulation model with 1×10^{6} atoms for a two year period. A total of 229,151 and 35,096 visits occurred for the periphyton and lake chub, respectively. The dashed line is the exponential distribution that fits each of these data histograms.

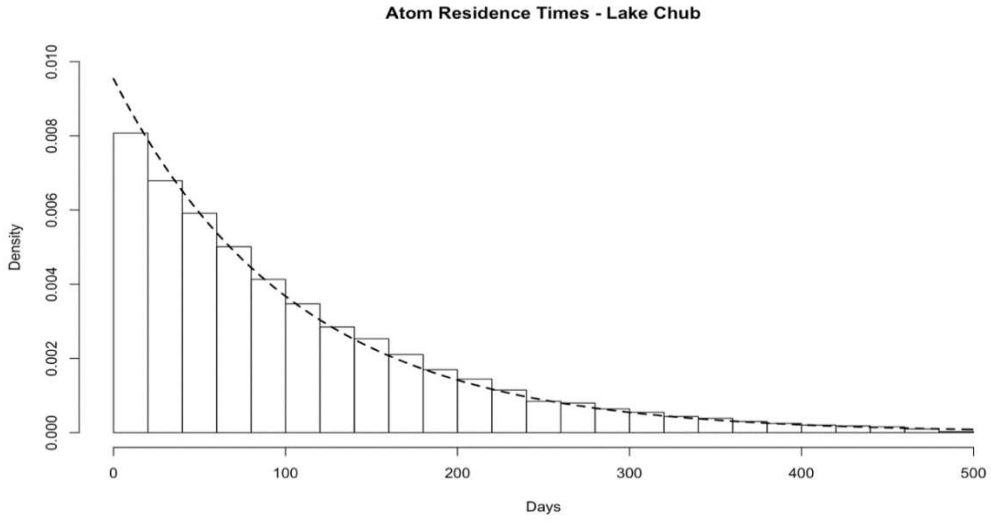

Figure 5.8A. Lake chub atom residence times predicted from the Markov Simulation of 1×10^{6} atoms for a two year period; the dashed line is the exponential distribution fit with a rate 0.00954

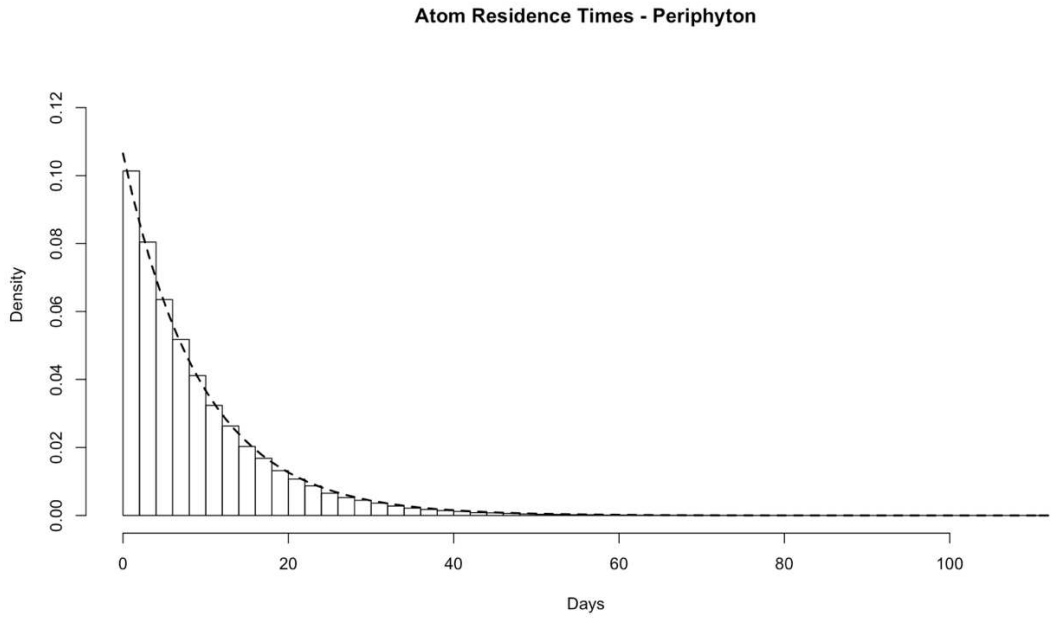

Figure 5.8B. Periphyton atom residence times predicted from the Markov Simulation of 1×10^6 atoms for a two year period; the dashed line is the exponential distribution fit with a rate 0.106

These results for additional biotic components are included in Appendix F of this dissertation along with QQ plots that provide a comparison of the actual model output to a synthetic exponential distribution data set of the same size as the model output.

5.4 Discussion

5.4.1. Assessment of the Markov models' ^{133}Cs Inventory Output

Conceptually, the discrete time Markov techniques provide an improved representation of the physical processes over time versus a numerical approximation solution that would be obtained from an ODE compartment model. Overall, the Markov matrix model and the Markov simulation model have ^{133}Cs inventory outputs that are within approximately 10% of the ODE kinetic model. The question of which model is preferable depends on the intended use, preference of the user, and the desired accuracy. The combination of the Markov matrix model and the simulation model offers the most comprehensive assessment of the Pond 4 system.

Additionally, the Markov probability transition matrix can be easily extended into an evaluation of steady state conditions.

One of the benefits of calculating the deterministic inventory output by use of the Markov matrix model is that it is more straightforward to use (in R or any similar programing language). Specifically, the Markov matrix model utilizes the Markov chain transition matrix of probabilities and Equation 5-1, and does not require detailing all of the differential equations, 13 in total for the Pond 4 ODE kinetic model. Solving Equation 5-1 in R software is straightforward and only requires one line of code using the Matrix package (Bates and Maechler, 2016). A potential additional benefit of the Markov matrix model to the ODE kinetic model is the computing speed. While the Markov matrix model has a speed approximately 10 times faster than R's differential equation numerical approximation code using the deSolve package, both techniques' speed is on the order of seconds, and hence the largest time advantage is with multiple calculation procedures.

Interestingly, when considering all components, including the physical components of water and sediment, the Markov matrix model and the mean output of the Markov simulation model (30 replications) ^{133}Cs inventories are almost identical at an input of 1×10^{6} atoms. The exceptions to this observation are the plankton and *Chaoborus* larvae ^{133}Cs inventories. The plankton and *Chaoborus* larvae do experience larger variability in the Markov simulation at 1×10^{6} atoms and it is likely that this exception may not remain with larger atoms numbers when their variability is lower. The agreement of the matrix model and the simulation model suggest that there could be some error (though not large) in the ODE kinetic model output due to the numerical approximation technique implemented, and supports the use of the Markov models over the ODE kinetic model if accuracy is desired.

The Markov matrix and simulation model results also suggest that these models better represent the days to maximum ^{133}Cs inventory for the Pond 4 model than the numerical approximation computation used in the ODE kinetic model, as almost every component has a better fit for days to maximum inventory when compared to the data based values. Table 5.1. provides a comparison for the Markov models and ODE kinetic model days until maximum ^{133}Cs inventories (recall the data based inventory values are from the tabular model, Jeong *et al., in press* 2018a). The Markov simulation mean inventories are used from 30 realizations of one million atoms. The largest improvement is in the plankton component where the ratio of days until maximum levels is 1.67 for the ODE kinetic model and 1.00 for the Markov matrix model, indicating an exact match for days until maximum between the Markov matrix model and the tabular model. The only exception to the better fit in the Markov models when compared to the ODE kinetic mode is the *Chaoborus* larvae of the Markov simulation model. At the higher input of 1×10^9 atoms, the days to peak for the *Chaoborus* larvae is the same as that in the ODE kinetic model (15 days). This suggests that this anomaly may only be seen at lower inputs to the Markov simulation model. Overall, the results of the days to peak ^{133}Cs inventory comparison suggests that the Markov matrix model framework should be applied instead of the ODE compartment modeling when the user is interested in assessing the temporal behavior, particularly for the primary producer components that are expected to uptake and then lose their ^{133}Cs inventories quicker than components higher in the food web.

5.4.2. Further Discussion on the Markov simulation model

While the ^{133}Cs inventory based framework (versus concentration) enabled a simulation of the movement of ^{133}Cs atoms, computing time needed to remain plausible. For this modeling effort, plausible is on the order of days. In the addition experiment, a total of 4 kg of ^{133}Cs was

added to Pond 4. When converted to atoms, four kg of ^{133}Cs is 1.4×10^{25} atoms. Clearly, to simulate this number of atoms would take a prohibitive amount of time and computer processing capacity. Instead, a much smaller number of atoms, $A = 1\times10^{6}$, was selected as an adequate number of atoms to balance computer processing time and having a large enough number of atoms to obtain useful results. A comparison at $A = 1\times10^{9}$ was also conducted, though this increased the simulation time to several days instead of 20 minutes. For perspective, 1×10^{9} atoms of the radioisotope ^{134}Cs (instead of ^{133}Cs) corresponds to 10.6 Bq. ^{134}Cs can be released from United States nuclear power plant operations in small authorized amounts on the order of 10s of kBq over a quarter of a year (NRC, 2016). As a hypothetical situation, assume that a nuclear power plant uniformly discharged 10 kBq of ^{134}Cs over one quarter of 120 days. At this rate, approximately 83 Bq per day would be released. While one billion atoms is much smaller than the total atoms in the Pond 4 experiment, it is an amount comparable to this hypothetical situation. Additionally, these simulation amounts are large enough to result in Cs atoms in the low probability components, plankton and *Chaoborous* larvae.

The computing time of the basic Markov simulation, when the history of individual atoms' pathways is not maintained, is 20 minutes for 1×10^{6} atoms and 300 days. When the atoms' Markov chain pathways are compiled in the pathway assessment (discussed further below) a larger amount of computer memory is needed. Currently, the Markov simulation pathway assessment takes approximately one day of computing time for 1×10^{6} atoms and two years. If the desired model input is 1×10^{9} atoms and 300 days, then the basic Markov simulation model takes several days to run. In our work on Pond 4, the use of 1×10^{9} atoms was only used to quantify the decrease in inherent variability at higher inventory amounts and was particularly useful to assess the plankton and *Chaoborus* larvae components, since the ^{133}Cs inventory levels

in these components are very small. However, for the pathway assessment 1×10^6 atoms was more than sufficient for most components and was sufficient for the plankton and *Chaoborus* larvae. In general, these computing times were not unreasonable for a simulation model that is investigative in nature, versus a model that would be used routinely, and it is possible that improvements could be made to improve the computing efficiency of the pathway assessment algorithm.

The overall inherent variability was found to be minor for the Pond 4 model framework and 1×10^6 atoms and even more so at 1×10^9 atoms. An assessment of the relative variability amongst the components was also accomplished. The results of the Markov simulation support that the largest component relative variability occurs 1) during time periods when components have smaller inventories of Cs and 2) for those components with smaller probabilities of retaining the Cs atoms per unit time. As can be seen in Figure 5.6A, in the Pond 4 system, the largest variability is observed in those components that have a smaller inventory levels and smaller retention probability, specifically, the plankton, *Chaoborus* larvae, and snails. As can be seen in Figure 5.6B, the fish initially have high inherent variability but this drops rapidly in the first couple weeks. Over a long period, the bluegill have the highest relative variability of this fish components, and the lake chub and largemouth bass have very similar levels of variability. This observation could be supported by the conclusion from Chapter 3 that the largest flux of ^{133}Cs is through the periphyton-lake chub-largemouth bass food chain.

Though the simulation does not show an overall large variability in the Pond 4 biotic components, this technique may be useful in evaluating variability in other systems, particularly those with lower retention probabilities. Given that, overall, the basic simulation does not have outliers suggests that the inventory based deterministic models provide a satisfactory

representation of the behavior of a large number of ^{133}Cs atoms in Pond 4 and are adequate for any future reverse engineering evaluations of the behavior of the ^{133}Cs inventories in Pond 4. However, it would be reasonable to use the Markov simulation to evaluate whether extensions of the model that significantly change the pathways or transition probabilities affect the inherent variability.

The ability to do a pathway assessment is a primary advantage of the Pond 4 Markov simulation model when compared to the deterministic approaches discussed in this paper. One aspect that cannot be assessed through the ODE kinetic model is the number of times an individual atom could be expected to visit a component over a specified time period (*i.e.*, the cycling of the system). The cycling observed of individual atoms in Table 5.2. for the fish components is small, and this was anticipated. However, the cycling through the macrophytes is larger than initially anticipated with 17% of the atoms making three or more visits to the macrophytes over a two year period. A small portion of these atoms made seven visits to macrophytes. The macrophytes were anticipated to have the most cycling due to being a primary producer and to the fact that they are not consumed in the Pond 4 model structure, and the pathway assessment of the Markov simulation results allowed for quantification of this cycling.

The fitted exponential distributions of the Markov simulation model atom residence time results are another outcome of the Markov chain pathway assessment (recall that the atom residence time was assessed as the time from entry to exit in the specified component). These distributions are useful in answering practical questions regarding the probability of an atom remaining in a biotic component for a specified duration of time. As one example of application, the probabilities predicted from the exponential distribution could be useful in assessing certain model assumptions. One such assumption in the model framework is that there is negligible Cs

loss from the food web components due decomposition (*i.e.* death by causes other than consumption) (Jeong *et al.*, *in press* 2018a). This assumption may not be supported by the model results if there is a significant chance that the ^{133}Cs atom is going to remain in the component longer than the upper range of the literature predicted lifespan (such lifespans are the predictions of time the biota would live if not consumed). Such an observation could also indicate a potential issue with the model transfer probabilities. A simple comparison between the mean of the model predicted atom residence times and the literature values for lifespan is useful for an initial assessment, and further quantification of probabilities can be done through use of the exponential distribution.

For the fish whose average lifespans range from five years to 16 years such as that of the largemouth bass (fishbase.org), loss due to death (other than consumption) over the two year period assessed is anticipated to be minor. The mean atom residence time for largemouth bass of 114 days is considerably less than five years, and supports the assumption that transition of ^{133}Cs from the bass to the sediment due to decomposition is minor. Further quantification of probabilities from the residence time exponential distribution are not needed. However, the evaluation is not as simple for a component with a shorter lifespan, such as the plankton. The average lifespan of plankton in laboratory studies where there is no prey can vary from a few days or less to upwards of 30 days depending on its species (Harris, 1986; Carron, 2009; Nandini, 2000; Tyrrell 2000). In Pond 4, clearly there is consumption of the plankton occurring, but these literature values provide an idea of the maximum potential plankton lifespan in Pond 4. The mean atom residence time from the simulation is about five days. Since the literature predicts that the average lifespan of the plankton component could be shorter than five days, it is worth quantifying this further by using the exponential distribution to calculate the probabilities

that the atom will remain in the biotic component longer than the literature supported lifespan. Unfortunately, resources were not available to specify the various plankton species and their abundances during the Pond 4 experiment, so it is not possible to determine the predominant species in the plankton component. Given this, the following examples are hypothetical.

First, consider a maximum plankton lifespan of approximately 20 days. Using the exponential distribution fit to the atom residence times of the plankton, we can conclude that there is a 1.6% chance that the ^{133}Cs atom will reside in the plankton longer than 20 days (see Appendix F for calculation). This low probability quantifiably supports the assumption that loss due to decomposition is negligible. However, it is possible that the maximum lifespan could have been around five days. Again using the exponential distribution calculation, there is a 36% chance that the Cs atoms will reside in the plankton component longer than five days (see Appendix F for calculation). If the maximum plankton lifespan was closer to 5 days, then our assumption may be weaker. While the data available for Pond 4 for plankton does not allow an actual assessment of the model assumption, this example illustrates the type of questions that could be answered with the exponential probability distribution fit to the atom residence times.

The pathway analysis could be extended further in future work. Additional example questions that could be investigated by analyzing the atoms' pathways are 1) the number of atoms that moved from the sediment to the water or 2) the number of atoms that are excreted by a given biological component, and 3) the number of decays in each organism if the model was applied to a radionuclide. Overall, insight on the behavior of the Cs in Pond 4 that cannot be obtained from the ODE kinetic model is a benefit from modeling with Markov methods.

5.5. Conclusion

The Markov models support 1) a useful deterministic alternative, the Markov matrix model, to the traditionally used ordinary differential equation compartment model, 2) a stochastic assessment of the inherent variability due to the different pathways within a system, 3) the ability to assess the cycling behavior of the system, and 4) a probabilistic assessment of the mean residence time in a component. Of these four benefits, the latter three provide insight on the system that cannot be obtained through compartment models. Additionally, the matrix model provides a simpler technique when compared to traditional ODE compartment model methods.

Future work will include an assessment of the absorbing Markov chain calculations as applied to Pond 4. For example, Markov methods can characterize the mean amount of time in each component and the total mean time prior to the atom transitioning to an absorbing state. Since Pond 5 is an absorbing state, the absorbing Markov methods can quantify the total mean amount of time until the atoms leave the Pond 4 system. The calculations can also quantify the mean amount of time in each biotic component prior to absorption. As another consideration, the sediments can also be estimated as an absorbing state for shorter time spans, and the same aspects can be evaluated. One benefit of these calculations in a modeling framework is that they provide a measure (in addition to the level of the ^{133}Cs inventory) to evaluate the effect of changing any conditions (i.e., remediation actions) on the behavior of the ^{133}Cs in Pond 4.

Finally, modeling at an atomic level enables an extension of the Pond 4 model and transition probability matrix to include radioactive isotopes of Cs. For an isotope such as Cs, the utilization of atoms instead of masses allows for the computation of the number of decays occurring in each of the components over time in the system. For example, by following the procedure given in this paper, the Markov simulation can be applied to a Pond 4 model extension

to the radioisotope ^{134}Cs, and the the following aspects can be evaluated 1) atom mean residence time in each biotic component, 2) the cycling of the atoms through the system, and 3) the intrinsic variation of the decay states in each component can be assessed.

It must be recalled that the aim of each of these models as applied to Pond 4 is to reverse-engineer and enable a thorough evaluation of the Pond 4 system under different conditions. The observations and assessments in this chapter support using the Markov matrix model for inventory determination and the Markov simulation model for pathway assessment in future Pond 4 system modeling evaluations. The methods described in this paper could be applied to any framework where a compartment model was traditionally used to obtain additional information on a system.

CHAPTER SIX. USE OF ABSORBING MARKOV CHAIN PRINCIPLES IN MODELING POND 4 CS DYNAMICS*

6.1. Introduction and objectives

Model development can be an objective of field experiments that is never fully accomplished for a variety of reasons, such as lack of resources or appropriate data. The Pond 4 ^{133}Cs addition experiment is unique in that it produced a robust set of data in field conditions and resulted in multiple previously published dynamic site specific models (Jeong, et al., 2018a; Jeong, et al., 2018b; Miller and Johnson, *in review*) in addition to predictions of concentration ratios at equilibrium (Pinder, et al., 2009; Pinder, et al., 2011). The overarching purpose of all the Pond 4 modeling effort thus far has been to increase understanding of the dynamics of the ^{133}Cs in the water, biota, and sediments of Pond 4 and to create a reverse-engineering type of model where different conditions may be applied and their effects on the Cs dynamics assessed. The use of absorbing Markov chains is applied to the previously developed Markov model framework (Miller and Johnson, *in review*) and investigated in the current work as a method to provide further insight on Cs dynamics, to include the mean amount of time for the Cs to exit Pond 4 and the degree of cycling that occurs prior to exiting. The following scenarios were assessed: 1) the baseline ^{133}Cs model, 2) varied resuspension probabilities, and 3) ^{133}Cs adjusted to ^{134}Cs, the shortest lived common radioisotope of Cs.

---

*Miller, V.J., and Johnson T.E., Use of Absorbing Markov Chain Principles in Modeling Pond 4 Cs Dynamics; pending submission to Journal of Health Physics

6.1.1. Absorbing Markov Chains and the application to Pond 4

Absorbing Markov chains are a specific type of Markov chain that has at least one state that is a sink, or per Markov terminology an absorbing (i.e., ergodic) state, where once the process enters this state it does not return to any of the other states. To our best knowledge, the current work is the first application of absorbing Markov chains in the physical modeling of radioecology or radiation protection processes. However, absorbing Markov chains methods have been used in a wide variety of other fields, to include the following examples from biogeochemistry, computer science, and forest science. In the biogeochemistry example, Liang *et al.* evaluated the importance of microbial necromass in soil carbon dynamics by using a three state absorbing Markov chain to quantify the movement of carbon through living microbial biomass in soil, microbial necromass in soil, and the atmosphere as carbon dioxide (the absorbing state). As another example, Jiang *et al.* utilized absorbing Markov chains to improve computer regeneration of images to detect the most informative region (i.e., saliency detection). And third, absorbing Markov chains have been used in forest science to evaluate lethal factors in plant populations and to assess different forest management strategies (Ronceros, *et al* and Feldman *et al*). A common denominator in all these studies is the usefulness of the absorbing Markov chain technique to quantify the mean duration that the process is in transitional states prior to being in the absorbing state(s).

Absorbing Markov chain equations, such as the one that quantifies the mean duration prior to absorption (i.e., exiting the defined system), can be directly and simply applied using the transition probabilities. Since the Pond 4 Markov model includes an absorbing state and possible reverse engineering scenarios include more than one absorbing state, the current work seeks to expand on previous efforts of Markov chain modeling of Pond 4 to assess the application of

Absorbing Markov chain methods in describing and analyzing the dynamics of Cs in the Pond 4 system.

6.1.2. Objectives

The objectives of this paper are to use absorbing Markov chain calculations (for objectives 1-5) and the previously developed Markov simulation model (for #1c and 5) to accomplish the following:

1) Calculate mean time ^{33}Cs spent in each component, and the total time, prior to exiting the system by:
    a. Transition into Pond 5
    b. Transition into Pond 5 and the sediments modeled as a sink.
    c. Through assessment of Markov simulation paths over two years for selected biota (and compare to a.)
2) Calculate the mean time spent in each biotic component prior to exiting the system, when extending the model to ^{134}Cs
3) Evaluate the change to the mean time due to different remobilization conditions for ^{133}Cs and ^{134}Cs
4) Quantify the probabilities of exit to each individual absorbing state for those scenarios with more than one absorbing state
5) Assess how or if decay affects the cycling behavior through the system for ^{134}Cs compared to ^{133}Cs prior to exiting the system over the entire process time and over a two year period

6.2. Methods

As described in Chapter 5 of this thesis, the movement or transition of all Markov chain processes through different states can be described by a set of transition probabilities which compose the elements of the transitional probability matrix, **P**. Since Markov chain processes are "memoryless" any state can be defined as the initial state. Though the water was the initial state in the experiment, the initial states of interest for this chapter are both the water and the biota. An example simulating a 10 day Markov chain for Cs in the Pond 4 system with plankton as the initial state is: "9" "9" "11" "11" "1" "6" "6" "6" "6" "6"; this atom spent one day in the plankton, two days in the Chaoborus larvae, one day in the water, and then transitioned to the sediments. The behavior of each individual Markov chain varies; a subsequent Markov chain also with an initial state of plankton spent 4 days in the plankton, then 24 days in the *Chaoborus* larvae, followed by two days in the water, and then also transitioned to the sediments. Though each simulated Markov chain is unique, their aggregate is described by the transition probabilities of the process.

Recall that the transitional probability matrix, **P**, is a square matrix with each dimension equal to the number of states, *m*.

$$\mathbf{P} = \begin{pmatrix} p_{1,1} & p_{1,2} & p_{1,3} & \cdots & p_{1,m} \\ p_{2,1} & p_{2,2} & p_{2,3} & \cdots & p_{2,m} \\ p_{3,1} & p_{3,2} & p_{3,3} & \cdots & p_{3,m} \\ \cdots & \cdots & \cdots & & \cdots \\ p_{m,1} & p_{m,2} & p_{m,3} & \cdots & p_{m,m} \end{pmatrix} \quad (6\text{-}1)$$

An element of **P**, $p_{i,j}$, indicates the probability of going from one state, *i,* to another state, *j*. The baseline ^{133}Cs Pond 4 model used for the calculations in this chapter is the same as that described in Chapter 5 where $m = 13$ states, and **P** is a 13×13 matrix. Three water components were

consistently used in the previous and current Pond 4 model frameworks as this was the number of components of the exponential fit to the water data (Pinder, 2005). In the current chapter, the results from these three water components are averaged or summed as appropriate and the water is given as one result.

6.2.1. Absorbing Markov Chain Theory and Calculations

The baseline Pond 4 model has one state, Pond 5, which is an absorbing state. Once the Cs transitions to Pond 5, it does not return to the Pond 4 system. While this is an assumption in the model framework, it is supported by the water flow direction to the adjacent Pond 5 and the predominant wind direction (Jeong et al., 2018b). Mathematically, an absorbing state will have a retention probability, $p_{i,i,}$ of 1. For Pond 4, state 13 is Pond 5, so $p_{13,13}$=1. The remaining elements of row 13 of the transition probability matrix will all be zero, $p_{i\neq 13,13}$. Such a state can be thought of either as a sink (a more common term in radioecology) or as exiting the system. These approaches are not as common in Markov chain literature and are referred to by the terms "absorbing state" or "ergotic state". For Pond 4 and the process of Cs movement, it is helpful to think of absorbed as meaning that the atom has exited the system of concern. This allows for the extension to different scenarios of what defines "exited system" and prevents potential confusion with the physical absorption of atoms to sediments, biota, etc.

There are multiple other descriptors of Markov chains, and Appendix C includes definitions that apply to the Pond 4 modeling in addition to the categorization as an absorbing Markov chain. Specifically, the Pond 4 model is also a discrete and stationary Markov chain. A discrete Markov chain is one where the transition probabilities are for discrete time steps. A stationary Markov chain is one where the probabilities do not change over time. For Pond 4, since each transition probability is for a one day time step, the output of calculations is in units of day. A

one day time step was selected because this is the time frame that 1) effects occur (for example, time until maximum ^{133}Cs inventory in a macrophytes); and 2) sampling supports (multiple sampling events in one day was not possible with available resources). Additionally, though transition probabilities undoubtedly changed over time, this simplifying assumption was applied for the initial Markov modeling efforts.

As mentioned previously, one of the primary calculations for absorbing Markov chains is the calculation of mean time in each biotic component prior to the atom exiting the system. The calculation procedure is straightforward and requires two steps to solve what is called the fundamental matrix, **N** (Kemney and Snell, 1976). The elements of the fundamental matrix, designated as $n_{i,j,}$ give the mean time (or more generally, the number of steps) in component *j*, given the atom started in component *i,* prior to exiting the system. The two steps to solve for **N** are:

Step 1. First, re-arrange the probability transition matrix **P** so that absorbing state row(s) are listed at the bottom, and then the matrix can be separated into the four sub-matrices **Q, R**, $\mathbf{I_s}$, and **Z**, as illustrated in Figure 6.1. These can be described as follows: 1) **Q** is a matrix describing the probabilities amongst the non-absorbing states; 2) **R** is matrix giving the probabilities of transitioning to the absorbing state(s); 3) $\boldsymbol{I_s}$ is an identity matrix (diagonal elements are equal to one); and 4) **Z** is a matrix of zeroes. As an example, consider the extension of the model where the sediments are also a sink (which was evaluated as part of this work). Given there are 13 states in the basic Pond 4 model and in this scenario two of them are absorbing (Pond 5 and sediments), the sub-matrices can be described as follows: 1) **Q** is a 11×11 matrix of the transition probabilities; 2) **R** is a 11×2 matrix; 3) $\boldsymbol{I_s}$ is a 2×2 identity matrix; and 4) **Z** is a 2×11 matrix of zeroes. For Step 2, **Q** is all that is needed.

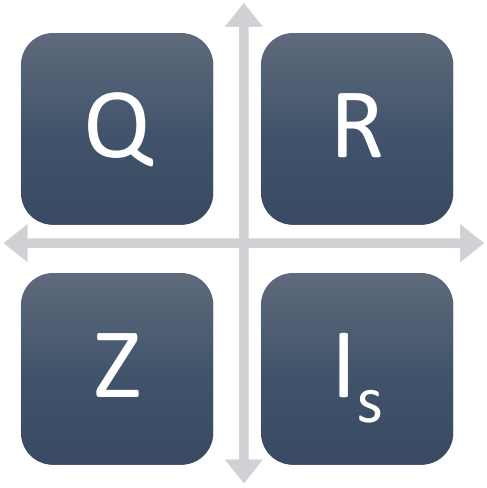

Figure 6.1. Division of transitional probability matrix

Step 2: Solve for the fundamental matrix **N** using the following equation:

$$\mathbf{N} = (\mathbf{I_{tr}} - \mathbf{Q})^{-1} \qquad (6-2)$$

$\mathbf{I_{tr}}$ differs from $\mathbf{I_s}$ in that it is an identity matrix of the same dimensions as **Q** (the matrix of the non-absorbing state transition probabilities). Further proof of Equation 6-2 is given in Appendix G for Pond 4 along with an example of the result of a calculation done for this chapter. The equation was solved in one line of code using the matrix package in R and the solve function (R core team; Bates, D. and Maechler, M., 2016). The vector $\boldsymbol{\tau}$ that expresses total days until ^{133}Cs exits the system given each starting component *i* is found by summing the rows of **N**:

$$\boldsymbol{\tau}_i = \sum_{j=1}^{j=12} \mathbf{N}_{i,j} \qquad (6-3)$$

For example, $\boldsymbol{\tau}_4$, is the total number of days until exiting the system given we are interested in a ^{133}Cs initial state in the macrophytes.

It is also possible to solve for the variance of the elements of **N** and $\boldsymbol{\tau}$. The variance of the mean steps to absorption (each element of **N)** is determined using the following equation (per Kemeny and Snell,1976):

$$\text{Var}[\mathbf{N}] = \mathbf{N}\,(2\,\mathbf{N_{dg}} - \mathbf{I_{tr}}) - \mathbf{N_{sq}} \qquad (6\text{-}4)$$

Where $\mathbf{N_{sq}}$ is **N** squared and $\mathbf{N_{dg}}$ is the diagonal matrix of **N.** The diagonal matrix only maintains the diagonal elements, and all other elements are zero. The variance in the total steps (i.e., total days for Pond 4) until exiting the system (per Kemeny and Snell,1976) is:

$$\text{Var}[\mathbf{N}] = (2\,\mathbf{N_{dg}} - \mathbf{I_{tr}})\,\boldsymbol{\tau} - \boldsymbol{\tau}_{sq} \qquad (6\text{-}5)$$

Where $\boldsymbol{\tau}_{sq}$ is $\boldsymbol{\tau}$ squared.

Equations 6-2 through 6-4 were also used to solve for the mean and variance of the total number of changes of state prior to exiting the system given a specified initial state. Doing this requires creating a new process described by the transitional probability matrix $\widehat{\mathbf{P}}$ using the original transitional probability matrix **P,** but with no retention in each transitional state (as described in Kemney and Snell, 1976). To do this for the Pond 4 baseline model, first $\widehat{\mathbf{P}}$ was set to equal **P**. Then $\widehat{\mathbf{P}}_{i,i}$ were set equal to zero for the transient states *i*= 1 to 12. Then each transient row of $\widehat{\mathbf{P}}$ was normalized by dividing each element of the row by its row-sum so that the elements of each row summed to one. Then $\widehat{\mathbf{N}}$**,** the fundamental matrix for $\widehat{\mathbf{P}}$, was solved in the same manner as previously described and $\widehat{\mathbf{D}}$ was determined, which for the baseline ^{133}Cs model is:

$$\widehat{\mathbf{D}}_{\mathrm{i}} = \sum_{j=1}^{j=12} \widehat{\mathbf{D}}_{i,j} \qquad (6\text{-}6)$$

The number of times a state changes from its initial starting point to exiting the system can also be described as the number of components visited prior to exiting a system. The previously developed Markov simulation model output includes a comparable descriptor of the system by assessing the percentage of atoms that revisited a component one or more times over a two year period. In the current work, the previous simulation output is compared to the

absorbing Markov chain calculation of $\widehat{\mathbf{N}}_{i,j}$ in terms of percentage of total as calculated by Equation 6-5. These values are not anticipated to be exactly the same because one is over a two year period and the other is over the mean time until the Cs exits the system (anticipated to be much longer than two years for ^{133}Cs).

The second equation, Equation 6-7, computes the probability matrix **B** whose elements give the probability of arriving in an absorbing state given the process starts in a transient state:

$$\mathbf{B}=\mathbf{NR} \tag{6-7}$$

Solving for **B** is most useful when comparing two or more absorbing states.

6.2.2. Applying AMC Computations to Pond 4

Equations 6-X through 6-Y are first applied to the basic Pond 4 framework, with only Pond 5 considered as exiting the system of concern (i.e., exiting Pond 4). The model framework was extended to considerations of the sediments as a complete sink and for ^{134}Cs instead of ^{133}Cs. The following further expounds the evaluated scenarios and additional methods applied:

A) Unmodified Pond 4 framework; ^{133}Cs exiting the system to Pond 5

B) ^{133}Cs exiting the system to Pond 5 and Sediments.

While re-suspension from the sediment has been modeled in the original ODE kinetic model (Jeong et al., 2018b) and was supported by experimental results, it is a small value in the model with a total probability of 0.0003 and a sediment retention probability of $P_{6,6}$ = 0.9997. The transition matrix was modified to make $P_{6,6}$ = 1 and all other elements of row six equal zero.

C) ^{134}Cs exiting the system by Pond 4, sediments, and/or decay.

Chemically, ^{134}Cs will behave the same as ^{133}Cs; however, exiting the system includes the process of radiological decay. Given a half life, $t_{1/2}$, of 2.0652 years (Chart of Nuclides),

the fraction or probability of decay each day is the decay constant, λ, expressed in days, calculated by Equation 6-8 as 9.14×10^{-4} d^{-1}.

$$\lambda = \frac{\ln(2)}{t_{1/2}} \tag{6-8}$$

λ was added in the transitional probability matrix **P** to each component within the system of interest for the three scenarios that will be subsequently explained. While it is possible to have each component transition to one "decay" state, individual decay sinks were created for each component within the system to allow for quantification and comparison of the probabilities of transition to decay from the different states (Equation 6-7 for **B**). To evaluate ^{134}Cs and to be able to make comparisons to ^{133}Cs scenarios, the following designations of exiting the system were applied to the ^{134}Cs model:

C1) Exiting the system by transition to Pond 5 or decay in all other model components. The ^{134}Cs atom that exits to Pond 5 can subsequently decay, but this is outside of the defined system for this scenario, as once the atom is in Pond 5, it already has exited the Pond 4 system. Scenario C1 was created to be comparable to scenario A. The transition probability matrix was adjusted with $p_{13,14}=0$ and the retention probabilities adjusted to ensure the rows summed to one.

C2) Exiting the system by transition to Pond 5 or sediments, or by decay in all other model components. Decay in Pond 5 or sediments is not an exit pathway since the ^{134}Cs has already exited the defined system of interest. This scenario was created to be similar to scenario B. The transition probability matrix was adjusted with $p_{13,14}=0$ and $p_{6,14}=0$, and the retention probabilities adjusted to ensure the rows summed to one.

C3) Exiting the system by decay alone; Pond 5 is included in the system of interest.

The fundamental matrix **N** was calculated for scenarios A, B, and C1-C3, and assessed for the initial state of the Cs in the water and for an initial state of the Cs in the biota. While the initial condition may be thought of as the start of the experiment (Cs added to the water), the initial condition can also be whenever one starts observing the process. Scenarios A and C1 were also evaluated to see whether there was an effect on the mean time until the Cs exits the system when changing remobilization probabilities by factors of 0.1, 0.5, 2, and 10.

The variance was evaluated for scenario A with baseline resuspension and adjusted resuspension using Equation 6-4 to quantify and assess the usefulness of this parameter. It is expected that the variance will be large since some atoms will exit the system quickly and others will take much longer to exit. Equation 6-7 was used to calculate and compare the probabilities of absorption from the transient states in scenarios B, C1, C2, and C3 since these were those scenarios where there was more than one absorbing state.

6.2.3. Comparison to Markov Simulation

The current work uses the previously developed Markov simulation model (Chapter 5) to 1) validate the mean days calculated by Equation 6-2 to exit the system given the atom entered a biotic component and to 2) validate the trend of the predicted state changes. For the first objective, 50,000 atoms' Markov chains were simulated for a two year period for each biotic component specified as the initial state. Those Markov chains that absorbed in a two year period were analyzed for the duration of time spent in each biotic component and the output was compared to that from Equation 6-2. Since the Markov simulation model was originally created to assess the dynamics over the first two years and the mean time until absorption could be longer than this, depending on the biotic component, this validation was performed for scenario C2. This scenario has the potential for the atom to exit the system over a shorter period of time

than the other scenarios due to having the most possibilities of exit (i.e., transition to the sediments, Pond 5, and decay).

For the second validation, the amount of cycling occurring over a two year period per the Markov simulation was assessed for both ^{133}Cs and ^{134}Cs with model baseline remobilization. 10,000 Markov chains were evaluated for each biota as the initial conditions. The Markov simulation cycling assessment output is the percentage of times an atom visits and revisits the given component over the user specified time period for a user specified number of atoms. This is somewhat different than the absorbing Markov chain that provides the mean number of state changes that is expected on average for the atom over the entire process time. To the authors' knowledge, it is not possible to determine the amount of cycling occurring over a set period without use of the Markov simulation model (Miller and Johnson, *in review*). While the exact results may not be comparable, the general trends predicted by the average total number of state changes and the Markov simulation cycling assessment should be comparable.

6.3. Results

6.3.1. Results for mean time until exiting the system

Since the results for the fundamental matrix **N** (Equation 1) of scenarios A, B, and C1-C3 have dimensions of 11×11, 12×12, or 13×13 depending on the scenario evaluated, there are at least 121 different values that could be meaningful for each scenario when assessing the mean times in each state until the Cs atom leaves the system and all initial conditions. The selection of which values to evaluate depends on the questions being asked and the initial conditions of interest. For example, if the initial condition was the macrophytes and changes were applied to the macrophytes uptake rate, the mean time in the periphyton ($N_{5,4}$) may be useful to assess the effect of these changes on the periphyton. However, of particular interest for this work is

determining whether parameters that can be obtained from Equations 6-1 through 6-7 are useful in describing dynamics of the system and useful for assessing the example reverse engineering scenario of increased/decreased sediment remobilization. For these objectives, the selected elements of interest are all transient states with the water as the initial state and the biota with the biota themselves as the initial state. The latter are the diagonal elements, for example $N_{12,12}$ for the largemouth bass. The following are examples of these results (from the fundamental matrix **N** for the appropriate scenario):

- It will take an average of 46 years for ^{133}Cs atom to be removed from the Pond 4 system (go to Pond 5) with the originally modeled sediment remobilization
- It will take an average of 2.8 years for the ^{134}Cs atom to be removed from the Pond 4 system (go to Pond 5 or decay)
- A ^{133}Cs atom that entered the largemouth bass will spend an average of 387 days in the bass prior to exiting the system, versus 206 days for ^{134}Cs

Tables 6.1 through 6.4 provide the results of mean time to exit Pond 4 for scenarios A-C given either the water or the specified biotic state as the initial condition. Table 6.1. lists the results for the total mean time for ^{133}Cs to exit Pond 4 to Pond 5 (scenario A) and ^{134}Cs to exit Pond 4 to Pond 5 or by decay (scenario C1) given the ^{133}Cs started in the water. Additionally, the table includes the results from different sediment remobilization probabilities applied at 0.1, 0.5, 2, and 10 times the original values.

Table 6.1. Comparison of total mean years until a Cs-133 and Cs-134 atom exits the Pond 4 system to Pond 5 given the atom started in the water for different remobilization conditions; Scenario A and C2 results

Scenario	Initial State	[Sed ⇒ Water] ×0.1	[Sed ⇒ Water] ×0.5	No change in sediment remobilization	[Sed ⇒ Water] ×2	[Sed ⇒ Water] ×10
Cs 133	Water	424 yr	88 yr	46 yr	25 yr	9 yr

Cs 134	Water	2.85 yr	2.79 yr	2.72 yr	2.61 yr	2.20 yr

The mean time spent in each component prior to exiting Pond 4 when the component itself is the initial state are listed in Table 6.2 for ^{133}Cs (scenario A) and ^{134}Cs (scenario C1). These results are the diagonal elements of the fundamental matrices, **N**, for scenarios A and C1. Additionally, the relative change for ^{134}Cs is listed when remobilization probabilities are increased by a factor of 10 and decreased by a factor of 10. The corresponding relative changes in mean days prior to exiting for ^{133}Cs due to varying remobilization conditions are not included in Table 6.2. because they were miniscule, if noticeable at all.

Table 6.2. Mean days in each initial state prior to exiting Pond 4 to Pond 5 and by decay (for ^{134}Cs); Scenario A and C2 results

Initial State	Cs- 133 (Days*)	Cs- 134 (Days)	Cs -134 [Sed ⇒ Water] × 0.1 (days)	Cs -134 [Sed ⇒ Water] × 10 (days)
Water	394	52	34% ↓	235 % ↑
Submerged Vegetation	189	28	28% ↓	212 % ↑
Periphyton	41	12	11% ↓	145 % ↑
Sediment	44 yrs	944	13% ↑	46 % ↓
Snails	6.7	5.2	1.3% ↓	5 % ↑
Bluegill	375	267	0.2% ↓	0.8 % ↑
Plankton	5.39	5.36	5.9×10^{-3} % ↓	0.02 % ↑
Chaoborus Larvae	11.6	11.5	2.7×10^{-3} % ↓	0.01 % ↑
Lake Chub	229	133	1.9 % ↓	4.7 % ↑
Largemouth Bass	387	206	1.8 % ↓	7.1 % ↑

Overall, the total and individual component mean times for ^{133}Cs to exit Pond 4 are much greater than for ^{134}Cs, as would be anticipated.

Results of both ^{133}Cs and ^{134}Cs in Table 6.1. and Table 6.2. allow for comparison of the two isotopes and their relative response to the same adjustments in remobilization probabilities. A much greater variation in the latter can be seen for ^{133}Cs than ^{134}Cs in Table 6.1. Specifically, when remobilization probabilities are decreased by an order of magnitude from that originally modeled, there was a factor of nine increase in the total mean time until the ^{133}Cs exits the system. Remobilization probabilities an order of magnitude larger than those originally modeled resulted in a factor of five decrease in the mean total time until the ^{133}Cs atom exits the system. The mean total time for the ^{134}Cs to exit the system only varied by a two percent decrease and a 24 percent increase for the same remobilization variations. The mean time until exiting is not a linear change with increasing or decreasing sediment remobilization. These variations in total mean time are caused by a change in the mean time in the sediments prior to exiting the system (the average of $N_{1\text{-}3,6}$), as changes in the biota mean times are not observed.

The total mean time until exiting the system from Table 6.1 can be expressed as the fraction of time spent in the sediments, water, and biota. For scenario A and unaltered remobilization, on average, the ^{133}Cs spends 90.4% of the total time prior to exiting Pond 4 in the sediments, 6.9% of the total time in the water, and 2.7% of the total time in the biota. An order of magnitude increase in remobilization probabilities showed a substantial decrease in the proportion of time prior to exiting Pond 4 in the sediments with 48.6% of the total time in the sediments and an increase in the water at 36.9% of the time and biota at 14.5% of the time. An order of magnitude reduction in remobilization results in the vast majority of the time being spent in the sediments; specifically, 98.95% of the time in the sediments, 0.75% of the time in

the water, and 0.30% of the time in the biota. As mentioned in the previous paragraph, it is changes to the time spent in the sediments prior to exiting Pond 4 that are driving these changes in proportions. When considering the biota individually, the longest proportions of the total time prior to exiting Pond 4 are spent in the submerged macrophytes and largemouth bass and the shortest proportions of time prior to absorption are spent in the plankton and *Chaoborus* larvae; this is consistent for scenario A regardless of changes to the remobilization probabilities.

The proportions of time prior to exiting Pond 4 for ^{134}Cs (scenario C1) with initial condition of water and the baseline remobilization rate are 86.5% of the time in the sediments, 10.1% in the water, and 3.4% in the biota, respectively. When the remobilization probabilities are increased by a factor of 10, these proportions are 93.7%, 4.8%, and 1.5%. When the remobilizations probabilities are decreased by a factor of 10, the ^{134}Cs on average spends 48.9% of the total time prior to exiting Pond 4 in the sediments, 37.8% of the total time in the water, and 13.3% of the time in the biota. Unlike ^{133}Cs, there are noticeable changes in the time spent in the individual biota and water for the different remobilization conditions. However, the changes are small, and the ^{134}Cs remains in the sediments for the majority of time. When considering just the biota, a ^{134}Cs atom that starts in the water will spend the longest proportions of total time prior to exiting Pond 4 in the submerged macrophytes and largemouth bass, and the shortest proportions of time are in the plankton and *Chaoborus* larvae; this is the same behavior as ^{133}Cs and again is consistent regardless of changes to the remobilization probabilities.

The mean time spent in each model component prior to exiting Pond 4, when the component itself is the initial state, is listed in Table 6.2. for ^{133}Cs (Scenario A) and ^{134}Cs (Scenario C1). Decreases of different proportions are seen in the times for ^{134}Cs when compared to ^{133}Cs. The largest decrease is a 95% decrease in the time in the sediment and the smallest

decrease is a 0.6% decrease in the time in the plankton. Table 6.2 also lists the percent change in each value for ^{134}Cs when the remobilization probabilities are decreased by a factor of 10 and increased by a factor of 10. Larger variation is seen in increasing the remobilization from sediment probabilities than in decreasing these probabilities. A less than one percent change is observed for the bluegill, plankton, and *Chaoborus* larvae. The percent change for ^{133}Cs is not listed because no change is seen in these values even at six decimal places.

A useful aspect of applying absorbing Markov chains is that the user can define "exiting the system" differently to assess variations in model structure. This was done in scenario B for ^{133}Cs and scenario C2 for ^{134}Cs by making the transition from water to sediments a point of exit and setting the remobilization probabilities to zero. Table 6.3. lists the results for the *total* mean time until exiting the system for each biotic state and the water as initial conditions. This allows for a comparison of the different states without the sediments taking up the large proportion of time prior to exiting.

Table 6.3. Total mean days until absorption in Pond 5, sediment (assuming it is a sink), and decay (for ^{134}Cs) given the atom started in the specified component; Scenario C2 results.

Initial State	Cs- 133 (days)	Cs- 134 (days)
Water	64	57
Submerged Vegetation	72	65
Periphyton	145	117
Snails	170	129
Bluegill	570	399
Plankton	128	101
Chaoborus Larvae	196	147

Lake Chub	433	331
mouth Bass	302	241

An example interpretation of the table values for the bluegill, which has the largest value, is: If the ^{134}Cs starts in the bluegill, it will take an average of 399 days until it exits to the sediments, Pond 5, or decays. Not all of these days will be in the bluegill itself, as at minimum it will need to transition through the Pond 4 water prior to exiting. As seen in the first row of Table 6.3, a ^{133}Cs atom that starts in the water will take 64 days, on average, to exit the defined system. 24% of this total time is in a biotic component, and 76% of the time is in the water, on average. It will take, on average, 57 days for a ^{134}Cs atom to make the same transition, with 24% of this time in a biotic component and 74% of the time in the water.

Table 6.4 lists the results for the mean time spent in the water and biota given the initial state is the given biota or the water for scenario C2 calculated by the deterministic equation 6-2, as done in the previous tables, and also estimated by the Markov simulation.

Table 6.4.; Mean days spent in the biotic components until transitioning to Pond 5, sediment (assuming it is a sink), and decay (for ^{134}Cs); scenario C2 results.

Initial State	Cs-133 Deterministic (days)	Cs-134 Deterministic (days)	Cs-134 Simulation (days)
Submerged Vegetation	19.8	19.2	19.3
Periphyton	10.7	10.4	10.4
Snails	5.17	5.14	5.10
Bluegill	353	266	199
Plankton	5.38	5.36	5.37
Chaoborus Larvae	11.6	11.5	11.5
Lake Chub	148	130	117
Largemouth Bass	249	202	176

An interpretation of Table 6.4 along with that of Table 6.3 for bluegill is: If the ^{134}Cs starts in the bluegill, it will spend an average of 266 days in the bluegill out of the total average 570 days until it transitions to the sediments, Pond 5, or decays in the Pond 4 system. The table also includes the results of the comparison to the Markov simulation method explained in Chapter 5 for Scenario C2. The Markov simulation and the absorbing Markov chain calculation produce comparable results for all the biotic components with the exception of the fish.

Scenario C3 was added to assess the behavior when exiting the system is only by decay for ^{134}Cs. In this scenario, both the sediments and Pond 5 are transient states and are included in the system of interest. Scenario C3's fundamental matrix **N** was calculated, and it is the same as scenario C1 with the addition of the mean amount of time spent in Pond 5 prior to decay for each initial state. The total amount of time prior to decay is 2.98 years and this is the same for every initial state; such a result is expected since the rate of decay is the same from each state.

Equation 6-3 for the variance in the mean time spent in each state prior to exiting and the total time were calculated for each scenario with baseline parameters and for scenario A for remobilization probabilities at 10% and 0.1% of the baseline parameters. Overall, the variance was consistently very large as can often be the result (Kemeny, 1976). For example, the variance in the 46 years that it takes on average for the ^{133}Cs to exit Pond 4 to Pond 5 is 8.4×10^5 years (scenario A). The variance in the equivalent parameter for ^{134}Cs (scenario C1) is likewise large; specifically, 2.03×10^3 years for the 2.72 year mean total time it takes for ^{134}Cs to exit either to Pond 5 or by decay. As would be expected for a large total variance, the variance in the mean time spent in each state prior to exiting is also large. Changes in sediment remobilization probabilities did not make a significant difference in the relative size of the variances.

6.3.2. Results for probabilities of exiting the system to different absorbing states

Another parameter evaluated for use in adding insight on the dynamics of Pond 4 is **B**. When there are multiple absorbing states the probabilities of exiting to each of these states from a given initial state can be found by solving Equation 6-7 for **B**. These probabilities were calculated for scenarios B, C1, C2, and C3, as these were the scenarios that had more than one absorbing state (Pond 5 is the only absorbing state for scenario A, so there is a 100% probability of exiting the Pond 4 system to Pond 5)**.** For scenario B and ^{133}Cs starting in water, there is a 95.9% probability of exiting the system to the sediments and a 4.10% probability of exiting to Pond 5. For the comparable scenario C2, the probabilities for ^{134}Cs to exit the Pond 4 system when the initial state is the water are 91.04% to the sediments, 3.73% to Pond 5, and 5.23% to decay from all other states. In scenario C1, the sediment is not a sink and baseline remobilization probabilities are used. In this situation, the probability of a ^{134}Cs atom exiting to Pond 5 is 8.6% and the probability of exiting by decay is 91.4%. This probability of exiting by decay can be divided into probabilities of exiting by decay in the sediments of 79%, by decay in the Pond 4 water of 9%, and decay in biota of 3%.

Since the only "route of exit" in scenario C3 is by decay in each of the different components, including Pond 5, the probabilities given in the matrix **B** indicate where in the system ^{134}Cs decay is most likely to occur. For an initial state of interest being the water, the highest probability of transition of the ^{134}Cs by decay is in the sediments, at approximately 80%. The next highest probability of decay is in the Pond 4 water at 9.2%, followed by decay in the Pond 5 water at 8.6%, and with decay in the biota having a 3.1% probability. Of the biota, decay in the macrophytes, lake chub, and largemouth bass have the largest probabilities.

Using **B**, it is also possible to quantify the probabilities of decay given the ^{134}Cs initial state is a specific biota. The sediment remains the component with the highest probability of decay occurring, regardless of what biota is specified as the initial state. Decay in the water or in Pond 5 is more likely than decay in the biotic initial state for the primary producers and primary consumers. If a secondary consumer (i.e., the fish) is the initial state, then there is a larger probability that decay occurs in the fish than the water of Pond 4 or Pond 5 (approximately a factor of 2-3 × larger).

6.3.1. Results for cycling behavior of system

The mean number of state changes that are expected for each model component as the initial state was calculated for scenarios A and C1 following the procedure described in the methods section of this chapter. Given an initial state of the water, ^{133}Cs is predicted to change states 86 times on average prior to exiting the system and ^{134}Cs is predicted to change states 8 times on average prior to exiting the system. Given an initial state in the biota, ^{133}Cs is predicted to change states 90 times on average prior to exiting the system and ^{134}Cs is predicted to change states 8 times on average prior to exiting the system. The mean number of state changes was also assessed for different remobilization conditions for scenario A. While changing remobilization conditions of a scenario changes the mean time prior to exiting the system when compared to the baseline scenario, it does not change the average number of state changes prior to exiting the system.

Table 6.5 compares the mean number of state changes through the biotic states for scenarios A and C1 when the initial condition is the biota itself. As the initial state in the biota counts as the first state, all values are above one.

Table 6.5. Predicted mean number of state changes prior to exiting the system by absorbing Markov chain techniques given the initial state is the biotic component itself.

Initial State	^{133}Cs/Scenario A	^{134}Cs/Scenario C3
Submerged Vegetation	14.01	2.11
Periphyton	4.28	1.27
Snails	1.31	1.02
Bluegill	1.07	1.004
Plankton	1.0013	1.00011
Chaoborus larvae	1.0006	1.00005
Lake chub	1.58	1.0361
Largemouth bass	1.59	1.0357

The degree above a value of one indicates how much cycling is expected to occur. The largest degree of cycling is seen in the macrophytes with the smallest degree in the *Chaoborus* larvae. This is consistent whether the atom is ^{133}Cs or ^{134}Cs, but cycling is reduced substantially when decay occurs. For example, a ^{133}Cs atom in the macrophytes is expected to return to the macrophytes 13 times on average prior to transitioning to Pond 5. A ^{134}Cs atom is only expected to return to the macrophytes approximately 1 more time prior to exiting to Pond 5 or decaying in a Pond 4 component. For plankton, a ^{133}Cs atom will change states 1.0013 times on average. Since this value is only 0.0013 greater than 1, most Cs atoms will not return to the plankton prior to exiting to Pond 5. For example, if there were initially 10,000 ^{133}Cs atoms in the plankton, only 13 of these atoms would return to the plankton prior to transitioning to Pond 5. If the values in

Table 6.5 are less than 1.5 it is more likely that the atom will not return to the biotic component it started in than it is that it will return.

Table 6.6. lists the results from assessing the cycling occurring in Markov simulations for ^{133}Cs scenario A and ^{134}Cs scenario C1 of 10,000 atoms over a two year period with the initial condition in the listed biotic state.

Table 6.6. Cycling occurring in model components for ^{133}Cs scenario A and ^{134}Cs scenario C1 predicted by a Markov simulation

Initial State	Percent of atoms that visit once	Percent of atoms that visit twice	Percent of atoms >2 visits	Mean State Changes
Cs-133				
Bass	97.3%	2.7%	0.01%	1.027
Lake chub	97.3%	2.7%	0.01%	1.027
Periphyton	79.8%	17%	3.2%	1.33
Macrophytes	29%	42%	29%	2.47
Plankton	99.97%	0.03%	0%	1.0003
Cs-134				
Bass	99.25%	0.75%	0.01%	1.008
Lake chub	98.1%	1.9%	0.01%	1.019
Periphyton	85%	13%	2%	1.18
Macrophytes	29%	42%	29%	2.18
Plankton	99.97%	0.03%	0%	1.0003

The simulation was performed for largemouth bass, lake chub, periphyton, macrophytes, and plankton as the initial states for comparison to the state change results in Table 6.5. The

macrophytes showed the highest degree of cycling, followed by the periphyton, then fish and plankton. The simulation results indicate that over a two year period 15% of ^{133}Cs can be expected to visit the macrophytes once, 48% of the ^{133}Cs can be expected to visit the macrophytes twice, and 37% can be expected to visit more than twice. For ^{134}Cs, less cycling through the macrophytes occurs, and these values are 29%, 42%, and 29%. Overall, less cycling occurs for ^{134}Cs in each of the evaluated biota with the exception of plankton, where very minimal cycling is observed for both ^{134}Cs and ^{133}Cs.

While Table 6.6 is descriptive of the cycling and useful for comparison of ^{133}Cs and ^{134}Cs, the Markov simulation results can also be evaluated for an average number of state changes through a given component, and this is more directly comparable to the absorbing Markov chain results of Table 6.5. Specifically, the average number of state changes through the macrophytes after starting in the macrophytes, over the two year period, was calculated from the simulation results as 2.5 for ^{133}Cs and 2.2 for ^{134}Cs. For periphyton, the same parameters were 1.24 for ^{133}Cs and 1.18 for ^{134}Cs.

6.4. Discussion

Absorbing Markov chain techniques offer straight forward techniques to solve for several parameters that offer insight into the Cs dynamics for Pond 4. Of particular usefulness in understanding the unmodified Pond 4 system better are the parameters that describe the total mean time until the Cs exits the system to Pond 4, the time in each component prior to exiting, and the number of state changes that occur prior to exiting. These values were calculated as 46 years for ^{133}Cs to exit Pond 4 to Pond 5 and 2.8 years for ^{134}Cs to exit Pond 4 to Pond 5 or decay. While absorbing Markov chain calculations can calculate the variance in the mean times prior to exiting the system, these are overall very large values that do not add additional insight other

than confirming that the range in the mean times are substantially larger than the mean values themselves. The mean time of 46 years for ^{133}Cs is a long period of time and it is acknowledged that changes are likely to occur to the pond system that could change the ecosystem framework, population levels, or transfer probabilities. These changes could have an impact on the mean duration spent in the system, and it may be more useful to consider relative predictions of reverse engineering changes than absolute quantities.

The use of absorbing Markov chain methods was applied to two reverse engineering scenarios in the current work, first the extension of the model to ^{134}Cs and second the investigation of both the ^{133}Cs model and the ^{134}Cs model with different sediment remobilization probabilities. Prior to this effort, we have used primarily the change in inventory level from the ODE kinetic model (or Markov matrix model) to evaluate the changes. While useful, the change in inventory level is one measure. The use of absorbing Markov chain methods adds the possibility of three measures for comparing the dynamics of ^{134}Cs and ^{133}Cs and for assessing the effect of changes to the transfer probabilities. These measures are: 1) mean time prior to exiting the system; 2) number of state changes prior to exiting the system; and 3) probabilities of the different routes of exiting the system. The first and second measures can be assessed for total time and for time in each biotic component given water or of the different biotic components with only a few steps and simple calculation.

The absorbing Markov chain methods described and applied in this chapter to Pond 4 can be validated through a couple methods. One method of validation is recognizing that for scenario 3 the total mean time for the ^{134}Cs atom to leave the system should be equal to the mean life of a ^{134}Cs atom since decay is the only route of leaving the system. The mean life is defined as the average time it takes for an atom to decay. The mean life is different than the half life, $t_{1/2}$,

and the mean life is equal to 1.44 $t_{1/2}$. The mean life calculated using the ^{134}Cs half life is equal to 2.98 years, which is the same as predicted by **N** for the total mean duration of the ^{134}Cs in the system. This is what would be anticipated, and validates that the absorbing Markov chain calculations are being done correctly.

The previously developed Pond 4 Markov simulation model was used as validation of the absorbing Markov chain results. One comparison was the mean days spent in the biotic components prior to exiting the system for scenario C2. As can be seen in Table 6.4, the results for the submerged vegetation, periphyton, snails, plankton, and *Chaoborus* larvae are comparable for both the simulation model results and the absorbing Markov chain results. The results for the fish are not as comparable, but are only 10% shorter for lake chub and largemouth bass. Bluegill has the greatest disparity with the mean duration predicted by the simulation being 25% shorter than the mean time predicted by the absorbing Markov chain calculation. These results for the fish are not so different as to indicate a problem in either the simulation or the calculation. Shorter results would be expected for the fish since the simulation is only over a two year period and some of the Cs is anticipated to be in the fish still at the end of this period.

The absorbing Markov state change results were also compared to what would be predicted for a two year period by the Markov simulation. While the results in Tables 6.5 and 6.6 are not directly comparable due to the differences in each method's period of time, the general trend can be assessed. This trend is the same for both approaches: the most cycling occurs through the macrophytes, followed by the periphyton, the fish, and then the plankton. The comparable behavior of both methods supports the use of the absorbing Markov chain calculations if a quantitative description of cycling over a time period comparable to the mean time until absorption is desired, or qualitative assessment of the degree of cycling if timeframes

of interest are shorter than the mean time until absorption. For example, the mean time for ^{134}Cs to exit the system by decay is approximately two years, and the absorbing Markov chain state changes from Table 6.5 vary less than 10% from that predicted by the two year Markov simulation and given in Table 6.6. The mean time for ^{133}Cs to exit the system to Pond 4 is 46 years, and the state changes of the two year simulation are not quantitatively reflective of that from the absorbing Markov chain. This deviation is particularly noticeable for the macrophytes and periphyton where a higher degree of Cs cycling occurs. If a quantitative assessment of the cycling is desired over a shorter timeframe, such as a two year period for Pond 4, then the Markov simulation should be used.

The goal of decreasing the sediment remobilization is to capture more Cs in the sediments and lower the values in the biota. Suggested techniques to accomplish this include: 1) the addition of K to the water column; 2) the addition of lime to the water column; and 3) the addition of illite clays to the water (Smith et al., 2002, Hinton et al., 2006, Hakanson and Andersson, 1992). The absorbing Markov chain results suggest that if these techniques lower the resuspension probabilities by up to about 50% then there is minimal change seen in decreasing the mean time Cs spends in the biota prior to exiting the system, with the exception of the submerged macrophytes and periphyton for ^{134}Cs. However, there is a substantial increase in the total time spent in the system prior to exiting the system. The majority of this increase is spent in the sediments, as would be desired for lesser impact on the majority of biota in a typical aquatic ecosystem.

While absorbing Markov chain methods provide results that are descriptive of the system and its individual states, the question may be posed if determining the inventory levels alone is satisfactory to assess the effects of increasing and decreasing remobilization probabilities.

Figures 6.2A and 6.2B provide graphs of ^{133}Cs largemouth bass inventory results over 500 days after addition using the previously developed Pond 4 Markov matrix model (Miller and Johnson, *in review*) and increasing and decreasing sediment remobilization probabilities to the same degree as done for this paper. A nonlinear response to changes in remobilization is seen for inventory levels as was observed for the mean time until exiting calculated by the absorbing Markov chain method. For ^{133}Cs and remobilization probabilities that are 50% or 10% of the baseline levels, there is an average daily decrease in inventory levels of 9% or 16%, respectively, over the 500 day period. For ^{134}Cs the average daily percentage decreases are 26% or 32% for 50 or 10% of the baseline, respectively. These decreases in inventory are useful in assessing the impact of the decreased remobilization, but the most beneficial approach is the use of the inventory assessment in tandem to the absorbing Markov chain calculations. For example, an average decrease of 9% inventory level may not be much but it does cause the ^{133}Cs to stay in the Pond 4 system, primarily in the sediments, for about twice as long as the baseline time. The absorbing Markov chain indicators may provide a stronger rationale for decision making efforts than considering inventory levels alone.

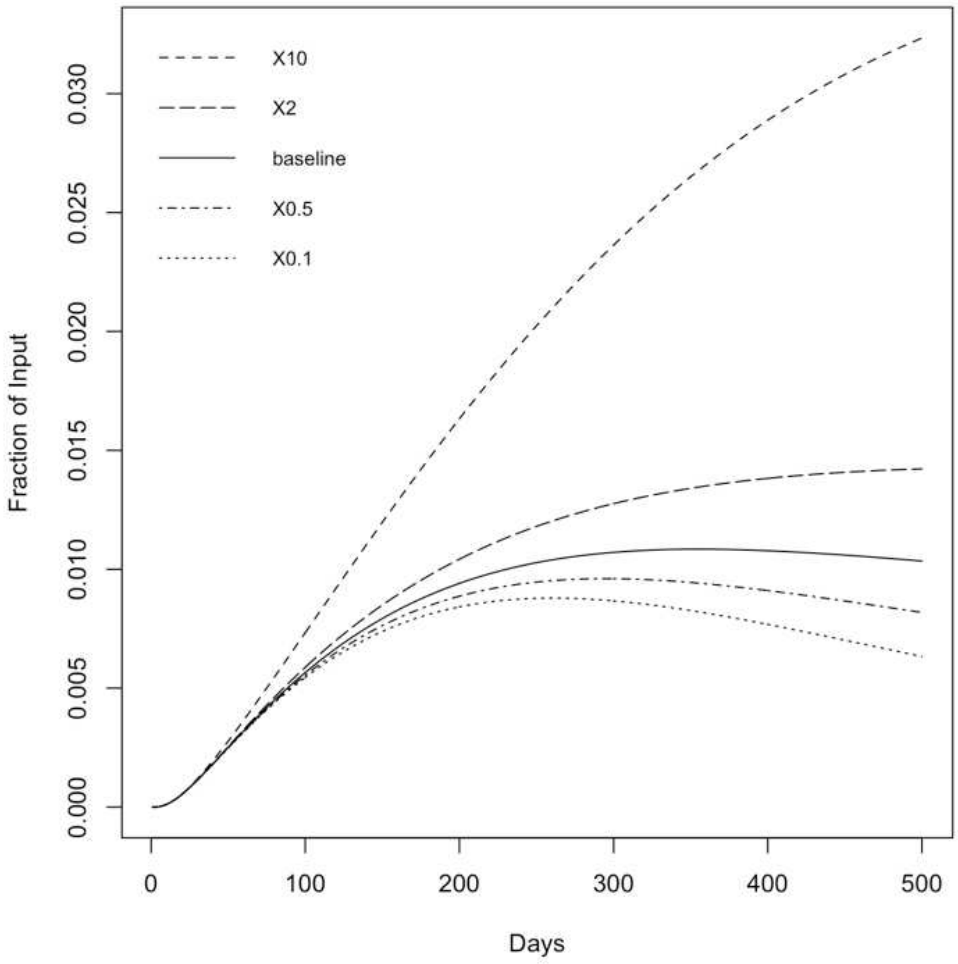

Figure 6.2A Largemouth bass ^{133}Cs inventory response to varying the remobilization probabilities, expressed as a fraction of input amount

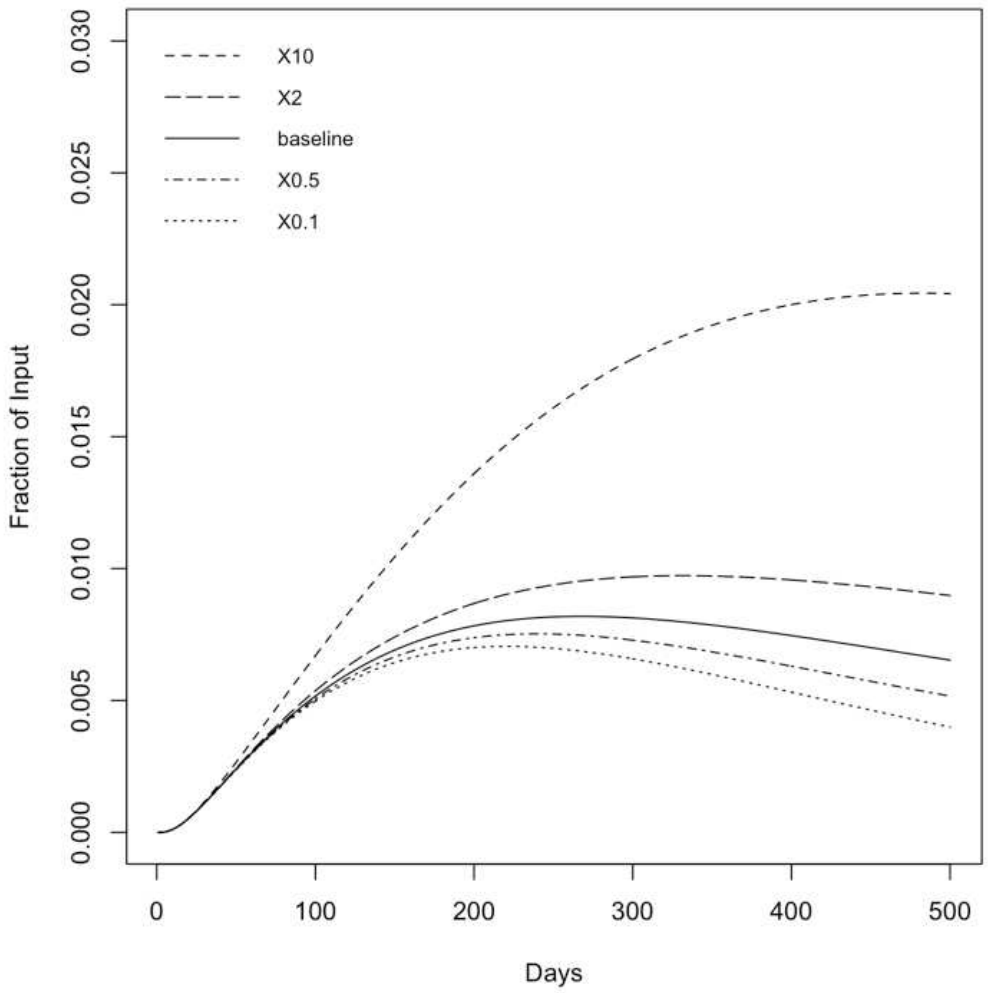

Figure 6.2B. Largemouth bass ^{134}Cs inventory response to varying the remobilization probabilities, expressed as a fraction of input amount

Last, a unique and useful absorbing Markov chain technique is to quantify which route of exit is most probable when there is more than one route of exit to the system. Though this parameter was not applied for the Pond 4 baseline ^{133}Cs because the only route of exit was Pond 5. Otherwise, it is useful in describing the system dynamics for the other exit scenarios and the reverse engineering scenario of a ^{134}Cs addition. Additionally, this technique could be used for comparing and contrasting reverse engineering remobilization probabilities. It would be most

useful in the situation where the probabilities of exits by different routes were close to each, and the question could be further specified as whether remobilization changes would make it more likely that the Cs would change its primary route of exit.

6.5. Conclusion

Absorbing Markov chain techniques provide information about system dynamics that are not possible to obtain through traditional compartment models. Additionally, the techniques were easily implemented to beneficially augment the previously developed Markov chain matrix modeling of the Pond 4 inventories (Miller and Johnson, *in review*). It is not a difficult extension to apply the calculations to the same transitional probability matrix used for this model. The absorbing Markov chain calculations provide several parameters that can be used in assessing reverse engineering scenarios. However, if the behavior over a specific time period is of interest, such as the first two years, the Markov simulation method should be used to evaluate the cycling in the system.

Further work could include extension to different reverse engineering scenarios such as: 1) remediation efforts targeting decreases in sediment remobilization implemented at a later time interval, for example 90 days after addition; 2) changes in the water flow out of Pond 4; or 3) changes in the excretion rates of the biota, as could be expected to occur during the winter months (Kryshev, et al., 1999). The same calculations and comparisons accomplished in this paper could also be performed for ^{137}Cs or a mixture of ^{134}Cs and ^{137}Cs as would be most realistic after an incident involving nuclear material. In the future, applying absorbing Markov chain procedures to a different compartment model system could provide interesting and heretofore unavailable system information.

CHAPTER SEVEN. CONSIDERATION OF A TEMPERATURE EFFECT ON ^{133}CS AND ^{134}CS USING POND 4 TIME INHOMOGENEOUS MARKOV MODEL

7.1. Introduction and Objectives

Cs levels in fish have been reported as having a seasonal variation per multiple studies (Peles, et al. 2000; Kolehmainen, 1979) with the effect attributed to varying temperatures in the water. In both of these studies, the Cs had been added tens of years earlier and the lakes would have been close to equilibrium conditions. The Kohleheim study, at White Oak Lake in Oakridge, TN, measured ^{137}Cs and ^{133}Cs concentrations in bluegill (and other fish studied) and concluded that 1) Cs levels varied in a sinusoidal manner over time; 2) maximum Cs levels occurred in late winter and minimum concentrations in late summer; and 3) the maximum seasonal Cs levels were about 35% greater than the minimum levels. The Peles' *et al.* study, which was for largemouth bass in a neighboring cooling pond to Pond 4 (Pond B), concluded that 1) the maximum levels occurred in September/October and were approximately 30% greater than the minimum levels which occurred in February/March; 2) the best fit to these data was an asymmetric saw tooth versus a sinusoidal behavior; and 3) that the month of sampling accounted for 17% of the variation seen in the results, per their analysis of covariance that also included size and sex. Since the Pond 4 models developed in this dissertation are population averaged, size and sex variation is not relevant. However, since the model is dynamic, an attempt was made to model variation in model behavior due to temperature through use of a time inhomogeneous Markov (TIM) model. It is possible that a temperature trend occurred during the Pond 4 experiment, but not enough samples were taken to observe a notable trend in the results when evaluating the fish of different size ranges separately.

After development of a ^{133}Cs TIM model in agreement with the baseline model inventories (does not deviate more than 30% from the baseline model), the TIM model was extended to model a ^{134}Cs input. The extension to ^{134}Cs enables:

1) Estimation of the dose to fish predicted by this model for an acute addition of Cs to the pond, and
2) Quantification of the effect of including versus not including temperature on this dose.

Additionally, the dynamic behavior of the concentration ratios over time was assessed for the TIM model and unmodified model and compared to what would be predicted at equilibrium.

The objectives of this chapter are to:

1) Evaluate the behavior of modifying elimination transfer probabilities to account for change due to temperature by use of a time inhomogeneous Markov chain
2) Evaluate what corresponding changes may be needed for uptake probabilities to maintain reasonable inventory levels
3) Apply the model to the reverse engineering scenario of ^{134}Cs added to the pond
4) Assess results on concentration ratio and internal dose

Objectives 2 through 4 were primarily limited to an evaluation of the largemouth bass inventories. The balance of elimination and uptake in biota over seasons is not straightforward and the scope of the current application is more focused on the largemouth bass due to 1) the larger amount of literature on this popular angling species, and 2) the bass had the longest timeframe of sampling in the Pond 4 experiment out of all the biota.

7.2. Methods

The Pond 4 time inhomogeneous Markov (TIM) model is simply an extension of the Markov matrix model explained in Chapter 5 (Equation 5-1), where the transfer coefficients are varied

for each time step to account for possible changes in the rates due to observed changes in the water temperature over the experimental period. A time inhomogeneous Markov chain has a different transfer probability matrix, $\mathbf{P_t}$, for each day *t* (Acevedo, 2013). The Pond 4 TIM model fractional distribution of Cs inventory levels was computed by:

$$\mathbf{S} = \mathbf{S_o} \prod \mathbf{P_t} \qquad (7-1)$$

As before, **S** is a vector where each element corresponds to a state in the model, and $\mathbf{S_0}$ is the initial distribution of Cs expressed as a fraction. The initial distribution was not varied from the previous chapters. State numbers for the TIM model indicating each model component are also the same as in previous models. Multiplying **S** by the initial input level gives the absolute values of inventory, though most results in this chapter are expressed as fractional inventories. For the Pond 4 TIM model, methods were first developed for a variation of the TIM model using only temperature adjusted elimination probabilities, followed by a version of the TIM model with elimination and uptake probabilities adjusted. The final TIM model selected was most appropriate for the largemouth bass. It was extended to a ^{134}Cs reverse engineering version. This version was used for the calculation of dose in the largemouth bass along with the calculation and comparison of largemouth bass concentration ratios over time.

7.2.1. General temperature behavior in Pond 4

The temperature data from 200 days prior to the experiment through about 550 days after the addition (through Jan 2002) was selected for an evaluation of a two year trend of behavior. The raw data are plotted in Figure 7.1..

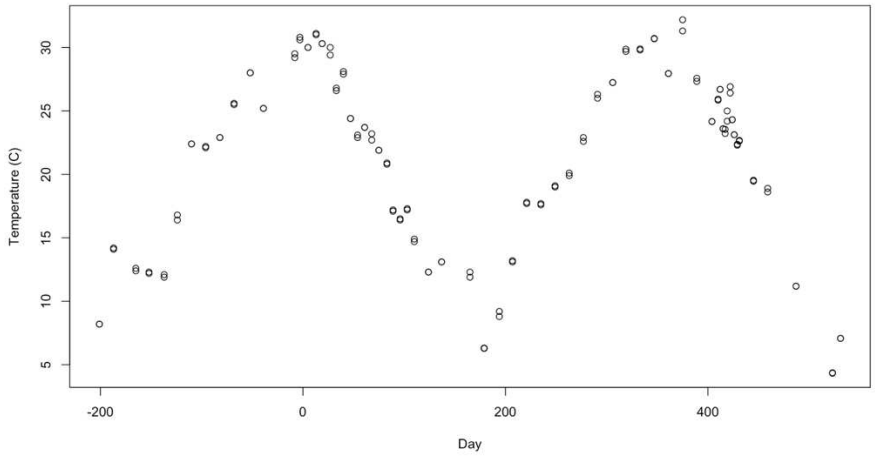

Figure 7.1. Plot of temperature data in Pond 4 for 200 days prior to the experiment to 530 days after the experiment.

Though the full depth profile was measured at 0.5 meter increments for temperature (at site A on Figure 1), the temperature measurements used in this chapter are from 0.5 and 1 meter depths where the biota would primarily reside. A sinusoidal curve in linear format of $y = a \sin\left(2\pi \frac{x}{365}\right) + b \cos\left(2\pi \frac{x}{365}\right) + c$ was fit to the temperature data. The constants *a*, *b,* and the intercept *c* were numerically solved using "lm" in the program R to do the regression (REF). A linear model can be applied instead of a nonlinear model due the following identity that $y = A \sin(x + \varphi)$, a sinusoidal curve, can be written in the linear form $y = a \sin(x) + b \cos(x) + c$ given the trigonometric principles $\sin(\varphi) = \frac{b}{\sqrt{a^2+b^2}}$, $\cos(\varphi) = \frac{a}{\sqrt{a^2+b^2}}$, $A = \sqrt{a^2 + b^2}$, and sin(a+b) = sin(a) cos(b)+cos(b) sin(a). The following shows the application of these principles:

$$a \sin(x) + b \cos(x) = \sqrt{a^2 + b^2}\left(\frac{a}{\sqrt{a^2 + b^2}} \sin(x) + \frac{b}{\sqrt{a^2 + b^2}} \cos(x)\right)$$

$$= A(\cos(\varphi) \sin(x) + \sin(\varphi) \cos(x)) = A \sin(x + \varphi) \qquad \text{Eq (7-1)}$$

For temperature data, $x = 2\pi \cdot \frac{t}{365}$, since we know the period of the sinusoidal behavior is 365 days.

Figure 7.2 illustrates the sinusoidal fit to temperature data for days 1-500 after addition. A decrease deviation from the fit was manually added for a one week span around day 179, where the measured temperature was 6.3 °C, to approximately account for a dip in observed temperatures that was outside of the sinusoidal fit. The temperature values were altered to vary one degree per day over this period, as a possible timespan for such a change to occur based on the temperature data. It is possible that the decrease lasted slightly longer than one week, but based on the behavior of the other temperature data it is unlikely to be shorter. It is likely the decrease and increase were not linear or balanced, but such deviations are not expected to significantly alter the model response. The model output was assessed with and without this added temperature deviation.

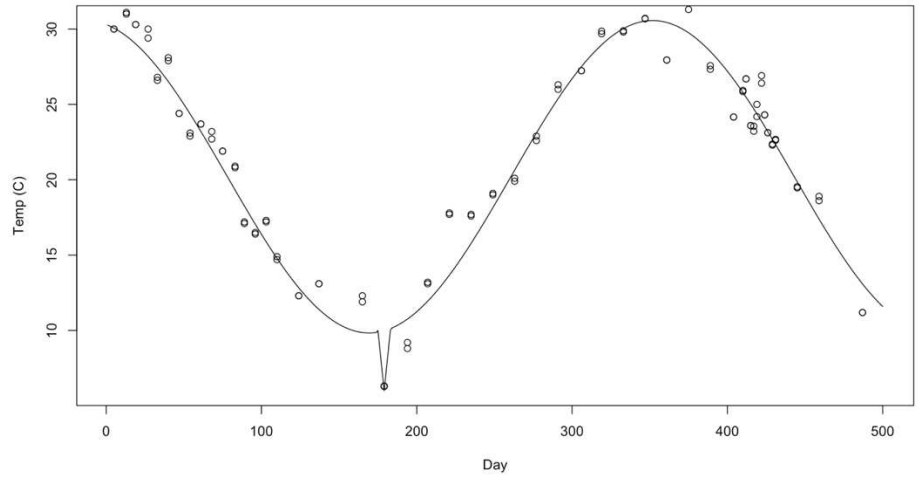

Figure 7.2. Sinusoidal fit with added cold weather deviation, as applied to temperature data

The results of the regression are given in Table 7.1. The *t* values indicate that the fit is statistically significant. The residuals for the fit are -5.66, -1.05, -0.04, 1.24, and 4.29 for the minimum, first quartile, median, third quartile, and maximum, respectively. The adjusted R squared value was 0.9327. The resulting equation for the linear model of temperature, *T*, on day

t is given below:

$$T(\mathrm{t}) = 10.1\cos\left(2\pi \cdot \frac{t}{365}\right) - 2.33\sin\left(2\pi \cdot \frac{t}{365}\right) + 20.2 \qquad \text{Eq (7-2)}$$

Table 7.1. Coefficients for sinusoidal fit to temperature data

	Estimate	Standard Error	*t* value	Pr(>|*t*|)
a	-2.3337	0.2298	-10.15	$<2\times10^{-16}$
b	10.1082	0.2395	42.20	$<2\times10^{-16}$
c	20.1711	0.1659	121.58	$<2\times10^{-16}$

7.2.2. Temperature correction factor applied to elimination transition probabilities for biota to water

Daily temperature correction coefficients, TCF_{ex}, for the excretion rates were computed based on the Q_{10} law, which states that there is approximately a two to three-fold change in reaction rates for every 10 degree change of water temperature (Leveque, 2003). Though a generality, this was applied for excretion rates of fish in the previous modeling discussed in Chapter two of this dissertation (VAMP, 2001). Mathematically, the Q_{10} law is stated as:

$$TCF_{ex} = Q_{10}^{(T2-T1)/10} \qquad \text{Eq (7-3)}$$

where Q_{10} is equal to the appropriate value between 2 and 3. There is little literature on the exact value between 2 and 3 to use for aquatic species, and 2 was selected for the current model efforts as was used in the VAMP model. Applying Equation 7-2 gives the following graph, Figure 7.3, for daily temperature based correction factors that can be applied to selected biotic component excretion rates. It is not surprising that the hottest temperatures (and TCF_{ex} ~1) were at the beginning of the addition experiment since it started on 1 August (day zero). For reference, day 153 of the experiment was 1 January; day 243 was 1 April, and day 426 was 1 October of the second year of the experiment. The coldest temperatures occurred in February.

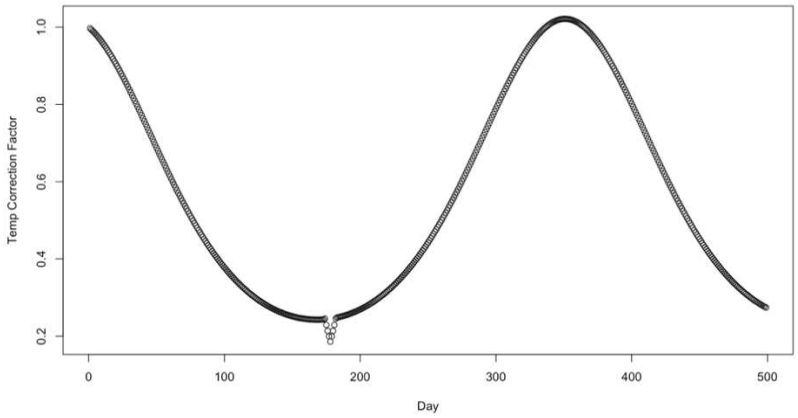

Figure 7.3. Temperature correction factor for excretion rates

These daily temperature correction factors were applied for three "options": 1) largemouth bass excretion, 2) all fish excretion, and 3) all food chain components. These factors were compared to the unadjusted baseline. Assessment of each of these scenarios was accomplished so that comparisons of the effect of applying the temperature corrections for elimination could be assessed in a step by step manner.

7.2.3. Temperature correction factor applied to transition probabilities for fish uptake by consumption

To account for decreased consumption rates by fish species during cooler temperature periods, three different approaches were applied and investigated to create a temperature correction factor for uptake, $TCF_{up,}$ to be applied along with the elimination correction factors. This correction was applied to:

1) The transition probabilities of largemouth bass uptake:
2) Lake chub to largemouth bass, $p_{11,12,}$ and
3) Bluegill to largemouth bass, $p_{8,12}$.

The correction factors for elimination from largemouth bass were also applied. If the response in the largemouth bass was reasonable, the method was also assessed for the uptake for the other fish, and the probabilities of transition from periphyton to lake chub, $p_{5,11}$, snails to bluegill, $p_{7,8}$, chaoborus larvae to bluegill, $p_{10,8}$ were altered. While it was anticipated that there were changes to the uptake rates of the primary producers due to less sun during the winter months, and likely a change also occurred in the snails and *Chaoborus* larvae, such an effect was not investigated in the current work since after approximately the first 30 to 60 days of the experiment, the ^{133}Cs levels had dropped to relatively low amounts in these biota compared to the fish.

The experimental results on largemouth bass consumption of Smagula and Adelman (1982) were used to develop two of the first approaches of model modifications for uptake. Smagula and Adelman's (1982) experiment was a laboratory experiment where young largemouth bass were fed a constant level of food while the temperature was varied and consumption rates at different temperatures were assessed. The results provided in their paper showed that consumption was reduced by a factor of two at 14°C compared to 20°C and increased by a factor of three for 26°C compared to 20°C. These results suggested an exponential decrease with decreasing temperature and the following fit was determined from relative change from 26°C, where T is temperature

$$\text{Relative change} = 0.0193\ e^{0.01493T} \qquad \text{Eq (7-4)}$$

with an R^2 value of 0.98. This relationship was applied to the estimated daily temperatures for Pond 4 (using Equation 7-2) and then normalized (such that day zero was equal to a value of one) to create the daily uptake correction factors, TCF_{up}, plotted in Figure 7.4. This prediction of reduced intake due to temperature is limited due to 1) the experiment being a laboratory versus

field study; 2) the behavior was reported at only three temperatures; and 3) young largemouth bass being the subject of the study as the Pond 4 fish are older and larger fish (>300 mm in length) whose consumption behavior is expected to be different. While these limitations are significant, a study that reported consumption over a range of given temperatures for largemouth bass (or lake chub or bluegill) was not found in the available literature.

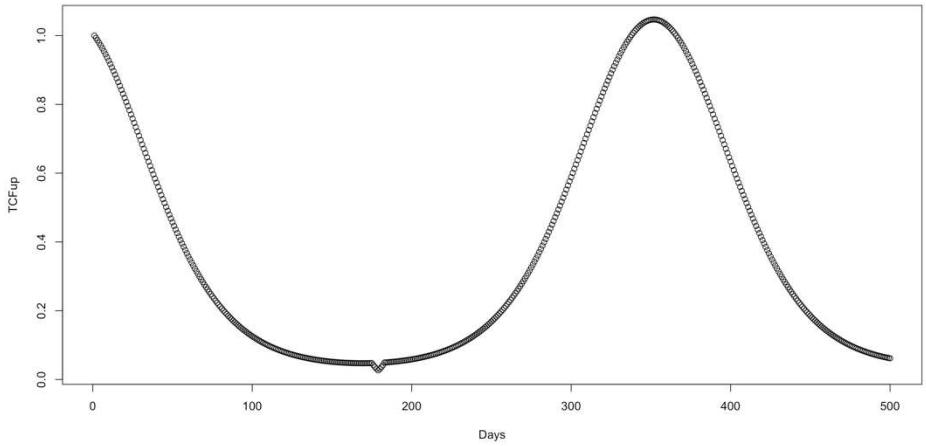

Figure 7.4. Correction factor for reduced consumption due to uptake

The lowest uptake correction factors of approximately 0.05 during the winter months are not unreasonable since the results of Peles et al. suggest that largemouth bass in nearby Pond B do not consume very much at all during this time period. Additionally, the sharpness of the decline and the duration of the lowest values (from approximately November-February) does match the period of time Peles *et al.* reported minimal to zero fish consumption by bass. However, it may be too large or long in duration for the model framework and transfer coefficient estimation methodology used in the Pond 4 modeling. Regarding the latter, since the transfer coefficients in the baseline model were originally optimized to match the behavior of the inventories over approximately a one year period for the bluegill and lake chub, and a 500 day

period for the largemouth bass, they represent a "time averaged" transfer coefficient. The two other uptake correction methods applied were developed to attempt to take this into consideration.

In the second approach, the probabilities describing consumption were reduced to 10% of the unmodified model levels for a period of the coldest temperatures in Pond 4, days 150 to 210 (Jan-Mar), and the other days' transfer coefficients were not altered. A value of 10% was selected as a reasonable estimate for an average reduction over this period of time based on the average behavior of the fish stomach analysis results from the Peles experiment. Such a step-wise approach may still not be an appropriate method, so a third approach of uniformly decreasing the transfer coefficients was applied. The degree of decrease was a constant and empirically derived reduction factor applied to the transfer coefficients for every day such that the adjusted inventory levels did not deviate more than approximately 25% from the unadjusted values. Approaches 2 and 3 were applied to the largemouth bass component first, and then to all fish components. The outputs of each of these models were compared to the unadjusted version, the Markov matrix model, which is time homogeneous (Chapter 5).

7.2.3. Concentration ratio and dose assessment in largemouth bass

The most reasonable time inhomogeneous Markov model for temperature correction was applied to the ^{134}Cs Markov model discussed in Chapter 6 where the decays occurring in each component were computed. The following procedures were followed just for largemouth bass. Though dose and concentration ratios could be assessed for each biota of the model, that is beyond the scope of the current work.

7.2.3.1. Procedures to compute concentration ratios

Since concentration ratios are simply the concentration of Cs in the biota of interest divided by the concentration in the water (in comparable units), it is possible to compute the daily concentration ratios from any of the Pond 4 models using the biomass values. The concentration ratios (CR) for largemouth bass can be computed by the following procedure:

$$\mathrm{CR} = \frac{\text{Fraction of Inventory in LMB x Input}/_{LMB\ biomass}}{\text{Fraction of Inventory in Water x Input}/_{pond\ volume}} = \frac{\text{Fraction of Inventory in LMB x Input}/_{360\ kg}}{\text{Fraction of Inventory in Water x Input}/_{1.5\times10^{8}L}}$$

Considering that 1 L of water is equal to 1 kg of water and that s_{12} is the largemouth bass element of the fractional distribution of Cs inventory, **S,** and s_1, s_2, and s_3 are the elements for water,

$$\mathrm{CR}(t) = 4.2\times10^{-11}\frac{s_{12}}{\Sigma_1^3 s_n} \qquad \text{Eq (7-5)}$$

The concentration ratio response over time was compared for the TIM model and the Markov matrix model for both ^{134}Cs and ^{133}Cs, and both were compared to literature values at equilibrium. Note that this is a wet weight concentration ratio; sometimes this value is reported in terms of dry weight (fish mass dried and then sampled). As explained in Chapter 2 of this dissertation, the Pond 4 model inventories were computed from daily estimates of wet weight concentrations.

7.2.3.1. Procedures to compute largemouth bass daily dose

Dose in a biota can be approximated by multiplying the biota concentration levels in Bq/kg by a dose conversion factor (DCF) which is generic for all pelagic fish, and given in ICRP report 108 as 2.0×10^{-4} μGy/h per Bq/kg of wet weight. Since the model output is daily fractional inventory, the largemouth bass fraction s_{12} of each day was multiplied by the input to the lake

(in Bq) and then divided by biomass to get concentration; this is then converted to dose using the DCF:

$$dose\ rate(t) = \frac{Input \cdot s_{12}}{360} DCF \qquad \text{Eq (7-6)}$$

The units above are μGy/h, so multiplying by 24 gives an approximation for the model predicted daily internal dose for the largemouth bass.

7.3. Results

7.3.1. Response of TIM model with excretion probabilities varied for temperature

The ^{133}Cs inventory results of the TIM model with excretion probabilities adjusted are given in Figures 7.5 through 7.9 for the largemouth bass, lake chub, bluegill, periphyton and plankton, respectively. The output of the Markov matrix model, the unmodified output, is also included in each plot for comparison. The legend of each figure indicates whether 1) just the largemouth bass, 2) all fish, or 3) all food chain excretion probabilities were modified. The difference in behavior due to the response due to the added one week drop in temperature was negligible.

Decreasing just the largemouth excretion probabilities per the temperature correction factor (option 1) resulted in the largemouth bass fractional inventories increasing by up to about 30% greater than the unadjusted model, as can be seen in Figure 7.5. The average of the daily ratios of the option (1) output compared to the unadjusted output for the 500 days modeled was 1.01 with a minimum of 0.98 and maximum of 1.28. The average of the daily ratios over the coldest timeframe, days 150 to 220, was 1.17. As can be seen in Figure 7.5, the TIM model largemouth bass output for option two, elimination probabilities of all the fish adjusted for temperature, is very close to that of option 1 (difference less than 2%). Lastly, in option 3, all the biota in the food chain are modified, and the largemouth bass inventory levels are the highest

compared to the baseline. The average ratio of the adjusted model to unadjusted for all the model components over the full 500 days modeled was 1.84 with a minimum of 0.94 and maximum of 5.3 occurring on day 7. The mean ratio for largemouth bass was 1.6 over the 500 day period and 1.5 over the period of coldest temperatures. These results are summarized in Table 7.1.

Table 7.1. Comparison of Results for TIM model with elimination probabilities temperature adjusted

	Ratio of Adjusted: Unadjusted				
	Days 0 to 500 Mean	Days 0 to 500 Min	Days 0 to 500 Max	Day of initial peak	Days of initial trough
Option 1; largemouth bass	1.01	0.98	1.28	303	412
Option 3; largemouth bass	1.6	1	2.09	305	411
Option 3; all model components	1.84	0.94	5.3	322	410

The temperature driven behavior of all three of these options is similar. As indicated in Table 7.1, the accumulation of ^{133}Cs continues for a longer period of time than the unmodified model before reaching a peak of day 303, 305, and 322 and then decrease for a span of 109, 106, 88 days, for options 1 through 3, respectively.

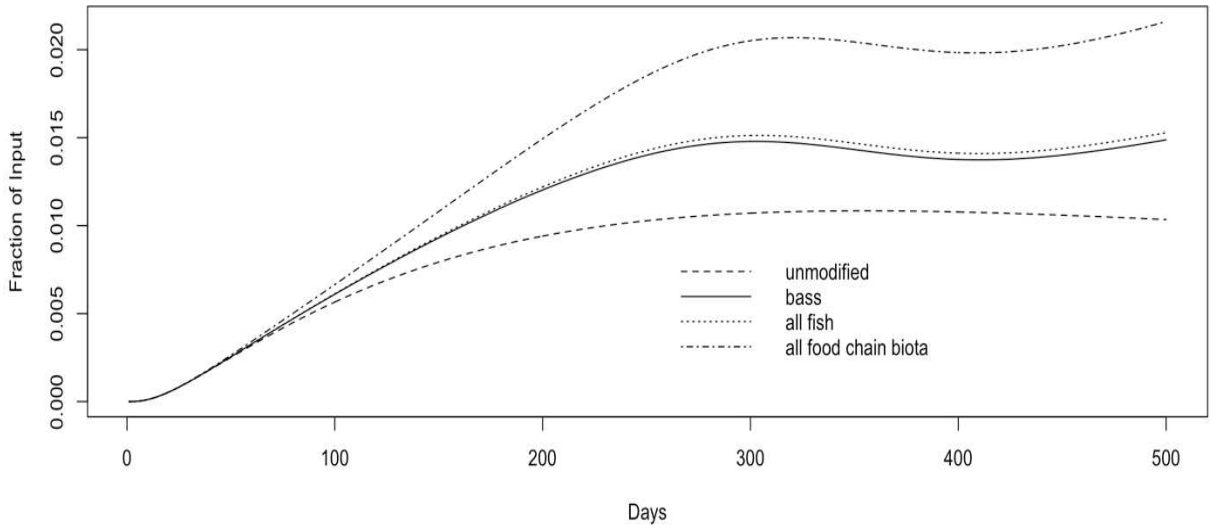

Figure 7.5. Largemouth bass results of temperature variation applied to elimination rates in ^{133}Cs TIM model.

Figures 7.6 and 7.7 illustrate the minimal difference between unmodified lake chub and bluegill results and the modeled results occurring when all the fish elimination probabilities are temperature adjusted. Though minimal, the modified response is higher as would be expected. When all of the food chain biota elimination rates are adjusted, then the lake chub values stay elevated through winter, and then begin to decline in the spring with the lowest levels occurring in approximately October. The response in the bluegill when all food chain biota are modified is notably different from the bluegill, and it is more similar in behavior to the largemouth bass. The increase in the bluegills over the winter months is slower, and a maximum occurs at the end of April. The minimum occurs at the end of October. This difference in behavior of the bluegill compared to lake chub could be expected since the bluegill component of the food chain model is higher in trophic level than the lake chub.

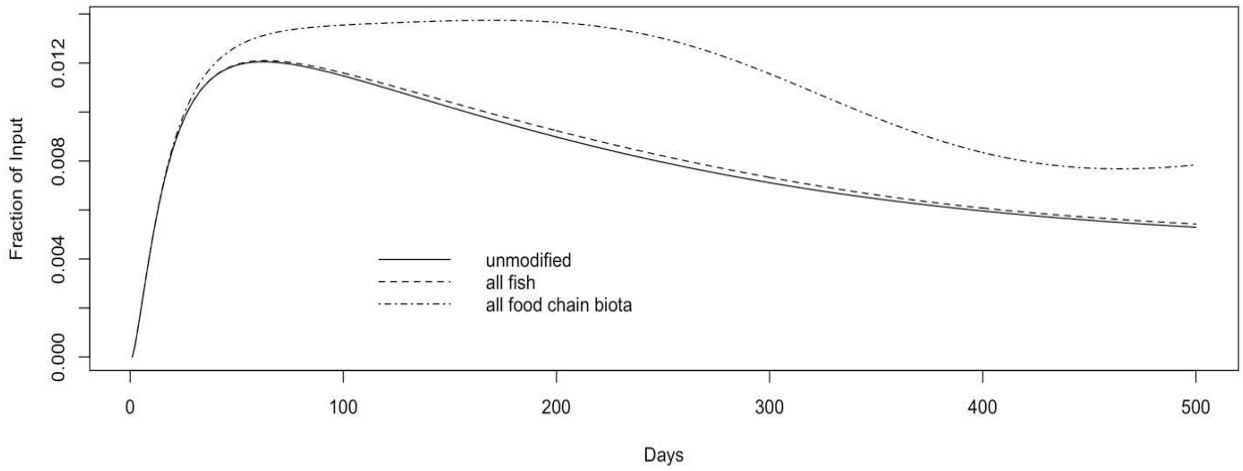

Figure 7.6. Lake chub results of temperature variation applied with the specified changes to elimination probabilities in ^{133}Cs TIM model.

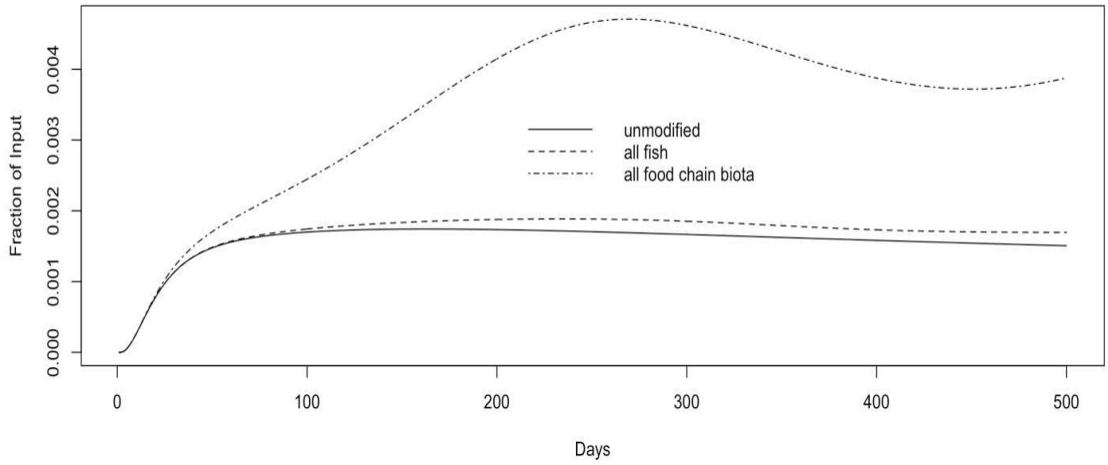

Figure 7.7. Bluegill results of temperature variation applied with the specified changes to elimination probabilities in ^{133}Cs TIM model.

The unmodified and modified periphyton and plankton results, as in Figure 7.8, do not deviate from each other until approximately day 30 after the primary increase in Cs.

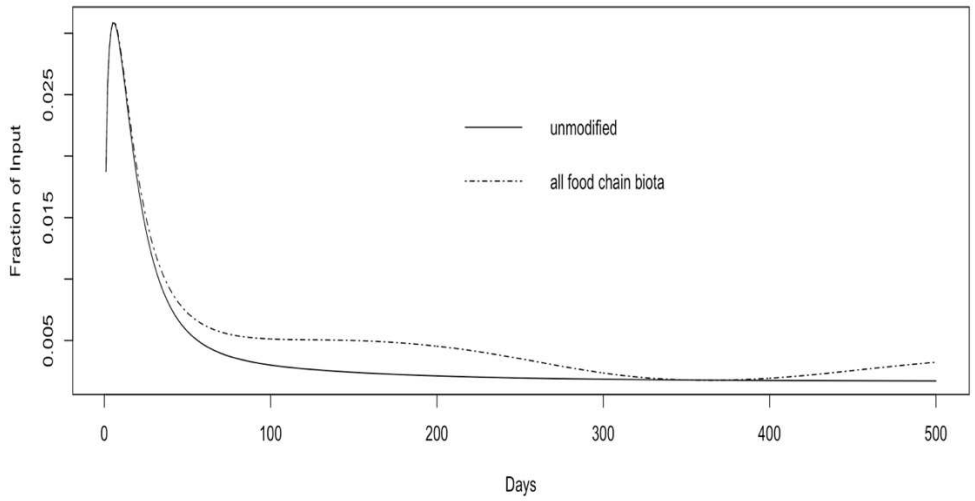

Figure 7.8. Periphyton results of temperature variation applied with the specified changes to elimination probabilities in ^{133}Cs TIM model.

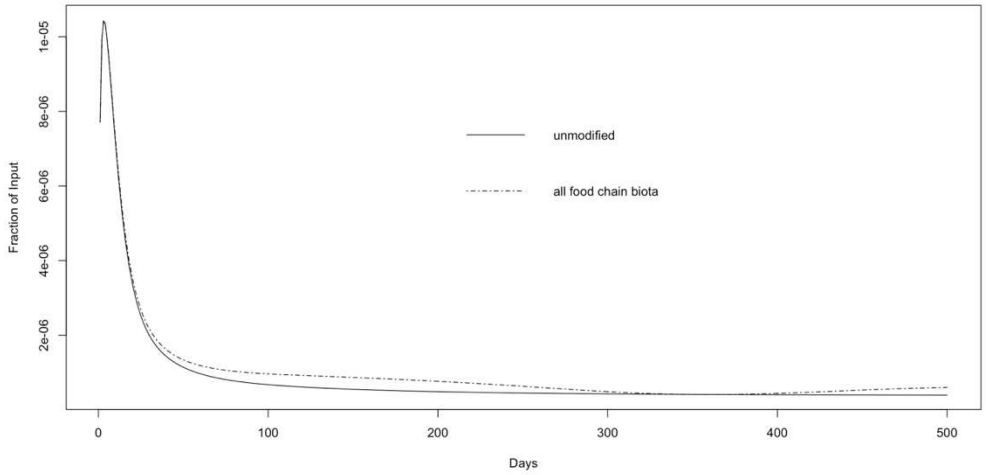

Figure 7.9. Plankton results of temperature variation applied with the specified changes to elimination probabilities in ^{133}Cs TIM model.

The snails and *Chaoborus* larvae ^{133}Cs levels increased between 100 and 200 days then decreased. Overall, these components followed a similar behavior to the plankton and periphyton, though the relative size of the increase over the cooler temperatures was larger.

7.3.2. Response of TIM model with uptake and excretion probabilities varied for temperature

As explained in section 7.2, three different approaches were investigated to determine the appropriate method of applying a reduction for uptake to account for the fish consuming less during the colder temperatures. Initially, uptake was only modified for the more simply assessed scenarios of temperature modified elimination probabilities for the largemouth bass and the fish. The first method discussed in section 7.2, the literature based uptake moderator, did not produce reasonable results in the largemouth bass. The largemouth bass fractional inventories dropped by approximately a factor of five from the unadjusted model levels over days 50 to 300 when applying this moderator to just the uptake probabilities for largemouth bass and using the elimination moderator to vary the largemouth bass elimination rates. From 300 to 500 days the inventory levels increased to approximately the same level as baseline by day 500. This approach was not investigated further since these results indicate that the literature-based uptake moderator would require substantial recalibration of the model to have the correct inventory levels. One approach to such a recalibration is to optimize all transition probabilities over a shorter initial period of the experiment versus the 400-500 day period that was used in the baseline model.

The result of applying the second method of developing an uptake moderator (reducing uptake over winter only) are shown in Figure 7.10 with elimination probabilities also adjusted for the largemouth bass and all the fish. Decreasing the uptake for just a few months period of time did not have prolonged effect on reducing the inventory levels. The substantial increase in Cs levels that occurred after the "flat" winter period is not a reasonable behavior for the actual largemouth bass behavior. As such, this approach was not investigated further, and use of a short term moderator was concluded to be an ineffective technique.

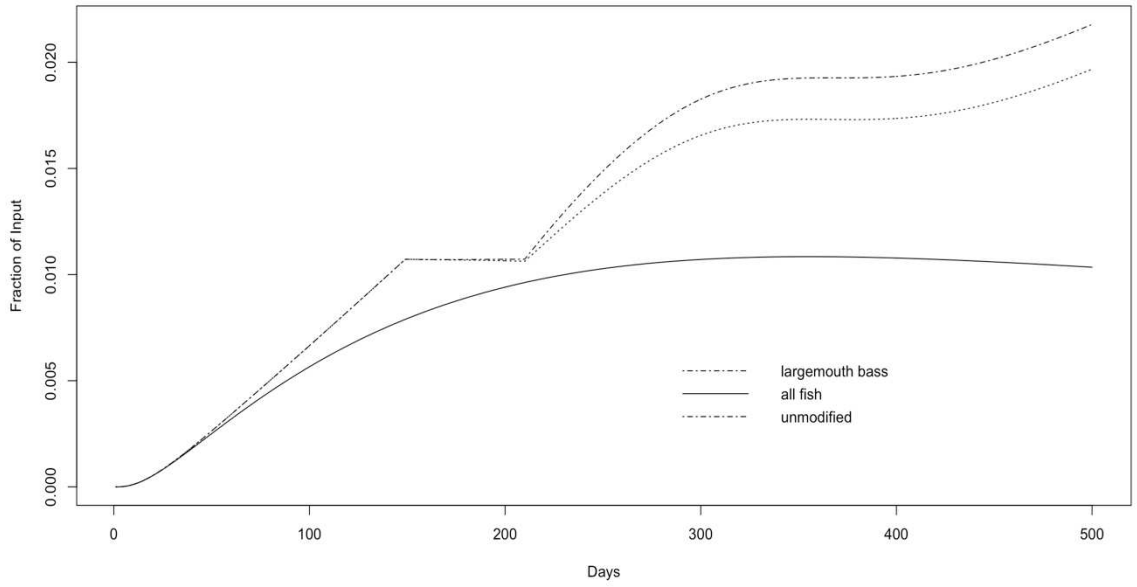

Figure 7.10. Results of applying a constant decrease over Jan-Mar to the uptake probabilities for largemouth bass and all fish, compared to unadjusted. The elimination moderator was applied to largemouth bass excretion probabilities.

Last, the approach of applying a constant reduction factor to the uptake probabilities for the largemouth bass was assessed. Again, the elimination factor was applied to the largemouth bass. The constant reduction factor of 0.8 was used to obtain the output graphed in Figure 7.11. and compared to the corresponding unmodified model output. The mean ratio of the adjusted to unadjusted outputs over the model timeframe was 1.1. Since the magnitude of the ^{133}Cs inventory level did not deviate substantially between the two models, this version of the TIM was selected for subsequent extension of the model to ^{134}Cs and for the concentration ratio and dose calculations.

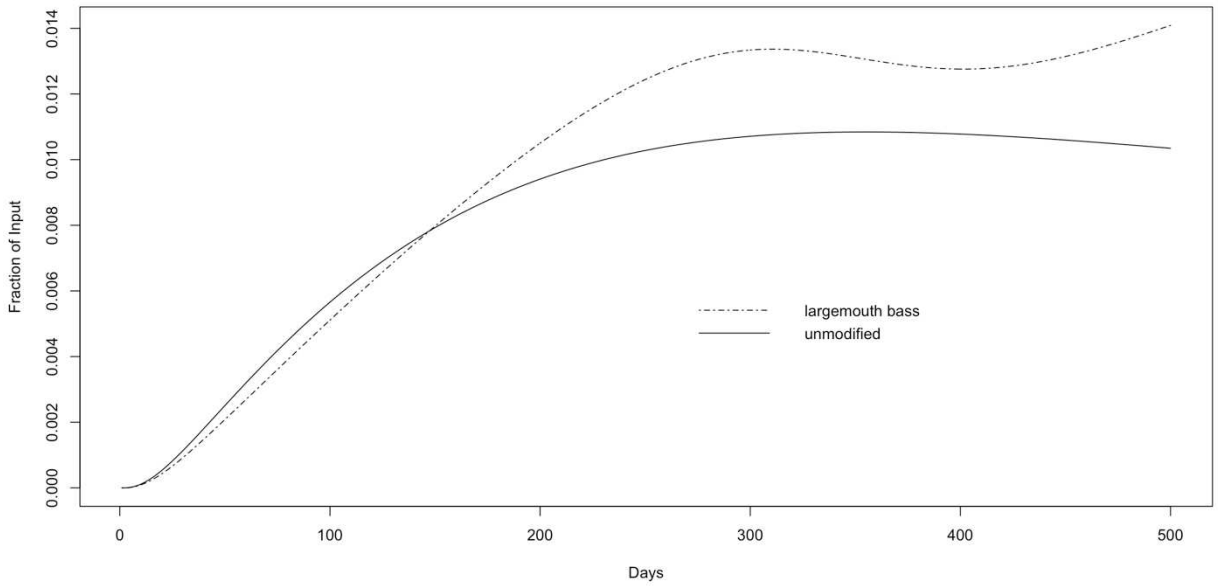

Figure 7.11. Results of applying a constant reduction factor over the entire 500 days to the uptake probabilities for largemouth bass, compared to unadjusted. The elimination moderator was applied to largemouth bass elimination probabilities.

While it could be possible to develop a TIM model with the elimination moderator applied to all the food web biotic components, as done previously, and the application of constant decrease factors for all the uptake probabilities of these biota, this was beyond the scope of the current work. The general behavior of the application of a temperature factor can be assessed for the other biota in the food web, but it is not the purpose of this paper to estimate daily doses and concentration factors for all of these biota.

7.3.3. Results of ^{134}Cs TIM model

Figure 7.12 is a graph of the ^{134}Cs with the final selected conditions for the largemouth bass TIM model of temperature adjustment factors applied to the elimination probabilities of the biota (per a Q_{10} of 2) and to the uptake rate of the largemouth bass. The unadjusted ^{134}Cs model and the comparable ^{133}Cs models are also included on the graph. The ^{134}Cs levels in the

largemouth bass of the TIM model increase until day 288 and then decrease until day 440 when they start to increase again.

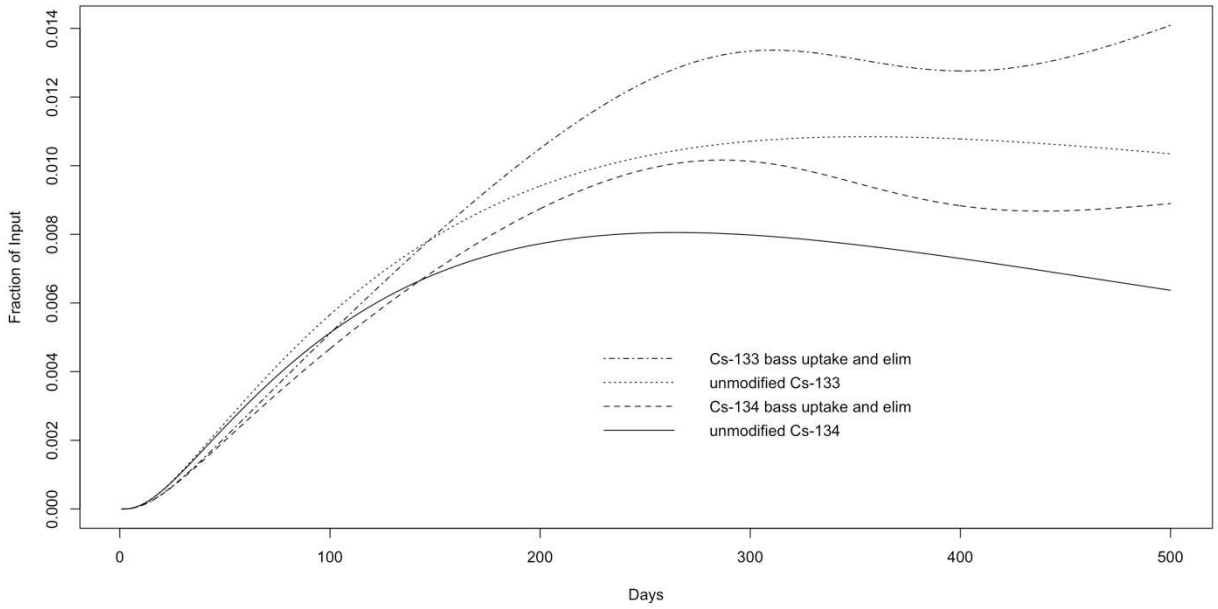

Figure 7.12. Comparison of ^{134}Cs and ^{133}Cs models for temperature varied (bass uptake and largemouth bass elimination probabilities modified) and the corresponding unmodified baseline models.

7.3.4. Results of daily concentration ratio calculation

The following is the results of calculating the concentration ratio predicted by the model output for largemouth bass (0.0099 inventory level, as a fraction of input) and water (0.0683) on day 250:

$$\frac{0.0099 \cdot \text{Input} \,/_{360\ kg}}{0.0683 \cdot \text{Input} \,/_{1.5\times10^{8} kg}} = 60289$$

Figure 7.13. is a graph of the results for all of the concentration ratios predicted by the model over the 500 day period modeled.

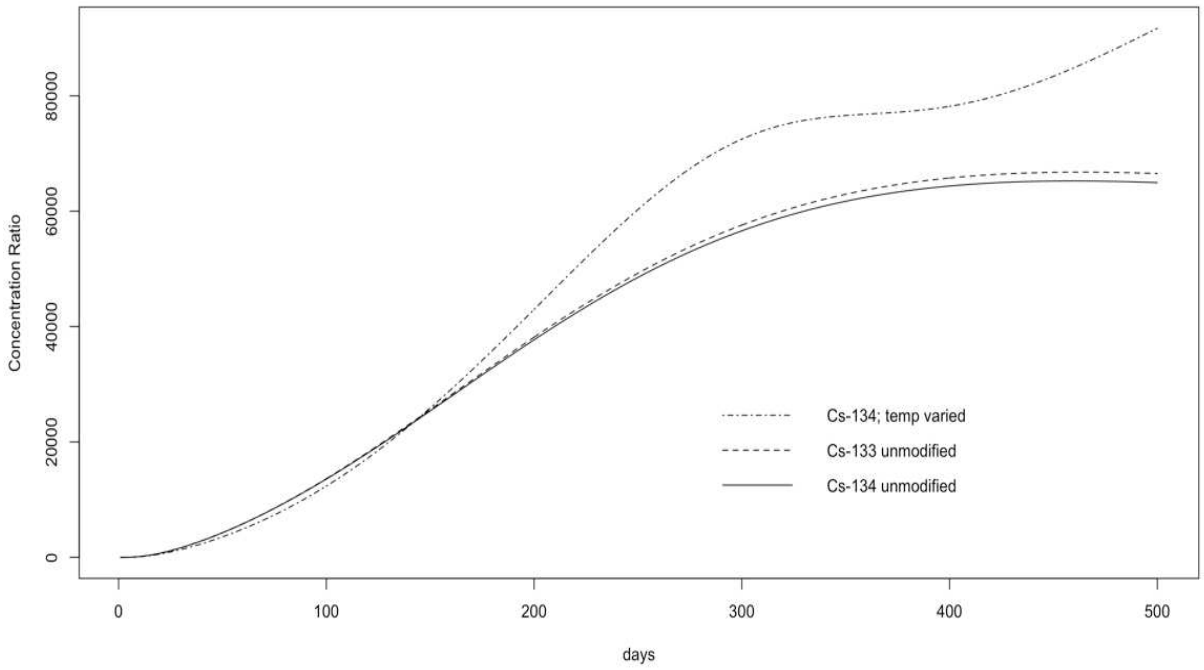

Figure 7.13. Concentration ratio results for the largemouth bass from the ^{134}Cs TIM model and the ^{134}Cs unmodified model. The ^{133}Cs unmodified results are included for comparison in behavior to ^{134}Cs.

7.3.5. Results of Largemouth Bass Internal Dose Calculation

Figure 7.14 is a graph of daily dose over time for the ^{134}Cs TIM model and the unmodified ^{134}Cs model for a 1.5×10^{8} Bq input into the pond, which is a water concentration level of 1 Bq/L (assuming constant initial distribution throughout the volume of the pond). The maximum daily dose occurred on day 288 and was 24.3 μGy. The dashed lines indicate the approximately 5 μGy variation that could possibly be attributed to temperature changes. This amount relates to a variation in concentration of about 860 Bq/kg.

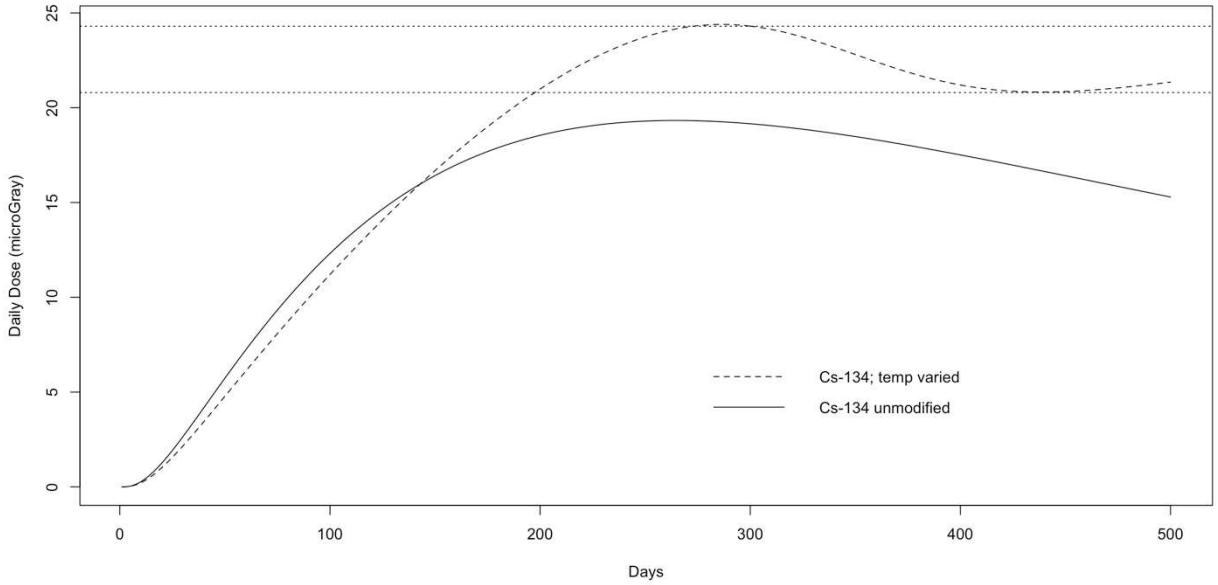

Figure 7.14. Daily dose results for the ^{134}Cs TIM model and the ^{134}Cs unmodified model. Though graphed as a continuous line, the results are discrete doses for each day.

7.4. Discussion

7.4.1. Responses of inventory output TIM modelling

Overall, the addition of a temperature driven changes to the daily elimination and uptake probabilities in the TIM model added a small sinusoidal deviation in the largemouth bass behavior, noticeable after the initial increase in uptake which took about 300 days for ^{133}Cs and slightly less for ^{134}Cs. The sinusoidal behavior is less than 10% deviation from the general increase in Cs inventory. In the largemouth bass, the TIM model also predicts a continual increase through the initial winter of the experiment, and indicates that the levels of Cs have a first peak in May/June before decreasing over the summer for approximately 3 months and then increasing again through the fall to winter (Figure 7.12). While the lag in overall Cs accumulation and consistently higher inventory levels after about day 130 when compared to the

unmodified model; these observations or the magnitude of the observations may be a result of inadequate balancing of uptake and elimination probabilities.

While the elimination moderator only TIM model over predicts the inventory levels (particularly in the fish) due to not taking into account the decrease due to reduced uptake in the winter, it can be used for an assessment of temporal behavior due to changing elimination rates in accordance with the Q_{10} law. Behavior in food web components that peaks quickly over the first 30 days of the experiment, such as the periphyton, is as anticipated with higher levels in the winter and lower levels in the summer. Accumulation of higher ^{133}Cs inventories is observed in the model overall. The lake chub response had a lag in the time until Cs levels dropped when compared to the unadjusted model, pointing to the need for a temperature based reduction in uptake probabilities. However, the initial approach of varying the elimination probabilities in the biota by the Q_{10} rule without complication of selecting the appropriate uptake factor allowed for an assessment of the seasonal behavior due to changes in the elimination rates. This change adds a small seasonal behavior and did not have a clear sinusoidal behavior after day 300 like the other fish. The bluegill response was more similar to the largemouth bass, with a sinusoidal behavior evident after day 250. Adequate experimental data was not available for comparison.

Of the three different approaches investigated as methods to decrease the uptake during colder periods, the most appropriate for the previously used Markov model development approach was to decrease the elimination rates by a constant rate over the modeled period. This initial attempt at a TIM model with temperature adjusted elimination and uptake was optimized just for the largemouth bass and compared to the experimental data for the largemouth bass for Pond 4. The model based observation of no temperature variability behavior over the first 300 days is the same as observed in the largemouth bass experimental data. Limited data from the

addition experiment exist for the largemouth bass of comparable sizes between days 300 to 400, and it is not possible to assess whether there is a temperature driven behavior in the data over this amount of time. It is possible that there is a temperature related trend in comparable sized bass experimental data between days 400 to 500, where a slight decrease followed by an increase occurs. If it exists, this trend matches the general behavior predicted by the TIM model for the largemouth bass during this period.

The model incorporation and assessment of the complex relation of uptake and elimination as temperature changes is further complicated in the Pond 4 experiment where levels in the fish were not in equilibrium with the water for the full period of the experiment. Given this, it was unknown if the model would behave similarly to the other studies, discussed in the introduction of this chapter, that were conducted at equilibrium conditions. These studies reported the highest levels of Cs in fish in late winter and the lowest in July/Aug or October, depending on the study (Peles 2000, Kolehmainen 1979). In contrast, the TIM model results indicated a continual increase in the fish through the initial winter of the experiment. Additionally, model results for largemouth bass indicate that the levels of Cs had a first peak in May/early June before decreasing over the summer for approximately 3 months with a minimum in September and then increasing again through the fall to winter (Figure 7.12). It may be that the acute addition accumulation causes a lag in seasonal variation when compared to equilibrium studies. This conclusion should be investigated further with subsequent refinements to the TIM model.

7.4.2. Concentration ratios and internal dose output TIM modelling

The largemouth bass optimized TIM model was modified to be a ^{134}Cs version of the model, and the behavior of concentration ratios and dose in the largemouth bass was assessed.

The concentration ratios range widely over the period of the experiment. The unmodified model concentration ratios approach a maximum value of approximately 60,000, which is higher than the literature reported equilibrium values for concentration ratios of 13,000 (NCRP 154, 2007) and 3,000 (IAEA TRS 472, 2010) for fish (non-benthic). These literature equilibrium values are an estimate based on multiple studies and are often incorporated into models, to include dynamic models such as those discussed in Chapter two of this dissertation. Use of the literature published equilibrium concentration ratios in Pond 4 instead of the modeled predictions of concentration ratios would result in an underestimation of Cs levels in the largemouth bass over much of the timeframe modeled (when the modeled concentration ratio is higher than the literature equilibrium values). Prior to approximately day 75 the model predicted concentration ratios are lower than the NCRP value, 13,000, and Cs levels in the largemouth bass may be overerestimated if the NCRP value was used to estimate Cs levels in the largemouth bass from water sample measurements; for the IAEA value of 3,000, the corresponding day is approximately day 25). Since it is plausible that water sampling and concentration ratios may be used in the early period after an accident (prior to having the resources to perform more sampling) the results of this modelling support prudence in such an application and promote using actual fish samples versus concentration ratios.

The sinusoidal behavior in the concentration ratios of the temperature modified TIM model is not particularly notable. The concentration ratios are notably higher in the temperature modified TIM model, likely due to the increased inventory level in the largemouth bass and minimal changes occurring in the water of the modified and unmodified models. The ^{134}Cs TIM model predicted internal dose rates, due to 1 Bq/L concentration in the pond's water are much lower than those which would be a concern for the biota. The levels reached a daily maximum of

about 18 μGy in the unmodified model versus 24 μGy in the TIM model, which is not a major difference. A value of 0.01 Gy/day absorbed dose for ^{134}Cs is the limiting dose to the maximally exposed biota recommended by the DOE to provide adequate protection of aquatic animal populations (DOE, 2002). The ERICA biota dose assessment tool has a screening level that is much lower than this, at 10 μGy/h or 240 μGy over a 24 hour period. In the Pond 4 model, this screening level would be exceeded in the TIM model for a level of 10 Bq/L. The seasonal behavior in dose is the same as described for the inventory output, and an approximately 5 μGy variation could possibly be attributed to temperature changes.

7.5. Conclusion

While computation of the TIM model is not more difficult than the standard Markov models, the selection of reasonable moderators for the effect of temperature on elimination and uptake is not simple. The application of the VAMP modeling project suggested Q_{10} value of two as a seasonal elimination moderator produced a small seasonal effect in the largemouth bass observable after day 300. Seasonal effects in the other biota were also evident when the elimination rate moderator was applied to all the biota in the Pond 4 model food web. The model results suggest that the temperature behavior in the largemouth bass is different for non-equilibrium conditions that result after an acute equilibrium than equilibrium conditions, though this conclusion should be confirmed by further refinements of the TIM model.

Further work would be to develop a more reasonable uptake moderator for temperature for all biota and possibly sediment resuspension which has been shown to have a seasonal effect (Alberts, 1979). Possibly, the initial moderator attempted in this work for

uptake would be more successful if reapplied for a Markov matrix model that was parameterized for the best fit over the first 90-100 days. Alternatively, the results from seasonal uptake studies of different fish could be applied, and possibly different uptake probabilities between the different fish species and/or other biota could be reasonably determined. Last, a different Q_{10} of 2.5 or 3 could be applied to see the relative change on model results.

CHAPTER EIGHT. FUTURE WORK

The Pond 4 modeling described in this dissertation produced a framework for descriptive site specific modeling of the dynamic Cs inventories in a basic lacustrine food web. Future work could further refine and extend this effort. Possible future work on the Pond 4 modeling project is summarized in the following list:

A) Further model application:

1) Assess effectiveness of additional remedial actions or of different timings, for example, reducing sediment resuspension probabilities on day 100

2) Submerged vegetation assessment; increase or decrease amount of ^{133}Cs and ^{134}Cs to simulate more or less macrophytes in the pond

B) Use of larger range of concentration data sampled

1) Use the upper/lower ends of the concentration curve fit coefficients' standard error values to determine inventory minima/maxima

2) Re-parameterize transition coefficients, as necessary, so the model output fits the upper/lower ends of these inventories

C) Re-parameterize model

1) A two water component equation instead of three water component

2) Two loss rates from the biota, slow and fast

3) A biomass change factor

D) Try different approach for Time-inhomogeneous Markov model using flux/day from tabular model to develop a time based moderator for select transition probabilities, possibly those most sensitive

E) Make the TIM model a Markov simulation model and evaluate changes from baseline model

F) Apply procedures to different ponds, where biomass can be measured and/or estimated and inventories determined

REFERENCES

Acevedo, M., Data Analysis and Statistics for Geography, Environmental Science, and Engineering. CRC Press; Taylor and Francis Group. 2013, 369-380.

Acevedo, Miguel F. Simulation of Ecological and Environmental Models. Second Edition. XanEdu Original Works. 2004.

Adams, M. S., and McCracken, M. D. 1974. Seasonal Production of the Myriophyllum component of the littoral of Lake Wingra, Wisconsin. Journal of Ecology 62, 457-465.

Alberg A1, MacLeod M, Wiberg K. Performance of the CalTOX fate and exposure model in a case study for a dioxin-contaminated site. Environ Sci Pollut Res Int. 2015 Jun;22(11):8719-27.

Alberts, J.J., Tilly, L.J., Vigerstad, T. J., 1979. Seasonal cycling of cesium-137 in a reservoir. Science 203, 649-651.

Alberts, J.J., Bowling, JW., Orlandini, KA. 1987. The effect of seasonal anoxia on the distribution of ^{238}Pu, ^{239,240}Pu, ^{241}Am, ^{244}Cm and ^{137}Cs in pond ecosystems of the southeastern United States. In: Pinder, III, J. E., Alberts, J. J., McLeod, K. W., R. G. Schreckhise, R. G, (Eds.), Environmental Research on Actinide Elements, CONF-84142 (DE86008713), NTIS, US Dept. Commerce, Springfield, VA, pp. 371-390.

Alhassan, A. and K.S. Nokoe. Modelling the Transitional Dynamics of Mycobacterium Tuberculosis Strain. Journal of Medical and Biomedical Sciences (2016) 5(2): 13-23

Alva, J.J., Gobas, F.A.P.C., 2016. Modeling 137Cs bioaccumulation in the salmon-resident killer whale food web of the Northeastern Pacific following the Fukushima Nuclear Accident. Science of the Total Environment 54, 56-67

Barnes, R. S. K. and Mann, K.H. Fundamentals of Aquatic Ecology. Wiley publishing. Jul 2009.

Bates, D. and Maechler, M., 2016. Matrix: Sparse and Dense Matrix Classes and Methods. R package version 1.2-7.1.

Becker, G.C., 1983. Fishes of Wisconsin. University of Wisconsin Press, Madison. 1052 pp.

Boeger, H., 1975. A comparison of the life cycle, reproductive ecologies and size-weight relationships of *Helisoma anceps*, *H. campanulatum*, and *H. trivolis*. Can. J. Zool. 53:1812-1824.

Chimney, M.J., Cody, W.R. and Starkel, W.M. 1985a. Final report on the water quality, phytoplankton and zooplankton of Par Pond and Pond B: I. Water Quality. Environmental and Chemical Services Report ECS-SR-20. Aiken, South Carolina.

Chimney, M.J., Cody, W.R., Starkel, W.M. 1985b. Water quality, phytoplankton and zooplankton of Par Pond and Pond B. Volume 1. Water Quality. Final Report. National Technical Information Service. Springfield, Virginia. Report DE86015868.

Clady, M.D., 1981. Survival and shifts in food of young-of-year Micropterus penned at high densities in an Oklahoma pond. Proceedings Oklahoma Academy of Sciences 61, 15-22.

Comans, R.N.J., Blust, R., Carreiro, M.C.V., Fernandez, J.A., Håkanson, L., Sansone, U., Smith, J.T., Varskog, P., 2001. Modelling fluxes and bioavailability of radiocaesium and radiostrontium in freshwaters in support of a theoretical basis for chemical/hydrological countermeasures. ECOPRAQ. Contract N° FI4P-CT95-0018, in: European Commission, Radiation protection. Fourth framework programme (1994–1998). Project summaries. EUR 19792 EN. 2001

Cuculeanu V., Lupu A., Romanof, N. 2002. Statistical characteristics of radionuclide concentration field around a nuclear power plant. Journal of Environmental Radioactivity 63, 231-237.

Dixon, Kenneth R. Modeling and Simulation in Ecotoxicology with Applications in MATLAB and Simulink. CRC Press Taylor & Francis Group, LLC. 2012

Durrett, Richard. Essentials of Stochastic Processes. 2011

Evans, D. W., Alberts, J. J., Clark, III, R. A., 1983. Reversible ion-exchange fixation of cesium 137 leading to mobilization from reservoir sediments. Geochemica et Cosmochemica Acta 47, 1041-1049.

Eversole, A.G. 1978. Life-cycles, growth and population bioenergetics in snail Heliosoma-trivolvis (Say). Journal of Molluscan Studies 44(2):209-222.

Flemer, D.A., Woolcott, W.S., 1966. Food habits and distribution of the fishes of Tuckahoe Creek, Virginia, with special emphasis on the bluegill, Lepomis m. macrochirus Rafinesque. Chesapeake Science 7, 75-89.

Gaul, W. and Underhill, D. 2001. A Simple Calculation for the Buildup and Decay of Radon Progeny. Health Physics. 80(6): 616-617.

Golikov, Vladislav. Modelling of long-term behavior of caesium and strontium radionuclides in the Artic environment and human exposure. Journal of Environmental Radioactivity 74. 159-169. 2004.

Grant W.E., Matis J.H., Miller T.H. 1991. A stochastic compartmental model for migration of marine shrimp.

Haque, M.E., Gomi, T., Sakai, M., Negishi, J.N., 2017. Developing a food web-based transfer factor of radiocesium for fish, whitespotted char (*Salvelinus leucomaenis*) in headwater streams. Journal of Environmental Radioactivity 172, 191-200.

Hakonson. T.E., Whicker, F.W. Cesium Kinetics in a Montane Lake Ecosystem. Health Physics. Pergamon Press 1975. Vol. 28 (June), pp. 699-706.

Hakanson, L., Andersson, T., Nilsson, A., 1992. Radioactive caesium in fish in Swedish lakes 1986-1988 – General pattern related to fallout and lake characteristics. Journal of Environmental Radioactivity 15, 207-229.

Hann, B.J., Mundy, C.J., Goldsborough, L.G., 2001. Snail-periphyton interactions in a prairie lacustrine wetland. Hydrobiologia 457, 167-175.

Harris. G.P., 1986. Phytoplankton Ecology; Structure, Function and Fluctuation. Springer Science+Business Media B.V. pg

Hewett, C.J., Jeffries, D.F., 1976. The accumulation of radioactive caesium from water by the brown trout (Salmo trutta) and its comparison with plaice and rays. Journal of Fish Biology 9, 479-489.

Hewett, C.J., Jeffries, D.F., 1978. The accumulation of radioactive caesium from food by the plaice (Pleuronetces platessa) and the brown trout (Salmo trutta). Journal of Fish Biology 13, 143-153.

Higley, K.A. Bytwerk, D.P. Generic Approaches to Transfer. Journal of Environmental Radioactivity 98. pp 4-23, 2007.

Hinton, T.G., Kaplan, D.I., Knox, A.S., Coughlin, D.P., Nascimento, R.V., Watson, S.I., Fletcher, D.E., Koo, B. 2006. Use of illite clay for in situ remediation of 137Cs-contaminated water bodies: Field demonstration of reduced biological uptake. Environ. Sci. Technol. 40, 4500-4505.

Hinton, T.G, Pinder, J.E, Whicker, F.W, Marsh, L., Joyner, J., Coughlin, D. Yi, Y, Gariboldi, J., 2006. Comparative kinetics of cesium from whole-lake, limnocorrals, and laboratory experiments. Radioprotection-Colloques. V37, C1, 605-610.

Hodgson, J.R., Kitchell, J.F., 1987. Opportunistic foraging by largemouth bass (Micropterus salmoides). The American Midland Naturalist 118, 323-336.

IAEA (International Atomic Energy Agency), IAEA-TECDOC-1143. Modelling of the transfer of radiocaesium from deposition to lake ecosystems; Report of the VAMP Aquatic Working Group. Part of the IAEA/EC Co-ordinated Research Programme on the Validation of Environmental Model Predictions (VAMP). ISSN 1011-4289. IAEA, 2000.

Jeong, H., Miller, V.J., Johnson, T.E., Hinton, T., Pinder J.E. III, 2018a. Model-based analyses of the cesium dynamics in the small mesotrophic reservoir, Pond 4. I. Estimating the inventories of and the fluxes among the pond's major biotic components. Journal of Environmental Radioactivity.

Jeong, H., Miller, V.J., Johnson, T.E., Hinton, T., Pinder J.E. III, 2018b. Model-based analyses of the cesium dynamics in the small mesotrophic reservoir, Pond 4. II. Development of a Rate-Based Kinetic Model. Journal of Environmental Radioactivity.

Johnson, J.C., Luczkovich, J.J., Borgatti, S.P., Snijders, T. A. Using social network analysis tools in ecology: Markov process transition models applied to the seasonal trophic network dynamics of the Chesapeake Bay. Ecological Modelling. 220 (2009) 3133-3140.

Kalos, Malvin H. and Whitlock, Paula A. Monte Carlo Methods. 2nd Edition. Wiley-VCH Verlag GmbH & Co. Weinheim. 2008.

Kelly, M.S. 1989. Distribution and biomass of aquatic macrophytes in an abandoned nuclear cooling reservoir. Aquatic Botany 35, 133-152.

Kelly, M.S. and Pinder, III, J.E. 1996. Foliar uptake of ^{137}Cs from the water column by aquatic macrophytes. Journal of Environmental Radioactivity 30, 271-280.

Kemney, John G. and Snell, J. Laurie. Finite Markov Chains. Springer-Verlag. 1976.

Kitchell, J.F., Windell, J.T., 1970. Nutritional value of algae to bluegill sunfish, *Lepomis macrochirus*. Copeia 1970, 186-190.

Kolehmainen, S., Romantschuk, H., Takatalo, S., Meittinen, J. K., 1967. Pollution experiments with Cs-137 in lakes of two limnologically different types. In: Congres International sur la Radioprotection du Milieu devant le Development des Utilizations Pacifques de l'Energie Nucleaire, Societe Franciase de Radioprotection, Paris, pp. II-20 – II-29.
Kolehmainen. S.E. 1979 The balances of 137cs, stable cesium and potassium of bluegill (lepomis macrochirus raf.) And other fish in white oak lake. Health Physics. 23: 301-315

La Row, E.J., Marzolf, G.R., 1970. Behavioral Differences Between 3rd and 4th Instars of Chaoborus punctipennis Say. The American Midland Naturalist, 84 (2), 428-436.

Lian, Chao. Cheng, G, Wixon, D, Balser, T. An Absorbing Markov Chain approach to understanding the microbial role in soil carbon stabilization. Biogeochemistry 106: 303-309. 2011

Lobinske, R.J., Cichra, C.E., Ali, A., 2002. Predation by bluegill (Lepomis macrochirus) on larval chironomidae (Diptera) in relation to midge standing crop in two central Florida lakes. Florida Entomologist 85, 372-375.

Lombardo, P., Cooke, G.D. 2002. Consumption and preference of selected food types by two freshwater gastropod species. Archiv fur Hydrobiologie 155, 667-685.

Malek, M. A., Nakahara, M., Nakamura, R., 2004. Uptake, retention and organ/tissue distribution of 137Cs by Japanese catfish (Silurus asotus Linnaeus). Journal of Environmental Radioactivity 77, 191-204.

Matis, J.H., Wehrly, T.E., Metzler, C.M., A semi-Markov process model for migration of marine shrimp. Ecological Modelinging 60:167-184 (1992).

McKone, T.E., UCRL- CR-U1456FtI CalTOX, A Multimedia Total-Exposure Model for Hazardous-Wastes Sites Part I: Executive Summary Prepared for: The Office of Scientific Affairs Department of Toxic Substances Control California Environmental Protection Agency June 1993

Monte, L., Fratarcangeli, S., Pompei, F., Quaggia, S., Batella, C. 1993. Bioaccumulation of 137Cs in the main species of fishes in the lakes of central Italy. Radiochemica Acta, 60, 249-222.

Monte, L., Brittain, J. E., Hakanson, L., Heling, R., Smith, J. T., & Zheleznyak, M. (2003). Review and assessment of models used to predict the fate of radionuclides in lakes. Journal of Environmental Radioactivity, 69(3), 177–205.

McElhany, P, Real, LA, Power, A.G., Vector Preference and Disease Dynamics: A Study of Barley Yellow Dwarf Virus. Ecology. 1 March 1995.

Moore, M.V. 2006. Differential use of food resources by the instars of Chaoborus punctipennis. Freshwater Biology 19, 249-268.

Morgan, I.J., Tytler, P., Bell, M.V. 1993. The accumulation of 137-caesium from fresh water by alevins and fry of Atlantic salmon and brown trout. Journal of Fish Biology 43, 877-888.

Mueller, F., State-of-the-art in ecosystem theory. Ecological Modelling 100, 135-161. 1997.

Nandini S. and Sarma. S. 2000. Lifetable demography of four cladoceran species in relation to algal food (Chlorella vulgaris) density. Hydrobiologia 435: 117–126, 2000.

NCRP Report No. 154; Cesium-137 in the Environment: Radioecology and Approaches to Assessment and Management. Recommendations of the National Council on Radiation Protection and Measurements; Sep 2007

Newman, M.C., Schalles, J.F. 1990. The water chemistries of Carolina Bays – a regional survey. Archiv for Hydrobiologie 118,147-168.

Nobriga, M.L., Feyrer, F., 2007. Shallow-water piscivore-prey dynamics in California's Sacramento-San Joaquin delta. San Francisco Estuary and Watershed Science 5, 1-13.

NRC Effluent Database for Nuclear Power Plants 2017. United States Nuclear Regulatory Agency. http://www.reirs.com/effluent/EDB_rptLicenseeReleaseAmts.asp.

Odum, E. P. 1959. Fundamentals of Ecology, 2nd edition. Philadelphia, W.B. Saunders, 62-64.

Pacholczyk, M, Borys, D, Kimmel, M. Finite absorbing Markov chain as a model of small-ligand binding process. 2013 International Work-Conference On Bioinformatics And Biomedical Engineering Proceedings. Pages: 747-751

Peles, J.D. Philippi, T., Smith, M.H. Brisbin, L Jr, Gibbons, J.W., Seasonal variation in radiocesium levels of largemouth bass (micropterus salmoides): implications for humans and sensitive wildlife species. Environmental Toxicology and Chemistry, 19(7), 2000

Pendleton, R.C., Hanson, W.C. 1958. Absorption of cesium-137 by components of an aquatic community. Second United Nations Geneva Conference, 18:419-422.

Peters, E.L., Newman, M.C. 1999. 137Cs elimination by chronically contaminated largemouth bass (Micropterus salmoides). Health Physics 76, 260-268.

Pinder III, J.E. et al., The Influence of a Whole-Lake Addition of Stable Cesium on the Remobilization of Aged ^{137}Cs in a contaminated reservoir. Journal of Environmental Radioactivity. 2004

Pinder III, J.E. et al., Foliar uptake of cesium from the water column by aquatic macrophytes, Journal of Environmental Radioactivity 85. 2006. pp 23-47

Pinder III, J.E. et al., Cesium accumulation by fish following acute input to lakes: a comparison of experimental and Chernobyl-impacted systems. Journal of Environmental Radioactivity. 2009. pp 256-467

Pinder III, J.E. et al., Contrasting cesium dynamics in neighboring deep and shallow warm-water reservoirs, Journal of Environmental Radioactivity 101. 2010. 659-669

Pinder III, J.E. et al., Cesium accumulation by aquatic organisms at different trophic levels following an experimental release into a small reservoir, Journal of Environmental Radioactivity 102. 2011. 283-293

R Software, R Core Team, 2016. R: A language and environment for statistical computing. R Foundation for Statistical Computing, Vienna, Austria. URL https://www.R-project.org/.

Radford, A.E., Ahles, H.E., Bell, C.R. 1968. Manual of the Vascular Flora of the Carolinas. University of North Carolina Press, Chapel Hill, NC. 1183 pp.

Rowan, D. J., Rasmussen, J. B., 1994. Bioaccumulation of radiocesium by fish: The influence of physiochemical factors and trophic structure. Canadian Journal of Fisheries and Aquatic Sciences 51, 2388-2410.

Rowan, D. J., Rasmussen, J. B., 1995. The elimination of radiocaesium from fish. Journal of Applied Ecology 32, 739-744.

Ross, S. 2007. Introduction to Probability Models. Amsterdam ; Boston Academic Press chp 4

Russell-Hunter, W.D., Browne, R. A., Aldridge, D. W. 1984. Overwinter tissue degrowth in natural populations of freshwater pulmonate snails (Helisoma trivolvis and Lymnaea palustris). Ecology, 65, 223-229.

SAS Institute Inc. 1989. SAS/STAT User's Guide, Version 6, Fourth Edition, Volume 2. SAS Institute Inc., Cary NC, 1684 pp.

Schell, WR, Linkov, I, Myttenaere, C., Morel, B. A Dynamic Model for Evaluating Radionuclide Distribution in Forests From Nuclear Accidents. Health Physics, 1996.

Smith, D.A. 1988. Radular kinetics during grazing in Helisoma trivolvis (Gastropoda: Pulmonata). Journal of Experimental Biology 136, 89-102.

Smith, J.T. Nice work-but is it science? Nature 408, 293. 2000.

Smith, J.T., Kudelsky, A.V., Ryabov, I.N., Daire, S.E., Boyer, L., Blust, R.J., Fernandez, J. A., Hadderingh, R.H., Voitsekhovitch, O.V., 2002. Uptake and elimination of radiocesium in fish and the "size effect." Journal of Environmental Radioactivity 62, 145-164.

Smith, J.T., Kudelsky, A.V., Fyabov, I.N., Hadderingh, R.H., Bugalov, A.A. 2003. Application of potassium chloride to a Chernobyl-contaminated lake; modeling the dynamics of radiocesium in an aquatic and decontamination of fish. Sci. Total Environ. 305, 217-227.

Smith, J.T., Belova, N.V., Bulgakov, A.A., Comans, R.N.J., Konoplev, A.V., Kudelsky, A.V., Madruga, M.J., Voitsekhovitch, O.V., Zibold, G., 2005. The "AQUASCOPE" simplified model for predicting ^{89,90}Sr, ^{131}I, and ^{134,137}Cs in surface waters after a large-scale radioactive fallout. Health Physics 89, 628-644.

Snip, L.J.P, Flores-Alsina, X., Plosz, B.G., Jeppsson, U., Gernaey, K.V., 2014. Modelling the occurrence, transport and fate of pharmaceuticals in wastewater systems. Environmental Modelling & Software 62, 1-16

Soetaert, K., Petzoldt, T., Setzer R.W., 2010. Solving Differential Equations in R: Package deSolve. Journal of Statistical Software, 33(9), 1--25.

Spedicato, G. 2017. Markovchain: discrete time Markov chains made easy

Stanley, R.A., et. al., 1976; Effect of Season and Water Depth on Eurasian Watermilfoil. Journal of Aquatic Plant Management, vol 14, pp 32-36.

Taylor, B. E., Aho, J. M., Mahoney, D. L., Estes, R. E., 1991. Population dynamics and food habits of bluegill (Lepomis macrochirus) in a thermally stressed reservoir. Canadian Journal of Fisheries and Aquatic Sciences 48, 768-775.

Teasley, R. Bernley, J. Davis, L.B., Erera, A., Chang, Y. A Markov chain model for quantifying consumer risk in food supply chains. 2016. Health Systems. Vol 5(2) 149-161.

Thomann, R.V., 1981. Equilibrium model of the fate of microcontaminants in diverse aquatic food chains. Canadian Journal of Fisheries and Aquatic Sciences 38, 280-296.

Thorp, J.H., Covich, A.P., 2001. Ecology and Classification of North American Freshwater Invertebrates, 2nd Edition. Elsevier Science and Technology Books. 1056 pp.

Tilly, L.J. 1975. Changes in water chemistry and primary productivity of a reactor cooling reservoir (Par Pond). In: Howell, F. G., Gentry, J. B., Smith, M. H. (Eds.), Mineral Cycling in Southeastern Ecosystems, CONF-740513, NTIS, U. S. Department of Commerce, Springfield, VA., pp. 394-407.

Topcuoglu, S. 2001. Bioaccumulation of cesium-137 by biota in different aquatic environments. Chemosphere 44, 691-695.

Tostowary, K. 2000. The assimilation and elimination of freshwater invertebrates. M. S. Thesis. Colorado State University. 91 p.

Tyrrell T. 2001. Redfield Ratio, in Encyclopedia of Ocean Sciences (Second Edition)

Vanderploeg, H. A., Booth, R. S., Clark, F. H., 1975a. A specific activity and concentration model applied to cesium-137 movement in a eutrophic lake. In: Cushing, -C. E., Jr. (Ed.), Radioecology and Energy Resources, Dowden, Hutchinson and Ross, Inc. Strousburg. Pennsylvania, pp. 164-177.

Vanderploeg, H. A., Booth, R. S., Clark, F. H., 1975b. A specific activity and concentration model applied to cesium-137 movement in a oligotrophic lake. In: Howell, F. G., Gentry, J. B., Smith, M. H. (Eds.), Mineral Cycling in Southeastern Ecosystems, CONF-740513, NTIS, U. S. Department of Commerce, Springfield, VA., pp. 142-165.

Van Donk, E., Grimm, M.P., Gulati, R.D., Klein Breteler, J. P. G. 1990. Whole-lake food-web manipulation as a means to study community interactions in a small ecosystem. Hydrobiologia 200/201, 275-289.

Venables, W. N. & Ripley, B. D. 2002. Modern Applied Statistics with S. Fourth Edition. Springer, New York.

Whicker, F. W., Shultz, V., 1982. Radioecology: Nuclear Energy and the Environment, Volume II. CRC Press, Inc. Boca Raton, Florida. 228 pp.

Winner, R.W., Greber, J.S. 1980. Prey selection by Chaoborus punctipennis under laboratory conditions. Hydrobiologia 68, 231-233.

APPENDIX A – ADDITIONAL DETAILS ON SAMPLING PROCEDURES OF ADDITION EXPERIMENT

A.1. Sampling of the primary producer components

The ^{133}Cs concentrations in three primary producer components that absorb Cs directly from the water column were measured in tissue samples collected before the addition and for at least 65 days following the addition. The three components were submerged aquatic macrophytes (which have been shown to absorb Cs from the water column; Pinder et al., 2006), plankton and periphyton.

To measure ^{133}Cs contents of the submerged aquatic macrophyte, *Myriophyllum spicatum* L, sections of leaf and stem tissue were clipped from the plants and gently shaken in the water to remove the loosely-attached periphyton, dried at 65 $^{\circ}C$ to a constant mass, and the concentrations of ^{133}Cs were measured by either NAA on dried and ground tissues or by ICP-MS after digesting dried and ground tissues in 10-mL HNO_3 and 5-mL H_2O_2. The ^{133}Cs concentrations in macrophytes were measured in replicate samples collected on day 0 and days 3, 8, 15, 22, 29, 44, 59, 65, 82 and 129 following the addition.

To collect periphyton material for determinations of ^{133}Cs concentrations, sections of *M. spicatum* were gently clipped from the plants while still in the water column, and the periphyton dislodged by vigorous shaking within submersed 80-µm mesh plankton nets. The contents of the net were back-washed into 1-L collection bottles, dried at 65 $^{\circ}C$, weighed and their ^{133}Cs were analyzed by NAA procedures on dried and ground replicate samples collected 13 days before the addition and on days 3, 8, 11, 15, 22, 29, 44, and 59 following the ^{133}Cs addition. The clipped plant material was retained, dried and measured for mass, and the ratio of periphyton mass to macrophyte mass was determined for each sample.

Plankton were collected from the upper 1.8 m of the water column in 40 vertical hauls of an 80-µm mesh plankton net before the addition and on days 0.25, 1, 3, 8, 15, 22, 29, 44, 59, 65, 82 and 129 following the addition. Additional samples were collected at weekly intervals through day 136 and on

days 164 and 178. The plankton net contents were back-washed into 1-L collection bottles, dried at 65 ºC, weighted and their ^{133}Cs concentrations were analyzed by NAA procedures. The sampled plankton probably included both primary producers such as phytoplankton and consumers such as zooplankton. Although this plankton sampling represents a mixed component of producers and consumers with alternative modes of accumulating Cs, this mixed component is the basis for most of the larger pelagic consumers such as *Chaoborus. punctipennis.*

A.2. Sampling of the animal components

The animal components of the biota analyzed in this study were 1) the plankton-feeding insect larvae of the insect *Chaoborus punctipennis*, 2) the periphyton-feeding aquatic snail *Helisoma trivolvis*, and the fishes 3) lake chub (*Erimyzon sucetta),* bluegill (*Lepomis macrochirus)* and largemouth bass (*Micropterus salmoides).* These five animal components were selected as representative and easily sampled trophic levels of distinct food chains, and limited analyses of ^{13}C:^{12}C and ^{15}N:^{14}N ratios verified distinctly different food chains for *C. punctipennis* larvae and *H. trivolis* (B. E. Taylor, unpublished data).

Chaoborus larvae pass through several stages, termed instars, before reaching lengths of 10 mm and emerging as a winged midge. All instars feed on phytoplankton and zooplankton with some changes in diet associated with instar stage and prey abundance (La Row and Marzolf, 1970; Winner and Greber, 1980; Chimney *et al*., 1981; Moore, 2006), and *Chaoborus* species have been proposed as potential biomonitors of metal contamination in lakes (Hare and Tessier, 1996; Croteau *et al*., 1998). Individual larvae of *C. punctipennis* were collected at dawn by trawling with 80-µm mesh nets in the open water areas on days 5, 12, 22, 29, 39, 65 and 94 days following the addition. The individuals were narcotized with carbonated water, sorted into four replicate samples of approximately 1000 individuals, and dried at 60 ºC to obtain about 50 µg dry mass for sample and the ^{133}Cs concentrations were determined by NAA procedures.

Heliosoma trivolis, which are aquatic snails, feed primarily by rasping periphyton from the surfaces of vegetation and other objects (Smith, 1988; Thorp and Covich, 2001; Lomardo and Cooke, 2002). The snail may live for two years and grow to 25-mm in size (Boeger, 1975; Eversole, 1978; Russell-Hunter *et al*., 1984). Individuals snails were collected using dip nets from the submerged surfaces of macrophytes before the addition and on days 5, 12, 22, 29, 39 65 and 94 days following the addition. The soft body parts of approximately 20 mg per snail were separated from the shell for approximately 10 individuals per sample, dried at 60 ºC, weighed, and the ^{133}Cs concentrations determined by NAA procedures.

Fish were collected by electroshocking from six locations along the margins of the submerged macrophytes beds**.** Stunned fish were collected using dip nets, sorted by species, and frozen for later analysis. Fish were collected before the ^{133}Cs addition and at 3-day intervals for the first 2 weeks following the addition, and at weekly intervals through the end of September, 1999, at bi-weekly intervals through March, 2000, and at monthly intervals through October 2000. The ^{133}Cs concentrations were measured by ICP-MS in dorsal muscle samples which were dried, weighed, digested in solutions of 10-ml of HNO_3 and 5-ml-H_2O_2. The ^{133}Cs concentrations in the muscle tissue were converted to a whole-fish basis using the value of 0.8 for the ratio of muscle mass to whole-fish mass (Peters and Newman, 1999).

Measurements of ^{133}Cs concentrations in fish were made for only the abundant species that can reach edible sizes. These species included the lake chub (*Erimyzon sucetta*), the bluegill (*Lepomis macrochirus*) and the largemouth bass (*Micropterus salmoides*). As individuals of these species grow, their diets can vary from algae and zooplankton through a mixture of zooplankton, insects and small fish, to predominantly larger fish (Hodgson and Kitchell, 1987; Taylor *et al*., 1991; Liao *et al*., 2002; Nobriga and Feyrer, 2007). Despite these variations, the lake chub is primarily an omnivore feeding on plants (Becker, 1983; *fishbase.org*) and small animals (*fishbase.org*). The bluegill is primarily an intermediate predator on zooplankton, crustaceans, insects and snails (Flemer and Woolcott, 1966; Kitchell and Windell, 1970; Taylor *et al*., 1991; Lobinske *et al*., 2002; *fishbase.org*) and larger individuals of

largemouth bass are apex predators feeding primarily on fish (Clady, 1981; Hodgson and Kitchell, 1987; Liao et al., 2002; Nobriga and Feyrer, 2007; *fishbase.org*).

A.3. Measurements for biomass of primary producers

The masses of the primary producers were estimated from the masses of these forms measured in samples multiplied by the area or volumes of the Pond that they occupied. The mass of submerged vegetation was measured by sampling 38 circular, 0.16-m^2 plots on the pond's bottom within the depths occupied by the submerged macrophytes. A circular approximately 3-m long tube with a 0.45-m diameter was lowered vertically to the pond bottom, and the vegetation in the tube removed using a 3-prong rake. The roots were removed from the sampled vegetation before it was separated into species, dried and weighed, and the total vegetation estimate of 35,000 kg wet mass was obtained as the mean dry biomass (g m^{-2}) multiplied by 1) a wet-mass to dry mass ratio of 10 and 2) the area of the pond occupied by the vegetation.

The mass of periphyton was estimated as the mean ratio of periphyton mass to submerged vegetation mass (0.170) times the wet mass of submerged vegetation in the pond (35,000 kg) to yield a periphyton wet mass of approximately 6,000 kg. The mass of phytoplankton collected in the plankton nets indicated a mean dry mass of 0.0134 g m^{-3} in the 68,000 m^3 in the upper 1-m of the open water area which indicates a wet mass for plankton of approximately 9 kg assuming a dry to wet ratio of 10. The low plankton mass may be a reflection of the abundances of the submerged macrophytes and periphyton which are thought to be competitively superior to phytoplankton with respect to nutrient uptake (Hann et al., 2001; van Donk et al., 1990).

APPENDIX B – FLUX CALCULATIONS

The following are the full set of equations for calculation of fluxes described in Chapter 3. The symbols are described in Table 3.5. Solving for the fluxes $F_{c,j\text{-}\rightarrow n}(t)$, U_1, U_2, and U_3 was accomplished as specified below:

n=8, largemouth bass

j=7, bluegills and j=6, lake chubs

$$U_8(t) = \Delta I_8 + F_{e,8}(t)$$

$$F_{c,7\rightarrow 8}(t) + F_{c,6\rightarrow 8}(t) = U_8(t)$$

$$F_{c,7\rightarrow 8}(t) = U_8(t)\, p_j = U_8(t)\ \frac{M_j}{\sum_i M_{j,i}} = U_8(t)\frac{M_7}{M_7+M_6}$$

$$F_{c,6\rightarrow 8}(t) = U_8(t)\, p_j = U_7(t)\ \frac{M_j}{\sum_i M_{j,i}} = U_8(t)\frac{M_6}{M_7+M_6}$$

n=7, bluegills

j=5, snails and j=4, chaoborus larvae

$$U_7(t) = \Delta I_7 + F_{e,7}(t) + F_{c,7\rightarrow 8}(t)$$

$$F_{c,5\rightarrow 7}(t) = U_7(t)\, p_5 = U_7(t)\frac{M_5}{M_4+M_5}$$

$$F_{c,4\rightarrow 7}(t) = U_7(t)\, p_4 = U_7(t)\frac{M_4}{M_4+M_5}$$

n=6, lakechubs

j=2, periphyton

$$U_6(t) = \Delta I_6 + F_{e,6}(t) + F_{c,6\rightarrow 8}(t)$$

$$F_{c,2\rightarrow 6}(t) = U_7(t)$$

n=5, snails

j=2, periphyton

$$U_5(t) = \Delta I_5 + F_{e,5}(t) + F_{c,5\rightarrow 7}(t)$$

$$F_{c,2\rightarrow 5}(t) = U_5(t)$$

n=4, Chaoborus larvae

j=3, plankton

$$U_4(t) = \Delta I_4 + F_{e,4}(t) + F_{c,4\rightarrow 7}(t)$$

$$F_{c,3\rightarrow 4}(t) = U_4(t)$$

n=3, Plankton

Uptake from water:

$$U_3(t) = \Delta I_3 + F_{e,3}(t) + F_{c,3\rightarrow 4}(t)$$

n=2, Periphyton

Uptake from water:

$$U_2(t) = \Delta I_2 + F_{e,2}(t) + F_{c,2\rightarrow 5}(t) + F_{c,2\rightarrow 6}(t)$$

n=1, Submerged Vegetation

Uptake from water:

$$U_1(t) = \Delta I_1 + F_{e,1}(t)$$

APPENDIX C – RATIOS OF ODE KINETIC MODEL TO TABULAR MODEL

Table C.1 below is ratios of kinetic model to tabular model for first 100 days and C.2 includes the same ratios for days 125 to 500 in 25 day interavals. Black text indicates model results are within a factor of two, orange text indicates within a factor of three, and blue text is larger than a factor of three.

Table C.1 Ratios of ODE kinetic model to tabular model for first 100 days

Day	Water	Macrophytes	Plankton	Periphyton	Snails	Chaob	Bluegill	Lakechub	Bass
5	0.85	1.21	1.53	1.21	0.71	1.00	0.10	0.45	0.01
10	0.80	1.26	1.46	1.46	1.34	1.52	0.37	0.83	0.05
15	0.82	1.25	1.18	1.51	1.61	1.59	0.61	1.03	0.10
20	0.87	1.23	0.98	1.47	1.69	1.52	0.79	1.15	0.16
25	0.92	1.21	0.85	1.39	1.65	1.42	0.91	1.22	0.22
30	0.96	1.17	0.77	1.29	1.57	1.32	1.00	1.25	0.28
35	1.01	1.12	0.72	1.19	1.45	1.22	1.05	1.27	0.34
40	1.05	1.07	0.69	1.10	1.33	1.13	1.08	1.28	0.39
45	1.08	1.01	0.66	1.01	1.22	1.05	1.10	1.29	0.45
50	1.10	0.96	0.63	0.94	1.13	0.98	1.11	1.29	0.50
55	1.12	0.90	0.61	0.88	1.04	0.92	1.11	1.28	0.55
60	1.12	0.85	0.59	0.83	0.97	0.86	1.11	1.28	0.60
65	1.12	0.80	0.57	0.79	0.91	0.81	1.11	1.27	0.64
70	1.12	0.76	0.56	0.75	0.86	0.77	1.11	1.26	0.68
75	1.12	0.72	0.54	0.72	0.81	0.74	1.10	1.25	0.72
80	1.11	0.69	0.53	0.70	0.78	0.71	1.10	1.25	0.75
85	1.10	0.66	0.52	0.68	0.75	0.68	1.09	1.24	0.78
90	1.09	0.64	0.51	0.66	0.73	0.66	1.08	1.23	0.81

95	1.08	0.62	0.50	0.65	0.71	0.64	1.08	1.22	0.84
100	1.07	0.60	0.50	0.63	0.69	0.63	1.07	1.21	0.87

Table C.2. Ratios of ODE kinetic model to tabular model for days 125 to 500

Day	Water	Macrophytes	Plankton	Periphyton	Snails	Chaob	Bluegill	Lakechub	Bass
125	1.03	0.56	0.48	0.60	0.65	0.59	1.04	1.18	0.97
150	0.99	0.55	0.48	0.59	0.63	0.57	1.03	1.15	1.05
175	0.98	0.55	0.48	0.60	0.64	0.57	1.01	1.13	1.10
200	0.97	0.56	0.50	0.61	0.65	0.58	1.01	1.11	1.14
225	0.98	0.58	0.51	0.63	0.67	0.60	1.01	1.11	1.16
250	1.01	0.60	0.54	0.65	0.69	0.62	1.02	1.11	1.18
275	1.04	0.63	0.56	0.69	0.72	0.65	1.03	1.12	1.19
300	1.09	0.66	0.59	0.72	0.76	0.69	1.05	1.13	1.20
325	1.15	0.70	0.63	0.77	0.81	0.73	1.07	1.15	1.20
350	1.22	0.74	0.67	0.81	0.86	0.77	1.09	1.18	1.21
375	1.31	0.79	0.71	0.87	0.91	0.82	1.12	1.21	1.21
400	1.42	0.84	0.76	0.93	0.97	0.88	1.16	1.25	1.21
425	1.54	0.90	0.81	0.99	1.04	0.94	1.19	1.30	1.21
450	1.67	0.96	0.87	1.06	1.12	1.01	1.24	1.35	1.21
475	1.83	1.03	0.94	1.14	1.20	1.08	1.29	1.41	1.21
500	2.00	1.11	1.01	1.22	1.29	1.16	1.34	1.49	1.21

APPENDIX D – MARKOV CHAIN TERMINOLOGY

Markov Chain: A general type of probabilistic model; consists of a series of random variables, X_i, that follow the Markov property (given below).

State: A state, ***S***, is the distribution that the random variables of the Markov chain, X_i, may be occupying. In the case of the Pond 4 model, or any compartment model, the states are the set of compartments. For the Markov chain model proposed by this document, the amount of ^{133}Cs atoms is the random variables that is changing through the states over a number of time steps, *n*.

Markov property: The Markov property specifies that the probability, $p_{i,j}$, of the system being in state *j* at step *n* is only dependent on that it was in state *i* during the previous step, *n-1*. A step is often expressed as a unit of time, Δt. The time, *t*, of the process at step *n*, is given by $n\Delta t$. The Markov property can be described mathematically as the following conditional probability (Acevedo, 2013):

$$p_{i,j} = P\left[S_j(n)\middle|S_i(n-1)\right] \tag{8}$$

$$\text{Where } 0 \leq p_{i,j} \leq 1 \quad \text{and} \quad \sum_i p_{i,j} = 1$$

Transitional probability matrix: A matrix **P** where the elements $p_{i,j}$ express the probability of the process transitioning from state *i* to state *j*.

Time-homogeneous Markov chain: Transition probabilities do not change over time

Non-homogeneous Markov chain: Transition probabilities can change over time

Discrete time Markov chain: Transition is discretized to set and uniform time steps

Continuous time Markov chain: Transition time from step to step is allowed to vary (often by an exponential function)

Transient Markov chain: A Markov chain that does not include absorbing states

Absorbing Markov chain: A Markov model wherein at least one state has a retention probability of one; no matter where the process starts, it will ultimately end up in this absorbing state

Ergotic state: An absorbing state

Transient states: Those states which are not absorbing, the process transitions from these states to at least one other state by the specified probability in the transitional probability matrix, **P**.

Fundamental Matrix: A matrix for absorbing Markov chains whose elements express the mean amount of time spent in transient states prior to transitioning to the absorbing state(s)

Two additional definitions worth inclusion in this appendix are:

Monte Carlo method – "One that involves deliberate use of random numbers in a calculation that has the structure of a stochastic process (Kalos, 2008)."

Stochastic Process- "A sequence of states whose evolution is determined by random events (Kalos, 2008)."

APPENDIX E – SENSITIVITY ANALSIS OF MARKOV MATRIX MODEL

Table E.1. Ratio of adjusted to unadjusted for each model component when the transition probabilities for movement of Cs through the food web and from the water to all directly connected components (periphyton, plankton, submerged vegetation, sediments, and Pond 5) are decreased by 20% individually. Overall model is not sensitive to such changes. The largest variation results from changing the water to sediment transition probabilities (second to bottom row in table). Additionally, the largemouth bass is most sensitive to changes in the water to periphyton followed by the periphyton to lake chub transition probabilities.

	Water	Sub Veg	Peri	Sediment	Snails	Bluegill	Plankton	Chaob larvae	Lake chub	Bass	Pond 5
peri to sn	1.00015	1.00013	1.02056	1.00001	0.81632	0.81536	1.00014	1.00013	1.01913	1.00901	0.99999
peri to lc	1.00312	1.00290	1.04135	1.00247	1.04104	1.03736	1.00300	1.00290	0.83074	0.83781	1.00228
lc to bass	0.99835	0.99842	0.99840	0.99943	0.99842	0.99940	0.99839	0.99843	1.18323	0.89831	0.99961
sn to bg	1.00045	1.00042	1.00043	1.00030	1.04465	0.83436	1.00044	1.00042	1.00034	0.99298	1.00027
bg to bass	0.99989	0.99990	0.99990	0.99997	0.99990	1.06086	0.99989	0.99990	0.99995	0.99279	0.99998
pl to ch	1.00000	1.00000	1.00000	1.00000	1.00000	0.99972	1.10880	0.88568	1.00000	0.99999	1.00000
ch to lmb	1.00000	1.00000	1.00000	1.00000	1.00000	1.00000	1.00000	1.00000	1.00000	1.00000	1.00000
W to peri	1.00223	1.00278	0.80214	1.00484	0.80217	0.80429	1.00256	1.00278	0.80343	0.80425	1.00197
W to pl	1.00000	1.00000	1.00000	1.00000	1.00000	0.99953	0.80000	0.80000	1.00000	0.99998	1.00000
W to subveg	0.99104	0.79570	0.99387	1.00643	0.99417	1.00615	0.99313	0.99457	1.00325	1.00966	0.99585
W to sed	1.23256	1.22475	1.22650	0.95092	1.22498	1.18808	1.22864	1.22400	1.19821	1.17739	1.14453
W to pnd5	1.01353	1.01270	1.01287	1.00551	1.01272	1.00574	1.01304	1.01262	1.00759	1.00436	0.80831

Table E.2. Ratio of adjusted to unadjusted for each model component when the transition probabilities for movement of Cs through the food web and from the water to all directly connected components (periphyton, plankton, submerged vegetation, sediments, and Pond 5) are increased by 20% individually. As in Table E.1., overall model is not sensitive to such changes and the largest variation comes from changing the water to sediment transition probabilities (second to bottom row in table).

	Water	Sub Veg	Peri	Sediment	Snails	Bluegill	Plankton	Chaob larvae	Lake chub	Bass	Pond 5
peri to sn	0.99986	0.99987	0.98026	0.99999	1.17649	1.17801	0.99986	0.99987	0.98158	0.99131	0.99986
peri to lc	0.99712	0.99732	0.96183	0.99770	0.96211	0.96528	0.99723	0.99732	1.15722	1.15142	0.99712
lc to bass	1.00125	1.00119	1.00120	1.00046	1.00119	1.00049	1.00122	1.00119	0.86176	1.08239	1.00125
sn to bg	0.99959	0.99961	0.99961	0.99972	0.95903	1.15272	0.99960	0.99961	0.99969	1.00647	0.99959
bg to bass	1.00010	1.00009	1.00009	1.00003	1.00009	0.94466	1.00010	1.00009	1.00005	1.00659	1.00010
pl to ch	1.00000	1.00000	1.00000	1.00000	1.00000	1.00023	0.91070	1.09430	1.00000	1.00001	1.00000
ch to lmb	1.00000	1.00000	1.00000	1.00000	1.00000	1.00000	1.00000	1.00000	1.00000	1.00000	1.00000
W to peri	0.99776	0.99721	1.19678	0.99521	1.19673	1.19387	0.99743	0.99722	1.19491	1.19372	0.99776
W to pl	1.00000	1.00000	1.00000	1.00000	1.00000	1.00047	1.20000	1.20000	1.00000	1.00002	1.00000
W to macro	1.00839	1.20600	1.00570	0.99381	1.00542	0.99408	1.00638	1.00505	0.99683	0.99079	1.00839
W to sed	0.83971	0.84352	0.84256	1.03627	0.84349	0.86408	0.84134	0.84403	0.85832	0.87027	0.83971
W to pnd5	0.98687	0.98767	0.98750	0.99460	0.98765	0.99439	0.98734	0.98774	0.99260	0.99572	0.98687

APPENDIX F – SUPPLEMENTAL PLOTS FOR CHAPTER FIVE

F.1. Additional plots illustrating similarity of Markov simulation model mean output to ODE kinetic model for 30 replications of one million atoms

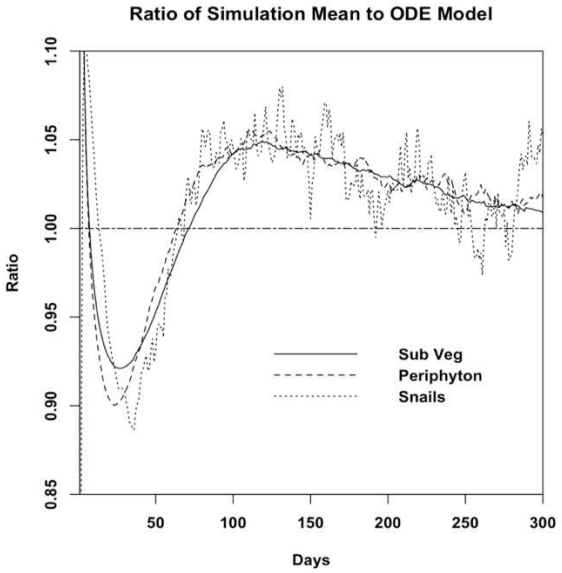

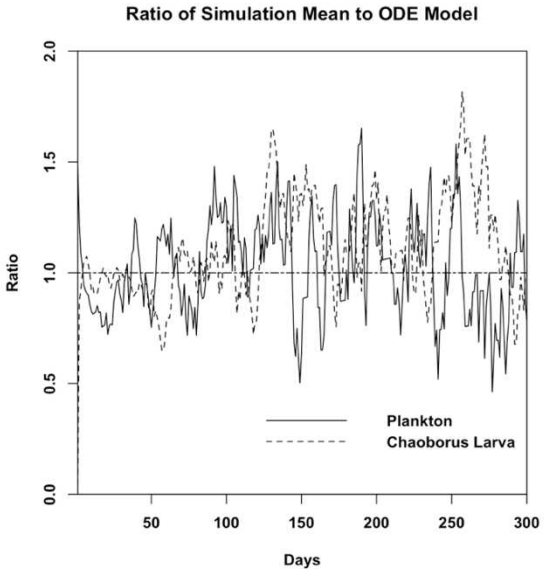

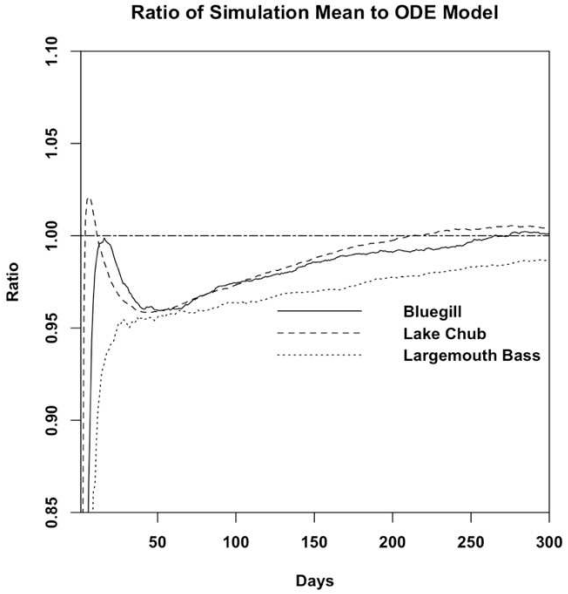

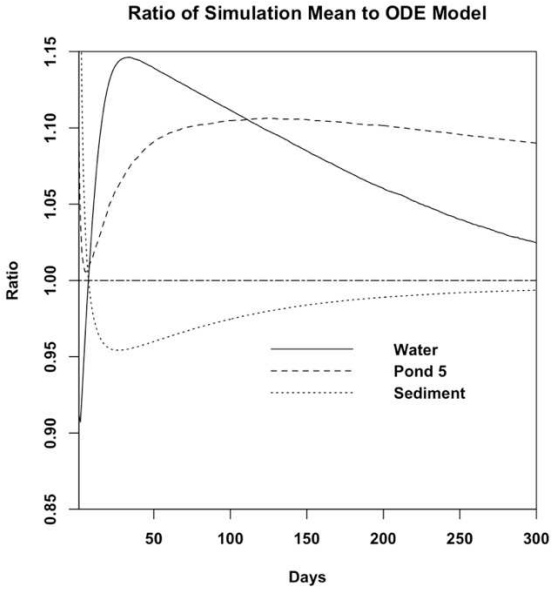

Figure F.1. Additional graphs of Markov simulation model compared to ODE model, illustrated as the ratio of the two models.

F.2. Atom residence time evaluation from Markov Simulation Model

Graphs of residence time (*i.e.* duration of visit from entry into given biotic component to exit of an atom) from Markov simulation results for additional biota results not included in Chapter 5. Figures F.2A to F.2C include the exponential distribution fit and a QQ plot of the results (x-axis) compared to a simulated distribution of the same amount of points (y-axis) from the exponential fit predicted parameters. Less than 10% of the fish results all exhibit a deviation from a 1.1:1 ratio of model results to the synthetic exponential distribution data; specifically, 4.5% of the bluegill are out of 1.1 ratio, 7.5% of the bass results 7.5% and 2.1% of the lake chub results

Table F.1. Additional Results Regarding the Markov Simulation Atom Residence Times

Biota State	Exponential Distribution Rate	Standard Error of Rate	Model Residence Time Mean (Days)
Snail	9.54×10^{-3}	5.096×10^{-5}	104.87
Plankton	0.206	0.022	4.86
Periphyton	0.106	2.22×10^{-4}	88.2
Macrophytes	0.0756	8.04×10^{-5}	13.3
Bluegill	7.11×10^{-3}	1.28×10^{-4}	140.5
Lake chub	9.54×10^{-3}	5.09×10^{-5}	104.9
Largemouth bass	8.81×10^{-3}	5.56×10^{-5}	113.6

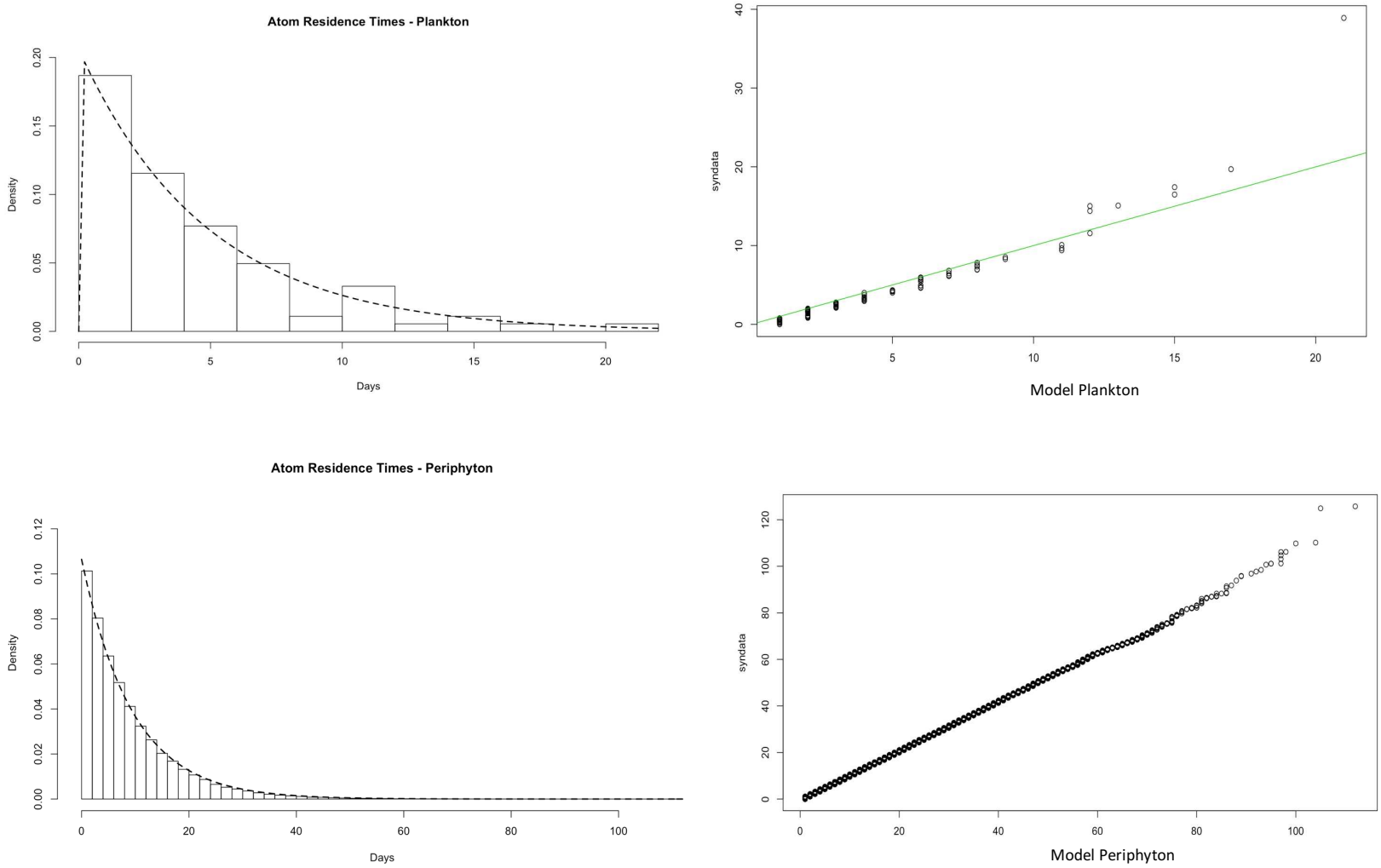

Figure F.2A. Model predicted atom residence times of the plankton and periphyton with exponential distribution fit and corresponding Q-Q plot

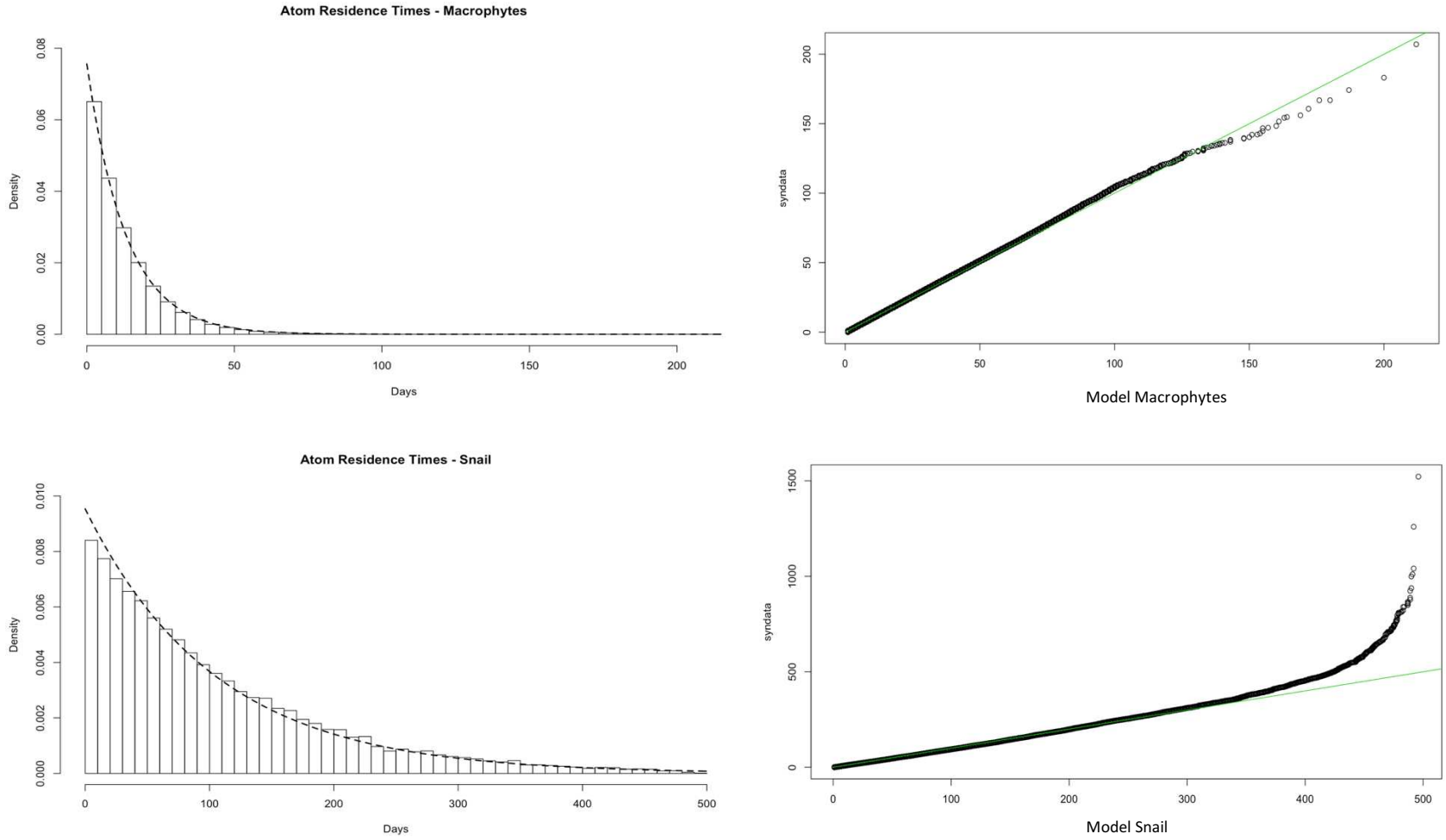

Figure F.2B. Model predicted atom residence times of the macrophytes and snail components with exponential distribution fit and corresponding Q-Q plot

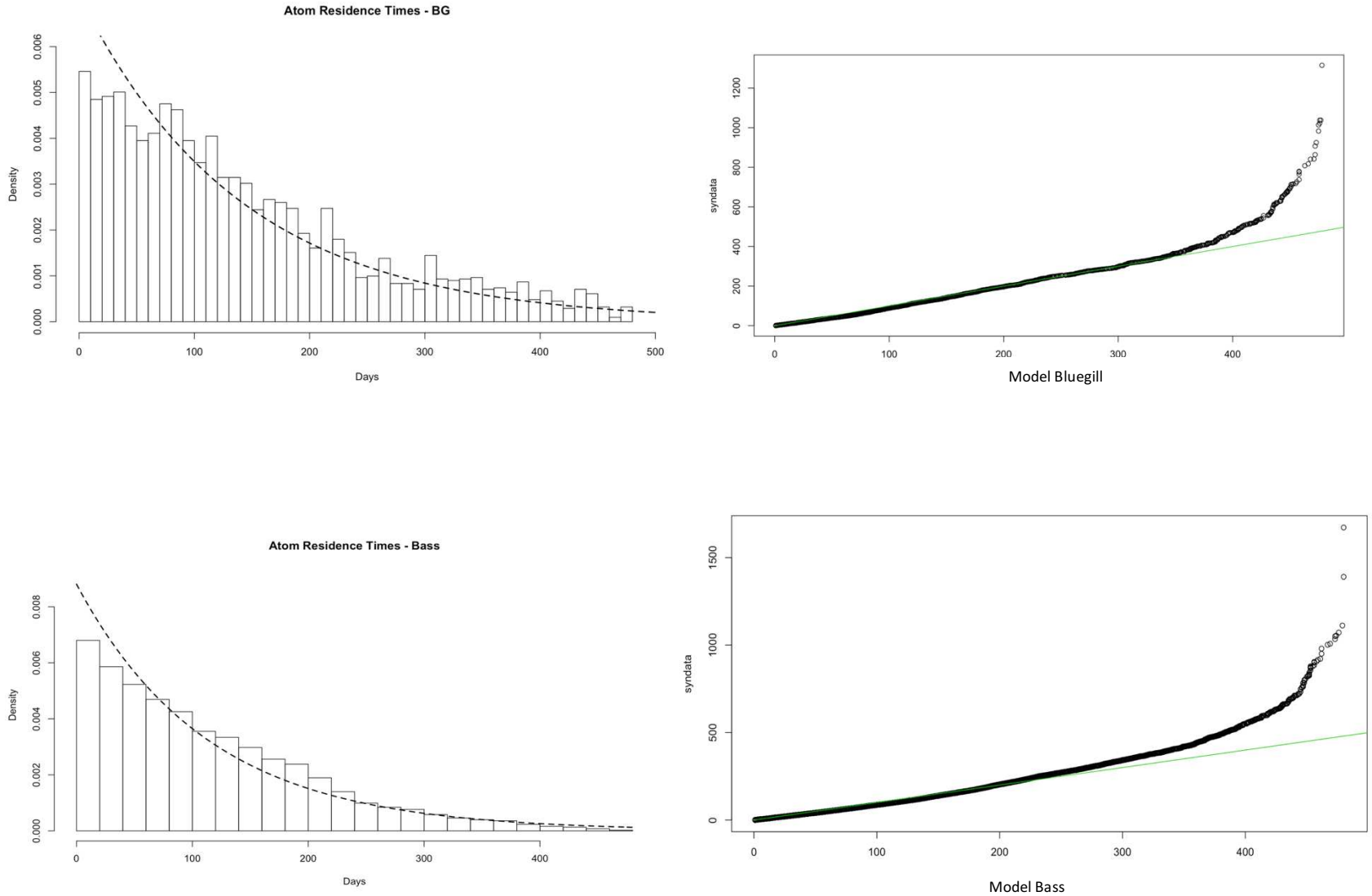

Figure F.1C. Model predicted atom residence times of the bluegill and bass components with exponential distribution fit and corresponding Q-Q plot

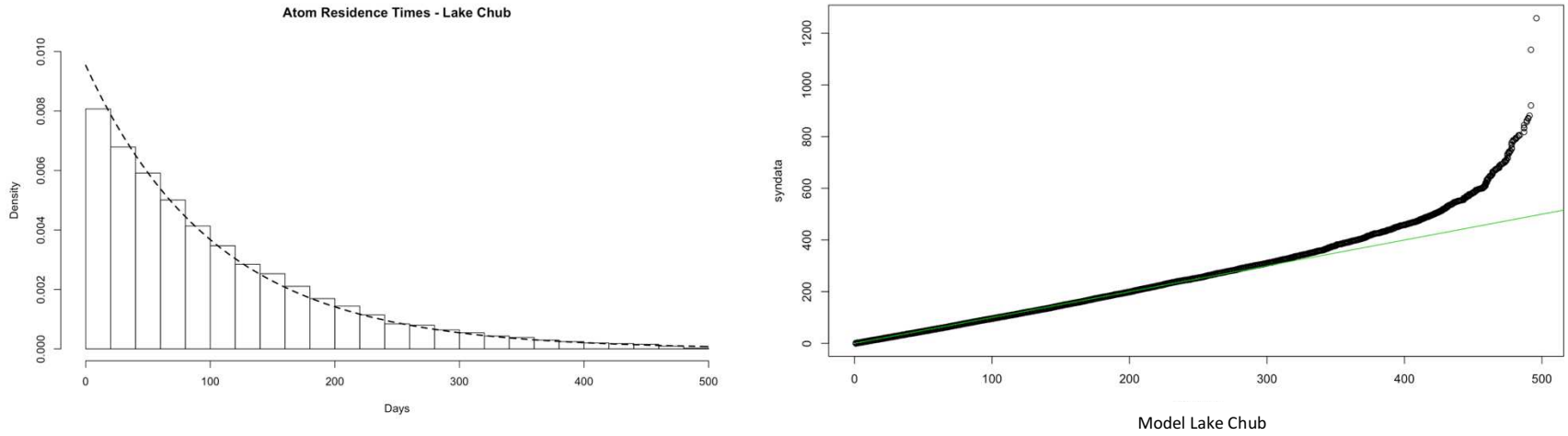

Figure F.2C. Model predicted atom residence times of the lake chub with exponential distribution fit and corresponding Q-Q plot

F.3. Exponential distribution principles and application

Probability density function: $f(t) = t\ exp(-\lambda t)$

λ = rate

$1/\lambda$ = mean

$1/\lambda^2$ = variance

Cumulative density function: $P(t) = 1 - \ exp(-\lambda t)$

*Recall that the cumulative density function is the integral (area under the curve) of the probability density function; $P(t)$ is used to answer the following questions in the main text of this manuscript:

Question One:

What is the probability that a ^{133}Cs atom will reside in the plankton longer than a lifespan of t=20 days?

From Plankton exponential distribution fit $\lambda = 0.20588$

$P(t > 20) = 1 - (1 - \ exp(-\lambda t)) = exp(-\lambda t) = exp(-0.20588 * 20) = 0.016$

Answer: There is a 1.6% chance that the ^{133}Cs atom will reside in the plankton longer than 20 days.

Question Two:

What is the probability that a ^{133}Cs atom will reside in the plankton longer than a lifespan of t=5 days?

$P(t > 5) = 1 - (1 - \ exp(-\lambda t)) = exp(-\lambda t) = exp(-0.20588 * 5) = 0.36$

APPENDIX G – ABSORBING MARKOV CHAIN SUPPLEMENTAL

G.1. Mathematical Basis of Absorbing Markov Chain Equation for N

This appendix provides definitions and theorems supporting the fundamental matrix, ***N***, and equations for the properties of an absorbing matrix. Recall that $\boldsymbol{Q}$ is the matrix of the transition probabilities for non-absorbing states. $\boldsymbol{I_{tr}}$ is an identity matrix of the same dimensions as $\boldsymbol{Q}$ and *n* is the number of steps. Each element of the matrix **N** gives the mean number of time steps that the system was in state *j* prior to being absorbed, given it started in state *i*. It can be shown that:

$$\boldsymbol{N} = (\boldsymbol{I_{tr}} - \boldsymbol{Q})^{-1} = \sum_{n=0}^{\infty} \boldsymbol{Q}^n \qquad \text{(G-1)}$$

Proof:

1. $(\boldsymbol{I_{tr}} - \boldsymbol{Q})$ must have a defined inverse
    a. If $\boldsymbol{Q}^k \to \boldsymbol{0}$ as $k \to \infty$ then $(\boldsymbol{I_t} - \boldsymbol{Q})$ has an inverse (see Kemney, 1976, page 22 for proof of this theorem). For an absorbing matrix, $\boldsymbol{Q}^k \to \boldsymbol{0}$ as *k* goes to infinity because ultimately the process ends in an absorbing state. For Pond 4, ultimately as time goes to infinity the atoms will all go to an absorbing state.
2. Given $\boldsymbol{Q}^k \to \boldsymbol{0}$ *as* $k \to \infty$ the following can be shown to be true:

$$\boldsymbol{N} = (\boldsymbol{I} - \boldsymbol{Q})^{-1} = \boldsymbol{I} + \boldsymbol{Q} + \boldsymbol{Q}^2 + \boldsymbol{Q}^3 + \cdots = \sum_{k=0}^{\infty} \boldsymbol{Q}^k$$

Proof:

- Utilize the identity:

$$(\boldsymbol{I}-\boldsymbol{Q})*(\boldsymbol{I}+\boldsymbol{Q}+\boldsymbol{Q}^2+\ldots+\boldsymbol{Q}^{k-1})=\boldsymbol{I}-\boldsymbol{Q}^{\boldsymbol{k}}$$

The following example illustrates this identity for *k*=4 given the principles: 1) $\boldsymbol{I}^{\boldsymbol{k}}=\boldsymbol{I}$ and 2) $\boldsymbol{I}\boldsymbol{Q}^{\boldsymbol{k}}=\boldsymbol{Q}^{\boldsymbol{k}}$, since $\boldsymbol{I}\,\boldsymbol{A}=\boldsymbol{A}$, where $\boldsymbol{A}$ is any matrix.

$$(\boldsymbol{I}-\boldsymbol{Q})*(\boldsymbol{I}+\boldsymbol{Q}+\boldsymbol{Q}^2+\boldsymbol{Q}^3)=\boldsymbol{I}^{\boldsymbol{2}}+\boldsymbol{I}\boldsymbol{Q}+\boldsymbol{I}\boldsymbol{Q}^{\boldsymbol{2}}+\boldsymbol{I}\boldsymbol{Q}^3-(\boldsymbol{Q}\boldsymbol{I}+\boldsymbol{Q}^2+\boldsymbol{Q}^3+\boldsymbol{Q}^4)=\boldsymbol{I}-\boldsymbol{Q}^{\boldsymbol{4}}$$

- When each side of the identity is multiplied by $(\boldsymbol{I}-\boldsymbol{Q})^{-1}$, the following is obtained

$$(\boldsymbol{I}+\boldsymbol{Q}+\boldsymbol{Q}^2+\ldots+\boldsymbol{Q}^{k-1})=\ (\boldsymbol{I}-\boldsymbol{Q})^{-1}(\boldsymbol{I}-\boldsymbol{Q}^{\boldsymbol{k}})$$

- The right side of the above equation, $(\boldsymbol{I}-\boldsymbol{Q})^{-1}\left(\boldsymbol{I}-\boldsymbol{Q}^{\boldsymbol{k}}\right)$**,** tends to $(\boldsymbol{I}-\boldsymbol{Q})^{-1}$ given 1) that $\left(\boldsymbol{I}-\boldsymbol{Q}^{\boldsymbol{k}}\right)$ tends to **I** given $\boldsymbol{Q}^k\rightarrow\boldsymbol{0}$ as $k\rightarrow\infty$ and 2) that $\boldsymbol{I}\,\boldsymbol{A}=\boldsymbol{A}$, where $\boldsymbol{A}$ is any matrix.

Probabilistically:

$\boldsymbol{N}$ can also be stated as:

$$\boldsymbol{N}=\left\{\,Mean_i\left[n_j\right]\right\} \qquad \text{(G-2)}$$

where n_j is a function that gives the total number of times that the process is in s_j prior to being absorbed. If u_j^k is a function that is 1 if the process is in state *j* after *k* steps and 0 otherwise, then $n_j=\sum_{k=0}^{\infty}u_j^k$. s_i and s_j are transient states that make up $\boldsymbol{Q}$. Equation X can be proven by:

$$\left\{\,Mean_i\left[n_j\right]\right\}=\ Mean_i\left[\sum_{k=0}^{\infty}u_j^k\right]=\ \sum_{k=0}^{\infty}\ Mean_i[u_j^k]$$

$$=\sum_{k=0}^{\infty}\ \left(\left(1-p(k)_{ij}\right)*0+p(k)_{ij}*1\right)=\sum_{k=0}^{\infty}\ \left\{p(k)_{ij}\right\}=\sum_{k=0}^{\infty}\ \boldsymbol{Q}^k=\mathbf{N}$$

where $p(k)_{ij}$ is the probability after *k* steps of being in state *j* given the initial state *i*, where *i* and *j* are both transient states.

G2. Example results from absorbing matrix calculations for Fundamental Matrix

Table G.1 gives an example of the results for the Fundamental Matrix, **N**, (explained in Chapter 6). Each row gives the mean amount days an atom will spend in each column specified biota prior to exiting the system to pond 5 or the sediments modeled as a sink (Scenario B2), given the atom started in the biota listed for that row. For example, an atom starting in the periphyton is expected to spend an average of about 28 days in the lake chub prior to exiting the system. The sum of each row gives the total time prior to exiting the system, for the specified initial starting state. The water results, highlight blue, were summed in the results given in Chapter 6.

*Table G.1. Complete results of **N**, the fundamental matrix, for the baseline ^{133}Cs model.*

	W1	W2	W3	Subm Veg	Peri	Snails	Bluegill	Pl	Chaob	Lake Chub	Bass
Water 1	1.55	1.96	13.73	6.47	1.15	0.06	0.85	2.68E-04	2.75E-04	3.09	5.27
Water 2	0.18	8.17	13.67	6.44	1.15	0.06	0.85	2.66E-04	2.73E-04	3.08	5.24
Water 3	0.17	1.82	101.93	5.98	1.07	0.05	0.79	2.47E-04	2.54E-04	2.86	4.87
Subm Veg	0.47	5.19	36.30	19.82	1.13	0.06	0.83	2.62E-04	2.69E-04	3.03	5.15
Peri	0.47	5.19	36.30	6.33	10.66	0.55	7.86	2.62E-04	2.69E-04	28.61	48.69
Snails	0.47	5.19	36.30	6.33	1.13	5.17	74.23	2.62E-04	2.69E-04	3.03	38.28
Bluegill	0.47	5.19	36.30	6.33	1.13	0.06	353.14	2.62E-04	2.69E-04	3.03	164.17

Pl	0.53	4.97	35.63	6.33	1.13	0.06	42.00	5.39	5.53	3.03	23.74
Chaob ***larvae***	0.47	5.19	36.30	6.33	1.13	0.06	87.25	2.62E-04	11.61	3.03	44.16
Lake Chub	0.47	5.19	36.30	6.33	1.13	0.06	0.83	2.62E-04	2.69E-04	148.15	234.12
Bass	0.47	5.19	36.30	6.33	1.13	0.06	0.83	2.62E-04	2.69E-04	3.03	248.84